



**This electronic thesis or dissertation has been  
downloaded from Explore Bristol Research,  
<http://research-information.bristol.ac.uk>**

*Author:*

**Williams, Matt**

*Title:*

**Imaging the Heart Brain Interaction in Myocardial Infarction with Non-obstructive  
Coronary Arteries (MINOCA)**

**General rights**

Access to the thesis is subject to the Creative Commons Attribution - NonCommercial-No Derivatives 4.0 International Public License. A copy of this may be found at <https://creativecommons.org/licenses/by-nc-nd/4.0/legalcode>. This license sets out your rights and the restrictions that apply to your access to the thesis so it is important you read this before proceeding.

**Take down policy**

Some pages of this thesis may have been removed for copyright restrictions prior to having it been deposited in Explore Bristol Research. However, if you have discovered material within the thesis that you consider to be unlawful e.g. breaches of copyright (either yours or that of a third party) or any other law, including but not limited to those relating to patent, trademark, confidentiality, data protection, obscenity, defamation, libel, then please contact [collections-metadata@bristol.ac.uk](mailto:collections-metadata@bristol.ac.uk) and include the following information in your message:

- Your contact details
- Bibliographic details for the item, including a URL
- An outline nature of the complaint

Your claim will be investigated and, where appropriate, the item in question will be removed from public view as soon as possible.

# Imaging the Heart Brain Interaction in Myocardial Infarction with Non- obstructive Coronary Arteries (MINOCA)

**Dr Matthew Guy Lloyd Williams**

A dissertation submitted to the University of Bristol in accordance with the requirements for the award of the degree of Doctor of Philosophy in the Faculty of Health Sciences.

School of Translational Health Sciences, Bristol Medical School, Faculty of Health Sciences, August 2022.

**Word Count 40,613**

# Abstract

## Introduction

Patients presenting with a suspected myocardial infarction but who have normal coronary arteries at angiography (MINOCA) are a common clinical challenge. There is early evidence for a heart-brain link in several cardiac pathologies, including takotsubo syndrome (TS), which partly makes up the MINOCA population. The pathophysiological association of the heart-brain interaction in the wider MINOCA population has not been studied.

## Methods

In this single centre, prospective, longitudinal observational study, all patients who presented with a suspected myocardial infarction and non-obstructive coronary arteries on invasive angiography were approached. Age and sex matched patients with a ST elevation myocardial infarction (STEMI) and a group of healthy volunteers were control groups. Patients received routine care but underwent additional psychological questionnaires and cardiac and functional brain magnetic resonance imaging within 14 days of admission and at 6 months. Image pre-processing and analysis was undertaken in a blinded fashion.

## Results

72 participants, 27 STEMI controls and 28 healthy controls were recruited. There were widespread reductions in brain grey matter volume compared to healthy controls, but no differences compared to STEMI controls. These reductions largely normalised at follow up. There was reduced connectivity in the central executive network and default mode network compared to healthy controls in the acute phase, and these changes largely persisted at follow up. There were less extensive differences compared with STEMI patients. There were negative relationships between global brain efficiency, connectivity and measures

of anxiety and stress in the MINOCA population which may partly explain these findings.

## **Conclusion**

MINOCA patients have high levels of stress and anxiety at presentation and have dynamic anatomical and functional disruption in mainly limbic and autonomic brain networks. There are correlations between stress and anxiety scores and reduced connectivity and reduced global brain efficiency which may partly explain these findings. Further larger studies are needed in this area and in the wider myocardial infarction population as there may be potentially important implications for the follow up and management of these patients which requires investigation.



# COVID-19 Impact Statement

This study was affected by the global coronavirus pandemic. All research studies undertaken at University Hospital's Bristol and Weston NHS Foundation Trust deemed non-essential to the immediate management of the pandemic were suspended from 16<sup>th</sup> March 2020. Dr Matthew Williams returned to clinical cardiology practice from this date until July 2020. Recruitment and follow up visits were suspended between 16<sup>th</sup> March 2020 and 1<sup>st</sup> August 2020. As a result of this suspension 6 study visits were cancelled and 30 follow up visits were postponed. 13 people were lost to follow up from the study with at least 3 citing concerns over COVID as their main reason (if a reason was offered). There was also a notable increase in the number of potential participants who declined to participate in the study once recruitment restarted due to concerns over COVID. In addition, it was not deemed ethical to ask healthy volunteers from the community to come into the hospital, therefore our pool of healthy volunteers was limited to existing healthy healthcare workers. Dr Williams was allowed to extend his research fellowship by 6 months to allow the study to be completed to the best of our ability. However, the delay in the study meant that the original completion date was pushed back, and this then overlapped with the pre-planned MRI scanner replacement from April-June 2021 (which was meant to happen after the study was completed). This meant follow up visits were suspended again from April to late June 2021. The subsequent back log of follow up scans, slow recruitment and limited capacity on the scanner (due to large NHS backlog) all related to COVID meant that total recruitment was lower than was planned. There was also not the time or resources available to complete the 12 month follow up visits. Despite our best efforts, and support from the clinical and management teams, this was unavoidable.

The overall impact on the study is that recruitment was lower meaning that our subgroup analysis is underpowered, notably in the Takotsubo syndrome group (n=10, rather than our estimated 15). In addition, our loss to follow up may

be greater than it would otherwise have been which may lead to some bias in our results as these patients had to be excluded from the follow up brain analysis study.

## Author's Declaration

I declare that the work in this dissertation was carried out in accordance with the requirements of the University's ***Regulations and Code of Practice for Research Degree Programmes*** and that it has not been submitted for any other academic award. Except where indicated by specific reference in the text, the work is the candidate's own work. Work done in collaboration with, or with the assistance of, others, is indicated as such. Any views expressed in the dissertation are those of the author.

SIGNED: ..... DATE:.....

# Dedication

I dedicate this thesis to my family, without their patience, love and support over many years I would not have been able to achieve this milestone. To my wife, Jessica, children Arabella and Freya and to my parents, Jeremy and Caroline.

# Acknowledgements

I would like to acknowledge my supervisors, particularly Dr Chiara Bucciarelli-Ducci, Dr Ella Hinton and Dr Jade Thai. Their expertise and guidance have made this project possible. In addition, I would like to thank Mr Christopher ‘Benny’ Lawton, superintendent radiographer, for his vision and support in the study design, logistics and for helping me navigate the various challenges that have arisen. Thanks also go to the fantastic team of CMR radiographers at the Bristol Heart Institute for so skilfully, patiently, and willingly acquiring the several hundred scans needed. To the other CMR fellows, too many to mention but particular thanks to Dr Kate Liang, Dr Estefania De Garate, Dr Konstantina Mitrousi and Dr Iwan Harries. To Martin Nelson and Gui Rego for help with acquiring the echo images. To Jeremy Williams for proofreading the final draft. Finally, to all the patients and volunteers for giving up their time to allow this study to happen.

This study was generously supported by grants from the Rosetrees Trust, James Tudor Foundation and the Above and Beyond Charitable Trust.

# Publications

The following work was published (or is currently under review) during my PhD:

**Matthew GL Williams;** Ngoc Jade Thai; Kate Liang *et al.* Functional Brain MRI Changes in the Limbic System in Patients with Suspected Myocardial Infarction and Non-Obstructive Coronary Arteries (MINOCA). Under review, *Circulation*, July 2022.

This paper is based on work presented in Chapter 4. Dr Matthew Williams was responsible for study design, data collection and analysis, data interpretation, drafting, finalising and submitting the manuscript.

**Matthew GL Williams;** Hinton, EC; Kate Liang *et al.* Reduced grey matter volume in patients with suspected myocardial infarction with non-obstructive infarction (MINOCA). In preparation, *Neuroimage - Clinical*, August 2022

This paper is based on work presented in Chapter 3. Dr Matthew Williams was responsible for study design, data collection and analysis, data interpretation, drafting, finalising and submitting the manuscript.

**Matthew GL Williams,** Kate Liang, Amardeep Dastidar *et al.* *The role of troponin in acute coronary syndrome with non-obstructive coronary arteries.* JACC: Cardiovascular Imaging 15 (2022) pp. 1578-1587  
<https://doi.org/10.1016/j.jcmg.2022.03.017>

This manuscript is based on a separate retrospective data set and the results are not featured in this dissertation. Dr Matthew Williams contributed significantly to data collection (extension of a pre-existing database). He was entirely responsible for study concept, study design, data analysis, data interpretation, drafting, finalising and submitting the manuscript.

**Matthew GL Williams**; Amardeep Dastidar; Kate Liang et al “*Sex differences in myocardial infarction with non-obstructive coronary arteries (MINOCA): presentation and outcome*”. Under review *IJC* August 2022

This manuscript is based on a separate retrospective data set and the results are not featured in this dissertation. Dr Matthew Williams contributed significantly to study design and data collection (extension of a pre-existing database). He was entirely responsible for data analysis, data interpretation, drafting, finalising and submitting the manuscript.

Ahmed Y El-Medany; Gui Rego; **Matthew Williams**; Stephen Lyen; Mark Turner. Multimodality imaging of Abernethy malformation. *Echocardiography*. Feb 16. 2022. DOI: 10.1111/echo.15324

Iwan Harries; Giovanni Biglino; Kerrie Ford; Martin Nelson; Gui Rego; Prashant Srivastava; **Matthew Williams** et al. Prospective Multiparametric CMR Characterization and MicroRNA Profiling of Anthracycline Cardiotoxicity: A Pilot Translational Study. Submitted to *IJC Heart and Vasculature* June 2022.

Kate Liang, **Matthew Williams**, Chiara Bucciarelli-Ducci. Cardiac MRI unmasks presumed embolic MI due to Patent Foramen Ovale. *European Heart Journal - Case Reports*, Volume 6, Issue 2, February 2022.  
<https://doi.org/10.1093/ehjcr/ytac029>

Nakou E, De Garate E, Liang K, **Williams M**, Pennell DJ, Bucciarelli-Ducci C. Imaging Findings of COVID-19-Related Cardiovascular Complications. *Cardiac Electrophysiology Clinics*. 2021 Oct 30. DOI: 10.1016/j.ccep.2021.10.008

Iwan Harries, Bostjan Berlot, Natasha ffrench-Constant, **Matthew Williams**, Kate Liang, Estefania De Garate, Anna Baritussio, Giovanni Biglino, Juan Carlos Plana, Chiara Bucciarelli-Ducci. Cardiovascular magnetic resonance characterisation of anthracycline cardiotoxicity in adults with normal left ventricular ejection fraction.

Int J Cardiol. 2021 Nov 15;343:180-186. doi: 10.1016/j.ijcard.2021.08.037. Epub 2021 Aug 26.

Kate Liang, Anna Baritussio, Alberto Palazzuoli, **Matthew Williams**, Estefania De Garate, Iwan Harries, Chiara Bucciarelli-Ducci. Cardiovascular Magnetic Resonance of Myocardial Fibrosis, Edema, and Infiltrates in Heart Failure. Heart Failure Clinics - (2020) doi:10.1016/j.hfc.2020.08.013

**Williams MGL**, Liang K and Bucciarelli-Ducci C. Transient Recurrent Takotsubo Cardiomyopathy Mimicking Apical Hypertrophic Cardiomyopathy. Eur Heart J Cardiovasc Imaging. 2021 May 10;22(6):e72. doi: 10.1093/ehjci/jeaa274.

**Williams MGL**, Thompson C, Johnson T, Bucciarelli-Ducci C. A Challenging and Unexpected Case of MINOCA Using Multimodality Imaging. J Am Coll Cardiol Case Reports. 2020. Aug, 2(10) 1564-1569

Iwan Harries, Kate Liang, **Matthew Williams** et al. Magnetic Resonance Imaging to Detect Cardiovascular Effects of Cancer Therapy J Am Coll Cardiol CardioOnc. 2020 Jun, 2 (2) 270-292.

Berlot, B; **Williams MGL**; Bucciarelli-Ducci, C – The Colours of Amphetamine-Induced Cardiomyopathy, Journal of Cardiovascular Medicine. 2020 May;21(5):396-397.



# Conference Abstracts

The following abstracts were presented during my PhD:

**Oral Poster Presentation** *“The heart brain interaction in acute coronary syndrome”*. European Society of Cardiology; August 2022.

**Poster Presentation** *“Sex and age differences in patients with a working diagnosis of myocardial infarction with non-obstructive coronary arteries (MINOCA): presentation and outcome”*. Presented at ESC Congress May 2021

**Poster Presentation** *“The role of peak troponin in patients with a working diagnosis of myocardial infarction with non-obstructive coronary arteries (MINOCA)”*. Presented at ESC Congress 2021

**Poster Presentation** *“Sex and age differences in patients with a working diagnosis of myocardial infarction with non-obstructive coronary arteries (MINOCA): presentation and outcome”*. Presented at EuroCMR Congress May 2021

**Poster Presentation** *“The role of peak troponin in patients with a working diagnosis of myocardial infarction with non-obstructive coronary arteries (MINOCA)”*. Presented at EuroCMR Congress 2021

**Poster Presentation** *“Sex differences in MINOCA: presentation and outcome”*. Accepted at Society of Cardiovascular Magnetic Resonance (SCMR) Scientific Sessions 2021.

**Poster Presentation** *“Transient Recurrent Takotsubo Cardiomyopathy Mimicking Apical Hypertrophic Cardiomyopathy”*. Accepted at Society of Cardiovascular Magnetic Resonance (SCMR) Scientific Sessions 2021.

**Poster Presentation,** *“Reduced orbitofrontal grey matter volume in myocardial infarction with non-obstructive coronary arteries (MINOCA)”*. Presented at ESC Congress: The Digital Experience. August 2020.

**Oral Presentation,** *“The Incremental Role of CMR in MINOCA”*. Special Research Institute Meeting November 2019.

**Poster Presentation,** *“An unexpected outpouching in an unexpected place”*. EuroCMR Congress 2019

**Poster Presentation,** *“Acute cocaine myocarditis, cardiac arrest and beyond”* EuroCMR Congress 2019

# Table of Contents

<b>CHAPTER 1</b>	<b>INTRODUCTION .....</b>	<b>1</b>
1.1	MINOCA .....	1
1.2	CMR IN MINOCA.....	3
1.2.1	CMR Validation in MINOCA .....	5
1.3	BRAIN MRI FOR THE CARDIOLOGIST .....	9
1.3.1	Anatomical Imaging .....	9
1.3.2	Functional Brain imaging.....	10
1.3.3	Summary .....	14
1.4	THE HEART-BRAIN INTERACTION IN MINOCA.....	14
1.4.1	Why is it important?.....	14
1.4.2	The Autonomic Nervous System .....	15
1.5	BRAIN-HEART INTERACTION .....	18
1.5.1	Myocardial Infarction .....	18
1.5.2	Takotsubo Syndrome .....	20
1.5.3	Depression and anxiety .....	25
1.6	UNANSWERED QUESTIONS.....	26
1.7	STUDY AIMS, OBJECTIVES AND HYPOTHESES .....	28
1.7.1	Aims.....	28
1.7.2	Objectives and hypotheses .....	28
1.8	CONCLUSIONS .....	31
<b>CHAPTER 2</b>	<b>METHODS.....</b>	<b>32</b>
2.1	STUDY DESIGN.....	32
2.2	STUDY REGISTRATION .....	32
2.3	RESEARCH TEAM .....	32
2.4	PATIENT AND PUBLIC INVOLVEMENT .....	33
2.5	RECRUITMENT OF MINOCA PATIENTS .....	33
2.5.1	Inclusion criteria .....	33
2.5.2	Exclusion Criteria .....	34
2.6	RECRUITMENT OF CONTROL PATIENTS .....	35
2.6.1	STEMI Patients.....	35
2.6.2	Healthy Volunteers .....	35
2.7	SAMPLE SIZE .....	35
2.8	OUTCOMES.....	36
2.9	STUDY SCHEMA .....	36

2.10	STUDY VISITS.....	37
2.10.1	<i>MINOCA Participants</i> .....	37
2.10.2	<i>STEMI Control participants</i> .....	39
2.10.3	<i>Healthy Volunteers</i> .....	39
2.11	STUDY PROTOCOLS.....	39
2.11.1	<i>Clinical History</i> .....	40
2.11.2	<i>Bloods</i> .....	40
2.11.3	<i>Electrocardiogram</i> .....	40
2.11.4	<i>Echocardiography</i> .....	40
2.11.5	<i>Questionnaires</i> .....	40
2.11.6	<i>CMR</i> .....	42
2.11.7	<i>Brain MRI</i> .....	44
2.11.8	<i>Follow up</i> .....	46
2.12	DATA ANALYSIS .....	46
2.12.1	<i>CMR Analysis</i> .....	46
2.12.2	<i>Brain analysis</i> .....	50
2.12.3	<i>Plan of Statistical analysis</i> .....	56
<b>CHAPTER 3</b>	<b>NOVEL INSIGHTS INTO BRAIN ANATOMICAL CHANGES IN MINOCA.....</b>	<b>57</b>
3.1	INTRODUCTION.....	57
3.2	METHODS .....	59
3.2.1	<i>MRI protocols</i> .....	60
3.2.2	<i>Voxel-based Morphometry</i> .....	61
3.2.3	<i>Limitations of VBM</i> .....	63
3.2.4	<i>Statistical Analysis</i> .....	63
3.3	RESULTS.....	64
3.3.1	<i>Study participants</i> .....	64
3.3.2	<i>Anatomical brain changes</i> .....	68
3.3.3	<i>Regression Analysis</i> .....	72
3.4	DISCUSSION .....	74
3.4.1	<i>Anatomical Differences</i> .....	74
3.4.2	<i>Relationship between brain volume and psychological and cardiac variables</i> .....	77
3.4.3	<i>Takotsubo Syndrome Subgroup Analysis</i> .....	78
3.4.1	<i>Study participants</i> .....	79
3.4.2	<i>Study Limitations</i> .....	80
3.5	CONCLUSIONS .....	81
<b>CHAPTER 4</b>	<b>NOVEL INSIGHTS INTO ACUTE FUNCTIONAL BRAIN CHANGES IN MINOCA.....</b>	<b>82</b>
4.1	INTRODUCTION.....	82

4.1.1	<i>Default Mode Network</i> .....	82
4.1.2	<i>Sympathetic and Parasympathetic Networks</i> .....	83
4.1.3	<i>Salience Network</i> .....	83
4.1.4	<i>Central Executive Network</i> .....	83
4.1.5	<i>Network Measures</i> .....	83
4.1.6	<i>MINOCA</i> .....	84
4.1.7	<i>Hypotheses</i> .....	85
4.2	<b>METHODS</b> .....	86
4.2.1	<i>Brain MRI</i> .....	86
4.2.2	<i>Functional Data Analysis</i> .....	86
4.2.3	<i>Global Network Measures</i> .....	87
4.2.4	<i>Functional analysis using network-based statistics</i> .....	87
4.2.5	<i>Regions of Interest</i> .....	89
4.2.6	<i>Power calculation</i> .....	89
4.2.7	<i>Statistical Analysis</i> .....	89
4.3	<b>RESULTS</b> .....	90
4.3.1	<i>Characterisation of the study population</i> .....	90
4.3.2	<i>Psychological questionnaires</i> .....	91
4.3.3	<i>Global network measures</i> .....	92
4.3.4	<i>Global network measures and psychological questionnaires</i> .....	92
4.3.5	<i>Subgroup Analysis</i> .....	95
4.3.6	<i>Network connectivity analysis</i> .....	96
4.3.7	<i>Takotsubo syndrome</i> .....	99
4.3.8	<i>Correlation Between Variables and Functional Networks</i> .....	101
4.4	<b>DISCUSSION</b> .....	109
4.4.1	<i>Psychological Profiles</i> .....	110
4.4.2	<i>Network Measures</i> .....	111
4.4.3	<i>Network connectivity</i> .....	112
4.4.4	<i>Network Connectivity in TS</i> .....	114
4.4.5	<i>Relationship between network measures and clinical variables</i> .....	114
4.4.6	<i>Limitations</i> .....	117
4.5	<b>CONCLUSIONS</b> .....	117
<b>CHAPTER 5 LONGITUDINAL CHANGES FROM THE ACUTE TO THE CHRONIC PHASE IN GREY MATTER VOLUME AND FUNCTIONAL CONNECTIVITY IN MINOCA</b> .....		<b>119</b>
5.1	<b>INTRODUCTION</b> .....	119
5.1.1	<i>Aims and Hypotheses</i> .....	122
5.2	<b>METHODS</b> .....	123

5.2.1	<i>Overview</i>	123
5.2.2	<i>Voxel-based morphometry</i>	123
5.2.3	<i>Functional connectivity analysis</i>	124
5.2.4	<i>Statistical Analysis</i>	124
5.3	RESULTS	125
5.3.1	<i>Investigations</i>	127
5.3.2	<i>Anatomical Analysis</i>	128
5.3.3	<i>Subgroup Anatomical Analysis</i>	131
5.3.4	<i>Global Brain Measures</i>	132
5.3.5	<i>Functional connectivity Analysis</i>	132
5.3.6	<i>Subgroup Functional Analysis</i>	136
5.4	DISCUSSION	142
5.4.1	<i>Longitudinal psychological profiles</i>	143
5.4.2	<i>Longitudinal grey matter volume and functional connectivity differences</i>	143
5.4.3	<i>Global network measures</i>	149
5.4.4	<i>Study Limitations</i>	150
5.5	CONCLUSIONS	150
<b>CHAPTER 6</b>	<b>GENERAL DISCUSSION, FUTURE DIRECTIONS AND CONCLUSION</b>	<b>152</b>
6.1	GENERAL SUMMARY OF RESULTS	152
6.1.1	<i>MINOCA patients</i>	152
6.1.2	<i>Takotsubo syndrome patients</i>	153
6.2	SYNTHESIS OF THEMES	153
6.2.1	<i>Disruption of the autonomic and limbic systems in MINOCA patients</i>	153
6.2.2	<i>Disruption in the CEN in Takotsubo Syndrome</i>	155
6.3	CLINICAL IMPLICATIONS	156
6.4	FUTURE DIRECTIONS	156
6.5	CONCLUSION	158
<b>CHAPTER 7</b>	<b>REFERENCES</b>	<b>160</b>
<b>CHAPTER 8</b>	<b>APPENDICES</b>	<b>177</b>
8.1	APPENDIX A	177
8.2	APPENDIX B	182
8.3	APPENDIX C	184
8.4	APPENDIX D	211

# List of Figures

FIGURE 1 STUDY SCHEMA .....	38
FIGURE 2 EXAMPLE OF HOW THE BASAL SLICE WAS CONTOURED FOR THE LV AND RV WHERE BOTH ATRIAL AND VENTRICULAR MYOCARDIUM WAS PRESENT. ....	47
FIGURE 3 ILLUSTRATIVE EXAMPLES OF DIAGNOSES ON CMR .....	49
FIGURE 4 STUDY FLOW CHART.....	64
FIGURE 5 BRAIN ACTIVATION MAP SHOWING REGION OF INCREASED GREY MATTER VOLUME IN MINOCA PATIENTS COMPARED TO HEALTHY CONTROLS .....	69
FIGURE 6 BRAIN ACTIVATION MAP SHOWING REGIONS OF REDUCED GREY MATTER VOLUME IN MINOCA PATIENTS COMPARED TO HEALTHY CONTROLS .....	69
FIGURE 7 BRAIN ACTIVATION MAP SHOWING REGION OF REDUCED GREY MATTER VOLUME IN TS PATIENTS COMPARED TO HEALTHY CONTROLS .....	72
FIGURE 8 STUDY FLOW CHART.....	91
FIGURE 9 BAR CHART DEMONSTRATING RESULTS OF PSYCHOLOGICAL QUESTIONNAIRES IN EACH GROUP .....	92
FIGURE 10A BAR CHART DEMONSTRATING NETWORK MEASURES BY ANXIETY, DEPRESSION AND STRESS SCORES IN MINOCA PATIENTS; FIGURE 10B TABLE SHOWING VALUES OF GLOBAL NETWORK MEASURES BY GROUP IN MINOCA PATIENTS, INCLUDING GLS-CMR. ....	94
FIGURE 11 BAR CHART DEMONSTRATING NETWORK MEASURES BY TS AND CONTROL GROUPS. ....	96
FIGURE 12 SUBNETWORKS WITH INCREASED FUNCTIONAL CONNECTIVITY IN PATIENTS WITH MINOCA COMPARED TO HEALTHY CONTROLS IN THE DEFAULT MODE NETWORK.....	97
FIGURE 13 SUBNETWORKS WITH REDUCED FUNCTIONAL CONNECTIVITY IN PATIENTS WITH MINOCA COMPARED TO HEALTHY CONTROLS (A) AND STEMI CONTROLS (B) IN THE CENTRAL EXECUTIVE NETWORK. ....	98
FIGURE 14 SUBNETWORKS WITH REDUCED FUNCTIONAL CONNECTIVITY IN PATIENTS WITH TS COMPARED TO HEALTHY CONTROLS (A) AND STEMI CONTROLS (B) IN THE CENTRAL EXECUTIVE NETWORK. ....	100
FIGURE 15 SUBNETWORKS IN MINOCA PATIENTS WITH A NEGATIVE CORRELATION WITH ANXIETY SCORE (A) AND WITH STRESS SCORES (B) IN THE SYMPATHETIC NETWORK. ....	102
FIGURE 16 SUBNETWORKS IN MINOCA PATIENTS WITH A NEGATIVE CORRELATION WITH STRESS SCORE IN THE PARASYMPATHETIC NETWORK.....	104
FIGURE 17 SUBNETWORKS IN MINOCA PATIENTS WITH A NEGATIVE CORRELATION WITH ANXIETY SCORE IN THE DMN.....	105
FIGURE 18 SUBNETWORKS IN MINOCA PATIENTS WITH A NEGATIVE CORRELATION WITH STRESS SCORE IN THE DMN. ....	106
FIGURE 19 SUBNETWORKS IN MINOCA PATIENTS WITH A NEGATIVE CORRELATION WITH PERCEIVED STRESS SCORE IN THE SALIENCE NETWORK.....	107

FIGURE 20 SUBNETWORKS IN MINOCA PATIENTS WITH A NEGATIVE CORRELATION WITH ANXIETY SCORE (A) AND GLS-CMR (B) IN THE CEN. ....	108
FIGURE 21 STUDY FLOW CHART .....	126
FIGURE 22 BEFORE AND AFTER PLOT SHOWING CHANGE IN PSYCHOLOGICAL SCORES AT EACH STUDY VISIT. ....	128
FIGURE 32 BRAIN ACTIVATION MAP SHOWING GREY MATTER REGIONS IN MINOCA PATIENTS DEMONSTRATING SIGNIFICANTLY INCREASED VOLUME IN THE CHRONIC PHASE COMPARED TO THE ACUTE PHASE. ....	129
FIGURE 24 BRAIN ACTIVATION MAP SHOWING GREY MATTER REGIONS IN MINOCA PATIENTS DEMONSTRATING SIGNIFICANTLY REDUCED VOLUME IN THE CHRONIC PHASE COMPARED TO THE ACUTE PHASE. ....	130
FIGURE 25 REGIONS OF THE BRAIN WITH REDUCED GREY MATTER VOLUME IN CHRONIC MINOCA PATIENTS VERSUS HEALTHY CONTROL PATIENTS.....	131
FIGURE 26 SUBNETWORKS WITH GREATER FUNCTIONAL CONNECTIVITY IN CHRONIC PHASE MINOCA PATIENTS COMPARED TO HEALTHY CONTROLS IN THE DEFAULT MODE NETWORK. ....	134
FIGURE 27 SUBNETWORKS WITH LOWER FUNCTIONAL CONNECTIVITY IN CHRONIC PHASE MINOCA PATIENTS COMPARED TO HEALTHY CONTROLS IN THE CENTRAL EXECUTIVE NETWORK. ....	135
FIGURE 28 SUBNETWORKS WITH REDUCED FUNCTIONAL CONNECTIVITY IN ACUTE PHASE TS PATIENTS COMPARED TO CHRONIC PHASE TS PATIENTS ON WHOLE BRAIN CONNECTIVITY ANALYSIS. ....	137
FIGURE 29 SUBNETWORKS WITH GREATER FUNCTIONAL CONNECTIVITY IN CHRONIC PHASE TS PATIENTS COMPARED TO HEALTHY CONTROLS IN THE CENTRAL EXECUTIVE NETWORK.....	138
FIGURE 30 SUBNETWORKS WITH LOWER FUNCTIONAL CONNECTIVITY IN CHRONIC PHASE TS PATIENTS COMPARED TO HEALTHY CONTROLS IN THE CENTRAL EXECUTIVE NETWORK.....	139
FIGURE 31 SUBNETWORKS WITH LOWER FUNCTIONAL CONNECTIVITY IN CHRONIC PHASE TS PATIENTS COMPARED TO STEMI CONTROLS IN THE CENTRAL EXECUTIVE NETWORK. ....	140



# List of Tables

TABLE 1 MINOCA DIAGNOSTIC CRITERIA .....	2
TABLE 2 LAKE LOUISE CRITERIA .....	6
TABLE 3 GRAPH THEORY TERMINOLOGY IN THE CONTEXT OF fMRI.....	12
TABLE 4 BREAKDOWN OF STUDY VISITS FOR MINOCA PARTICIPANTS.....	37
TABLE 5 BREAKDOWN OF STUDY VISITS FOR STEMI CONTROL PARTICIPANTS .....	39
TABLE 6 BREAKDOWN OF STUDY VISIT FOR HEALTHY VOLUNTEERS .....	39
TABLE 7 CMR SEQUENCE PARAMETERS .....	44
TABLE 8 REGION OF INTEREST COORDINATES FOR THE DEFAULT MODE NETWORK BASED ON THE MONTREAL NEUROLOGICAL INSTITUTE COORDINATE SYSTEM.....	53
TABLE 9 MNI COORDINATES FOR NODES ASSOCIATED WITH SYMPATHETIC AND PARASYMPATHETIC REGULATION. ..	54
TABLE 10 MNI COORDINATES FOR THE SALIENCE NETWORK. ....	55
TABLE 11 MNI COORDINATES USED FOR THE CENTRAL EXECUTIVE NETWORK ANALYSIS .....	55
TABLE 12 STUDY GROUP BASELINE DEMOGRAPHICS .....	65
TABLE 13 RESULTS OF THE PSYCHOLOGICAL QUESTIONNAIRES .....	67
TABLE 14 CMR FINDINGS .....	68
TABLE 15 DEMOGRAPHICS AND RESULTS BY SUBGROUPS.....	70
TABLE 16 REGIONS WHERE GREY MATTER VOLUME NEGATIVELY CORRELATES WITH PRIOR HISTORY OF MENTAL HEALTH DISEASE .....	72
TABLE 17 REGIONS OF THE BRAIN IN WHICH GREY MATTER VOLUME POSITIVELY CORRELATE WITH GLS .....	73
TABLE 18 SUMMARY OF PREVIOUS STUDIES EXAMINING GREY MATTER DIFFERENCES IN TS .....	79
TABLE 19 TABLE SHOWING GLOBAL NETWORK MEASURES BY GROUP .....	92
TABLE 20 GLOBAL NETWORK MEASURES BY MINOCA SUBGROUPS. ....	95
TABLE 21 SUMMARY TABLE SHOWING DIRECTION OF CORRELATION SEEN ON CORRELATION ANALYSIS BETWEEN VARIABLES AND NETWORKS IN EACH GROUP. ....	115
TABLE 22 DEMOGRAPHICS, INVESTIGATIONS, QUESTIONNAIRE AND CMR FINDINGS FOR THE DIFFERENT STUDY GROUPS. ....	127
TABLE 23 GLOBAL NETWORK MEASURES IN ACUTE AND CHRONIC PHASE MINOCA PATIENTS AND CONTROL PATIENTS .....	132
TABLE 24 TABLE ILLUSTRATING THE CHANGES IN CONNECTIVITY OVER TIME IN MINOCA VERSUS CONTROL PATIENTS .....	136
TABLE 25 TABLE ILLUSTRATING CHANGES IN FUNCTIONAL CONNECTIVITY FROM THE ACUTE TO CHRONIC PHASE COMPARED TO CONTROLS IN TS.....	141
TABLE 26 REGIONS WHERE GREY MATTER VOLUME NEGATIVELY CORRELATES WITH MMSE SCORE.....	182
TABLE 27 REGIONS OF THE BRAIN IN WHICH GREY MATTER VOLUME POSITIVELY CORRELATES WITH GLS IN STEMI PATIENTS.....	182

TABLE 28 REGIONS OF THE BRAIN IN WHICH GREY MATTER VOLUME POSITIVELY CORRELATE WITH LVEF IN HEALTHY CONTROLS PATIENTS.....	182
TABLE 29 TABLE DEMONSTRATING NETWORK MEASURES BY ANXIETY, DEPRESSION, STRESS AND GLS-CMR GROUPS IN STEMI CONTROL PATIENTS AND HEALTHY VOLUNTEERS. ....	184
TABLE 30 INCREASED CONNECTIVITY IN PATIENTS WITH MINOCA COMPARED TO HEALTHY CONTROLS IN THE DEFAULT MODE NETWORK AT TWO SET THRESHOLDS. ....	185
TABLE 31 REDUCED CONNECTIVITY IN PATIENTS WITH MINOCA COMPARED TO HEALTHY CONTROLS IN THE CENTRAL EXECUTIVE NETWORK AT TWO DIFFERENT SET THRESHOLDS. ....	185
TABLE 32 REDUCED CONNECTIVITY IN PATIENTS WITH MINOCA COMPARED TO STEMI CONTROLS IN THE CENTRAL EXECUTIVE NETWORK ....	186
TABLE 33 REDUCED CONNECTIVITY IN PATIENTS WITH TS COMPARED TO HEALTHY CONTROLS IN THE CENTRAL EXECUTIVE NETWORK. ....	187
TABLE 34 REDUCED CONNECTIVITY IN PATIENTS WITH TS COMPARED TO STEMI CONTROLS IN THE CENTRAL EXECUTIVE NETWORK. ....	188
TABLE 35 REDUCED CONNECTIVITY IN PATIENTS WITH TS COMPARED TO HEALTHY CONTROLS ON WHOLE BRAIN ANALYSIS. ....	189
TABLE 36 REDUCED CONNECTIVITY IN PATIENTS WITH TS COMPARED TO STEMI CONTROLS ON WHOLE BRAIN ANALYSIS. ....	190
TABLE 37 NETWORKS WITH A NEGATIVE CORRELATION BETWEEN CONNECTIVITY AND ANXIETY SCORES IN THE SYMPATHETIC NETWORK IN MINOCA PATIENTS. ....	191
TABLE 38 NETWORKS WITH A NEGATIVE CORRELATION BETWEEN CONNECTIVITY AND STRESS SCORES IN THE SYMPATHETIC NETWORK IN MINOCA PATIENTS. ....	192
TABLE 39 NETWORKS WITH A NEGATIVE CORRELATION BETWEEN CONNECTIVITY AND STRESS SCORES IN THE SYMPATHETIC NETWORK IN STEMI PATIENTS. ....	193
TABLE 40 NETWORKS WITH A NEGATIVE CORRELATION BETWEEN CONNECTIVITY AND STRESS SCORES IN THE PARASYMPATHETIC NETWORK IN MINOCA PATIENTS. ....	194
TABLE 41 NETWORKS WITH A POSITIVE CORRELATION BETWEEN CONNECTIVITY AND STRESS SCORES IN THE PARASYMPATHETIC NETWORK IN HEALTHY PATIENTS. ....	195
TABLE 42 NETWORKS WITH A NEGATIVE CORRELATION BETWEEN CONNECTIVITY AND ANXIETY SCORES IN THE DEFAULT MODE NETWORK IN MINOCA PATIENTS. ....	196
TABLE 43 NETWORKS WITH A NEGATIVE CORRELATION BETWEEN CONNECTIVITY AND PERCEIVED STRESS SCORES IN THE DEFAULT MODE NETWORK IN MINOCA PATIENTS.....	197
TABLE 44 NETWORKS WITH A POSITIVE CORRELATION BETWEEN CONNECTIVITY AND ANXIETY IN THE DEFAULT MODE NETWORK IN HEALTHY PATIENTS. ....	199
TABLE 45 NETWORKS WITH A POSITIVE CORRELATION BETWEEN CONNECTIVITY AND PERCEIVED STRESS SCORES IN THE DEFAULT MODE NETWORK IN HEALTHY PATIENTS.....	199
TABLE 46 NETWORKS WITH A NEGATIVE CORRELATION BETWEEN CONNECTIVITY AND PERCEIVED STRESS SCORES IN THE SALIENCE NETWORK IN MINOCA PATIENTS. ....	200

TABLE 47 NETWORKS WITH A NEGATIVE CORRELATION BETWEEN CONNECTIVITY AND ANXIETY SCORES IN THE CENTRAL EXECUTIVE NETWORK IN MINOCA PATIENTS. ....	201
TABLE 48 NETWORKS WITH A NEGATIVE CORRELATION BETWEEN CONNECTIVITY AND GLS-CMR IN THE CENTRAL EXECUTIVE NETWORK IN MINOCA PATIENTS. ....	202
TABLE 49 NETWORKS WITH A POSITIVE CORRELATION BETWEEN CONNECTIVITY AND GLS-CMR IN THE CENTRAL EXECUTIVE NETWORK IN HEALTHY PATIENTS.....	203
TABLE 50 NETWORKS WITH A NEGATIVE CORRELATION WITH ANXIETY SCORE IN MINOCA PATIENTS ON WHOLE BRAIN ANALYSIS.....	204
TABLE 51 NETWORKS WITH A NEGATIVE CORRELATION WITH PERCEIVED STRESS SCORE IN MINOCA PATIENTS ON WHOLE BRAIN ANALYSIS .....	207
TABLE 52 NETWORKS WITH A POSITIVE CORRELATION WITH ANXIETY SCORE IN HEALTHY PARTICIPANTS ON WHOLE BRAIN ANALYSIS .....	209
TABLE 53 REGIONS OF THE BRAIN IN MINOCA PATIENTS WITH <i>REDUCED</i> GREY MATTER VOLUME FROM THE ACUTE TO CHRONIC PHASE .....	211
TABLE 54 REGIONS OF THE BRAIN IN ACUTE MINOCA PATIENTS WITH INCREASED GREY MATTER VOLUME COMPARED TO CHRONIC MINOCA PATIENTS.....	211
TABLE 55 REGIONS OF THE BRAIN WITH REDUCED GREY MATTER VOLUME IN CHRONIC MINOCA PATIENTS VERSUS HEALTHY CONTROL PATIENTS. ....	213
TABLE 56 GREATER CONNECTIVITY IN PATIENTS WITH A PREVIOUS EPISODE OF MINOCA COMPARED TO HEALTHY CONTROLS IN THE DEFAULT MODE NETWORK. ....	213
TABLE 57 LOWER CONNECTIVITY IN PATIENTS WITH A PREVIOUS EPISODE OF MINOCA COMPARED TO HEALTHY CONTROLS IN THE CENTRAL EXECUTIVE NETWORK. ....	213
TABLE 58 GREATER CONNECTIVITY IN PATIENTS WITH A PREVIOUS EPISODE OF TS COMPARED TO HEALTHY CONTROLS IN THE CENTRAL EXECUTIVE NETWORK. ....	214
TABLE 59 LOWER CONNECTIVITY IN PATIENTS WITH A PREVIOUS EPISODE OF TS COMPARED TO HEALTHY CONTROLS IN THE CENTRAL EXECUTIVE NETWORK. ....	214
TABLE 60 LOWER CONNECTIVITY IN PATIENTS WITH A PREVIOUS EPISODE OF TS COMPARED TO PATIENTS WITH A PREVIOUS STEMI IN THE CENTRAL EXECUTIVE NETWORK. ....	214
TABLE 61 REDUCED CONNECTIVITY IN PATIENTS WITH AN ACUTE EPISODE TS COMPARED TO CHRONIC TS ON WHOLE BRAIN ANALYSIS.....	215

## Chapter 1 INTRODUCTION

---

Coronary heart disease is the leading cause of death worldwide. It was responsible for 200,000 hospital visits and 66,000 deaths in 2018 in the UK(1). Acute coronary syndrome (ACS) is a term that is frequently used in clinical practice and refers to a range of conditions initially attributable to acute myocardial ischaemia and/or infarction, usually due to a sudden reduction in coronary blood flow (2). Patients classically present with chest pain, electrocardiogram (ECG) changes and a dynamic change in a cardiac biomarker, usually cardiac troponin. The immediate clinical pathway is determined by the clinical history and ECG. Patients with acute chest pain and ST-segment elevation on the ECG are taken for primary percutaneous coronary intervention (PPCI)(3), and patients without ST-segment elevation are assessed and risk stratified prior to potential revascularisation(4). The most common mechanism for an ACS is plaque rupture with a subsequent sudden reduction in calibre (or occlusion) of the culprit vessel. However around 5-10% of patients who present with an ACS are found to have non-obstructive coronary arteries at invasive coronary angiography(5-8). The majority of these patients have an alternative explanation for their presentation (e.g. pulmonary embolus, cardiomyopathy, sepsis, arrhythmia, myo/pericarditis) but in the absence of another specific cause for the presentation, the European Society of Cardiology (ESC) deem these patients as having a myocardial infarction with non-obstructive coronary arteries (MINOCA)(9).

### 1.1 MINOCA

DeWood's landmark studies in the 1980s suggested that around 10% of patients presenting with an acute coronary syndrome had non-obstructive disease on angiography(10, 11). Since then it has evolved from myocardial infarction with normal coronaries (MINC)(12) to myocardial infarction with normal

coronary arteries (MINCA)(13) and ultimately MINOCA. The ESC were the first to formally recognise this working diagnosis in 2017 and offer an investigative strategy (9). Recently the American Heart Association (AHA) (14) have published a scientific statement which takes into account the updated 4<sup>th</sup> Universal definition of myocardial infarction (15). This latest definition tries to separate out ‘ischaemic’ (plaque rupture, supply-demand mismatch etc.) from ‘non-ischaemic’ (myocarditis, takotsubo syndrome (TS) etc.) aetiologies. The scientific statement would only classify patients with an ‘ischaemic’ basis for their presentation as having MINOCA. Their diagnostic criteria are shown in Table 1.

Table 1 MINOCA diagnostic criteria

cTn indicates cardiac troponin; and MINOCA, myocardial infarction in the absence of obstructive coronary artery disease. \*Note that additional review of the angiogram may be required to ensure the absence of obstructive disease. Adapted from Tamas-Holland et al 2019(14).

<b>The diagnosis of MINOCA is made in patients with acute myocardial infarction that fulfills the following criteria:</b>
<b>1. Acute myocardial infarction (modified from the “Fourth Universal Definition of Myocardial Infarction” Criteria)</b>
<i>Detection of a rise or fall of cTn with at least 1 value above the 99<sup>th</sup> percentile upper reference limit</i>
<b>and</b>
<i>Corroborative clinical evidence of infarction evidenced by at least one of the following:</i>
<ul style="list-style-type: none"> <li><i>a) Symptoms of myocardial ischemia</i></li> <li><i>b) New ischemic electrocardiographic changes</i></li> <li><i>c) Development of pathological Q waves</i></li> <li><i>d) Imaging evidence of new loss of viable myocardium or new</i></li> <li><i>e) regional wall motion abnormality in a pattern consistent with an ischemic cause</i></li> <li><i>f) Identification of a coronary thrombus by angiography or autopsy</i></li> </ul>
<b>2. Non-obstructive coronary arteries on angiography:</b>
<i>Defined as the absence of obstructive disease on angiography (ie, no coronary artery stenosis ≥50%) in any major epicardial vessel*</i>
<b>3. No specific alternate diagnosis for the clinical presentation:</b>
<i>Alternate diagnoses include but are not limited to nonischemic causes such as sepsis, pulmonary embolism, and myocarditis</i>

Thus, an extensive search to exclude non-ischaemic causes is recommended prior to diagnosing MINOCA including, amongst others, cardiac magnetic resonance

imaging (CMR), intravascular ultrasound (IVUS), optical coherence tomography (OCT) and coronary functional assessment(14)

However, as the definition of MINOCA has evolved, and not all centres have access to recommended investigations (e.g. CMR, OCT), the cohort of patients with MINOCA in the literature is extremely heterogenous and will include a significant proportion of patients who do not have an ischaemic basis for their presentation, and indeed have myocarditis or TS. The vast majority of the existing literature is in line with the 2017 ESC definition of MINOCA(9) which is a “working diagnosis analogous to heart failure” with the aim of prompting further evaluation. Patients with a clear alternate diagnosis at presentation are excluded based on the clinical context (e.g. a clear diagnosis of myocarditis in a 21 year old man with a preceding viral illness presenting with position chest pain, ST elevation on the ECG, elevated troponin and normal coronary arteries). However, the clinical context is not always clear and therefore the ESC definition of MINOCA encompasses non-ischaemic and ischaemic causes. This is a clinically much more practical definition than the AHA version as the working diagnosis can be applied immediately after angiography rather than several days/weeks down the line after all comprehensive investigations to exclude a non-ischaemic aetiology have been completed. As the 2019 definition was not yet published at the time of the protocol design and for the reasons outlined above, this study will use the 2017 ESC definition. For comparison purposes for this study, if the AHA definition was used, it would mean that only patients with a myocardial infarction on the CMR would be classified as MINOCA.

### *1.2 CMR IN MINOCA*

Once a diagnosis of MINOCA has been made this should trigger a search for the underlying cause. Failure to do so may result in “inadequate and inappropriate” therapy(3). Clinical acumen is not enough to make a diagnosis and the presence of non-obstructive coronary arteries does not mean the patient has not had a myocardial infarction. CMR has evolved as an excellent test for the investigation of these patients and is an ESC class IB recommendation in the work-up of

MINOCA(4). This is highlighted by two papers. Firstly, Pathik *et al* showed only a 52% concordance between a panel of consultants blinded to the CMR result and the subsequent CMR diagnosis (16). Secondly, Dastidar *et al* showed CMR led to a new diagnosis in 54% and a change in management in 41% (17) compared to clinical acumen alone. The diagnosis that the consultant panel most struggled with was acute myocardial infarction which, in terms of prognosis and therapeutics, is the most important diagnosis to make.

CMR has emerged as the preferred imaging modality in MINOCA due to its ability to accurately identify regional wall motion abnormalities and presence and pattern of oedema and myocardial scar/fibrosis. Newer techniques such as feature tracking, T1 and T2 mapping sequences can be added to allow more detailed diagnostics and increase sensitivity and specificity(18-20). CMR can establish the diagnosis in around 79% of patients when performed within 6 weeks of the MI. Typical causes identified included myocarditis (38%), myocardial infarction (24%) and TS (16%) (8) but the frequency of each vary with the inclusion criteria of each study. Determining a precise diagnosis allows treatment of the underlying condition. It could also lead to appropriate changes in clinical management, such as stopping (or starting) anti-ischaemic therapies, initiating subsequent further diagnostic investigations and altering follow up arrangements. A cardiac MRI led diagnosis can modify medical therapy in 32% of patients when compared to standard care (21). A robust diagnosis can also allow for more specific risk stratification and prognostication and can identify complications which can be missed by other imaging modalities, notwithstanding the psychological benefit to the patient of having a 'diagnosis'.

The ESC does not mandate when CMR should be performed in MINOCA, however there may be significant benefit in performing CMR early due to a fall in the diagnostic pick up rate from 82% to 54% when CMR was performed more than 2 weeks after the myocardial infarction (17, 22). There is also a more general trend of higher diagnostic yield when MRI is performed early – for example 77-87% diagnostic yield when CMR performed within 1-6 days (16, 21, 23) compared

to a yield of 65% when performed up to 3 months after presentation (24). This appears to be driven by a decrease in the rate of diagnosis of TS and acute myocarditis. Furthermore, in a sub-group analysis of patients with myocarditis, high T2 signal (indicating oedema) and gadolinium enhancement (representing scar/fibrosis) was detected in 81% and 100% of patients with suspected myocarditis respectively if the scan was performed within 2 weeks, but only 11% and 76% respectively of scans performed after this time (25).

### 1.2.1 CMR VALIDATION IN MINOCA

The three most common aetiologies for MINOCA and the expected CMR findings will be described below.

#### 1.2.1.1 Myocardial Infarction

This is a broad cohort of patients who have CMR evidence of subendocardial or transmural late gadolinium enhancement (LGE) in a typical coronary artery territory distribution (**Error! Reference source not found.**). The aetiology may represent plaque disruption(26, 27), epicardial coronary vasospasm(28), coronary microvascular dysfunction, coronary embolus/thrombosis, spontaneous coronary artery dissection or supply-demand mismatch(14).

The presence of myocardial oedema allows timing of the infarct as during acute myocardial ischaemia, myocardial oedema can be delineated with T2-weighted imaging. This cohort is important to identify because this diagnosis has important diagnostic and therapeutic implications as they are usually managed with antiplatelet medications and secondary prevention therapies.

#### 1.2.1.2 Myocarditis

Myocarditis is simply inflammation of the myocardial tissue. The most common causes of myocarditis are viral infection, immune-mediated diseases, endocrine disorders, drugs and toxins. It can be identified on CMR using the Lake-Louise criteria to examine the presence and pattern of late gadolinium



distribution, hyperaemia and oedema (Table 2) (29). The Lake Louise criteria were subsequently updated in 2018 (30) to include the use of myocardial T1 and T2 relaxation times as diagnostic criteria. As our study largely did not include mapping as originally planned due to a scanner software malfunction 2 months into recruitment, the original Lake Louise criteria are shown below and were used in our study.

Table 2 Lake Louise Criteria

<b>In the setting of clinically suspected myocarditis, CMR findings are consistent with myocardial inflammation, if at least 2 of the following criteria are present:</b>	
<ul style="list-style-type: none"> <li>• <i>Regional or global signal intensity increase of <math>\geq 2.0</math> on T2 weighted images</i></li> <li>• <i>Increased global myocardial early gadolinium enhancement ratio between myocardium and skeletal muscle of <math>\geq 4.0</math> in gadolinium-enhanced T1-weighted images.</i></li> <li>• <i>There is at least 1 focal lesion with nonischemic regional distribution in inversion recovery-prepared gadolinium-enhanced T1-weighted images ("late gadolinium enhancement").</i></li> </ul>	
<b>Supportive Criteria</b>	
<ul style="list-style-type: none"> <li>• <i>Pericardial effusion on cine CMR images.</i></li> <li>• <i>Systolic LV wall motion abnormality in cine CMR images.</i></li> </ul>	

The pattern of late gadolinium enhancement is typically epicardial, in the mid-wall, patchy or transmural. Oedema, appearing as an area of high-signal intensity in T2-weighted images, can be regional or global. The 2013 ESC Task Force on myocarditis (31) recommend CMR in the evaluation of myocarditis.

Many studies have validated the diagnostic accuracy of cardiac MRI compared to the historical 'gold-standard' of endomyocardial biopsy and clinical criteria. There is good diagnostic accuracy of CMR of 79% in acute myocarditis, with a sensitivity and specificity of 81% and 71% respectively using T1 weighted imaging before and after contrast and T2 imaging (32, 33). In acute myocarditis (which will comprise all the patients in this study) diagnostic sensitivity and

specificity of the Lake Louise criteria against clinical parameters has been reported at between 82%-76% and 98%-96% respectively (18, 34). Novel techniques, such as tissue characterisation techniques and extra-cellular volume (ECV) quantification further improve the diagnostic accuracy (18, 35-38). These new techniques have also been successfully validated against endomyocardial biopsy(38).

Finally, global longitudinal strain analysis may give further diagnostic benefit in acute myocarditis as strain measurement by feature tracking has been shown to be impaired despite normal ejection fraction (39). Feature tracking using CMR can be done offline using the existing cine images. It relies on measurement of the degree of myocardial deformation from its original length to its final length, expressed as a percentage (i.e. the longitudinal shortening of the ventricle from base to apex during the cardiac cycle)(40). By combining strain, native T1 and T2 mapping techniques diagnostic accuracy could be increased to 96% without the need for contrast (18). Combining strain and T2 mapping was also shown to be a highly accurate way of diagnosis acute myocarditis (41).

The evolution of myocarditis on CMR was first shown by Friedrich in 1998. Using contrast enhanced T1 weighted images, the inflammatory process appeared to spread from a focal area to a more disseminated process over the first 2 weeks after disease onset (42). More recently many studies have shown the gradual reduction in oedema with time. For example, repeat CMR at a median time of 76 days following presentation showed T2 signal in only 39% of patients compared to 84% at presentation (25). In another study, 86% of myocarditis patients showed complete resolution of oedema at 106 days with 36% showing late gadolinium, whereas at 350 days there was no oedema and only 1 patient had late gadolinium (23). Similar results have been shown using more novel techniques; native T1, T2 and ECV volumes decrease from the acute stage over 3-12 months (43). This again highlights the diagnostic value in early CMR imaging.

### 1.2.1.3 Takotsubo Syndrome

TS is characterised by acute, reversible left ventricular (LV) dysfunction in the absence of significant explanatory coronary disease and is usually triggered by acute emotional or physical stress. It is usually associated with acute ECG changes and cardiac troponin elevation. Formal diagnostic criteria have been proposed (International Takotsubo Diagnostic Criteria) (44). CMR will typically demonstrate a combination of regional wall motion abnormalities (RWMAs) on cine imaging, high T2 signal (oedema), and the absence of late gadolinium enhancement (myocardial scar/fibrosis) (45).

The cause is not precisely understood and is likely to be multifactorial (46). There is a heart-brain connection which contributes to the pathophysiology of TS as will be discussed later. The condition usually affects post-menopausal women but almost anyone can be affected. CMR has added value over echocardiography due to its higher spatial resolution, 3D image acquisition and myocardial tissue characterisation. It is also better at identifying complications (such as thrombi which are seen in 2-8% of cases) and assessing the right ventricle which is involved up to 48% of the time (47). CMR allows detection of myocardial oedema and myocardial fibrosis (not usually present in TS – although a small focal or patchy area can be seen using a threshold of 3 SDs above mean signal intensity (45)) allowing differentiation between myocarditis and ischaemic causes. It is thought up to 7% of patients who are presumed to have had an MI actually have TS (48). Sequential scans allow accurate documentation of the resolution of LV systolic impairment and regional wall motion abnormalities which is one of the key diagnostic criteria. The ventricular function usually returns to normal by 12 weeks (49). Urgent inpatient scanning is essential as recovery of function can be faster; CMR at presentation showed significantly reduced ejection fraction ( $37\% \pm 6\%$ ) but by discharge this had normalised ( $58\% \pm 6\%$ ) (50) meaning this important diagnosis could be missed if imaging is delayed. The ESC taskforce recommend scanning all patients with TS within 7 days (49). However, novel CMR techniques

have suggested that TS is not truly fully reversible. 12 months after presentation with TS there are still parameters of reduced global longitudinal strain and elevated whole heart native T1 values(51).

The primary aim of this thesis is to address the heart brain interaction in patients presenting with MINOCA and so to facilitate that I will discuss the theory behind brain imaging before going on to discuss the current literature on the heart-brain interaction.

### *1.3 BRAIN MRI FOR THE CARDIOLOGIST*

Brain MRI, including functional brain MRI (fMRI), is a widely used, non-invasive method to study the anatomy and function of the brain in health and pathology. Analysis of the brain in our study will focus on structural (anatomical) analysis or functional (connectivity) analysis. The methods for conducting the analyses described below will be described in full in chapter 2.

#### *1.3.1 ANATOMICAL IMAGING*

Disease processes in the brain can result in cell loss which manifests as atrophy. Automated techniques to quantify these changes have been developed. Voxel-based morphometry (VBM) is a key technique which is applied using parametric mapping by neuroscientists to assess macroscopic grey matter differences between individuals (see Chapter 2 for the methods). It allows recognition of changes in anatomy before overt cortical atrophy is observed. Very simply, it requires T1-weighted volumetric MRI scans of the brain and after pre-processing it performs t-tests across all voxels in the brain to identify differences in grey matter volume between groups. Regression analysis can be applied across all the voxels to assess variables which correlate with grey matter volume. This method has been applied to a number of pathologies (including neurodegenerative disease(52), schizophrenia(53) and movement disorders(54), with good correlation with previous methods of manual measurement(55, 56). For the purposes of our study, we investigated whether patients with MINOCA had grey matter loss which predisposed them to developing this condition.

### 1.3.2 *FUNCTIONAL BRAIN IMAGING*

A simple understanding of the image acquisition process and the commonly used terminology is helpful for any cardiologist who is hoping to understand the literature in this area.

#### 1.3.2.1 Technique

Functional magnetic resonance imaging (fMRI) utilises the magnetic properties of haemoglobin to look at variations in brain metabolism over time in different anatomical regions. Areas of the brain that are metabolically active utilise energy in the form of adenosine triphosphate (ATP) and this changes the regional cerebral metabolic rate of oxygen. Fully oxygenated haemoglobin signal is indistinguishable from brain tissue signal, but deoxygenated haemoglobin is strongly paramagnetic. Specific blood oxygen level dependent (BOLD) sequences can detect these changes in signal and are used to infer metabolic activity in a region. fMRI can be used to assess task-induced regional changes or simply used to evaluate resting state connectivity(57). Resting state analysis focuses on spontaneous variations in BOLD signal while at rest which reflects the intrinsic activity of the brain.

fMRI can be performed on 1.5- or 3-Tesla scanners, take minutes to acquire, are well tolerated by patients and do not require contrast administration which means they are relatively cheap and are possible on almost all MRI scanners.

#### 1.3.2.2 Graph Theory

Once the data has been acquired it needs to be meaningfully and reproducibly interpreted. Pre-processing occurs before statistical analysis can begin (see methods). The mathematical study of networks, otherwise known as graph theory, forms the basis of one of the most common methods of complex network analysis. The founding principle of graph theory is that the behaviour of very large, complex systems (such as the brain, or social networks) share macroscopic patterns despite profound microscopic differences in structure and

interaction(58). These patterns can be quantified and studied. Examples of macroscopic behaviours include ‘small worldness’, ‘modularity’ and ‘centrality’ (Table 3).

The brain is of course extremely complex but for the purposes of network analysis it can be broken down into neurones or brain regions (*nodes*) which are connected to each other via functional or anatomical connections (*edges*). Anatomical connections are typically synapses or axonal projections between two nodes. Functional connections represent two nodes which may not be anatomically connected but demonstrate temporal correlations in their BOLD activity which infers they are connected. Edges can be weighted whereby the edge carries information on the strength of the association, or unweighted, whereby there simply is or is not a connection. Edges can also be directed, meaning one node influences another node but not the other way around, or undirected, where there is no information on the directionality of the connection. Following statistical analysis, adjacency matrices can be created and are presented as tables with rows and columns representing nodes and the matrix representing the edges(59). These matrices can then be compared between groups (i.e. exposed or unexposed groups) or longitudinally (paired data analysed over time). To put this into a more digestible context using the social network example, nodes represent people and edges represent friendships. Network measures represent quantitative measurements of how the social network functions.

### 1.3.2.3 Network Measures

Network measures are the statistical representations of brain networks which allow us to quantify global and regional networks (58). Table 3 summarises the key network measures. Comparisons of these network measures across populations or diseases may highlight differences in connectivity in different brain pathologies(60).

Table 3 Graph theory terminology in the context of fMRI

Term	Definition	Function
<b>Node degree</b>	The number of connections an individual node has	A measure of centrality. The most fundamental of network measures. Reflects the importance of a node in a network.
<b>Degree distribution</b>	The degrees of all the network's nodes	Marker of network development and resilience.
<b>Path length</b>	The minimum number of edges between nodes	Efficiency is inversely related to path length.
<b>Segregation</b>	The ability for specialised processing to occur within densely interconnected groups of brain regions.	A measure of the presence of clusters or modules within the network.
<b>Integration</b>	The ability to rapidly combine specialised information from distributed brain regions.	A measure of the ease at which distinct brain regions communicate – dependent on paths. Shorter paths suggest greater integration.
<b>Clustering coefficient</b>	A measure of the number of connections between nearest neighbours of a node as a proportion of the maximum number of possible connections.	Random networks demonstrate low average clustering whereas complex networks have high clustering (local efficiency and high resilience).
<b>Hub</b>	A node with a high degree	Nodes with high degrees are essential for efficient communication.
<b>Centrality</b>	A measure of how many of the shortest path between other node pairs in the network pass through it.	High centrality is key to efficient communication
<b>Resilience</b>	A measure of the structural integrity of the network following deletion of nodes or edges.	A measure of how compromised a network becomes with disruption (e.g. an insult such as Alzheimer's or a stroke).
<b>Global efficiency</b>	The average inverse shortest path length	Measure of efficiency and integration. Short mean path lengths have a high global efficiency and suggests high integration.
<b>Modularity</b>	The degree to which nodes are connected <i>within</i> groups and not <i>between</i> groups.	A measure of segregation.
<b>Small world propensity</b>	A measure of the extent a network has small world characteristics.	Networks with small world characteristics have high local clustering amongst nodes but short path lengths due to the presence of long-range paths to distant nodes. These networks are highly segregated and integrated.

Our study will focus on three of the key network measures, global efficiency (as this can be applied on unconnected functional networks like ours), modularity and small world propensity.

### 1.3.2.4 Atlases

Automated anatomical labelling of brain activations (AAL) is a commonly used method to parcellate the brain into distinct regions of interest thus creating an 'anatomical atlas' onto which any brain can be mapped onto (61). These anatomical regions can then define the 'nodes' used in the data analysis. This atlas can be used to conduct whole brain analysis or specific, pre-defined regions of interest. The AAL atlas consists of 116 individual regions of interest, or 90 if the cerebellum is excluded(61). Coordinates of brain regions generated from the statistical analyses can also be applied to atlases to identify the anatomical brain regions involved.

### 1.3.2.5 Resting state brain networks

Several resting state brain networks of interest have been identified by prior neuroimaging studies as being abnormal in patients with TS and thus are of interest to our study. These include the default mode network(62), central autonomic network(62), salience network(63) and the central executive network(63, 64). The anatomical components of these functional networks will be included in our region of interest analyses and are described in Methods.

Resting state networks are active at rest rather than during active tasks. The default mode network is active during wakeful rest and has importance in thinking about oneself and others, mind-wandering, remembering the past and planning for the future(65). The central autonomic network influences the activity of the preganglionic neurons of the autonomic nervous system. The salience network is involved in complex functions including communication and self-awareness(66) and the central executive network which is involved in sustained attention, problem-solving and reasoning(67).



### 1.3.3 SUMMARY

Therefore by putting together all the information that has been summarised so far we can quantitatively measure differences in the anatomy or connectivity of brain regions/networks which have plausible mechanisms for affecting the heart using the pathways described in 1.4.2. This study will use these techniques to quantify brain and cardiac changes in patients presenting with MINOCA.

## 1.4 THE HEART-BRAIN INTERACTION IN MINOCA

### 1.4.1 WHY IS IT IMPORTANT?

The heart must provide the body with the necessary oxygen and nutrients it requires to function. It must be able to respond to the specific needs of the body in a range of different physiological scenarios. On its own, the intrinsic automaticity of the heart would have a pacing rate of 100 bpm which is not physiologically appropriate most of the time(68). As a result, the human body has complex neural and endocrine mechanisms which influence and manipulate cardiac function. These mechanisms are primarily coordinated in the brain. Pathological or physiological changes in these complex mechanisms can lead to cardiac pathologies. In addition, pathologies which primarily affect the heart can influence the brain. This connection between the heart and the brain was first theorized 350 years ago by William Harvey (69) and this link has subsequently been implicated in a multitude of cardiovascular pathologies including coronary atherosclerotic disease (70, 71), stroke (72), heart failure (73), atrial fibrillation(74), hypertension (75) and many more. In response to this, the World Stroke Organisation Brain and Heart Task Force was created to highlight the growing importance of a potential new sub-speciality, neurocardiology (76).

It should be noted that the connection between the heart and the brain is bidirectional: the heart can affect the brain (such as embolic stroke, patent foramen ovale's (PFO's) association with migraines, ACS/heart failure and

increased risk of dementia etc) and the brain affects the heart (e.g. neurogenic heart disease)(77). This thesis will focus on the brain's affects on the heart.

The brain can exert beat-to-beat control over the heart. According to Palma et al (78) the anterior insula, anterior cingulate cortex, amygdala, hypothalamus, periaqueductal gray matter, parabrachial nucleus and the medulla exert this control via the autonomic nervous system. Many of these brain regions also process emotional behaviours, stress responses and homeostatic mechanisms which is relevant in several disease states. In addition, the intrinsic cardiac nervous system is controlled by the extrinsic autonomic nervous system. We need to understand how these systems work to understand how the brain and heart interact.

### *1.4.2 THE AUTONOMIC NERVOUS SYSTEM*

The ANS comprises the sympathetic (SNS) and parasympathetic nervous systems (PSNS) and is characterised by a preganglionic and a postganglionic neuron unlike the single neuron used in the somatic nervous system.

#### **1.4.2.1 Sympathetic Nervous System**

Cardiac sympathetic innervation originates in the C3-T3 segments of the spinal cord (intermediolateral cell columns) and it receives excitatory inputs from the rostral ventrolateral medulla (RVLM) in the brain. Several regions of the brain, including the insular cortex, anterior cingulate cortex and the amygdala project to the medullary and spinal nuclei. The neurons in the RVLM activate in response to psychological stress and pain amongst others. These cholinergic pre-ganglionic neurons of the spinal cord activate adrenergic neurons of the paravertebral sympathetic ganglia which project axons to the heart(79). Sympathetic and parasympathetic nerves are concentrated towards the base of the heart rather than the apex (76). The receptors of the SNS are either  $\beta$  or  $\alpha$  adrenergic receptors. In the heart there are two main receptors:  $\beta_1$  and  $\beta_2$ .  $\beta_1$  receptors are located in the SA node, AV node and on cardiomyocytes.  $\beta_2$  receptors are located in vascular smooth muscle and the coronary circulation and

are mainly stimulated by systemic circulating catecholamines(68). Activation of  $\beta_1$  receptors increases the heart rate by increasing SA node automatism, speed of conduction through the AV node and His/Purkinje system and shortening diastole. It also has positively inotropic effects on the cardiomyocytes. Thus, there is a well-established pathway for external emotional and physical triggers to modulate the nervous control of the heart.

In addition, the SNS has pre-ganglionic fibres which extend to the adrenal medulla and directly innervate adrenal chromaffin cells to release adrenaline and noradrenaline, and to the kidneys to stimulate the release of dopamine. These systemic catecholamines can also directly stimulate the adrenoreceptors located in the heart and vasculature(68).

### 1.4.2.2 Parasympathetic Nervous System

Parasympathetic control of the heart is via the vagus nerve. Preganglionic cholinergic neurons of the nucleus ambiguus in the medulla (and less so in the dorsal motor nucleus of the vagus) send axons to the cardiac ganglia(80, 81). From there they synapse with muscarinic receptors which are activated by the neurotransmitter acetylcholine. The sinoatrial and atrioventricular node, atria and ventricular conducting system are well innervated whereas the myocardium is relatively spared. The muscarinic receptors found in the heart are  $M_2$  and  $M_3$ .  $M_2$  receptors are mainly located in the AV node and atria and when they are activated, they have the opposite effects of  $\beta_1$  receptors on heart rate.  $M_3$  are mainly in the vascular endothelium and their activation leads to vasodilatation (68). In the resting state, parasympathetic inputs predominate over sympathetic.

### 1.4.2.3 Hypothalamic-pituitary-adrenal axis

The hypothalamic-pituitary-adrenal (HPA) axis consists of the hypothalamus, pituitary and adrenal endocrine glands. The hypothalamic paraventricular nucleus (PVN) is the control centre of the HPA axis and secretes corticotropin releasing hormone which stimulates the anterior lobe of the pituitary gland to secrete adrenocorticotrophic hormone (ACTH) amongst others. In response to ACTH the adrenal cortex secretes glucocorticoid steroid hormones

such as cortisol(68). These stress hormones have diffuse effects on the human body and the cardiac response to stress is a key research area.

### 1.4.2.4 Higher brain control of efferent autonomic function

As briefly mentioned in section 1.4.2.1, the insular cortex, anterior cingulate cortex, amygdala and several hypothalamic nuclei regulate autonomic control(78). The function of these regions are complex.

The rostroventral insular cortex is closely linked with the anterior cingulate cortex and amygdala and together they receive, process and respond to afferent signals which are key in emotional processing(82). The anterior cingulate cortex also has extensive connections and is part of the default mode network (ventral anterior cingulate cortex) which is active at rest, and the salience network (dorsal anterior cingulate cortex) which is involved in cognitive processes (83, 84). The amygdala is central to the brain's response to fearful stimuli and it has sympathoexcitatory effect on the RVLM in response to fear driving the body's autonomic response(85). In addition, the orbitofrontal cortex and ventromedial prefrontal cortices are interconnected with the amygdala and exert an inhibitory effect and modulate the individual response to fearful stimuli(86, 87). Finally, the hypothalamus has direct and indirect projections to the RVLM, inferomediolateral cell columns and dorsal motor nucleus of the vagus and so is in a key position to modulate the autonomic response of the heart in response to its extensive sensory inputs(88, 89).

Knowledge of these complex interactions is crucial for understanding the pathophysiological processes which may affect the heart but also for the potential development of novel therapies. The next section will now review the current neuroimaging literature in relation to cardiac pathology. For the purposes of this thesis, I will only consider the brain's effect on the heart in patients with myocardial infarction and takotsubo cardiomyopathy (there have been no imaging studies looking at patients with acute myocarditis). I will focus on *human*

*neuroimaging studies* examining the anatomical and functional connections between the brain and the heart as this has the most relevance to this thesis.

## 1.5 BRAIN-HEART INTERACTION

### 1.5.1 MYOCARDIAL INFARCTION

Negative emotions such as stress, sadness, anger and anxiety can independently increase the risk of major adverse cardiovascular events (MACE) (90-93). Elevated risk of MI has been documented in the minutes to hours following episodes of anger, anxiety and depressed mood (94). Myocardial infarctions are more likely on a Monday which is typically the start of the working week and when stress levels are at their highest(95). Stress is perhaps the best-known neurological risk factor for cardiac disease(96) with a risk similar to established cardiovascular risk factors. However, the mechanisms underlying these associations are only starting to become understood. There are very limited neuroimaging studies to date, and these are PET/CT studies which focus on how stress modulates the risk of MI. There are no neuroimaging studies assessing patients with major depressive disorder or anxiety *prior* to myocardial infarction despite this being a recognised independent risk factor.

There are several plausible explanations for how stress contributes to MACE. Mental stress can induce ischaemia due to the increase in afterload due to peripheral vasoconstriction(92). However, the most convincing arguments involve its effect on inflammation and the vascular endothelium. Mental stress can rapidly increase circulating adrenaline and noradrenaline, and this has been shown to induce endothelial dysfunction which is an important predictor of atherosclerosis (97). Activation of the SNS due to stress causes a systemic inflammatory response increasing circulating inflammatory biomarkers including IL-6, MCP-1 and MMP-9 (98, 99). Thirdly, direct inhibition of nitric oxide has been shown in depressed patients(100) and this also has the potential to cause endothelial dysfunction. Fourthly, it has been shown that patients with an emotional trigger prior to their myocardial infarction demonstrated heightened

platelet activation which could increase the chances of a thrombotic event(101). A recent seminal neuroimaging study suggested that resting amygdala activity may predispose to adverse cardiovascular events(102). The amygdala is a key part of the salience network which is involved in cognition and emotion(103) and has previously been shown to be upregulated in stress, anxiety and depressive disorders (104). The study demonstrated that for each 1 standard deviation (SD) increase in resting amygdala activity on  $^{18}\text{F}$ -FDG PET/CT imaging the risk of an atherosclerotic major adverse cardiovascular event increased by 1.59 (1.27-1.98,  $p<0.001$ )(102) and these events occurred sooner than those with lower activity and independently of established cardiovascular risk factors. Amygdala activity also correlated with arterial  $^{18}\text{F}$ -FDG-uptake (a measure of arterial inflammation) and activity in the bone marrow and spleen. The authors undertook a serial two-mediator analysis which was consistent with a pathway of increased amygdala activity leading to increased haematopoiesis in the bone marrow and spleen, subsequent arterial inflammation and therefore increased major cardiovascular events.

Further to this, the same group investigated socioeconomic class as a marker of stress. Lower socioeconomic class is known to be associated with MACE and this is not all solely down to the higher risk profile of these patients and their reduced interaction or access to healthcare professionals(105). Low socioeconomic class is associated with increased psychosocial stress(106, 107). The stress response is controlled by the SNS of which the amygdala is also key central component. SNS activation induces stress-induced leukopoiesis which drives atherosclerotic inflammation(108) which increases cardiovascular risk and the chance of myocardial infarction(102, 109). Metabolic activity in the amygdala, bone marrow and arterial walls was quantified in a retrospective observational study of 289 individuals with lower socioeconomic status in the USA(110). They demonstrated that for every SD increase in neighbourhood median income there was a 0.156-SD decrease in amygdala activity and a resultant decrease in arterial inflammation despite correction for age, sex and cardiovascular risk factors. The lowest quartile of median neighbourhood income was also associated with

increased MACE with a HR of 6.31 (95% CI: 1.41 to 11.83;  $p = 0.016$ ) when adjusted for CVD risk factors, and other confounders including health behaviours and obesity. Using mediation analysis, which is a statistical tool to explore the underlying mechanism of a known relationship, the authors showed for the first time that lower socioeconomic class was associated with increased amygdala activity which increased haematopoietic activity which increased arterial inflammation and increased MACE. In a separate cross-sectional substudy, the same authors demonstrated a strong correlation between the perceived stress scale (PSS-10) and amygdala activity, arterial inflammation and C-reactive protein(102). The salience and autonomic networks are therefore of particular interest in our study.

Most recently, increased brain emotional neural activity, as measured by amygdala activity on  $^{18}\text{F}$ -FDG-PET/CT, was associated with acute plaque instability via increased macrophage haematopoiesis and arterial inflammation(111). Plaque instability is a precursor to acute myocardial infarction. Reducing plaque inflammation was associated with reducing amygdala activity 6 months following presentation with myocardial infarction. Although cause and effect cannot be elucidated, it suggests that stress and emotional processing pathways which affect amygdala activity could potentially be modifiable factors in the future to help patients move from a high-risk plaque to more stable plaques.

### 1.5.2 TAKOTSUBO SYNDROME

Takotsubo syndrome is preceded by an emotional or physical stressful trigger in more than 70% of cases (112). This has led to an increasing amount of research into potential neural mechanisms of TS. The precise pathophysiology of the condition is not understood and is likely to be multifactorial (46). There are now a substantial number of neuroimaging studies implicating the autonomic nervous system as a key player.

The first report in 2014 measured cerebral blood flow (CBF) by SPECT, and showed increased flow in the subcortical brain regions (hippocampus, brainstem

and basal ganglia) in *the acute phase* of patients with TS that was triggered by a stressor(113). These regions are involved in the acute stress response. There was reciprocal reduced CBF in the prefrontal cortex which is also seen in acute stress. The subcortical regions remained activated to a lesser degree in the chronic phase after resolution of the wall motion abnormality which may reflect ongoing stress in these patients or a pre-existing underlying vulnerability to stress. This first report was a very small study including 3 patients and it is not possible to ascertain cause and effect. The brain activation may simply represent a state of sympathetic activation but the persistence of these changes into the chronic phase may suggest there is a role for cognitive therapies in at risk populations or to prevent relapse.

Klein demonstrated that there are homogenous alterations across areas of the brain associated with emotional control, cognitive function and the central part of the autonomic nervous system which are predictive of TS (64). These are the same regions that are affected by common comorbidities such as depression and anxiety. Hiestand performed MRI on twenty Caucasian female patients, a mean of  $342 \pm 274$  days after a Takotsubo event, and 39 healthy female controls. They found decreased cortical thickness in both insulae and cingulate cortices in patients with previous TS together with reduced gray matter volume in the left and right amygdala and at the right amygdala/hippocampus border. These regions partly comprise the limbic network which is a region of the brain that is critical for emotional processing, cognition, and the autonomic nervous system (114). Most recently Dichtl used voxel-based morphometry (VBM) to quantify grey matter volume in patients with TS acutely. Amongst others, they demonstrated reduced grey matter volumes in the right insula, right and left thalamus, left cerebral cortex and left amygdala suggesting disruption of brain regions controlling the SNS (115).

There are several small studies using rs-fMRI to examine brain connectivity networks in TS. Resting state networks, including the DMN, are active at rest and are responsible for self-related thinking and cognition. Sabisz et al. investigated



thirteen women 12-18 months after a TS event and found that there were increased connections in the precuneus, a key component of the DMN. In addition, there was hypoconnectivity in the ventromedial prefrontal cortex which is responsible for emotional processing and control. They concluded that these changes may suggest that patients with TS have a greater focus on self, a greater tendency to experience negative affectivity and problems with emotional control(116). Hiestand showed in their earlier study that there was reduced connectivity in the limbic system in patients who had an episode of TS (117). Pereira showed that regions of the brain that are responsible for control of the autonomic nervous system (namely the insular cortex, amygdala and right hippocampus) respond differently to autonomic stressors (Valsalva manoeuvre) in individuals with a previous episode of TS compared to control patients(118). Silva et al also demonstrated increased connectivity in areas of the brain that are responsible for emotional and autonomic control. In response to a cold trigger stress there was increased connectivity in nodes located in the amygdala, left putamen, right insula and right cerebellum. They theorised that patients with previous TS have abnormal autonomic modulation in response to stress compared to healthy controls.

The most relevant contemporary study was conducted by Templin et al (62) and this merits closer analysis. Resting state functional MRI (rs-fMRI) was performed in 15 patients with previous TS and 39 age and gender-matched controls. They demonstrated reduced connectivity in the areas of the brain responsible for autonomic control, regulation of cardiac function, emotions, learning and memory compared to healthy controls. In addition, there was hypoconnectivity in the default mode network (DMN). They hypothesised that a triggering emotional event in people with this abnormal functional substrate leads to a more pessimistic evaluation of the event, increasing stress levels and subsequently adversely affecting the central autonomic nervous system which could lead to an exaggerated sympathetic response. However, as with many of the studies described, it is important to note that participants were scanned a median of 378 days (interquartile range: 116-564 days) after the diagnosis was

made. This delay to brain imaging means that any acute changes associated with the acute, reversible presentation of takotsubo cardiomyopathy would be missed. In addition, the control group only included normal patients so it seems plausible that the functional changes seen may represent changes that developed after any stressful event. It would have been interesting to compare the TS group with a control group who had another stressful event. It is also relevant to note some of the inconsistencies from these studies. For example, the Silva study demonstrated increased connectivity in a subnetwork of the autonomic nervous system and salience network including the left hippocampus, left ACC, left inferior frontal cortex and superior temporal cortex. They did not demonstrate reduced connectivity in any network. However, the majority of the other studies demonstrated reduced connectivity in networks involving these nodes. These inconsistencies are not uncommon in neuroimaging studies and are likely to reflect relatively small numbers in each study, retrospective design (and subsequent bias), different methodology, acquisitions and analytical techniques and heterogeneity in the study population.

Furthermore, a  $^{18}\text{F}$ -FDG-PET imaging study showed that higher amygdala activity was associated with greater odds of developing TS but also those with higher activity developed TS ~2 years before those with lower amygdala activity(119). This demonstrates that increased amygdala activity predates the onset of TS rather than being a consequence of it.

Marijuana use has recently been linked to TS in a number of case reports and as an independent risk factor (120). The endocannabinoid and emotional processing systems largely overlap (hypothalamus, hippocampus, amygdala and prefrontal cortex). It has been proposed that exogenous cannabis use may lower the threshold for HPA axis activation during stressful events by affecting the inhibitory influences within the amygdala. This has been shown in cannabis users without takotsubo cardiomyopathy(120) but, given the small numbers involved, high quality evidence is lacking in this area. In addition, marijuana use is strongly associated with underlying stress and mental health disorders, and this is a clear

confounder in this cohort. Nevertheless, it is another piece of evidence highlighting potential links between the heart and the brain in TS.

A unifying hypothesis that has been put forward which could link these results would be that chronically elevated stress levels lead to chronically elevated neural activity in autonomic and emotional processing pathways which predisposes these individuals to an exaggerated neurophysiological response to a stressor(121). However, all of these studies are limited by their small sample size, retrospective design and, in most cases, long interval between diagnosis and scanning. It is not possible to ascertain a causal relationship between the two or decipher which event precedes the other, with the exception of using mediation analysis. Despite this there is now a growing body of evidence which suggests that TS may be a primary neurological condition with remote cardiac effects.

### **1.5.2.1 Stroke and Takotsubo Syndrome**

Subarachnoid haemorrhage (SAH) is the most common neurological disorder associated with myocardial injury. One study suggested that up to 68% of patients presenting with SAH had detectable cardiac troponin I release and 99% of patients with elevated cardiac troponin had either abnormal clinical examination, abnormal ECG or RWMA on cardiac imaging. The degree of troponin release correlated with markers of severity of the neurological insult and the peak troponin was associated with severe disability or death at discharge(122). It has been postulated that these changes reflect a stress cardiomyopathy caused by catecholamine surges aimed to relieve the fall in cerebral perfusion pressure due to the raised intracranial pressure or a direct effect on the cardiac control centres in the brain. Classical contraction band necrosis, seen in extreme sympathetic discharge and in TS, is also seen in neurogenic stress cardiomyopathy suggesting a similar underlying process. The phenotype of neurocardiogenic stress cardiomyopathy (or neurocardiogenic stunned myocardium) is different to that of traditional apical TS in that the pattern of RWMA is more often basal or mid wall compared with the traditional apical RWMA seen in classical TS (123). It is also more likely to affect males, have a lower peak troponin, present without ST

elevation, have a higher ejection fraction at presentation and have a higher inpatient mortality(124, 125). This has led to these conditions being referred to as 'takotsubo phenocopies' or 'secondary stress cardiomyopathies' as although the pathophysiological mechanisms are similar, they appear to have difference clinical presentations and outcomes(126). The proinflammatory state following damage to the neuronal and glial cells in ischaemic and haemorrhagic stroke can directly stimulate the hypothalamus to increased sympathetic activity and circulating catecholamines(127).

The insula is a key region of cerebral cortex located in each hemisphere in the lateral sulcus separating the temporal lobe from the parietal and frontal lobes. It is densely interconnected and is thought to be a key component of the central autonomic network (CAN) and in emotional control(128). This is the network responsible for the control of the sympathetic nervous system and thus the catecholamine release which is the favoured cause for TS. It is supplied by the middle cerebral arteries and as such is at particular increased risk of the consequences of cerebrovascular disease. In a sample of 50 patients who had an unexplained troponin rise following an acute ischaemic stroke, infarcts in the right insula (posterior, superior and medial aspects) and the right inferior parietal lobule were particularly associated with troponin elevation (129). Damage to the insular cortex has been associated with myocardial injury, increasing BNP levels and takotsubo syndrome(128, 130). Ischaemic stroke affecting the right insular cortex and peri-insular areas were more commonly detected in patients with a takotsubo like myocardial dysfunction on echocardiography(131). The right insular cortex appears to be implicated particularly in sympathetic autonomic tone, whereas the left insular cortex more with parasympathetic autonomic tone(132).

### *1.5.3 DEPRESSION AND ANXIETY*

There are no neuroimaging studies in humans which look at the link between the brain and the heart in depression or anxiety and myocardial infarction. There are, however, multiple rs-fMRI studies in people with anxiety and depression. People with major depressive disorder have evidence of

hypoconnectivity in the central executive network(133), limbic network (including the amygdala, OFC and hippocampus), salience network(134) and hyperconnectivity in the default mode network(135). Major depressive disorder is also associated with increased global efficiency and reduced modularity suggesting that these patients have a more random arrangement of brain topology rather than small world features which reflects less optimal brain organisation(136). Depression is also associated with reduced orbitofrontal cortex, hippocampal and insula grey matter volume (amongst other regions) which could also feasibly affect the functioning of the ANS (137).

Patients with generalised anxiety disorder may have heightened activation of the amygdala and aberrant connections between the amygdala and the prefrontal cortex(138). There is also evidence for lower global efficiency in patients with generalised anxiety disorder(139) . Therefore, it is quite plausible that patients with high depression or anxiety scores or a history of depression or anxiety would have brain changes which could modulate the risk of myocardial infarction, and this warrants investigation.

### *1.6 UNANSWERED QUESTIONS*

There is huge scope for research in this field. Much of the work carried out so far is interesting but only hypothesis generating. fMRI and PET are well established non-invasive investigations which could be used to assess brain structure, markers of neuroinflammation, cerebral blood flow and functional connectivity in patients with cardiac disease. Future studies need to be larger and prospective in design. Ideally patients would be recruited before developing cardiac or brain pathology and followed prospectively, but the relative infrequency of these conditions (particularly takotsubo cardiomyopathy) means cohorts would have to be prohibitively large. A compromise therefore of recruiting patients at presentation, following them up over time and comparing them to well defined age and sex-matched controls also undergoing an acute stressful event but who do not develop TS (not just healthy volunteers) is justified. Cohorts need to have robust diagnoses (including with CMR for takotsubo

cardiomyopathy, or CT or invasive angiography for myocardial infarction) to prevent mimics contaminating the data and diluting any small effects.

Given the described association between stress and inflammation, there is yet to be any significant neuroimaging work on the relationship between depression and anxiety and myocardial infarction. It is not unrealistic to think that the structural and function brain changes associated with these conditions will also impact on the autonomic nervous system and modulate arterial inflammation.

Furthermore, the clinical relevance of the heart-brain interaction in MINOCA is unknown, especially regarding TS. Most of the studies described are descriptive in nature, highlighting interesting findings which may have clinical significance. There is not yet any clinically relevant outcome data, such as associated morbidity and mortality related to patients who develop neuroinflammation or who have altered limbic system connectivity in their brain. As such there are no clinically relevant therapeutic options, be it pharmacological or psychological. Subsequent studies may evaluate the role of cognitive therapies in at risk cohorts or in patients with previous TS to see if this reduces the likelihood of repeat events.

This study aims to fill some of these knowledge gaps by investigating the MINOCA population acutely using a prospective cohort of patients. It will also aim to recruit sufficient participants to allow for meaningful subgroup analysis (including TS). Furthermore, our study will include patients presenting with an ST-segment elevation myocardial infarction (STEMI) to ensure that any acute anatomical or connectivity changes seen are not simply secondary to a stressful cardiac event. Finally, for the first time, participants will be followed up with sequential cardiac and brain imaging to delineate changes between the acute and chronic phases of the condition.

## *1.7 STUDY AIMS, OBJECTIVES AND HYPOTHESES*

### *1.7.1 AIMS*

The overall aim of the study is to comprehensively characterise the global and regional anatomical and functional brain changes in patients with MINOCA and how they evolve over time.

### *1.7.2 OBJECTIVES AND HYPOTHESES*

The objectives for each of our studies are described below.

#### **1.7.2.1 Chapter 3**

*Objective 1:* Quantify acute anatomical grey matter volume differences in MINOCA and to compare them with patients with an acute ST-elevation myocardial infarction (STEMI) and healthy control participants using whole brain voxel-based morphometry (VBM).

*Objective 2:* Identify any associations between grey matter volume and cardiac and psychological variables.

*Hypothesis 1:* there will be a reduction in grey matter volume in regions of the brain associated with the limbic and autonomic nervous systems in MINOCA compared to STEMI and healthy controls

*Hypothesis 2:* there will be associations between measures of heart function, anxiety, stress and depression and grey matter volume in the MINOCA group and if present, these will be different to such associations in the STEMI and healthy control groups.

*Hypothesis 3:* any differences/associations seen will also be present in a subgroup analysis comprising only patients with TS when compared to healthy and STEMI controls.

**1.7.2.2 Chapter 4**

*Objective 1:* Characterise the differences in global network measures and network functional connectivity between MINOCA, STEMI and healthy participants,

*Objective 2:* Correlate global network measures and network functional connectivity with measures of anxiety, depression, stress and global longitudinal strain (GLS-CMR) in MINOCA patients and in both control groups where a correlation is found in the MINOCA group.

*Objective 3:* Conduct the same analysis as per objectives 1 and 2 in a subgroup of patients with TS

*Hypothesis 1:* patients with MINOCA would have higher anxiety and stress scores than both control groups.

*Hypothesis 2:* patients with MINOCA would have reduced global efficiency, modularity and small world propensity compared to control patients compared to both control groups.

*Hypothesis 3:* anxiety, depression, stress and GLS-CMR would negatively correlate with global efficiency, modularity and small world propensity in MINOCA patients.

*Hypothesis 4:* patients with MINOCA would have reduced connectivity on region of interest and whole brain network analysis in networks comprising the autonomic and limbic systems compared to both control groups.

*Hypothesis 5:* anxiety, depression, stress and GLS-CMR would negatively correlate with whole brain and regional connectivity in MINOCA patients.

*Subgroup Analysis*

*Hypothesis 6:* patients with TS would have reduced global efficiency, modularity and small world propensity compared to both control groups



*Hypothesis 7:* patients with TS would have reduced connectivity in subnetworks involving the amygdala and autonomic nervous system compared to both control groups.

### 1.7.2.3 Chapter 5

*Objective 1:* Investigate if the changes in psychological state, grey matter volume or connectivity in MINOCA and TS patients at presentation are reversible at 6 months.

*Hypothesis 1:* patients with MINOCA would have higher anxiety and stress scores than both control groups

*Hypothesis 2:* there will be no difference in grey matter volume in any region compared to MINOCA patients in the acute phase

*Hypothesis 3:* there would be no change in the grey matter volume differences identified in the acute phase analysis compared to healthy controls.

*Hypothesis 4:* there would be no change in the grey matter volume differences identified in the acute phase analysis between TS patients and healthy controls.

*Hypothesis 5:* there would be no difference in global efficiency, modularity and small world propensity compared to the acute phase.

*Hypothesis 6:* there would be no difference in the connectivity changes seen on the DMN and CEN analysis in the acute phase between MINOCA and control patients.

*Hypothesis 7:* there would be no difference in the connectivity changes seen on the CEN and whole brain analysis in the acute phase between TS and control patients.

## 1.8 CONCLUSIONS

MINOCA is a working diagnosis and is typically characterised by participants with myocardial infarction, myocarditis and TS. They are more likely to have a history of anxiety, depression or previous psychological disorders but the reasons for this are not understood. CMR is a well-validated tool for identifying the diagnosis in these patients. Brain MRI is non-invasive imaging technique which can be used to characterise anatomical and functional brain changes in these patients. A range of anatomical and connectivity differences have been shown in the autonomic nervous system as well as the regions involved in the regulation of emotions in patients with myocardial infarction and TS which provide clues to the underlying pathophysiology of these conditions. In this study we build on this work to help address several unanswered questions.

## Chapter 2 METHODS

---

### 2.1 *STUDY DESIGN*

A prospective, single centre, observational cohort study was undertaken at University Hospitals Bristol and Weston NHS Foundation Trust (UHBW). The study was sponsored by the University of Bristol and was approved by the Health Research Authority (HRA) on 24<sup>th</sup> August 2018. Confirmation of capacity and capability was received from UHBW on 8<sup>th</sup> January 2019 and recruitment started on 1<sup>st</sup> February 2019.

The study was funded by grants from the Rosetrees Trust (£15, 500), James Tudor Foundation (£15, 500) and Above and Beyond Charitable Trust (£18, 517).

### 2.2 *STUDY REGISTRATION*

The study protocol was registered prospectively on a primary clinical trial registry (<https://doi.org/10.1186/ISRCTN15878953>).

### 2.3 *RESEARCH TEAM*

Chiara Bucciarelli-Ducci (CBD) was the chief investigator for the study. Matthew Williams (MW) was the principal investigator (PI). MW was responsible for designing the study protocol and related documentation, completing funding applications, obtaining ethics and relevant local approvals, recruitment of participants, study oversight and interim review, data collection, data analysis and dissemination of results. Kate Liang (KL) and Estefania De Garate were cardiac MRI fellows in the department who assisted with patient recruitment. Ngoc Jade Thai (JT) was a principal investigator and supervised the design of the neuroimaging protocols and provided training for MW to analyse the brain data. Giovanni

Biglino (GB) provided statistical review of the protocol and advice on the study design.

### *2.4 PATIENT AND PUBLIC INVOLVEMENT*

During the design of the study protocol 5 patients with MINOCA or STEMI were approached on the ward (MW). They were asked to review the study protocol and comment on the patient information leaflets (PIL) and invitation letter, the demands of the study, give their opinion on whether the study was worthwhile and say whether they would have taken part in the study or not and why. 3/5 people (60%) said they would take part. All patients said the study was worthwhile and justified the time and expense. Minor changes were made to the language of the patient facing documents. The reasons given for not taking part in the study were both related to being unable to travel to UHBW, one patient did not have a car and the other patient lived too far away and had cost concerns. As a result of these comments, we applied for further grants to support an allowance of £20 per person per study visit, which was not part of their routine clinical care.

### *2.5 RECRUITMENT OF MINOCA PATIENTS*

All patients presenting to UHBW between 1<sup>st</sup> February 2019 and 31<sup>st</sup> January 2021 with MINOCA, as defined by the 2017 ESC working group paper on MINOCA(9), were screened for inclusion in the study. Recruitment was suspended from the 16<sup>th</sup> March 2020 to the 1<sup>st</sup> August 2020 due to the coronavirus pandemic.

#### *2.5.1 INCLUSION CRITERIA*

1. Age 18-80 years
2. Met the ESC 3<sup>rd</sup> universal definition of myocardial infarction(140)
3. <50% epicardial coronary artery stenosis on invasive or computed tomography (CT) coronary angiography in any potential infarct related territory

4. No other clinical overt specific cause for the acute presentation at the time of angiography
5. Written informed consent

### 2.5.2 EXCLUSION CRITERIA

1. Invasive or CT coronary angiography not performed or not diagnostic
2. Previous coronary artery bypass grafting (CABG)
3. Previous cerebrovascular event (CVE) or other known neurological disorder/disease
4. Contraindications to CMR, including severe renal insufficiency (eGFR <30), implanted pacemaker/defibrillator, ferromagnetic metal implant, severe claustrophobia
5. Pregnancy or breast feeding
6. Prisoners
7. Unable to meet the follow up requirements
8. Timing of the initial CMR >2 weeks after admission

The 3<sup>rd</sup> universal definition of MI requires measurement of troponin levels. In our centre we use the Elecsys high sensitivity troponin T (hs-TnT). The 99<sup>th</sup> percentile upper reference limit is >14 ng/l. “*Rise or fall*” in hs-TnT was regarded as a 20% change on consecutive measurements. Patients with previous CABG were excluded due to anticipated challenges interpreting the cardiac MRI in the context of known significant multivessel coronary disease. All CMRs were planned to occur within 2 weeks of admission to ensure a higher diagnostic yield as described in chapter 1(17).

Patients who met the inclusion and exclusion criteria were approached by a member of the research team (MW, KL or EDGI) whilst they were on the ward and were given written information about the study. All patients were given *at least* 2 hours to read the information and sign a consent form if they agreed to take part.

## *2.6 RECRUITMENT OF CONTROL PATIENTS*

### *2.6.1 STEMI PATIENTS*

Age and sex matched control patients presented to UHBW with an acute STEMI and had an occluded epicardial coronary artery at invasive angiography. Otherwise, the inclusion and exclusion criteria were the same as for the MINOCA patients. Recruiting STEMI control patients allowed for direct comparison to a cohort who had also been admitted to the same department, undergone angiography and had a stressful event.

### *2.6.2 HEALTHY VOLUNTEERS*

Age and sex matched healthy volunteers were recruited using local publicity. Inclusion and exclusion criteria are described below.

#### **2.6.2.1 Inclusion Criteria**

1. Age 18-80 years
2. Written informed consent

#### **2.6.2.2 Exclusion Criteria**

1. Prior history of cardiovascular disease
2. Prior history of a neurological disorder/disease
3. Contraindications to CMR (including severe renal insufficiency (eGFR <30), implanted pacemaker/defibrillator, ferromagnetic metal implant, severe claustrophobia)
4. Pregnancy or breast feeding

## *2.7 SAMPLE SIZE*

This was a novel study, and no formal sample size calculation was performed prospectively. Previous comparable retrospective studies in patients with TS recruited 13-20 participants(64, 114, 116). A meta-analysis of recent highly cited fMRI studies reported a median sample size of 14.5(141). Previous work in our department suggested the prevalence of each sub diagnosis was 33%

for acute myocarditis, 26% AMI, 16% TS, 9% other cardiomyopathies and 16% normal scans(17). Therefore, to ensure a minimum of 15 participants in each of our predefined MINOCA subgroups we planned to recruit 100 participants. The prevalence of MINOCA is estimated at 6%(8). On average, our tertiary cardiology centre treats ~700 STEMI patients and ~2500 non-ST-elevation myocardial infarction (NSTEMI) patients each year (as documented in the BCIS database). Therefore, we would expect ~192 patients a year with MINOCA in our centre. Patient and public involvement suggested around 60% of patients would take part in the study. Using a more conservative figure of a 50% recruitment rate we anticipated recruitment to last ~12 months. This time frame would also be in keeping with the time constraints of undertaking a 3-year PhD which needed to include time for study set up, analysis and writing up.

STEMI and healthy control participants were recruited in a 2:1 ratio (aiming for 50 healthy and STEMI controls). These numbers were decided by balancing the need for adequately sized control groups for statistical power and the available time on the CMR scanner. A 2:1 ratio was the minimum ratio that would provide large enough subgroups for meaningful analysis and enough controls to provide statistical power to detect differences in grey matter volume or connectivity. This ratio has previously been used in the fMRI literature(142). The predicted number of participants and controls are significantly larger than the comparable studies discussed in the Introduction.

### 2.8 *OUTCOMES*

Specific outcomes for each study will be described in the relevant chapters. In short, primary outcomes were grey matter volume and measures of brain connectivity. The secondary outcomes were anxiety and depression scores and the perceived stress score.

### 2.9 *STUDY SCHEMA*

The study schema is shown in

Figure 1. Due to restrictions resulting from the coronavirus pandemic the research echocardiograms at 4-6 weeks and at 6 months were removed from the protocol in March 2020 as the close personal contact could not be justified.

### 2.10 STUDY VISITS

#### 2.10.1 MINOCA PARTICIPANTS

MINOCA participants were asked to take part in four study visits to help answer the clinical questions. The contents of each study visit are shown in Table 4.

Table 4 Breakdown of study visits for MINOCA participants

	Study visit 1 - < 14 days	Study visit 2 – 4-6 weeks	Study visit 3 – 6 months	Study visit 4 – 12 months
CMR	✓	✓	✓	
Brain MRI	✓		✓	
Questionnaires	✓		✓	
Routine bloods	✓	✓	✓	
ECG	✓	✓	✓	
Echo	✓			
Follow up				✓



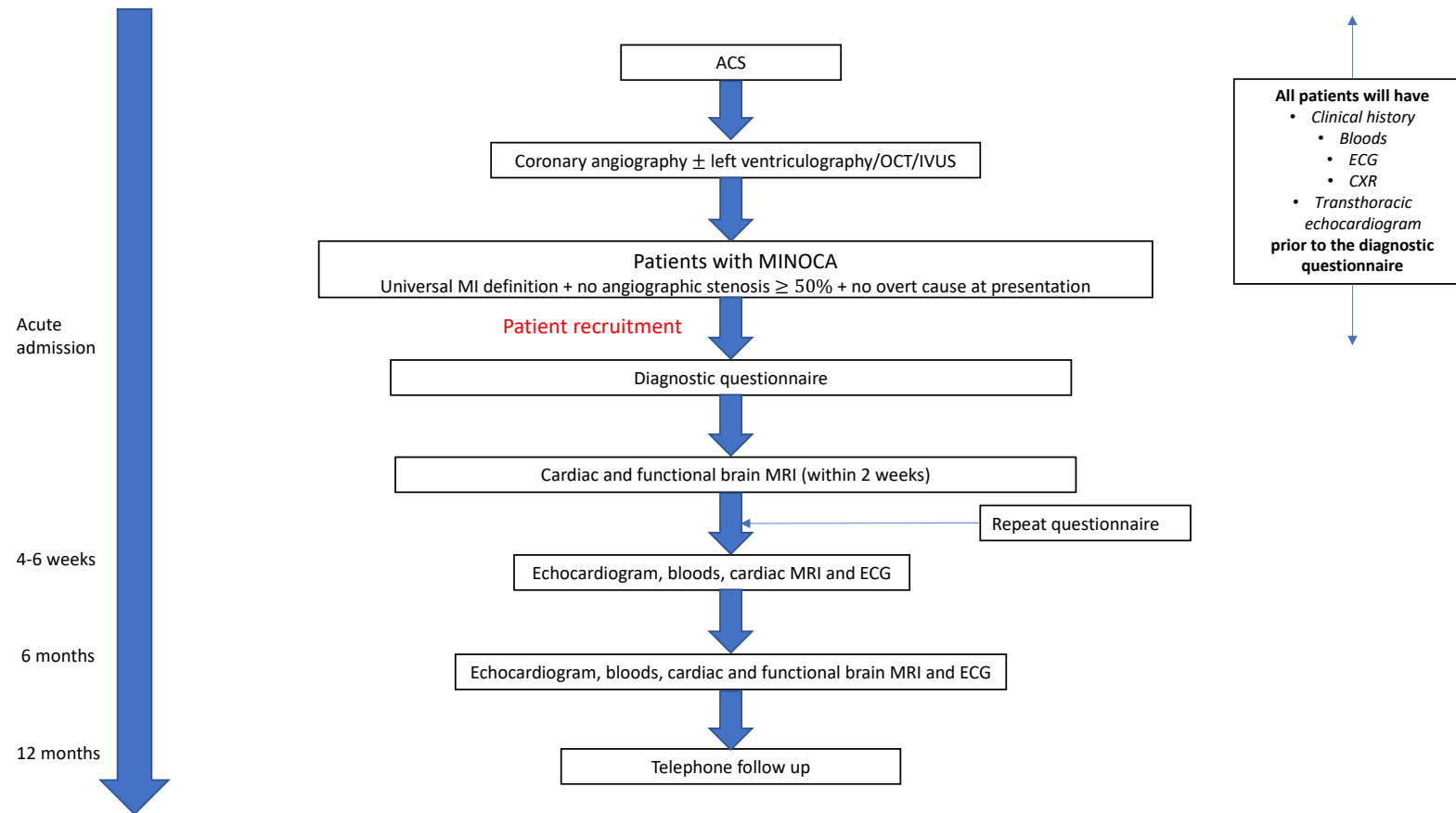


Figure 1 Study Schema

### 2.10.2 STEMI CONTROL PARTICIPANTS

STEMI control participants took part in 3 study visits as outlined in Table 5.

**Table 5 Breakdown of study visits for STEMI control participants**

	Study visit 1 - < 14 days	Study visit 2 – 6 months	Study visit 3 – 12 months
CMR	✓	✓	
Brain MRI	✓	✓	
Questionnaires	✓	✓	
Routine bloods	✓	✓	
ECG	✓	✓	
Echo	✓		
Follow up			✓

### 2.10.3 HEALTHY VOLUNTEERS

Healthy volunteers only required 1 study visit which is outlined in Table 6.

**Table 6 Breakdown of study visit for healthy volunteers**

	Study visit 1
CMR	✓
Brain MRI	✓
Questionnaires	✓
Routine bloods	✓
ECG	✓
Echo	
Follow up	

## 2.11 STUDY PROTOCOLS

To maintain consistency across all study visits, participants and researchers, a case report form was designed and used to standardise all study visits.

### *2.11.1 CLINICAL HISTORY*

Relevant demographic information and details of the participants' clinical presentation, past medical history, drug and social history and clinical examination were recorded for all MINOCA and STEMI participants.

### *2.11.2 BLOODS*

All participants had a full blood count (FBC), urea and electrolytes (UEs), c reactive protein (CRP), full lipid profile, hs-TnT and NT-proBNP collected by the time of the first study visit. These bloods were repeated at visits 2 and 3, if applicable.

### *2.11.3 ELECTROCARDIOGRAM*

All participants had a standard 12 lead electrocardiogram recorded at admission and at visits 2 and 3.

### *2.11.4 ECHOCARDIOGRAPHY*

All MINOCA and STEMI control participants had an echocardiogram prior to CMR as part of the standard clinical pathway for STEMI and for the further investigation of patients with MINOCA. Subsequent echocardiography at visits 2 and 3 were planned but this requirement was removed to allow the safe restart of the study during the coronavirus pandemic.

### *2.11.5 QUESTIONNAIRES*

All participants underwent standardised screening questionnaires at visit 1 for cognitive impairment (mini-mental state examination (MMSE)), anxiety and/or depression (hospital anxiety and depression score (HADS)) and perceived stress (perceived stress scale (PSS) and the brief illness perception questionnaire (B-IPQ)). These questionnaires were repeated at 6 months for the MINOCA and STEMI control participants and an extra questionnaire (impact of event scale – revised (IES-R)) was performed. Copies of the questionnaires are in Appendix A.

These questionnaires are well established and well validated methods for screening for cognitive impairment(143, 144), anxiety or depression(145) and stress perception(146-148). The collection of this data allowed for direct comparison of psychological differences between the three study groups and for quantitative comparison with the cardiac and brain MRI data.

The MMSE is a 30-point test which is quick and easy to perform. It comprises mainly verbal tasks which assess registration, attention and calculation, repetition, language, orientation to time and place, recall and requires patients to follow simple commands. It is routinely used as a screening test for cognitive impairment. However, it is poor at assessing visuospatial dysfunction and is thought to be influenced by age and education(149). A score of  $\geq 24$  suggests normal cognition.

The HADS is another very commonly used screening tool which was designed to identify anxiety and depression over the past 7 days in patients with a physical illness. It therefore does not assess somatic symptoms. It is split into two scores, HADS-D (depression) and HADS-A (anxiety) which are combined into a 14 multiple choice questions. A score of 0-7 is normal and  $\geq 8$  suggests the presence of anxiety or depression(145, 150).

The PSS-10 is a popular self-reported questionnaire for measuring the perception of stress during the past month. It comprises 10 questions answered on a 5-point Likert scale. It has been shown to correlate with biomarkers of stress such as cortisol(151). The questions are general in nature and assesses to what extent the patient's life has been 'unpredictable, uncontrollable and overloaded'(146). Although it not meant to be used as a diagnostic tool, it is accepted that the higher the score the higher the perceived stress. A score of 13 is around average (although this does vary slightly with age) and a score of  $>20$  is generally felt to represent high stress(152).

The B-IPQ comprises 8 questions each assessed on a 10-point scale and one open ended causal question which quickly assesses cognitive and emotional representations of illness. It is not assessed over a particular length of time. The patients' emotional representation of their illness affects patient behaviour and changing their emotional representation can improve recovery following myocardial infarction(153). The questionnaire assesses cognitive illness representations, emotional representations, and illness comprehensibility. Higher scores represent linear increases in the dimension being measured(147).

The IES-R scale comprises 22 questions assessed on a 5-point Likert scale. It is designed to assess the subjective distress caused by a traumatic event over the past 7 days. Questions address 14 of the 17 DSM-IV symptoms of post-traumatic stress disorder. A score of  $\geq 33/88$  is thought to be the best discriminator for a diagnosis of post-traumatic stress disorder(154) although this is not recommended for clinical practice.

### *2.11.6 CMR*

CMR was performed at 1.5-T (Magnetom Avanto, Siemens Healthineers, Erlangen, Germany) with a standard 12 channel matrix coil configuration. A comprehensive CMR protocol was conducted including

- i) short and long axis localisers
- ii) axial whole thorax half-Fourier acquisition single-shot turbo spin echo (HASTE)
- iii) coronal whole thorax single shot fast imaging with steady-state free precession (FISP)
- iv) steady-state free precession sequence images (SSFP) acquired in the standard 3 long-axis planes and a stack of short axis cines covering the left ventricle.
- v) T2-weighted short T1 inversion recovery (T2-STIR) sequence acquired in at least 5 slices in the short axis and a 4-chamber long axis plane

- vi) post gadolinium images in the same planes as the SSFP images performed 2 to 3 minutes post contrast administration (early gadolinium enhanced images (EGE)) and 8-10 minutes post contrast administration (late gadolinium enhanced images (LGE)).

Intravenous gadobutrol (Gadovist; Bayer Schering Pharma, Berlin-Wedding, Germany) was administered at a dose of 0.1 mmol/kg-1.

### **2.11.6.1 Steady-state free precession imaging**

This was a breath-hold segmented gradient echo sequence using conventional prospective ECG triggering with an 8mm slice thickness and no slice gap. If the image quality was deemed non-diagnostic due to arrhythmia then cine imaging with prospective triggering was used. If there was severe artefact due to poor breath holding technique then retrospective gating was used.

### **2.11.6.2 T2-weighted STIR sequence**

These were acquired using a breath-hold black-blood segmented turbo spin-echo technique with a triple inversion-recovery preparation module. This enabled the suppression of signal from fat and flowing blood with surface coil normalisation. The typical breath hold was 10-15 seconds depending on the patient's heart rate. To help with poor breath holders, turbo factor was increased as necessary.

### **2.11.6.3 Early gadolinium enhancement**

These images were acquired using an inversion-recovery prepared breath-hold gradient-echo sequence which was performed 3 minutes following gadolinium contrast administration.

### **2.11.6.4 Late gadolinium enhancement**

Firstly, a single-shot shallow breathing phase-sensitive inversion recovery (PSIR) SSFP sequence was performed increasing the yield of diagnostic images in patients who had significant difficulty holding their breath or had significant

arrhythmia. Following this, an inversion recovery prepared breath-hold segmented T1 gradient echo with a manually adjusted inversion time to effectively null the normal myocardium was performed 8-10 minutes post contrast administration. PSIR image reconstruction was performed using the same acquisition protocol which minimises the dependence of the image quality on the manually selected T1.

The full parameters for all sequences are described in Table 7.

Table 7 CMR sequence parameters

PARAMETER	SSFP	T2-STIR	EGE	LGE (MAG/PSIR)
FIELD OF VIEW	259x319	variable	260x320	260x320
FIELD OF VIEW PHASE (%)	81.3	81.3	81.3	81.3
REPETITION TIME (MSEC)	40	700	700	1022
ECHO TIME (MSEC)	1.13	74	3.17	3.17
FLIP ANGLE (DEGREES)	75	90	25	25
MATRIX	156x192	208 x 256	208 x 256	208 x 256
BANDWIDTH (HZ/PIXEL)	930	235	140	140
ECHO SPACING (MSEC)	variable	6.74	8.2	variable
trigger pulse	1	2	2	2
VOXEL SIZE	1.7x1.7x8	2.3 x 1.4 x 8	1.9 x 1.4 x 8	1.3 x 1.3 x 8
COIL NORMALISATION	No	yes	yes	No

The original protocol included native and post contrast T1 mapping and T2 mapping sequences. Unfortunately, due a scanner malfunction very early into recruitment (early April 2019), the mapping works-in-progress (WIPs) sequences were lost and so mapping was removed from the imaging protocol.

### 2.11.7 BRAIN MRI

The brain MRI was performed prior to the CMR on the same MRI scanner at 1.5-T using a 12-channel head coil. Participants underwent the following sequences:

- i) brain localisers
- ii) a T1 full volume high resolution 3D magnetisation prepared - rapid gradient echo (MP-RAGE)) sequence for volumetric quantitative analysis and to co-register the functional images
- iii) a T2\* weighted gradient echo planar sequence optimised for blood oxygen level dependent imaging (BOLD) for functional connectivity analysis.

The widespread availability of 1.5-T scanners means that this field strength has been the most commonly used for functional imaging previously, including in previously published retrospective rs-fMRI studies in takotsubo syndrome(63, 118). Although 3-T imaging brings higher sensitivity it can be limited by the increased susceptibility artefacts associated with scanning at increasing field strength(155). However, it was not ethically acceptable to transfer inpatients acutely to the 3-T scanner in a separate local hospital. During study design the clinical 1.5-T scanner in our unit was found to produce images of good diagnostic quality that would allow us to scan patients in the acute setting.

### **2.11.7.1 MP-RAGE sequence**

This acquisition lasted 5 minutes and the patient was instructed to lie as still as possible. The technical parameters were: TR 1900 ms; TE 2.91 ms; flip angle 15 degrees; N = 176 slices with 1.0 mm<sup>3</sup> voxel resolution; matrix 246 x 256; bandwidth 130Hz/Px.

### **2.11.7.2 BOLD sequence**

This acquisition lasted 12 minutes and the participant was instructed to lie as still as possible, with their eyes open in a resting state. The images were acquired in the axial plane parallel to the anterior and posterior commissure, excluding the cerebellum. The sequence parameters were 268 measurements, 38 slices, 3.1 mm slice thickness, TR 2620 ms, TE 40 ms, flip angle 80 degrees, matrix 64x64, voxel size 3.1 x 3.1 x 3.1mm, bandwidth 3552 Hz/Px, echo spacing 0.56 ms, EPI factor 64.



### *2.11.8 FOLLOW UP*

Telephone follow up was planned at 12 months following recruitment. Due to the unavoidable and unforeseen delays in the progression of the study and lack of resources it was not possible for this to be completed.

### *2.12 DATA ANALYSIS*

All the data generated from the study was manually inserted from the case report forms into a purpose built, pseudonymised excel spreadsheet.

#### *2.12.1 CMR ANALYSIS*

All scans were analysed offline using cvi42 (Circle Cardiovascular Imaging; Release 5.9.4 (1161)). Investigators were blinded to the CMR diagnosis, clinical details and the prior CMR (for visits 2 and 3).

##### **2.12.1.1 Volumes**

To quantify volumes the epicardium and endocardium were delineated on each axial slice using semi-automated feature recognition at end-diastole and end-systole. Any errors in contouring were manually corrected. The end-diastolic and end-systolic phases were assessed visually as the phase with the largest and smallest intra-cavity blood pool at mid ventricular level. Papillary muscles and non-compacted trabeculae were included as LV blood pool. LV slices were identified by the presence of >50% myocardium surrounding the blood pool. If the basal slice contained ventricular and atrial myocardium, then contours were manually drawn up to the junctions and joined together (Figure 2).

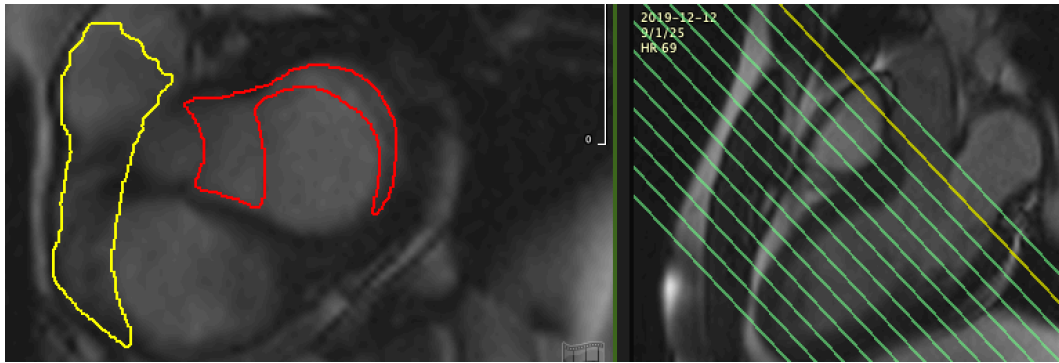


Figure 2 Example of how the basal slice was contoured for the LV and RV where both atrial and ventricular myocardium was present.

#### 2.12.1.2 Global longitudinal strain

Endocardial and epicardial borders were automatically contoured and manually adjusted on the end-diastolic phase for the whole short axis and 3 long axis slices. Subsequently the software's feature tracking algorithm was applied to determine the global longitudinal strain over the whole myocardium. Accurate tracking of the myocardium was checked visually and corrected manually. Scans which did not allow for accurate analysis were excluded.

For the functional analyses, global longitudinal strain as assessed by CMR (GLS-CMR) was chosen to be the only cardiac variable included in the regression analyses. Originally LVEF, LGE mass and oedema mass were also going to be included. However due to the large number of analyses which needed to be completed across several networks and multiple thresholds (see Chapter 4 Methods) this was not feasible. Therefore GLS-CMR was chosen as the sole variable to allow a representative analysis in a timely fashion. GLS-CMR is a measure of the global longitudinal function of the left ventricle and therefore is strongly correlated with the LVEF and is more sensitive to left ventricular dysfunction than LVEF (39, 156). It is not constrained by the falsely normal ejection fraction when the stroke volume to LV cavity size ratio is preserved. It is also likely to be related to the amount of oedema and LGE which may impair cardiac deformation. Therefore, it was felt to be the optimal measure to reflect all our previously chosen variables.

### 2.12.1.3 Oedema

Myocardial oedema was identified per segment and quantitatively. A 16 segment AHA model was used to identify myocardial segments. For the per segment analysis a region (>10 contiguous pixels) was manually drawn in each segment and in a region of remote normal skeletal muscle on the same axial slice (or nearest available slice if no skeletal muscle was visible). Care was taken to avoid contouring the endocardial border as this region frequently demonstrates very high T2 signal due to blood pooling. Myocardial oedema was deemed to be present, in the absence of artefact, if T2 signal intensity (T2SI) was  $\geq 2.0$  compared to skeletal muscle as per the updated Lake Louise criteria(30). For the quantitative analysis the previously drawn contours were derived onto the matching T2-STIR SA stack and manually adjusted. The Otsu method was selected to quantify the volume of myocardial oedema. This has been shown to be the superior method in terms of test-retest variability(157) for oedema analysis. This method estimates the threshold intensity from a histogram of all intensities to ensure there is minimal variance either side of the threshold(158). Scans which were deemed non-diagnostic due to suboptimal image quality were excluded from analysis.

### 2.12.1.4 Late gadolinium enhancement

LGE was identified by pattern (ischaemic, mid-wall, subepicardial, transmural/diffuse), per segment and quantitatively. Presence and pattern of LGE was assessed visually. If LGE was present in any part of a myocardial segment, then the whole segment was counted in the per segment analysis. Short axis contours were derived onto the matching short axis LGE images and manually corrected. A region of interest (ROI) was drawn in the area of highest signal intensity in affected myocardium and a separate ROI was drawn in a remote unaffected area. The full width half maximum (FWHM) method was used to quantify the mass of LGE as this has been shown to have good inter and intra-observer variability and test-retest repeatability(159). This method uses a threshold intensity as one midway between the mean intensity of normal remote myocardium and the maximal signal intensity within the affected area(160). Areas of microvascular obstruction or myocardial haemorrhage, which may affect the

FWHM method, were manually contoured separately so they were excluded from thresholding but included in the infarcted volume. Images which were deemed non diagnostic for pattern, segment or quantitative analysis were excluded (for example scans may have been of sufficient quality to determine the pattern of distribution or number of segments involved but not for quantitative analysis).

### 2.12.1.5 Diagnosis

The CMR diagnosis was recorded by a consultant cardiologist or radiologist with level 3 CMR accreditation at the time of imaging and recorded in the clinical notes as per the usual clinical pathway. The diagnosis was verified to meet the specified diagnostic definitions of the study by a member of the research team. If there was uncertainty regarding the final diagnosis this was reviewed by the second investigator and, if necessary, a third investigator adjudicated. Myocardial infarction was defined by the presence of subendocardial or transmural late gadolinium enhancement (LGE) in a typical coronary artery territory (Figure 3A). Acute myocarditis was defined by the presence of both myocardial oedema on T2-based imaging AND an area of high signal intensity in a nonischaemic pattern on LGE images as per the 2018 modified Lake Louise criteria(30)(Figure 3B). Previous myocarditis was defined by the presence of nonischaemic LGE if no oedema was present. TCM was defined by the presence of myocardial oedema  $\pm$  regional wall motion abnormality (RWMA) in a non-coronary distribution and the

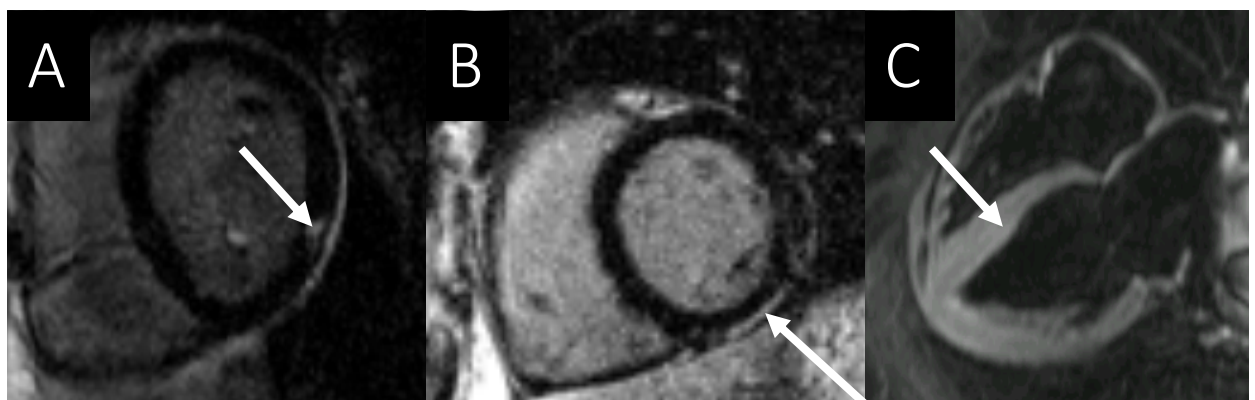


Figure 3 Illustrative examples of diagnoses on CMR

A - Short axis slice in the mid ventricle demonstrating focal near transmural LGE in the inferolateral segment (white arrow) in keeping with a focal myocardial infarction; B - Short axis slice in the basal ventricle demonstrating subepicardial LGE in the inferior segment (white arrow) in keeping with myocarditis; C – T2-STIR sequence demonstrating high signal and increased wall thickness in the mid and apical segments (white arrow) in keeping with diffuse myocardial oedema.

absence of LGE consistent with the international takotsubo (InterTAK) diagnostic criteria(161) (Figure 3C). Normal scans were defined by the absence of a RWMA (excluding dyssynchrony), oedema or LGE (excluding non-specific LGE at the left/right ventricular insertion points). Other diagnoses including hypertrophic cardiomyopathy, dilated cardiomyopathy and cardiac amyloidosis were defined using established tissue characterisation characteristics.

### *2.12.2 BRAIN ANALYSIS*

The DICOM images were transferred to the University of Bristol (UoB) DICOM server for analysis. All images were pseudonymised with a specific random 3 letter patient code (e.g. YDI) and visit code (e.g. P49) to ensure participant confidentiality and blinding of the investigators. All the DICOM files generated by the scanner were converted to NIfTI-1 format to ensure compatibility with the pre-processing software. SPM12 (Statistical Parametric Mapping) software was used within the Matlab environment for analysis of the data on a UoB workstation(162).

#### **2.12.2.1 Anatomical analysis**

The images were analysed using voxel-based morphometry (VBM)(163). To standardise the MRI scans across all the individuals to allow for meaningful statistical analysis, extensive pre-processing must occur. The key stages to this are spatial registration, segmentation, normalisation and spatial smoothing (163, 164). This process will be explained in more detail in Chapter 3.

#### **2.12.2.2 Functional analysis**

268 volumes were acquired by the scanner which corresponded to 268 NIfTI files per participant per visit. Once again, extensive pre-processing in line with existing literature and the SPM12 guide was carried out prior to statistical analysis as will be explained in chapter 4(162). Firstly, the images were adjusted to correct any differences in slice acquisition times caused by echo-planar scanning. This ensures the data on each slice corresponds to the same point in time. Next the images were realigned to match all the images to each other. This

acts to correct the images for movement over the duration of the scan. The images were then resliced to generate a new adjusted file(165). The adjusted images were then segmented as described previously into grey matter, white matter, CSF, bones, soft tissue and air. The images were then normalised to MNI space and resliced into another new file using a voxel size of 2x2x2 mm and a -90 to 90, 126 to 90, -72 to 108 bounding box. The new files were smoothed as previously described using a Gaussian kernel of 8mm full width at half maximum(166). The 3D volumes were then concatenated into a single 4D file. Finally, the segmented white matter and csf files were normalised using the existing deformation field to allow for nuisance regression in the statistical analysis.

Further preprocessing of the 4D file was required prior to statistical analysis. Previously written scripts by Christelle Langley and Jade Thai were used within Matlab for this purpose. Firstly, nuisance regression was performed where CSF, white matter and movement were regressed out from the signal generating a new 4D file. Next the timeseries for each region were extracted and bandpass filtered (0.01-0.08 Hz) to obtain the frequency of interest and remove filter activity not associated with the brain. We used the Automated Anatomical Labelling (AAL) atlas(61) to obtain neuroanatomical labels for our data. The cerebellum was excluded from analysis as this region was not required for our analysis, therefore the atlas included 90 brain regions. A simple weighted Pearson correlation matrix (90 x 90) was created to assess for correlations between each brain region described by the atlas and this was Fisher transformed to standardise it across different subjects. Finally, all negative correlations were removed and made positive to allow for analysis of the strength of correlation rather than the direction. As a result, a final weighted undirected correlation matrix was generated which was used for the final statistical analysis.

The statistical analysis of the functional brain data was divided into two parts: a global analysis and a more focussed hypothesis driven analysis focussing on specific brain networks.

For the global analysis, scripts from the brain connectivity toolbox(60) and a small world propensity script(167) were used. These scripts generate the measures of global efficiency, modularity and small world propensity described in Chapter 1. These global network measures could then be correlated with the clinical data and the measures for the whole MINOCA cohort could be compared with the control participants. In addition, the participants could be further subdivided into MINOCA subgroups to analyse for differences in global connectivity between subgroups. Further details about statistical methods used to answer the specific hypotheses are described in the relevant chapters.

For the hypothesis driven analysis, brain networks were chosen a-priori based on the existing literature as described in Chapter 1. These included sympathetic and parasympathetic networks(168), the default mode network(169), salience network(83) and central executive network(83) as described in chapter 4. The specified MNI coordinates were converted to AAL regions using xjView 10 (<https://www.alivelearn.net/xjview>). A new weighted connectivity matrix was then generated for each new network which only contained the specific AAL nodes. This was then used for the ROI analysis using network-based statistics (see Chapter 4).

### **2.12.2.3 Default Mode Network**

Table 8 shows the MNI coordinates used to determine the AAL network nodes of the default mode network.

**Table 8** Region of interest coordinates for the Default Mode Network based on the Montreal Neurological Institute coordinate system.

ROI in both hemispheres were included in the analysis. Table adapted from Andrews-Hanna et al. (2010) (169)

Region	X	Y	Z	AAL region
<b>PCC-aMPFC Core</b>				
Anterior medial prefrontal cortex	-6	52	-2	Cingulum_Ant
Posterior cingulate cortex	-8	-56	26	Precuneus
<b>dMPFD Subsystem</b>				
Dorsal medial prefrontal cortex	0	52	26	Frontal_Sup_Med
Temporal parietal junction	-54	-54	28	Supramarginal
Lateral temporal cortex	-60	-24	-18	Temporal_Inf
<b>MTL Subsystem</b>				
Ventral medial prefrontal cortex	0	26	-18	Rectus
Posterior inferior parietal lobule	-44	-74	32	Occipital_Mid
Retrosplenial cortex	-14	-52	8	Calcarine
Parahippocampal cortex	-28	-40	-12	Fusiform
Hippocampal formation	-22	-20	-26	Parahippocampal

#### 2.12.2.4 Central autonomic network

Table 9 shows the MNI coordinates for the regions of the sympathetic and parasympathetic networks which were taken from a meta-analysis which assessed central autonomic processing in humans(168) and are consistent with the nodes used in the recent Templin paper(62). The MNI coordinates were converted to AAL regions as previously explained.



**Table 9 MNI coordinates for nodes associated with sympathetic and parasympathetic regulation.**

Table adapted from Beissner et al 2013.

Region	x	y	z	Hemisphere	AAL region
<b>Sympathetic</b>					
Midcingulate cortex, paracingulate cortex, supplementary motor area	0	10	40	L/R	Cingulate_Mid
Supramarginal gyrus, superior parietal lobule, primary somatosensory cortex	48	-26	46	R	Postcentral
Amygdala, subgenual anterior cingulate cortex, nucleus accumbens, caudate, hippocampal formation	-20	-8	-12	L	Hippocampus
Ventromedial prefrontal cortex, pregenual/subgenual anterior cingulate cortex	-2	38	-18	L/R	Rectus
Anterior insula ventrolateral prefrontal cortex	44	18	-6	R	Insula
Thalamus, nucleus ruber, periaqueductal gray	-4	-16	6	L/R	Thalamus
Supramarginal gyrus, superior parietal lobule, primary somatosensory cortex	-44	-36	42	L	Parietal_Inf
Secondary somatosensory cortex, posterior insula, putamen	-32	-20	14	L	Insula
Dorsolateral prefrontal cortex	20	36	34	R	Frontal_Sup
<b>Parasympathetic</b>					
Hippocampal formation	30	-22	-16	R	Hippocampus
Amygdala, ventral tegmental area, hypothalamus	-20	-6	-18	L	Amygdala
Anterior insula, caudate	-40	0	12	L	Insula
Precuneus, dorsal posterior cingulate cortex	-6	44	34	L/R	Cingulate_Mid
Primary motor cortex, temporal pole	-56	6	8	L	Frontal_Inf_Oper
Middle temporal gyrus, superior temporal gyrus	50	-24	2	R	Temporal_Sup
Supramarginal gyrus, angular gyrus,	44	-38	14	R	Temporal_Sup
Anterior insula	40	2	12	R	Insula

### 2.12.2.5 Salience Network

Table 10 shows the MNI coordinates used for the region of interest analysis of the salience network. These are taken from Seeley et al(83) and were also referenced in the Silva paper showing increased connectivity (63) .

Table 10 MNI coordinates for the salience network.

FEF – frontal eye field;

Region	x	y	z	Hemisphere	AAL region
<b>Paralimbic</b>					
Orbital frontoinsula	42	10	-12	R	Insula
	-40	18	-12	L	Frontal_Inf_Orb
Temporal pole	52	20	-18	L/R	Temporal_Pole_Sup
Paracingulate	0	44	28	L	Frontal_Sup_Med
Dorsal ACC	6	22	30	R	Cingulate_Mid
	-6	18	30	L	Cingulate_Ant
SMA/pre-SMA	6	8	58	L/R	Supp_Motor_Area
<b>Neocortical</b>					
Superior temporal	64	-38	6	R	Temporal_Mid
	-62	-16	8	L	Temporal_Sup
Parietal operculum	58	-40	30	R	Supramarginal
	-60	-40	40	L	Parietal_Inf
Frontal pole	-24	56	10	L	Frontal_Sup
Ventrolateral PFC	42	46	0	R	Frontal_Mid
Dorsolateral PFC	-38	52	10	L	Frontal_Mid
<b>Subcortical/Limbic</b>					
Ventral striato-pallidum	22	6	-2	L/R	Putamen
Thalamus, dorsomedial	12	-18	6	R	Thalamus
SLEA/paraolfactory	-28	4	-18	L	Amygdala

### 2.12.2.6 Central executive network

Table 11 shows the ROI coordinates for the central executive network which is also taken from the Seeley paper and was referenced in a recent neuroimaging study(170).

Table 11 MNI coordinates used for the central executive network analysis

Region	x	y	z	Hemisphere	AAL region
<b>Paralimbic</b>					
Orbital frontoinsula	-26	24	-10	L	Insula
<b>Neocortical</b>					
Dorsolateral PFC	46	46	14	L/R	Frontal_Mid
Ventrolateral PFC	34	56	-6	L/R	Frontal_Mid_Orb
Frontal operculum	56	14	14	R	Frontal_Inf_Oper
DM PFC	0	35	46	L	Frontal_Sup_Med
Lateral parietal	38	-56	44	L/R	Parietal_Inf
Inferior temporal	58	-54	-16	R	Temporal_Inf
<b>Subcortical</b>					
Caudate, dorsal	12	14	4	L/R	Caudate
Thalamus, anterior	10	2	8	L/R	Thalamus

### *2.12.3 PLAN OF STATISTICAL ANALYSIS*

Specific details on statistical methods used to answer specific hypotheses are described in each chapter.

STATA (version 17) was used for all statistical analysis. In summary, continuous data will be presented as mean  $\pm$  SD or median (IQR) as appropriate. Categorical variables will be presented as counts or proportions. Normality will be assessed by visual assessment of histograms and by using the skewness and kurtosis tests for normality where necessary. Comparisons between groups will be performed using the student t test or the Mann Whitney U test, or with ANOVA or Kruskal-Wallis when comparing multiple groups for continuous variables. The chi square test will be used for categorical variables. For data involving repeated measurements in the same group of patients over time, the corresponding paired tests will be used. Variables included in regression models will be pre-specified on clinical grounds or based on previously published associations.

## Chapter 3 NOVEL INSIGHTS INTO BRAIN ANATOMICAL CHANGES IN MINOCA

---

### 3.1 INTRODUCTION

Patients presenting with a myocardial infarction but who have non-obstructive coronary arteries (MINOCA) on angiography are commonly encountered in cardiology. These patients can have a wide range of diagnoses but typically are found to have a myocardial infarction, myocarditis or takotsubo syndrome (TS) (8, 17). Patients with TS have a higher prevalence of neurological and psychiatric disorders than patients with obstructive disease and around two-thirds of patients have a physical or emotional trigger in the 12 hours before the onset of symptoms(112, 171). The autonomic nervous system is thought to be a key driver of inflammation and forms a central part of the proposed pathomechanism of TS(46). These findings have led several investigators to explore if there are particular anatomical differences in the brain structure of these patients. There are now several small retrospective neuroimaging studies which have identified structural brain differences in patients with TS. Hiestand et al showed decreased grey matter volume in the left and right amygdala and at the amygdala/hippocampus border compared to healthy controls(114). Klein et al identified several anatomical differences in regions of the brain involved in autonomic cardiac control (supplementary motor areas, both paracentral gyri, left superior parietal lobe, putamen, hippocampus, precuneus and medial temporal gyrus) and emotional processing (insula, amygdala and orbitofrontal areas) compared to healthy controls. The amygdala, an important component of the autonomic nervous system and in the response to stress, has been shown to have increased activity on 18 F-FDG-PET/CT imaging in patients who go on to develop TS years before its onset(119).

In patients with MINOCA, there is a higher prevalence of anxiety and depression than the healthy population(172) and a higher incidence of preceding emotional stress and psychiatric illness compared to patients with obstructive

coronary disease even when patients with TS are excluded(173). The reasons for this are unknown. A recent PET/CT study has shown that amygdala activity is strongly associated with adverse cardiovascular outcomes (including myocardial infarction), which is likely to be mediated by arterial inflammation which might partly explain the finding in the MINOCA population (102). Yet there are no neuroimaging studies examining the MINOCA population as a whole. Given the potential importance of the link between brain function and cardiovascular outcomes in this patient group, further research is warranted.

The overall aim of the study therefore, was to investigate anatomical grey matter volume differences in patients with MINOCA compared to patients with an acute ST-elevation myocardial infarction (STEMI) and healthy control participants. A further aim was to explore any differences in a subgroup of patients with acute TS.

Our hypotheses were:

*Hypothesis 1:* there will be a reduction in grey matter volume in regions of the brain associated with the limbic and autonomic nervous systems in MINOCA compared to STEMI and healthy controls

*Hypothesis 2:* there will be associations between measures of heart function, anxiety, stress and depression and grey matter volume in the MINOCA group and if present, these will be different to such associations in the STEMI and healthy control groups.

*Hypothesis 3:* any differences/associations seen will also be present in a subgroup analysis comprising of just patients with TS when compared to healthy and STEMI controls.

### 3.2 *METHODS*

The study design and recruitment are explained in detail in Chapter 2 and will only be summarised here.

In this prospective cohort study, all patients presenting to a single tertiary cardiology centre (Bristol Heart Institute, Bristol, UK) with MINOCA, as defined by the 2017 ESC working group paper on MINOCA(9), were approached for inclusion in the study. The full inclusion and exclusion criteria are described in Chapter 2.

Two control groups were recruited. The STEMI control group included patients who were admitted to the Bristol Heart Institute with ST-segment elevation on the ECG and who had an occluded epicardial coronary artery at invasive angiography. The second 'healthy control' group included volunteers with no prior known history of cardiovascular or neurological disorders. Volunteers were recruited through advertising in local media and within the Bristol Heart Institute. Due to the ongoing coronavirus pandemic and changing restrictions imposed on visiting the hospital, the healthy volunteers largely comprised NHS staff who were already based at the University Hospitals Bristol and Weston NHS Foundation Trust (UHBW). The study was reviewed and approved by the local institutional review board (South Hampshire B research ethics committee) and all patients gave written informed consent.

All patients completed a standardised proforma documenting their demographics, clinical history, past medical history, cardiovascular risk factors and medications at presentation. All patients underwent routine blood testing including full blood count, high sensitivity C reactive protein (CRP), high sensitivity Troponin T and NT-proBNP. MINOCA and STEMI control patients had transthoracic echocardiography (TTE) performed as part of their routine clinical care. In addition, all patients underwent a mini mental state examination (MMSE), the hospital anxiety and depression score (HADS), perceived stress scale (PSS) and the brief illness perception questionnaire (B-IPQ) to evaluate their baseline psychological status immediately prior to the CMR and brain MRI.

### *3.2.1 MRI PROTOCOLS*

#### **3.2.1.1 CMR**

CMR was performed at 1.5-T (Magnetom Avanto, Siemens Healthineers, Erlangen, Germany). A comprehensive CMR protocol was performed including steady-state free-precession sequence images acquired in the standard 3 long-axis planes and a stack of short axis cines covering the left ventricle; T2-weighted short T1 inversion recovery (T2-STIR) sequence images acquired in at least 5 slices in the short axis and 4-chamber long axis plane; post gadolinium images were acquired using standard inversion recovery segmented gradient echo sequences performed 2-3 minutes post contrast administration (early gadolinium enhanced images) and 8-10 minutes post contrast administration (late gadolinium enhanced images). Intravenous gadolinium-chelate contrast agent (gadobutrol) was administered at a dose of 0.1 mmol/kg<sup>-1</sup>.

#### **3.2.1.2 Brain MRI**

Brain MRI was performed immediately prior to CMR at 1.5-T (Magnetom Avanto, Siemens Healthineers, Erlangen, Germany) using a 12-channel head coil. A T1-weighted inversion recovery 'magnetisation prepared rapid acquisition gradient echo' (MPRAGE) scan was acquired for volumetric anatomical quantitative analysis.

#### **3.2.1.3 Analysis**

All CMR studies were reviewed by a consultant with >15 years of CMR experience. Scans were analysed using cvi42 (Circle Cardiovascular Imaging; Release 5.9.4 (1161). Myocardial oedema was identified by regional (>10 contiguous pixels) high T2 signal intensity (T2SI) or a global T2SI  $\geq 2.0$  on T2 weighted images as per the updated Lake Louise criteria (30). LGE distribution was assessed visually.

Myocardial infarction was defined by the presence of subendocardial or transmural LGE in a typical coronary artery territory. Myocarditis was defined by

the presence of both of the 2018 modified Lake Louise criteria(30). TS was defined by the presence of myocardial oedema, regional wall motion abnormality (RWMA) in a non-coronary distribution and the absence of LGE consistent with the international takotsubo (InterTAK) diagnostic criteria (2018)(161). Normal scans were defined by the absence of a RWMA (excluding dyssynchrony), oedema or LGE (excluding non-specific LGE at the left/right ventricular insertion points). Other diagnoses including hypertrophic cardiomyopathy, dilated cardiomyopathy and cardiac amyloidosis were defined using established tissue characterisation characteristics.

### 3.2.2 *VOXEL-BASED MORPHOMETRY*

The pseudonymised brain scans were analysed using VBM to quantify grey matter volume(163, 164). Statistical parametric mapping package (SPM12; Wellcome Trust Centre for Neuroimaging, <http://www.fil.ion.ucl.ac.uk/spm>) was implemented in MATLAB (Mathworks Inc., Matick, MA, USA; release 2015a) for the pre-processing and analysis of the data. Firstly, every region of the brain was registered to the Montreal Neurological Institute (MNI) template which standardises brain structure across patients. The images were checked to ensure they approximately matched the standard MNI space and orientation. Default parameters were used unless specified. Secondly, the images were segmented to separate out tissue classes such as CSF, grey and white matter. Segmentation works by using tissue probability maps which calculate the chance of a certain tissue type being present in each voxel. Segmentation is also used to normalise the scan into the standard stereotactic MNI space which is achieved by generating deformation fields for each scan. Finally, the images were smoothed to correct for any remaining slight anatomical differences between subjects. This changes the intensity of each voxel to the weighted average of the surrounding voxels. A FWHM of 8 mm was used for smoothing to determine the size of the Gaussian used to define the weight of the neighbouring voxels.

Statistical analysis could then be performed using SPM12. The statistical model was specified, and the relevant images were selected for analysis. An



explicit mask was created based on the average grey matter probability map in MNI space using a threshold of 0.05. This explicit mask visually had a better fit to the AAL template than the default mask. Covariates were pre-specified as age, gender and total intracranial volume (TIV) as these variables are known to influence brain anatomy. Comparison of grey matter volume between cohorts was carried out using a two-way unpaired student t-test using the specified covariates. T contrasts were specified as [1 -1] and [-1 1] to assess for increased or decreased grey matter volume between the two groups being assessed. This has the effect of subtracting the beta of the second group from the first and testing it against zero. Multiple regression analyses were performed using variables (e.g. anxiety score) which would test for associations between grey matter volume and test scores.

Finally, the selection of significance level is very important in this type of analysis. As the analysis is applied across very many voxels, the analysis must be corrected for multiple comparisons to prevent false positives. Simple Bonferroni correction is not suitable as it too conservative and will lead to very many false negatives due to the fact that the Z scores at each voxel are highly correlated with their neighbours and not 'independent'. Family-wise error (FWE) uses random field theory and is a better way to deal with the problem of multiple comparisons. It is the most stringent at reducing false-positives with a very low rate, but consequently has a higher false negative rate, meaning potentially important areas of reduced grey matter volume will be missed(174). The false discovery rate (FDR) correction is more lenient and allows the user to apply their own statistical threshold. However, the lower the threshold the higher the proportion of false positives and thus this will greatly influence the pattern of grey matter loss and the results of the study. Larger studies, or studies with a large effect size, will tend to use the FWE method. Our results will be presented as FWE corrected with an  $\alpha < 0.05$ (174). Voxel level results are reported rather than cluster levels due to inconsistencies in smoothness in VBM image data. The results were visualised using xjView toolbox (<https://www.alivelearn.net/xjview>).

### 3.2.3 LIMITATIONS OF VBM

There are some important limitations of VBM to be aware of. Firstly, the normalisation process is imperfect, and accuracy will vary between subjects and between brain regions depending on the correspondence between subjects and the complexity of the brain region being normalised. Smoothing can aid normalisation, but this relies on an arbitrary kernel size. This can lead to variations in statistical sensitivity across different regions of the brain(175).

### 3.2.4 STATISTICAL ANALYSIS

Statistical analysis was performed using STATA (version 17). Normality of continuous data was assessed by visually assessing histograms and by using the skewness and kurtosis tests for normality where necessary. Continuous data are presented as mean  $\pm$  standard deviation or median  $\pm$  interquartile range dependent on the normality of their distribution. Categorical variables are presented as counts and proportions. Based on the normality of the data, comparisons of continuous variables between groups were performed using the student t test or the Mann Whitney U test and categorical variables using the chi square test.

To address the first hypothesis, comparison of grey matter volume in each voxel between MINOCA and each of the control groups separately was carried out using a one-way unpaired student t-test including age, gender and total intracranial volume as covariates. To address the second hypothesis, multiple regression analyses were used to assess for associations between pre-specified cardiac variables (left ventricular ejection fraction (LVEF,) global longitudinal strain (GLS), oedema mass, late gadolinium enhancement mass (LGE) mass, MMSE score, anxiety and depression scores, PSS, presence of self-reported mental health illness) and grey matter volumes in each group. For the final hypothesis the analysis was repeated but only including patients with a CMR diagnosis of TS. All statistical analyses were corrected for multiple comparisons using the stringent family-wise error method (FWE). A very conservative T threshold of  $T > 5$  was

selected to minimise the chance of false positive results(174). Values of  $p < 0.05$  were deemed as demonstrating evidence against the null hypothesis.

### 3.3 RESULTS

#### 3.3.1 STUDY PARTICIPANTS

239 consecutive patients presented to the Bristol Heart Institute with MINOCA over the study period and were screened by the research team. Figure 4 details the study flow chart. The study period ran from 1/2/2019 to 16/3/2020 and 1/08/2020 to 31/01/2021 due to an enforced suspension related to the global coronavirus pandemic. 127 patients were recruited in total including 72 patients who met the MINOCA inclusion criteria, 27 STEMI controls and 28 healthy controls. Two healthy controls were subsequently excluded due to the presence of a previous episode of myocarditis and a dilated RV on the CMR.

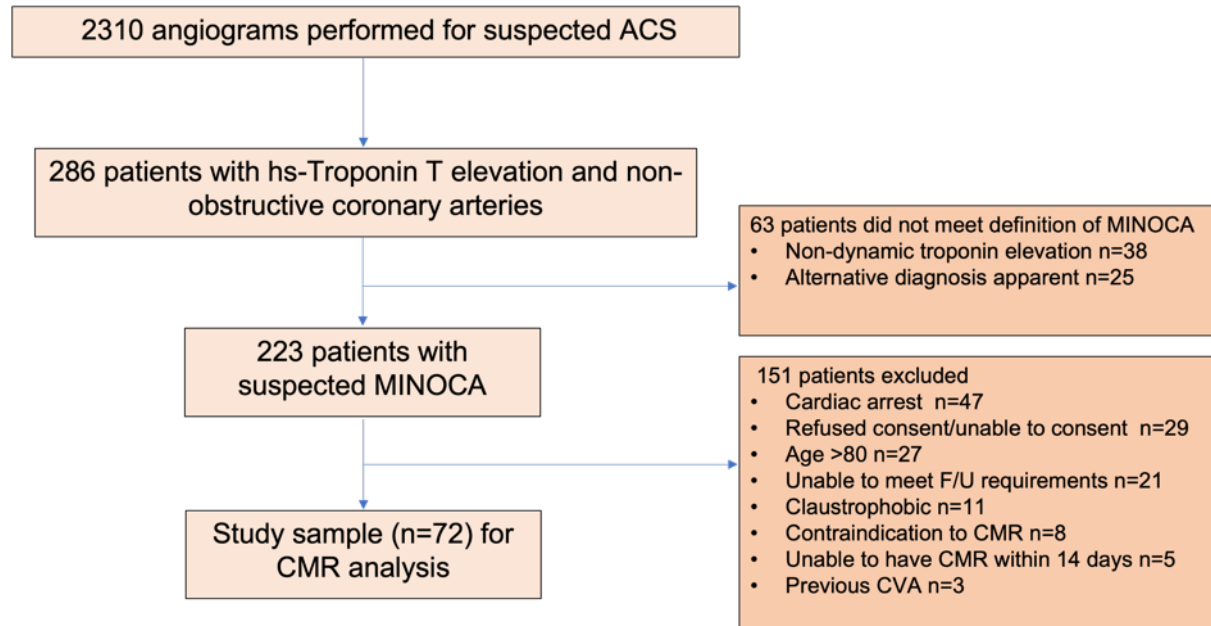


Figure 4 Study Flow Chart

ACS – acute coronary syndrome, CVA – cerebrovascular accident

Table 12 illustrates the demographics of the study groups. There was no significant difference in age and sex between the MINOCA group or the STEMI or healthy control group.

Table 12 Study group baseline demographics

Variable	MINOCA (n=72)	STEMI (n=27)	P value MINOCA v STEMI	Healthy (n=26)	P value MINOCA v Healthy
Age, median [IQR], years	57 [47-66]	61 [49-70]	0.229	53 [47-60]	0.183
Female sex, n (%)	34 (47)	8 (30)	0.115	15 (58)	0.360
Caucasian, n (%)	66 (92)	27 (100)	0.495	24 (92)	0.671
BMI, mean [SD], kg/m <sup>2</sup>	28.0 [6.2]	29.3 [4.4]	0.333	27.3 [5.6]	0.6303
Right-handed, n (%)	61 (85)	25 (93)	0.510	21 (81)	0.506
<b>Medical history, n (%)</b>					
Hypertension	26 (36)	13 (48)	0.275	2 (8)	<b>0.006</b>
Diabetes	9 (13)	5 (18)	0.586	1 (4)	0.211
Dyslipidaemia	17 (24)	12 (44)	<b>0.043</b>	1 (4)	<b>0.026</b>
<b>Smoking status</b>					
Current smoker	18 (25)	6 (22)	0.709	1 (4)	<b>0.044</b>
Former smoker	18 (25)	9 (33)		6 (23)	
Never smoker	36 (50)	12 (44)		19 (73)	
Family history of MI	17 (24)	7 (26)	0.811	3 (12)	0.709
Prior MI	5 (7)	1 (4)	0.709	0 (0)	0.168
Malignancy	7 (10)	3 (11)	0.838	0 (0)	0.099
Mental health disease	24 (33)	3 (11)	<b>0.027</b>	2 (8)	<b>0.011</b>
<b>Symptoms at presentation, n (%)</b>					
Chest pain	71 (99)	25 (93)	0.120	n/a	n/a
Breathlessness	28 (39)	12 (44)	0.616	n/a	n/a
Palpitations	14 (19)	2 (7)	0.147	n/a	n/a
Syncope	3 (4)	4 (15)	0.066	n/a	n/a
Recent viral illness	12 (17)	4 (15)	0.824	0 (0)	<b>0.026</b>
Recent physical or mental stressor	6 (8)	0 (0)	0.122	0 (0)	0.129
ST-elevation myocardial infarction presentation	22 (31)	27 (100)	<b>&lt;0.001</b>	n/a	n/a
<b>Medication on Admission n (%)</b>					
Single antiplatelet	8 (11)	2 (7)	0.586	0 (0)	0.076
Dual antiplatelet	0 (0)	0 (0)	n/a	0 (0)	n/a
Beta-blocker	11 (15)	1 (4)	0.116	0 (0)	<b>0.034</b>
ACEi/ARB	17 (24)	7 (26)	0.811	0 (0)	<b>0.006</b>
Statin	15 (21)	4 (15)	0.498	1 (4)	<b>0.045</b>
<b>Electrocardiogram findings, n (%)</b>					
Heart rate, mean [SD], bpm	76 [17]	75 [16]	0.770	71 [16]	0.146
ST-segment depression	9 (13)	20 (77)	<b>&lt;0.001</b>	0 (0)	0.059
T-wave inversion	12 (17)	4 (15)	0.824	0 (0)	<b>0.026</b>
Left bundle-branch block	0 (0)	0 (0)	n/a	0 (0)	n/a
Q waves	3 (4)	4 (15)	0.824	0 (0)	0.287
Normal electrocardiogram	33 (46)	0 (0)	<b>&lt;0.001</b>	24 (92)	<b>&lt;0.001</b>
<b>Echocardiography (n=91)</b>					
Segmental RWMA, n (%)	23 (35)	23 (92)	<b>&lt;0.001</b>	n/a	n/a
LVEF, median [IQR], %	55 [52-60]	55 [45-58]	0.071	n/a	n/a
<b>Laboratory Investigations</b>					
Peak Troponin T, median [IQR], ng/L	187 [54-517]	3095 [1450 – 5616]	<b>&lt;0.001</b>	5 [5-6]	<b>&lt;0.001</b>
CRP, median [IQR], mg/L	5 [2-17]	2 [1-8]	0.186	1 [1-2]	<b>&lt;0.001</b>
NT-pro-BNP, median [IQR], pg/ml	139 [69-517]	1085 [711-1766]	<b>&lt;0.001</b>	42 [21-59]	<b>&lt;0.001</b>
Total cholesterol, median [IQR], mmol/L	3.4 [2.6-4.3]	5.3 [3.2-6.5]	<b>0.021</b>	n/a	n/a

LDL-cholesterol, median [IQR], mmol/L	2.2 [1.5-3.0]	3.2 [2.2-3.9]	<b>0.004</b>	n/a	n/a
Triglycerides, median [IQR], mmol/L	1.5 [1-2.1]	1.4 [1-2.5]	0.809	n/a	n/a
<b>Coronary Angiography</b>					
<b>Maximal stenosis by visual estimation by operator</b>					
<b>LAD</b>			n/a		
0%	47 (65)	2 (7)			
1-29%	17 (24)	7 (25)			
30-49%	8 (11)	0 (0)			
50-69%	0 (0)	3 (11)			
70-99%	0 (0)	4 (15)			
100%	0 (0)	11 (41)			
<b>Cx</b>					
0%	55 (76)	13 (48)			
1-29%	15 (21)	4 (15)			
30-49%	2 (3)	1 (4)			
50-69%	0 (0)	3 (11)			
70-99%	0 (0)	2 (7)			
100%	0 (0)	4 (15)			
<b>RCA</b>					
0%	53 (74)	10 (37)			
1-29%	16 (22)	6 (22)			
30-49%	3 (4)	1 (4)			
50-69%	0 (0)	0 (0)			
70-99%	0 (0)	0 (0)			
100%	0 (0)	10 (37)			

### 3.3.1.1 Risk Factors

There were no significant differences between any self-reported cardiovascular risk factors (hypertension, diabetes mellitus, hypercholesterolaemia, smoking and family history of premature myocardial infarction (<65 years)) between MINOCA and STEMI groups. Patients with MINOCA were significantly more likely to self-report a history of previous mental health disease than both STEMI and healthy controls. There was no difference between the presence of a recent mental or physical stressor between MINOCA or the control groups, but there was in TS patients compared to STEMI and healthy controls respectively ( $p=0.003$  and  $p=0.004$ ).

### 3.3.1.2 Cardiac Investigations

31% of MINOCA patients presented with ST-segment elevation on the ECG. MINOCA patients had a lower peak troponin, NT-pro-BNP, total cholesterol and LDL-cholesterol than STEMI patients (Table 12). There was weaker evidence of a difference in ejection fraction during the index admission on

echocardiography. On angiography, 40 (56%) MINOCA patients had smooth coronary arteries without any degree of obstruction.

### 3.3.1.3 Psychological Questionnaires

MINOCA patients had lower baseline MMSE scores and higher anxiety, depression and perceived stress scores (PSS) than healthy controls (Table 13). MINOCA patients had higher anxiety scores than STEMI patients but there was no strong evidence for a difference in MMSE, depression score or PSS. MINOCA patients had less understanding of their condition compared to STEMI patients on the B-IPQ.

Table 13 Results of the psychological questionnaires

Variable	MINOCA (n=72)	STEMI (n=27)	P value MINOCA v STEMI	Healthy (n=26)	P value MINOCA v Healthy
<b>MMSE, median [IQR]</b>	29 [28-29]	29 [28-30]	0.780	30 [29-30]	<b>0.001</b>
<b>Anxiety, mean [SD]</b>	8.0 [4.0]	6.0 [3.3]	<b>0.025</b>	4.4 [3.2]	<b>&lt;0.001</b>
<b>Depression, median [IQR]</b>	4 [2-6.5]	2 [1-4]	0.057	1 [0-3]	<b>&lt;0.001</b>
<b>Perceived Stress Scale, mean [SD]</b>	17.2 [8.0]	14.5 [7.8]	0.136	9.5 [6.2]	<b>&lt;0.001</b>
<b>Understanding, median [IQR]</b>	6.5 [4-8]	8 [6-9]	<b>0.048</b>	n/a	n/a

### 3.3.1.4 CMR Findings

Table 14 summarises the CMR findings. MINOCA patients were scanned a median of 4 days later than STEMI patients and had significantly higher EF than STEMI patients and lower GLS. MINOCA patients had significantly less LGE and oedema than STEMI patients.

CMR identified a diagnosis in 76% of MINOCA patients with acute myocardial infarction being the most frequent diagnosis. 100% of STEMI patients had evidence of a myocardial infarction on the CMR.

Table 14 CMR Findings

Variable	MINOCA (n=72)	STEMI (n=27)	P value MINOCA v STEMI	Healthy (n=26)	P value MINOCA v Healthy
Days from admission to CMR, median [IQR]	6 [3-8]	2 [1-2]	<0.001	n/a	n/a
LVEF, median [IQR], %	59 [53-61]	51 [45-56]	<0.001	62 [60-65]	<0.001
iLVEDV, median [IQR], ml/m <sup>2</sup>	80 [74-88]	79 [69-91]	0.670	86 [68-97]	0.545
iLVSV, median [IQR], ml/m <sup>2</sup>	46 [41-53]	37 [35-44]	<0.001	53 [41-59]	0.030
iLV mass, median [IQR], g/m <sup>2</sup>	55 [48-64]	62 [55-66]	0.080	51 [46-62]	0.119
RVEF, median [IQR], %	57 [53-61]	56 [52-60]	0.452	58 [51-63]	0.533
iRVEDV, median [IQR], ml/m <sup>2</sup>	79 [70-91]	72 [64-86]	0.032	95 [73-110]	0.058
MAPSE, median [IQR], mm	12 [10-13]	10 [8-11]	0.013	14 [12-15]	0.003
TAPSE, mean [SD], mm	21 [4.9]	21 [3.5]	0.483	24 [5.0]	0.016
GLS, mean [SD], %	-16.0 [-17.4 - 13.9]	-12.4 [-14.3 - -11.2]	<0.001	-17.9 [-20 - -15.9]	<0.001
Presence of LGE, n (%)	44 (61)	25 (93)	0.002	0 (0)	<0.001
<b>Pattern of LGE n. (%)</b>					
Ischaemic	27 (61)	25 (100)	0.019	n/a	n/a
Mid-wall	7 (16)	0		n/a	
Subepicardial	8 (18)	0		n/a	
Diffuse/patchy	1 (2)	0		n/a	
Insertion point	1 (2)	0		n/a	
Number of segments of LGE, median [IQR]	1 [0-2]	5 [3-6]	<0.001	0 [0]	<0.001
LGE mass, median [IQR], g	0.6 [0-4.8]	18.4 [7.1 - 32]	<0.001	0 [0]	<0.001
MVO, n (%)	2 (3)	13 (48)	<0.001	0 (0)	0.391
Presence of oedema, n (%)	45 (63)	27 (100)	<0.001	0 (0)	<0.001
Number of segments of oedema, median [IQR]	1 [0-5]	7 [5-8]	<0.001	0 [0]	<0.001
Oedema mass, median [IQR], g	7 [0-24]	44 [28 - 53]	<0.001	0 [0]	<0.001
<b>CMR Diagnosis</b>					
Myocarditis	15 (21)	0 (0)	<0.001	0 (0)	<0.001
MI	27 (38)	27 (100)		0 (0)	
TS	11 (15)	0 (0)		0 (0)	
Other cardiomyopathy	2 (3)	0 (0)		0 (0)	
Normal/non-specific	17 (24)	0 (0)		26 (100)	

LVEF – left ventricular ejection fraction; RVEF – right ventricular ejection fraction; iLVEDV – indexed left ventricular end-diastolic volume; iLVSV – indexed left ventricular stroke volume, iLV mass – indexed left ventricular mass; MAPSE – mitral annular plane systolic excursion; TAPSE – tricuspid annular plane systolic excursion; GLS – global longitudinal strain; LGE – late gadolinium enhancement; MVO – microvascular obstruction; MI – myocardial infarction; TS – takotsubo syndrome

### 3.3.2 ANATOMICAL BRAIN CHANGES

The two-sample t-tests comparing grey matter volumes between MINOCA patients and healthy controls showed that MINOCA patients had increased grey matter volume in the putamen compared to healthy controls (Figure 5) and reduced grey matter volume in widespread regions of the brain (Figure 6).

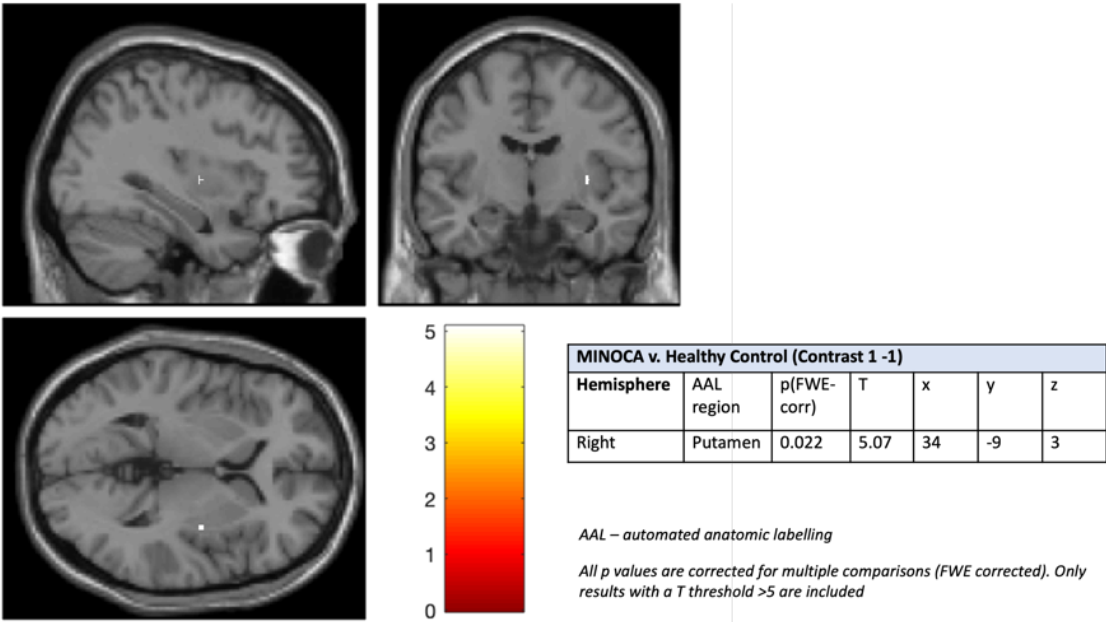


Figure 5 Brain activation map showing region of increased grey matter volume in MINOCA patients compared to healthy controls

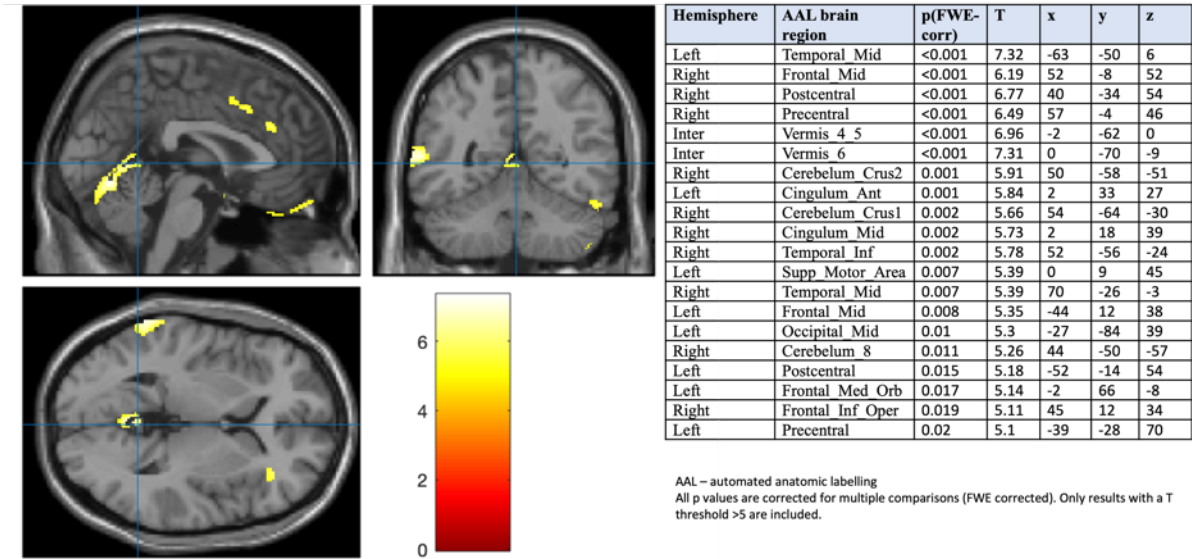


Figure 6 Brain activation map showing regions of reduced grey matter volume in MINOCA patients compared to healthy controls



There were no significant differences between grey matter volume between MINOCA patients and STEMI patients at the high significance level applied.

### 3.3.2.1 Subgroup Analysis

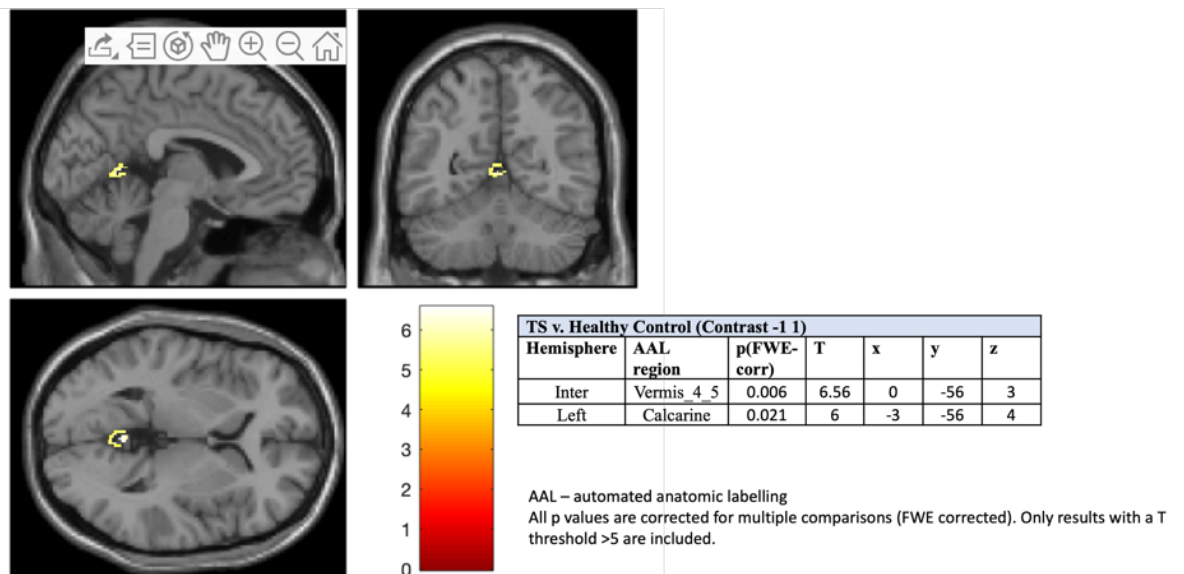
Demographics broken down by subgroup are shown in Table 15.

Table 15 Demographics and results by subgroups

Variable	Acute Myocarditis	MINOCA	TS
Age, median [IQR], years	51 [25-64]	53 [47-61]	68 [60-70]
Female sex, n (%)	6 (43)	9 (35)	9 (90)
Caucasian, n (%)	14 (100)	24 (92)	10 (100)
BMI, mean [SD], kg/m <sup>2</sup>	25.6 (6.5)	29.7 (6.5)	23.7 (5.9)
Right-handed, n (%)	12 (86)	21 (81)	9 (90)
<b>Medical history, n (%)</b>			
Hypertension	3 (21)	8 (31)	3 (30)
Diabetes	1 (7)	2 (8)	2 (20)
Dyslipidaemia	5 (36)	4 (15)	3 (30)
<b>Smoking status</b>			
Current smoker	3 (21)	7 (27)	4 (40)
Former smoker	6 (43)	5 (19)	2 (20)
Never smoker	5 (36)	14 (54)	4 (40)
Family history of MI	3 (21)	8 (31)	4 (40)
Prior MI	0 (0)	1 (4)	0 (0)
Malignancy	1 (7)	2 (8)	2 (20)
Mental health disease	3 (21)	9 (34)	6 (60)
<b>Symptoms at presentation, n (%)</b>			
Chest pain	14 (100)	26 (100)	10 (100)
Breathlessness	3 (21)	11 (42)	2 (20)
Palpitations	1 (7)	1 (4)	2 (20)
Syncope	0 (0)	1 (4)	2 (20)
Recent viral illness	6 (43)	3 (12)	0 (0)
Recent physical or mental stressor	0 (0)	3 (12)	4 (40)
ST-elevation myocardial infarction presentation	8 (57)	7 (27)	4 (40)
<b>Laboratory Investigations</b>			
Peak Troponin T, median [IQR], ng/L	135 [94-663]	333 [114-525]	497 [286-1225]
CRP, median [IQR], mg/L	23 [5-54]	5 [2-15]	3 [1-15]
NT-pro-BNP, median [IQR], pg/ml	132 [93-292]	142 [69-260]	2940 [609-6246]
Total cholesterol, median [IQR], mmol/L	3.4 [2.7-3.6]	4.3 [2.8-5.2]	2.8 [2.5-4.1]
<b>Psychological Questionnaires</b>			
MMSE, median [IQR]	29 [28-29]	29 [28-29]	29 [27-30]
Anxiety, mean [SD]	7.0 [6-12]	6.5 [4-10]	8.0 [7-9]
Depression, median [IQR]	2.5 [2.4]	5.4 [4.6]	4.7 [4.2]
Perceived Stress Scale, mean [SD]	16.0 [8.7]	17.4 [8.0]	16.0 [7.3]
<b>CMR Findings</b>			
Days from admission to CMR, median [IQR]	4.5 [2-11]	4.5 [2-7]	3 [2-7]
LVEF, median [IQR], %	60 [56-62]	57 [54-61]	47.5 [42-59]

iLVEDV, median [IQR], ml/m <sup>2</sup>	81 [74-96]	81 [75-89]	78.5 [70-81]
iLVSV, median [IQR], ml/m <sup>2</sup>	48.5 [46-54]	46 [42-54]	37 [34-46]
iLV mass, median [IQR], g/m <sup>2</sup>	59 [48-75]	56.5 [48-65]	54.5 [48-60]
RVEF, median [IQR], %	58 [52-62]	57.5 [54-61]	59 [56-61]
iRVEDV, median [IQR], ml/m <sup>2</sup>	83.5 [70-110]	81.5 [72-98]	68.5 [60-76]
GLS, mean [SD], %	-18.1 [2.4]	-17.3 [2.3]	-9.2 [4.4]
Presence of LGE, n (%)	14 (100)	24 (92)	2 (20)
<b>Pattern of LGE n. (%)</b>			
Ischaemic	0 (0)	24 (100)	2 (20)
Mid-wall	7 (50)	0 (0)	0 (0)
Subepicardial	7 (50)	0 (0)	0 (0)
Diffuse/patchy	0 (0)	0 (0)	0 (0)
Insertion point	0 (0)	0 (0)	0 (0)
Number of segments of LGE, median [IQR]	1 (1-2)	2 [1-2]	0 [0-0]
LGE mass, median [IQR], g	0.92 [0.30-3.1]	3.12 [1.78-6.45]	0 [0-0]
Presence of oedema, n (%)	8 [57]	23 [88]	10 [100]
Number of segments of oedema, median [IQR]	1 [0-4]	2 [1-4]	7.5 [6-9]
Oedema mass, median [IQR], g	1.1 [0-38]	11.8 [4.9-16.5]	32.8 [25.8-42.7]

Patients with TS had reduced grey matter volume in the cerebellar vermis and left calcarine fissure and surrounding cortex compared to healthy controls (Figure 7). Our study did not demonstrate any other significant differences in grey matter volumes between patients with TS compared to healthy or STEMI patients.



**Figure 7 Brain activation map showing region of reduced grey matter volume in TS patients compared to healthy controls**

A sensitivity analysis was performed as 3/11 patients with TS had a previous episode of TS and thus may not have had ‘acute’ brain changes. When these patients were excluded from analysis the difference in the cerebellar vermis remained ( $p^{\text{FWE}} = 0.01$ ,  $T 6.55$ ) but not in the calcarine fissure and surrounding cortex. There remained no grey matter differences between TS patients and STEMI patients.

### 3.3.3 REGRESSION ANALYSIS

#### 3.3.3.1 Psychological

There was a negative association between a self-reported history of mental health disease and grey matter volume in the left opercular part of the inferior frontal gyrus (Table 16). There was also a negative association between MMSE score and grey matter volume in the right putamen (Appendix B). There were no associations between grey matter volume and anxiety, depression or perceived stress scores seen in patients with STEMI or healthy controls.

**Table 16 Regions where grey matter volume negatively correlates with prior history of mental health disease**

Hemisphere	AAL region	p(FWE-corr)	T	x	y	z
Left	Frontal_Inf_Oper	0.023	5.27	-44	18	14

#### 3.3.3.2 Cardiac

There was a positive association between global longitudinal strain as measured by CMR (GLS-CMR) and grey matter volume in multiple brain regions (Table 17). There were no other correlations between LGE mass, oedema mass, LVEF or peak troponin T. In the STEMI group there were also positive correlations in similar frontal and temporal brain regions to the MINOCA group (Appendix B).

However, there was no association between grey matter volume and GLS-CMR in the healthy control group, although there were positive correlations with LVEF (Appendix B).

Table 17 Regions of the brain in which grey matter volume positively correlate with GLS

Hemisphere	AAL region	p(FWE-corr)	T	x	y	z
Left	Frontal_Inf_Orb	<0.001	8.67	-18	24	-24
Left	ParaHippocampal	<0.001	8.6	-28	-20	-26
Right	Frontal_Sup_Orb	<0.001	7.75	16	21	-22
Right	Occipital_Mid	<0.001	7.67	26	-88	2
Right	Cingulum_Mid	<0.001	7.65	10	-40	42
Right	Lingual	<0.001	7.5	12	-60	6
Right	Hippocampus	<0.001	7.48	30	-4	-24
Right	Fusiform	<0.001	7.3	38	-20	-32
Left	Temporal_Mid	<0.001	7.22	-52	-69	20
Right	ParaHippocampal	<0.001	7.22	28	-16	-26
Right	Temporal_Mid	<0.001	7.11	56	-8	-22
Left	Occipital_Mid	<0.001	7.04	-39	-80	18
Left	Frontal_Mid	<0.001	7.01	-40	45	27
Left	Frontal_Sup_Medal	<0.001	6.98	-8	18	39
Right	Precuneus	<0.001	6.93	3	-51	27
Left	Rolandic_Oper	<0.001	6.84	-57	10	2
Left	Lingual	<0.001	6.76	-14	-82	-10
Left	Parietal_Sup	<0.001	6.72	-33	-69	54
Left	Frontal_Sup	<0.001	6.68	-24	36	46
Left	Occipital_Inf	<0.001	6.63	-33	-90	-12
Left	Cingulum_Mid	<0.001	6.47	-6	27	33
Right	Occipital_Inf	<0.001	6.46	36	-78	-2
Left	Frontal_Inf_Oper	<0.001	6.41	-56	6	16
Left	Parietal_Sup	<0.001	6.41	-21	-56	60
Left	Supp_Motor_Area	0.001	6.38	-6	9	44
Right	SupraMarginal	0.001	6.38	58	-36	27
Right	Cerebelum_8	0.001	6.31	26	-68	-44
Right	Parietal_Inf	0.001	6.18	51	-57	38
Left	Frontal_Sup_Orb	0.002	6.07	-15	44	-22
Left	Frontal_Inf_Oper	0.002	5.99	-51	14	33
Left	Cingulum_Mid	0.002	5.95	-12	-38	40
Right	Postcentral	0.003	5.92	27	-46	57
Left	Fusiform	0.003	5.87	-42	-64	-14
Right	Paracentral_Lobule	0.003	5.85	9	-38	58
Left	Precuneus	0.004	5.81	-8	-64	39
Right	Cerebelum_6	0.005	5.75	44	-38	-30

Right	Insula	0.005	5.74	38	-15	14
Left	SupraMarginal	0.006	5.68	-54	-44	34
Left	Supp_Motor_Area	0.006	5.67	-9	-12	60
Left	Thalamus	0.007	5.64	-10	-9	3
Right	Cuneus	0.008	5.59	16	-94	8
Left	SupraMarginal	0.014	5.42	-64	-38	30
Left	Cerebelum_6	0.02	5.31	-27	-51	-34
Right	Temporal_Inf	0.02	5.31	52	-22	-22
Left	Temporal_Pole_Sup	0.024	5.25	-34	12	-28
Left	Precentral	0.025	5.24	-46	-8	44
Right	Temporal_Sup	0.029	5.19	45	-20	-2
Left	Cerebelum_8	0.032	5.16	-34	-62	-48
Right	Supp_Motor_Area	0.034	5.14	8	-16	62
Right	Angular	0.035	5.13	62	-56	24
Right	Frontal_Sup	0.039	5.1	15	-6	64
Right	Frontal_Sup_Medial	0.04	5.09	9	36	44
Right	Frontal_Mid	0.041	5.09	39	21	32
Left	Calcarine	0.041	5.08	-15	-56	10
Right	Angular	0.042	5.08	46	-54	32
Left	Caudate	0.045	5.06	-4	12	4

AAL – automated anatomic labelling

All p values are corrected for multiple comparisons (FWE corrected).

### 3.4 DISCUSSION

Our results show for the first time that: 1) there are widespread reductions in grey matter volume in patients with MINOCA compared to healthy controls, although there was no difference compared to STEMI controls; 2) MINOCA patients have increased grey matter volume in the putamen compared to healthy controls, but not STEMI controls; 3) there are widespread positive associations between grey matter volume and GLS-CMR in the MINOCA group; 4) there is reduced grey matter volume in the cerebellar vermis and left calcarine fissure and surrounding cortex in patients with acute TS

#### 3.4.1 ANATOMICAL DIFFERENCES

We have shown, for the first time, widespread reductions in grey matter volume in patients with MINOCA compared to healthy controls. Our sample was large (72 MINOCA patients) with robust correction for multiple comparisons (FWE method). This suggests that patients with MINOCA have diffuse structural abnormalities across the brain which may affect multiple functional networks. The most significant of these were in the bilateral middle temporal gyrus, bilateral postcentral and precentral gyri, left anterior cingulate gyrus, right median cingulate gyrus, right inferior temporal gyrus, left middle frontal gyrus and right inferior frontal gyrus. There were also several locations in the cerebellum. Interestingly, there were no differences between the MINOCA and STEMI groups suggesting that these differences are not unique to MINOCA and may also be present in the STEMI population. It is plausible that there is an acute change in grey matter volume in acutely unwell patients generally. Because the MINOCA group included 39% of patients with an MI, the phenotype of the MINOCA and STEMI groups overlapped, and this also may have reduced the subsequent ability to detect a difference between the groups. However, this is only hypothesis generating and further studies looking at the STEMI population are warranted.

There is early evidence linking anatomical and functional changes in the brain to adverse cardiovascular outcomes(102, 110, 111, 119), but there are no studies examining this link in patients with MINOCA, despite the higher prevalence of mental health disease in this cohort(112). Anxiety and depression are very common conditions globally and have been associated with several anatomical brain changes(176, 177). Patients with major depressive disorder have been shown to have widespread and varied reductions in grey matter volume following VBM analysis (137, 176). The largest VBM study in non-geriatric patients with major depressive disorder demonstrated significant volume reductions in regions including the dorsolateral prefrontal cortex, anterior cingulate cortex and medial orbital frontal cortex, but it also included a small cluster in the left putamen(176). These regions are typically shown to be abnormal in functional brain analyses of patients with depression(137). In comparison, patients with generalised anxiety disorder have been shown to have reduced grey matter

volume in the dorsolateral prefrontal cortex, hippocampus, insula, thalamus, superior temporal gyrus but increased volume in the amygdala(178-181). These anatomical locations are areas of the brain integral to several established functional networks which have direct control over cardiac function via the autonomic nervous system and the hypothalamic-pituitary-adrenal axis(78).

The middle temporal gyri have been shown to be activated in response to happy and fearful audio-visual stimuli and is thus important in the audio-visual perception of emotion(182). The anterior and medial cingulate gyri are part of the cingulate cortex which has multiple projections to the medullary and spinal nuclei and central to the autonomic nervous control of the heart(79). It has an important role in reward and learning pathways(183) and demonstrates reduced grey matter volume in patients with major depressive disorder (177). The cingulate cortex are also part of the default mode network and salience networks (83, 84). The default mode network is active during wakeful rest and has importance in thinking about oneself and others, mind-wandering, remembering the past and planning for the future(65). The salience network is involved in complex functions including communication and self-awareness(66). Finally, reduced grey matter volume has also been previously shown in the right inferior frontal gyrus in patients with depression (184, 185) and this region is also thought to be involved in empathy, interpersonal interaction and communication(186).

We have also shown increased grey matter in the right putamen in MINOCA patients compared to healthy controls. The putamen is a subcortical structure which forms part of the striatum and is involved in social learning and reward processing(187). The striatum also receives dopaminergic inputs and has extensive connections with emotional processing regions such as the amygdala(187). Previous studies in patients with social anxiety disorder have shown reduced grey matter volume in the left putamen (188, 189) but there are no VBM studies in MINOCA for comparison. We speculate that increased volume in the putamen in patients with MINOCA contributes to their increased emotional

dysregulation and this leads to overactivity of the amygdala and subsequent overactivity of the autonomic nervous system.

In summary there are extensive structural differences in multiple brain regions involved in the emotional processing centres of the brain which may provide a substrate for the pathogenesis of MINOCA and explain the high prevalence of anxiety, depression and psychiatric comorbidity in these patients. However, since MINOCA is a heterogenous cohort of patients and no difference was seen with the STEMI control arm, these results are exploratory and further work is required.

### *3.4.2 RELATIONSHIP BETWEEN BRAIN VOLUME AND PSYCHOLOGICAL AND CARDIAC VARIABLES*

#### **3.4.2.1 Psychological**

Patients with MINOCA who had a history of mental health disease had reduced grey matter volume in the opercular part of the inferior frontal cortex compared to those without such a history. This area is part of the ventrolateral prefrontal cortex, is typically involved in speech and has been shown to have reduced volume in schizophrenia(190) although it is not known to have any definite role in anxiety, depression or stress. The ventrolateral prefrontal cortex does however have functions within the reward and motivation systems. It has inputs from the orbitofrontal cortex and the amygdala(191) and shows increased activation in reward sensitive individuals (192). It is possible that individuals with MINOCA have lower reward sensitivity and therefore are less likely to display goal-directed behaviours due to the reduced sensation of pleasure when achieving a goal. This may partly explain the association with prior mental health disease which are often characterised by loss of motivation.

#### **3.4.2.2 Cardiac**

This is the first study to associate markers of cardiac function with grey matter volume. Our results showed that there are widespread positive associations between grey matter volume and GLS-CMR in patients with MINOCA.



Therefore, patients with MINOCA with a higher GLS (i.e. worse LV function, normal GLS is  $<-18\%$ ) have increased grey matter volume in many areas of the brain. In the STEMI control group, there were also relatively widespread associations between grey matter volume and GLS-CMR and many of these areas overlapped with the MINOCA group, most notably in frontal lobe regions of the brain (Appendix B). The diffuse nature of our findings suggests there may be previously underappreciated complex interactions between brain structure and/or function and cardiac systolic function. As this is the first time this analysis has been performed and the associations are so extensive it is difficult to interpret but this could be used as a basis for future studies.

In the healthy control group, there was no association between GLS-CMR and grey matter volume, although there were multiple positive associations with LVEF (Appendix B). Higher LVEF typically represents greater LV function (and lower GLS). The association with LVEF was surprising, but they are notable as many of these regions (bilateral hippocampus, right insula, cingulate cortex) are key components of many known emotional processing networks and have outputs to the autonomic nervous system. Thereby there may be a mechanism linking increased grey matter volume, and therefore a greater ability to process emotion or stress and increased LV function in the healthy population.

### *3.4.3 TAKOTSUBO SYNDROME SUBGROUP ANALYSIS*

Previous work has focussed on the heart-brain interaction in TS. Our subgroup analysis of patients with takotsubo syndrome showed reduced grey matter volume in the cerebellar vermis and left calcarine fissure and surrounding cortex, which includes part of the posterior cingulate cortex (PCC). This is a surprising result and is not entirely consistent with previous literature which is summarised in Table 18. This may be because our sample size was smaller and so lacked the power to identify small differences, the shorter interval to scanning or due to the different methodology between the studies. The cerebellar vermis is primarily involved in movement but has recently been implicated in cognitive and mood dysregulation(193, 194). Connections from the vermis to the hypothalamus

and limbic system have been demonstrated(195) confirming the anatomical substrate for the involvement in the emotional processing centres which have been described previously in TS(114, 115). The most important regions in animal models for the interaction with the autonomic nervous system and emotional response were lobuli III to VII of the vermis which would be in keeping with our findings (196). Our results would support a role for the cerebellum in the pathophysiology of takotsubo syndrome, but further work is required to assess this hypothesis.

Table 18 Summary of previous studies examining grey matter differences in TS

Reference	Method	TS Participants	Time to brain MRI	Anatomical Region	Result
Klein et al (2017)(64)	VBM	19	168 $\pm$ 267 days	Nil	n/a
Hiestand et al (2018)(114)	VBM	20	342 $\pm$ 274 days	Amygdala (bilateral) Right amygdala/hippocampus border	Reduced
	SBM			Antero-ventral insula (bilateral) Cingulate cortex (bilateral)	Reduced
Dichtl et al (2020)(115)	VBM	13	<72 hours	Right middle frontal gyrus Right insula Left central opercular cortex Right paracingulate gyrus Thalamus (bilateral) Left cerebral cortex Left amygdala Right subcallosal cortex	Reduced

VBM – voxel based morphometry; SBM – surface based morphometry

#### 3.4.1 STUDY PARTICIPANTS

Our MINOCA population demographics are aligned with the existing literature, confirming our representative population and that the only significant difference between the MINOCA and STEMI group is the presence of hyperlipidaemia(8). MINOCA patients were more likely to have a history of self-reported mental health illness than STEMI patients as previously reported (172, 173). This was supported by the fact that our MINOCA patients had significantly higher baseline anxiety scores compared to both STEMI and healthy control groups. MINOCA patients were scanned a median of 4 days later than STEMI

patients. This was largely unavoidable due to the difference in priority for invasive angiography. STEMI patients are taken directly to the catheter lab on admission whereas patients with an NSTEMI presentation (which made up 69% of the MINOCA cohort and 0% of the STEMI cohort) generally have to wait several days for their procedure. Theoretically, as oedema is known to reduce over time, this could lead to a systematic bias which would underestimate oedema in patients presenting with an NSTEMI compared to STEMI. Nevertheless, any reduction in oedema over this short period is likely to be small and is unlikely to have a significant material impact on our results. This is because we know the diagnostic yield of CMR is high up to 2 weeks after presentation(17). The ESC taskforce recommend scanning all patients with TS within a window of 7 days (49) and 81% of patients with myocarditis still had oedema present at up to 2 weeks from presentation. This all suggests that oedema is still demonstrable and diagnostic when our MINOCA patients were scanned.

### 3.4.2 *STUDY LIMITATIONS*

There are several limitations to our work. Firstly, it was not possible to collect cardiac physiological data during acquisition of the neuroimaging data as our study used the clinical MRI scanner. This means it was not possible to regress out possible nuisance variables like cardiac and respiratory deformation. Although our recruitment was strong (49% of eligible MINOCA patients were recruited), there may still be recruitment bias with frailer, 'sicker' or more anxious patients less likely to be recruited. In addition, recruitment occurred before and during the COVID-19 pandemic; this was a highly stressful event and may have led to increased stress, anxiety and depressive symptoms in patients recruited during the pandemic compared to those before (57 MINOCA, 21 STEMI recruited before COVID-19; 15 MINOCA, 6 STEMI and 27 healthy volunteers recruited after COVID-19).

Due to a scanner malfunction 2 months into recruitment, T1/T2 mapping and ECV quantification was not possible in 90% of our cohort and so this was excluded from the analysis. These quantitative measures are known to increase

diagnostic sensitivity and specificity and would have provided an alternative method to quantify myocardial oedema and scar/fibrosis.

#### 3.4.2.1 Clinical Implications

This exploratory study raises several further important clinical questions that need addressing. Patients with MINOCA are distinct from the healthy population in terms of their psychological and neuroanatomical state. These differences may provide future therapeutic targets for psychological or pharmacological therapies. Indeed, there may even be novel therapeutic options which could target autonomic brain activation or modulate its potentially harmful pro-inflammatory consequences. The lack of a significant grey matter volume difference between MINOCA and STEMI patients is interesting and, given the overlap with MI, may suggest there are structural brain differences across all patients with acute myocardial infarction. This is a potentially very significant finding given how frequently MIs occur and the high morbidity and mortality. This study was not designed to address the STEMI population and, as such, further work is urgently needed to investigate this potentially important finding.

### 3.5 CONCLUSIONS

Patients with MINOCA have diffuse reductions in grey matter volume compared to healthy controls, but not compared to STEMI patients. There are strong associations between grey matter volume and GLS-CMR in MINOCA and STEMI patients and between LVEF and grey matter volume in healthy patients. A history of previous mental health disease correlates with reduced grey matter volume in the left inferior frontal gyrus. Our novel results suggest there are complex diffuse anatomical brain changes in MINOCA patients which provide a basis for further work in understanding the brain-heart interaction in these patients.

## Chapter 4 NOVEL INSIGHTS INTO ACUTE FUNCTIONAL BRAIN CHANGES IN MINOCA

---

### 4.1 INTRODUCTION

The brain consists of many spatially distant but functionally connected regions which form networks(197, 198). In graph theory, a network is made up of nodes (anatomical regions in our study) and the connections (edges) between them (see chapter 1 for full explanation). Resting-state fMRI measures spontaneous low-frequency fluctuations in the Blood -Oxygen-Level -Dependant (BOLD) signals to investigate the functional connectivity of brain networks(199). The default mode network (DMN)(169, 200), central executive network (CEN)(83), sympathetic and parasympathetic networks(168) and salience network(83) are examples of such networks which have previously been shown to be altered compared to healthy controls in patients with takotsubo syndrome(TS), as described in chapter 1(62, 63, 115). The idea that dysfunction within a node or an edge results in abnormal signalling which can influence the whole subnetwork is key to all neuroimaging studies(67).

#### 4.1.1 DEFAULT MODE NETWORK

The DMN is a resting state 'core intrinsic' network. It is therefore activated during the resting state or 'free-thinking' and is deactivated during tasks(200). It is comprised of three brain regions: i) the ventral medial prefrontal cortex, ii) the dorsal medial prefrontal cortex and iii) the posterior cingulate cortex, adjacent precuneus and lateral parietal cortex. The role of the DMN is not fully understood but it is involved in emotional processing, the recollection of previous events and self-referential judgements(201). The components of the DMN used in this study are shown in Chapter 2 Table 8

#### *4.1.2 SYMPATHETIC AND PARASYMPATHETIC NETWORKS*

The central autonomic network has been characterised by Beisnner et al(168) in a meta-analysis of human neuroimaging studies. The autonomic nervous system can exert beat to beat control over cardiac function so understanding the higher cortical control of this network is important in helping our understanding of cardiac physiology and pathophysiology. The sympathetic and parasympathetic networks have different components which are shown in Chapter 2 Table 9, but they include core regions in the left amygdala, right anterior insula and midcingulate cortices.

#### *4.1.3 SALIENCE NETWORK*

The salience network is another core intrinsic network which is built around paralimbic structures including the dorsal anterior cingulate cortex and the anterior insula(83). The full list of nodes is shown in Chapter 2 Table 10. The individual components of the salience network have diverse functions but overall, the network is thought to integrate incoming sensory data with the internal environment to aid decision making. Hyperactivity in the anterior insula has been consistently shown in anxiety disorders (67, 202).

#### *4.1.4 CENTRAL EXECUTIVE NETWORK*

The CEN is a fronto-parietal system which includes core regions in the dorsolateral prefrontal cortex and the lateral posterior parietal cortex(83). The full description of the nodes in our study are shown in chapter 2, Table 11. The CEN is implicated in working memory, decision making and problem-solving and is disrupted in nearly every major psychiatric disorder (67).

#### *4.1.5 NETWORK MEASURES*

In addition, the application of graph theory to brain imaging has allowed the characterisation of complex networks through measures of global brain network connectivity called network measures (58, 60). Measures such as global efficiency (60, 203) (a measure of brain integration), modularity (60, 204) (a

measure of segregation of brain networks) and small world propensity (167) (a measure of efficiency but adjusted for network density) provide quantification of global properties of the brain network. Larger values suggest greater brain integration, segregation, and a more efficient structure, greater synchronisation and information flow (205, 206). These global network measures have been shown to be abnormal in patients with anxiety and depression, although results are inconsistent(136, 139, 207-209). Differences in global network measures in patients with MINOCA and how these global network measures may be associated with psychological scores (anxiety, depression and stress) and measures of cardiac function (GLS-CMR), is not known.

### 4.1.6 MINOCA

MINOCA is a common working diagnosis in cardiology(9). These patients have been shown to have a higher prevalence of anxiety and depression than the healthy population(172) and, compared to patients with obstructive coronary disease, have a higher prevalence of preceding stress and psychiatric illness, even when excluding the patients with TS (173). MINOCA is a heterogenous group, usually encompassing patients who will have had a myocardial infarction, an episode of myocarditis or TS(8). The reasons for why this diverse group should have similar psychological and psychiatric profiles are not known. However, there is recent evidence to suggest that upregulation of the amygdala, a key component in the autonomic nervous system and often dysregulated in anxiety, depression and stress(104), increases the risk of major adverse cardiac events due to increased arterial inflammation(102) and plaque instability(111). Dysregulation of the autonomic nervous system is also likely to be a contributing factor in the aetiology of TS(46, 210). Therefore, it is possible that there is overlap in the risk factors for both myocardial infarction and TS to explain their similar psychological profiles.

Global longitudinal strain (GLS-CMR) as measured by feature tracking on CMR is a quantitative measure of left ventricular systolic function and is more sensitive measure of early systolic dysfunction than ejection fraction(39, 211). The

larger the insult to the myocardium, the greater the degree of dysfunction and the worse the prognosis(212, 213). No previous studies, to our knowledge, have examined the quantitative relationship between cardiac dysfunction and brain connectivity. It is plausible that these variables will be correlated, with patients with greater anxiety, depression and stress scores having greater LV dysfunction due to more extensive dysregulation in the brain networks regulating the autonomic nervous system e.g. sympathetic and parasympathetic networks.

#### 4.1.7 HYPOTHESES

Our hypotheses for this study were that:

- i) patients with MINOCA would have higher anxiety and stress scores than both control groups.
- ii) patients with MINOCA would have reduced global efficiency, modularity and small world propensity compared to both control groups.
- iii) anxiety, depression, stress and GLS-CMR would negatively correlate with global efficiency, modularity and small world propensity in MINOCA patients.
- iv) patients with MINOCA would have reduced connectivity on region of interest and whole brain network analysis in networks comprising the autonomic and limbic systems compared to both control groups. Anxiety, depression, stress and GLS-CMR would negatively correlate with whole brain and regional connectivity in MINOCA patients.

##### *Subgroup Analysis*

- v) patients with TS would have reduced global efficiency, modularity and small world propensity compared to both control groups
- vi) patients with TS would have reduced connectivity in subnetworks involving the amygdala and autonomic nervous system compared to both control groups.



## 4.2 *METHODS*

The study design has been described in full elsewhere (Chapters 2 and 3) and so is only summarised here. All patients presenting to a single tertiary cardiology centre (Bristol Heart Institute) with MINOCA(9) were approached for inclusion in the study. The study flow chart is shown in chapter 3 Figure 4. All study participants underwent routine blood sampling, electrocardiography, echocardiography and psychological questionnaires prior to brain MR and CMR. Psychological questionnaires included the hospital anxiety and depression scale (HADS), perceived stress scale (PSS) and the brief illness perception questionnaire (bIPQ) which are well established and have been extensively validated(145, 147, 214). The CMR protocol is described in full in chapter 3 and included standard SSFP cine, T2-STIR and post gadolinium imaging.

### 4.2.1 *BRAIN MRI*

Brain MRI was acquired prior to CMR at 1.5T (Magnetom Avanto, Siemens Healthineers, Erlangen, Germany) using a 12-channel head coil. For the functional analysis, a T2\* weighted gradient echo planar sequence optimised for blood oxygen level dependent imaging (BOLD) was acquired. The acquisition lasted 12 minutes and the patient was asked to remain as still as possible with their eyes open in the resting state. The images were acquired in the axial plane parallel to the anterior and posterior commissure, excluding the cerebellum. The sequence parameters were 268 measurements, 38 slices, 3.1 mm slice thickness, TR 2620 ms, TE 40 ms, flip angle 80 degrees, matrix 64x64, voxel size 3.1 x 3.1 x 3.1mm, bandwidth 3552 Hz/Px, echo spacing 0.56 ms, EPI factor 64.

### 4.2.2 *FUNCTIONAL DATA ANALYSIS*

268 volumes were acquired. Statistical parametric mapping software (SPM12) implemented in MATLAB (release 2015a) was used for pre-processing. Firstly, the images were corrected to adjust for differences in the acquisition time between slices. The images were realigned and resliced to remove movement artefact. The adjusted images were then segmented into grey matter, white

matter, CSF, bones, soft tissue and air and then normalised to MNI space and orientation and resliced again using a voxel size of 2x2x2 and a -90 to 90, 126 to 90, -72 to 108 bounding box. The new images were smoothed with a Gaussian kernel (FWHM of 8 mm). The final 3D volumes were concatenated into a single 4D file and the segmented white matter and CSF were normalised using the existing deformation field.

Nuisance regression was performed to regress out CSF, white matter and movement from the signal generating a new 4D file. Next, the timeseries for each region were extracted and bandpass filtered (0.01-0.08 Hz) to obtain the frequency of interest and discard nuisance frequencies. We used the Automated Anatomical Labelling (AAL) atlas(61) to obtain neuroanatomical labels for our data. The cerebellum was excluded as this region was not required for our analysis and so the atlas included 90 brain regions. A simple weighted Pearson correlation matrix (90 x 90) was created to assess for correlations between each brain region described by the atlas and this was Fisher transformed to standardise it across different subjects. Finally, all negative correlations were removed and made positive to allow for analysis of the strength of correlation rather than the direction. As a result, a final weighted correlation matrix was generated which was used for the final statistical analysis.

#### 4.2.3 GLOBAL NETWORK MEASURES

For the global analysis, scripts from the brain connectivity toolbox(60) and a small world propensity script(167) were used. These scripts generate the global efficiency, modularity and small world propensity network measures described in chapter 1.

#### 4.2.4 FUNCTIONAL ANALYSIS USING NETWORK-BASED STATISTICS

The network-based statistic (NBS) toolbox(215) (<https://www.nitrc.org/projects/nbs/>), implemented in Matlab (version R2019b; <https://www.mathworks.com>), was used to analyse the weighted connectivity matrices derived from the rs-fMRI data. NBS is a statistical method to adjust for

multiple comparisons based on cluster-based statistical methods in mass univariate testing. This method allows for increased power to detect distributed networks rather than being able to test significance of single connections.

NBS uses the well-established general linear model (GLM) approach for analysis. The hypothesis that there was no significant increase or decrease in connectivity in each specified network between each group was tested in turn using an unpaired one-tailed t-test (MINOCA v STEMI or MINOCA v healthy control). NBS tests the specified hypothesis at every connection in the network (mass univariate testing). Using guidelines in the NBS manual and in line with previous studies(62), a threshold was manually determined through experimentation and all connections with a value higher than this set threshold were further assessed. NBS then identifies 'topological clusters' within these supra-threshold connections which is a set of supra-threshold connections joining two specified nodes. Finally, to determine the significance of each network a FWER-corrected p-value was calculated using permutation testing (5000 permutations). The component extent option was specified to allow detection of weak effects but distributed across many connections. Our analysis tested for reduced and increased connectivity, and we tested across a wide range of set thresholds ( $t=1.0$  to  $t=\text{maximum threshold}$ ) to fully explore the networks. One was a more stringent threshold and the other was a lower, more liberal threshold. Effects seen at the more stringent thresholds are likely to be characterised by strong, topologically focal differences and at the lower threshold subtle yet topologically extended. The arbitrariness these thresholds could be seen as a criticism of NBS because as the threshold changes, new networks can appear, and existing statistically significant networks can change in size. However, NBS always ensures control of the FWER regardless of the set threshold. The NBS guide actively advocates experimenting with a wide range of t thresholds.

For the correlation analysis the hypothesis that there was no significant positive or negative correlation between a specified variable (e.g. anxiety score or

GLS-CMR) and connectivity (in a specified network) in MINOCA patients was tested in turn using t tests at set thresholds.

#### *4.2.5 REGIONS OF INTEREST*

In addition to the global functional analysis encompassing all 90 AAL regions, five other networks were pre-specified based on the existing literature. These included sympathetic and parasympathetic networks(168), the default mode network(169), salience network(83) and central executive network(83) as described in chapter 2. The specified MNI coordinates were converted to AAL regions using xjView 10 (<https://www.alivelearn.net/xjview>). A new weighted connectivity matrix was then generated for each new network which only contained the specific AAL nodes. This was then used for the ROI analysis using NBS to compare the connectivity in each network between MINOCA and control patients.

#### *4.2.6 POWER CALCULATION*

This was an exploratory study and as such no formal power calculation was performed. The predicted smallest subgroup would be TS (~16-27% of MINOCA presentations) (8, 16). Previously published fMRI studies in TS included 15(62), 13(115) and 20(64) subjects and so we aimed to prospectively recruit 100 patients with MINOCA with the aim of having a similar number (~20) of patients with TS. Control participants were recruited in a 2:1 ratio with patients with the aim of balancing power in the control groups with the feasibility and cost of running the study.

#### *4.2.7 STATISTICAL ANALYSIS*

STATA (version 17) was used for all statistical analysis. Normality of continuous data was assessed by visual assessment of the histogram or, if necessary, a Kolmogorov-Smirnov test. Continuous data is presented as mean  $\pm$  standard deviation or median (IQR) depending on the normality of the data. Categorical variables are presented as counts and proportions. Comparison of

means between two groups was assessed using the Students unpaired two-way t-test for parametric data (e.g. TIV between MINOCA and STEMI patients) or the Wilcoxon Rank sums test for non-parametric data (e.g. global efficiency between MINOCA and STEMI patients).

Connectivity in each network between groups was assessed in each direction separately using an unpaired one-tailed t-test between every connection in the specified network. The result was FWE-corrected as described in section 4.2.4 to control for the effect of multiple comparisons. No covariates were specified 'a priori' as the groups were age and sex-matched at recruitment. There was no significant difference in total intracranial volume (TIV) between groups and so this was not included as a covariate. Two t (test statistic) thresholds were chosen from a wide range of tested thresholds to help demonstrate the nature of any effect shown. To check for positive or negative correlations between pre-specified variables (anxiety score, perceived stress score, GLS-CMR) and connectivity at two set t thresholds in each specified network, further unpaired one-tailed t-tests were performed and results were FWE-corrected. Only the three variables most clinically relevant were pre-specified for the correlation analysis due to the large number of analyses that needed to be performed (multiple t thresholds need to be tested for each contrast (positive or negative) for each of the three variables in each specified ROI network in each group). GLS-CMR was chosen as the most relevant CMR variable as it is a global representation of cardiac function, is more sensitive than LVEF, is clinically useful and significantly correlates with the of amount of LGE and oedema seen.

A p value<0.05 was considered as strong evidence against the null hypothesis.

## *4.3 RESULTS*

### *4.3.1 CHARACTERISATION OF THE STUDY POPULATION*

This has been described in chapter 3. Due to the impact of the global coronavirus pandemic and lower incidence of MINOCA than anticipated, 72 of the

planned 100 MINOCA patients were recruited. The recruitment flow chart is shown in Figure 8. For the functional brain analysis, a further 4 MINOCA, 2 STEMI and 1 healthy control were excluded due to incorrect slice acquisition (n=5), inability to lie flat for brain imaging (n=1) and excessive artefact (n=1). Ten patients were included in the TS subgroup analysis.

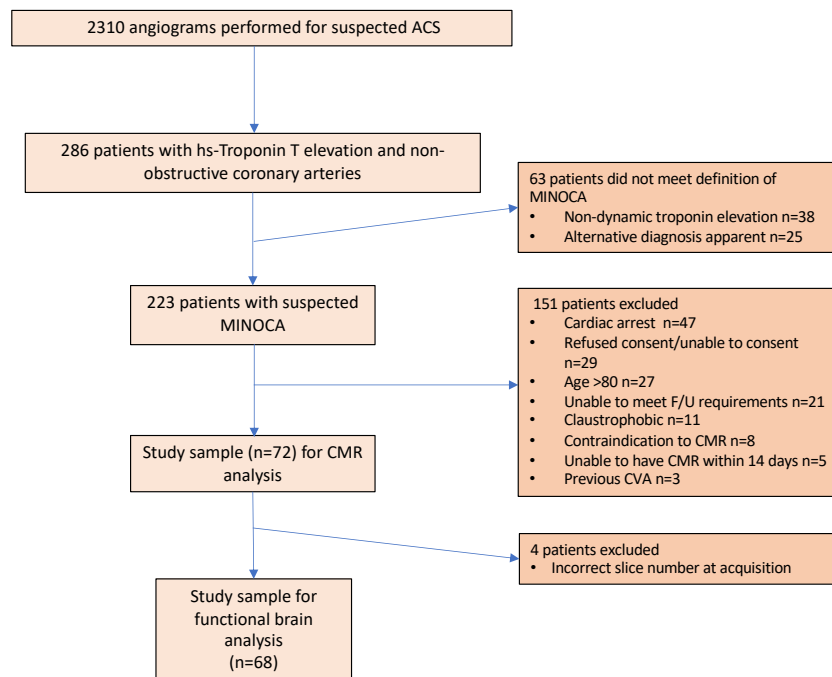


Figure 8 Study Flow Chart

#### 4.3.2 PSYCHOLOGICAL QUESTIONNAIRES

MINOCA patients had lower baseline MMSE scores and higher anxiety, depression and perceived stress scores (PSS) than healthy controls. MINOCA patients had higher anxiety scores than STEMI patients but no strong evidence for a difference in MMSE, depression score or PSS (Figure 9). MINOCA patients had less understanding of their condition compared to STEMI patients on the B-IPQ questionnaire (Table 2, Chapter 3).

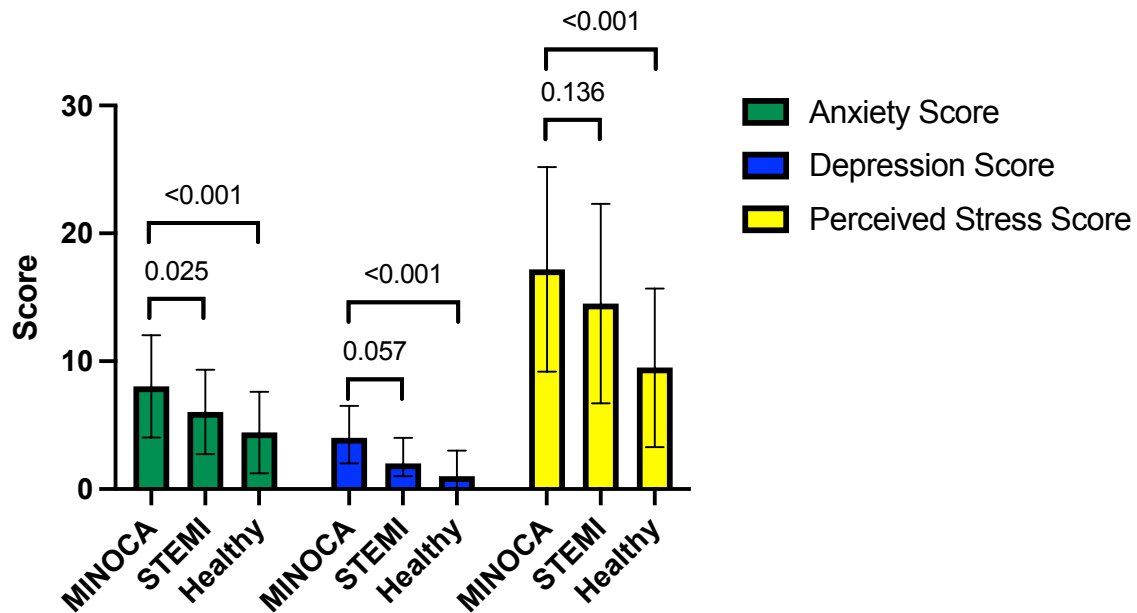


Figure 9 Bar chart demonstrating results of psychological questionnaires in each group

The bar chart displays mean anxiety score ( $\pm$ SD), median depression score ( $\pm$ IQR) and mean perceived stress score ( $\pm$ SD) for each group. P values are shown for direct comparisons between MINOCA and STEMI groups (lower) and MINOCA and healthy groups (upper).

#### 4.3.3 GLOBAL NETWORK MEASURES

There were no significant differences between total intracranial volumes, global efficiency, modularity or small world propensity between MINOCA and STEMI or healthy controls (Table 19).

Table 19 Table showing global network measures by group

	MINOCA (n=68)	STEMI (n=25)	P value (MINOCA v STEMI)	Healthy (n=25)	P value (MINOCA v Healthy)
Total intracranial volume, mean [SD]	1534 [187]	1543 [130]	0.816	1534 [171]	0.985
Global efficiency, median [IQR]	0.324 [0.301 - 0.353]	0.331 [0.297 - 0.354]	0.768	0.319 [0.305 - 0.352]	0.934
Modularity, mean [SD]	0.131 [0.018]	0.132 [0.025]	0.902	0.127 [0.018]	0.314
Small world propensity, median [IQR]	0.675 [0.592 - 0.763]	0.640 [0.615 - 0.754]	0.588	0.690 [0.580 - 0.763]	0.979

#### 4.3.4 GLOBAL NETWORK MEASURES AND PSYCHOLOGICAL QUESTIONNAIRES

Patients were categorised into high or low anxiety and depression scores (high score  $\geq 8$ ) (145, 150) and high or low perceived stress scores (high score  $> 20$ )

(216) as is consistent with the literature. In addition, GLS-CMR was binarized into normal ( $\leq -17.9\%$ ) and abnormal ( $> -17.9\%$ ) based on the median GLS-CMR in our healthy control group ( $-17.9\%$ ). Results for the MINOCA group are described below results for the STEMI control groups and healthy volunteers are in Appendix C.

#### **4.3.4.1 Anxiety and Global Network Measures**

Patients with MINOCA who had a high anxiety score had lower global efficiency and SWP than those with a low anxiety score. There was no difference in modularity, SWP or GLS-CMR in patients with high or low anxiety in the MINOCA group (Figure 10). There was no difference in any global network measure by anxiety group in the STEMI control or healthy volunteer groups (Appendix C).

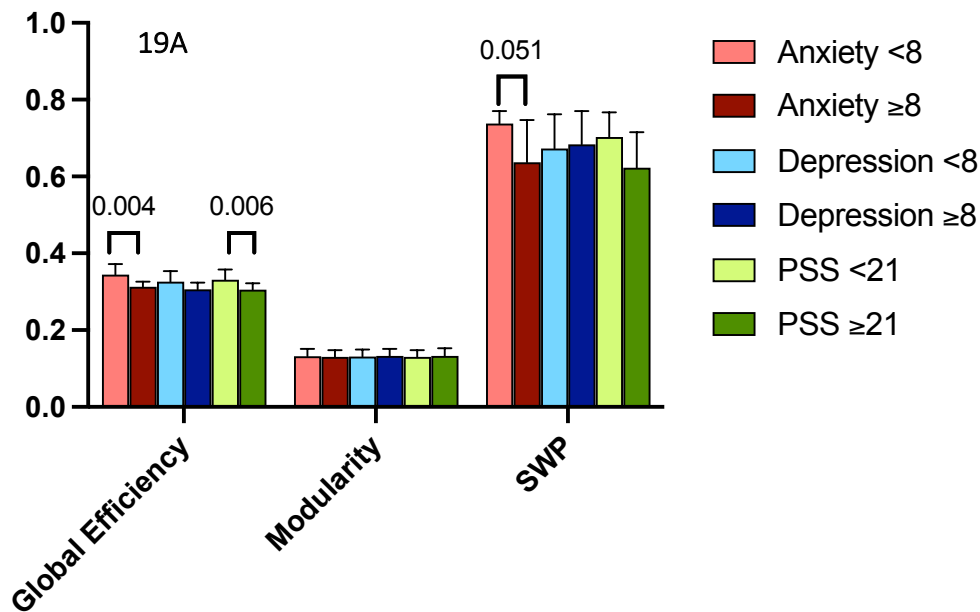
#### **4.3.4.2 Depression and Global Network Measures**

There was no difference in global efficiency, modularity, SWP or GLS-CMR in the MINOCA group in patients with high or low depression scores (Figure 10). There was no difference in any global network measure by depression group in the STEMI control or healthy volunteer groups (Appendix C).

#### **4.3.4.3 Stress and Global Network Measures**

In the MINOCA group, patients with a high stress score had lower global efficiency than those with a low stress score. There was no difference in modularity, SWP or GLS-CMR in MINOCA patients with high or low stress scores (Figure 10). STEMI patients with a high stress score has lower SWP than STEMI patients with a low stress score. There were no other differences in global network measures by stress group in the STEMI control or healthy volunteer groups.





19B

Score	Global Efficiency	Modularity	SWP
Anxiety <8 (n=34)	0.345 [0.323-0.372]	0.132 [0.019]	0.738 [0.611-0.770]
Anxiety ≥8 (n=34)	0.313 [0.293-0.326]	0.130 [0.018]	0.636 [0.579-0.747]
P value	<b>0.004</b>	0.806	0.051
Depression <8 (n=55)	0.326 [0.305-0.354]	0.131 [0.019]	0.673 [0.581-0.762]
Depression ≥8 (n=13)	0.306 [0.294-0.324]	0.133 [0.018]	0.684 [0.631-0.770]
P value	0.132	0.618	0.498
PSS <21 (n=48)	0.331 [0.314-0.358]	0.130 [0.018]	0.703 [0.602-0.767]
PSS ≥21 (n=20)	0.305 [0.287-0.321]	0.132 [0.012]	0.622 [0.568-0.715]
P value	<b>0.006</b>	0.698	0.067
GLS-CMR ≤-17.9% (n=14)	0.342 [0.304-0.353]	0.134 [0.023]	0.664 [0.582-0.753]
GLS-CMR >-17.9% (n=54)	0.323 [0.298-0.353]	0.130 [0.017]	0.685 [0.593-0.766]
P value	0.354	0.564	0.448

Figure 10A Bar chart demonstrating network measures by anxiety, depression and stress scores in MINOCA patients; Figure 10B Table showing values of global network measures by group in MINOCA patients, including GLS-CMR.

The bar chart displays median global efficiency  $\pm$  IQR, mean modularity  $\pm$  SD and median SWP  $\pm$  IQR by anxiety, depression and stress groups. P values are shown where this is strong evidence of a difference between the scores. In Figure 3B, efficiency and SWP are displayed as median [IQR] and modularity as mean [SD].

#### 4.3.5 SUBGROUP ANALYSIS

The MINOCA group was further divided into diagnostic groups (Table 20). There was no significant difference in any global measure of brain function between the subgroups ( $p < 0.05$ ).

Table 20 Global network measures by MINOCA subgroups.

TIV – total intracranial volume; SWP – small world propensity; MI – myocardial infarction; TS – takotsubo syndrome; OCM – other cardiomyopathy

Subgroup analysis: Functional Brain MRI					
	Myocarditis (n=14)	MI (n=27)	TS (n=9)	OCM (n=2)	Normal/non-specific (n=16)
TIV, mean [SD]	1592 [156]	1578 [184]	1410 [175]	1480 [64]	1486 [204]
Global efficiency, median [IQR]	0.323 [0.297 – 0.346]	0.336 [0.314 – 0.383]	0.323 [0.307 – 0.343]	0.290 [0.276 – 0.303]	0.319 [0.291 – 0.350]
Modularity, mean [SD]	0.132 [0.014]	0.132 [0.018]	0.141 [0.019]	0.119 [0.037]	0.123 [0.018]
SWP, median [IQR]	0.750 [0.591 – 0.772]	0.684 [0.609 – 0.759]	0.655 [0.602 – 0.706]	0.563 [0.513 – 0.613]	0.668 [0.586 – 0.761]

Patients with TS were also compared to healthy and STEMI control groups to address hypothesis 6. Patients with TS had higher modularity compared to healthy controls (0.141 v 0.127,  $p=0.047$ ) but there were no other significant differences in global network measures between patients with TS and either control group (Figure 11).

There was no difference in global efficiency, modularity or swp and high or low anxiety, depression and perceived stress score in TS. Patients with TS with an abnormal GLS-CMR had a lower modularity than those with a normal GLS (0.135 v 0.165;  $p=0.027$ ).

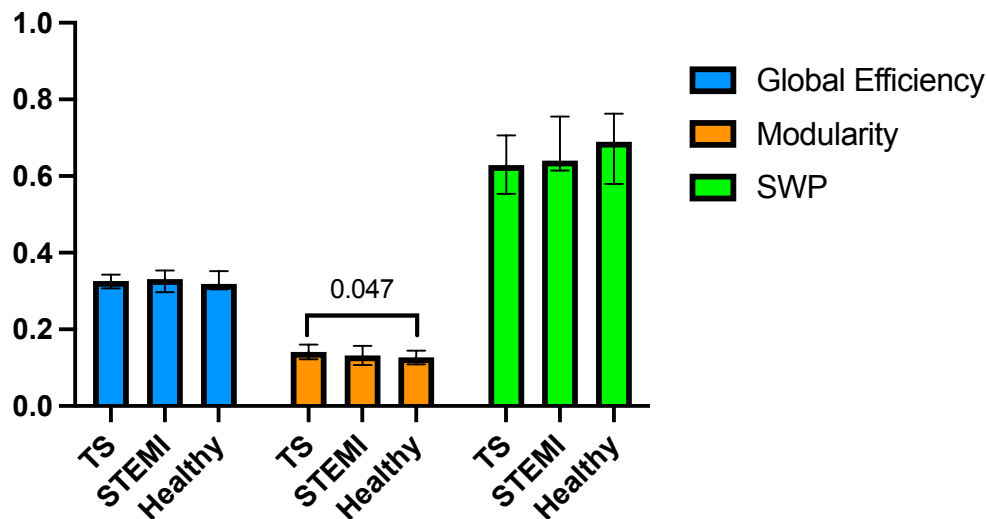


Figure 11 Bar chart demonstrating network measures by TS and control groups.

The bar chart displays the median global efficiency  $\pm$  IQR, mean modularity  $\pm$  SD and median swp  $\pm$  IQR for each group. Significant p values are shown for direct comparisons between TS and STEMI groups or healthy groups.

#### 4.3.6 NETWORK CONNECTIVITY ANALYSIS

There was no difference in connectivity between MINOCA and STEMI or healthy controls in the sympathetic, parasympathetic or salience networks or on whole brain connectivity analysis (90 nodes).

##### 4.3.6.1 Default Mode Network

At the higher set threshold ( $t=3.1$ ), there was increased connectivity in the MINOCA-related network compared to healthy participants consisting of 2 edges over 3 nodes ( $p=0.012$ , Figure 12). The nodes involved were left and right parahippocampus and the right supramarginal gyrus. At the lower set threshold ( $t=2.35$ ), there was increased connectivity in MINOCA patients compared to healthy controls in the DMN comprising 7 edges over 6 nodes ( $p=0.016$ , Appendix C). There was no difference in connectivity compared to STEMI patients.

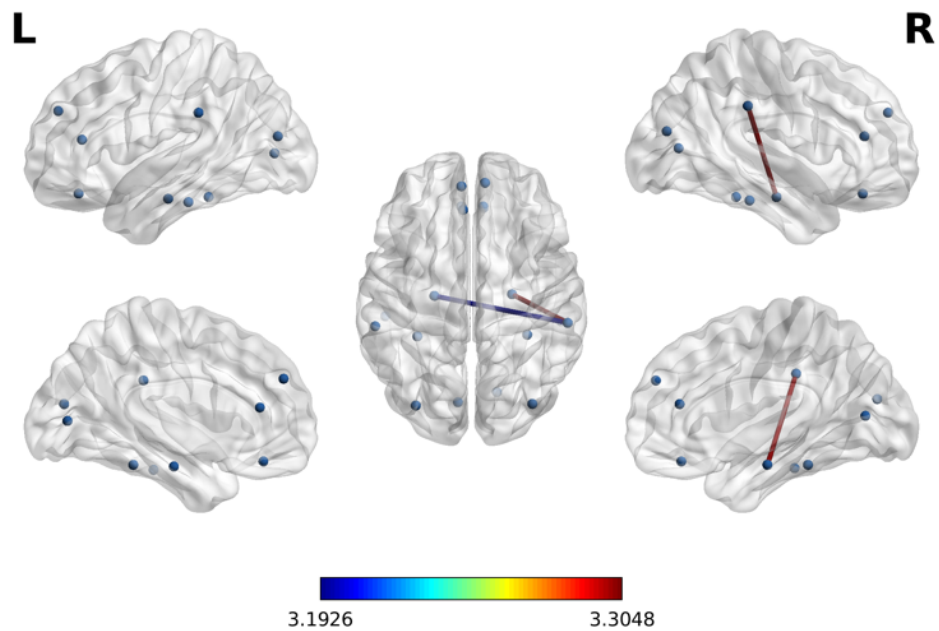


**Figure 12** Subnetworks with increased functional connectivity in patients with MINOCA compared to healthy controls in the default mode network.

Only subnetworks at the higher set threshold ( $t=3.1$ ) are shown. The subnetworks at the lower set threshold are shown in the appendix with a table of the nodes. The colour bar signifies the t-value of the strength of the difference in connectivity between the subnetworks in each group. The blue dots represent the nodes that comprise the DMN.

#### 4.3.6.2 Central Executive Network

At the higher set threshold ( $t=3.8$ ), there was reduced connectivity in the MINOCA-related network compared to healthy participants comprising 1 edge over 2 nodes ( $p=0.02$ , Figure 13A). The nodes involved were the left frontal middle gyrus (orbital part) and the left frontal inferior gyrus (orbital part). At the lower set threshold ( $t=1.9$ ), the network consisted of 9 edges over 8 nodes ( $p=0.048$ , Appendix C).

At the higher set threshold ( $t=2.2$ ), there was reduced connectivity in the MINOCA-related central executive network comprising 5 edges over 6 nodes ( $p=0.05$ ; Figure 13B) compared to STEMI controls. These nodes included the left frontal middle gyrus (orbital part), right middle frontal gyrus, right thalamus, right inferior temporal gyrus and the bilateral inferior parietal gyri. At the lower threshold ( $t=1.8$ ) there were 11 edges over 9 nodes ( $p=0.045$ , Appendix C).

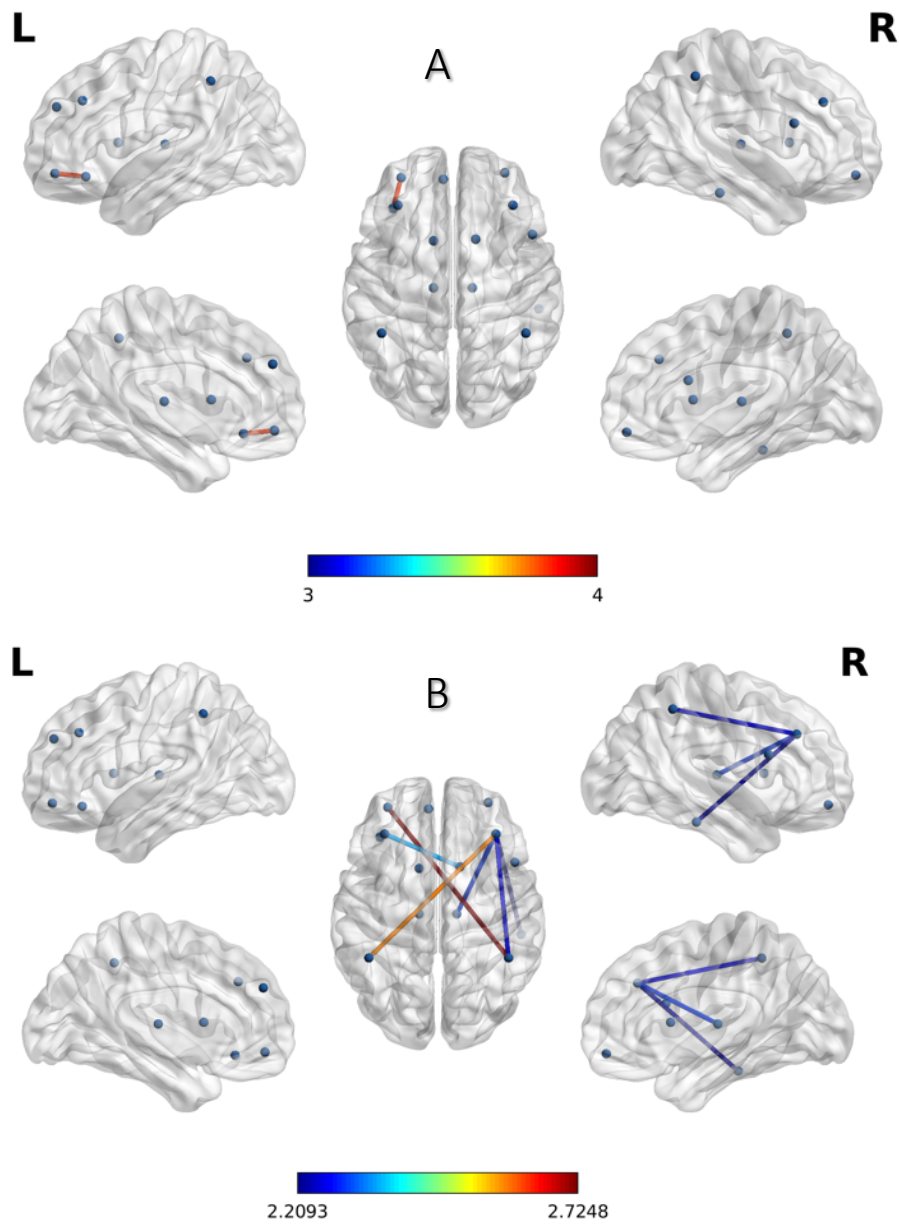


Figure 13 Subnetworks with reduced functional connectivity in patients with MINOCA compared to healthy controls (A) and STEMI controls (B) in the central executive network.

Only subnetworks at the higher set threshold are shown. The subnetworks at the lower set threshold are shown in the appendix with a table of the nodes. The colour bar signifies the t-value of the strength of the difference in connectivity between the subnetworks in each group. The blue dots represent the nodes that comprise the CEN.

#### 4.3.7 *TAKOTSUBO SYNDROME*

There was no difference in connectivity compared to controls in the sympathetic, parasympathetic, salience or default mode networks.

##### 4.3.7.1 Central Executive Network

At the higher set threshold ( $t=2.2$ ), there was reduced connectivity in the TS-related network compared to healthy controls comprising 5 edges over 6 nodes ( $p=0.030$ ; Figure 14A). Amongst these nodes were the left frontal middle gyrus (orbital part), bilateral inferior parietal gyri, left frontal middle gyrus, left medial frontal superior gyrus and the bilateral frontal inferior gyri (orbital parts). At the lower threshold ( $t=1.7$ ) there was a trend towards hypoconnectivity in a network comprising 10 edges over 8 nodes ( $p=0.053$ ; Appendix C). There were no networks demonstrating increased connectivity.

When compared to STEMI patients, at the higher set threshold ( $t=3.7$ ), there was reduced connectivity in the TS-related network comprising 1 edge over 2 nodes ( $p=0.008$ , Figure 14B). These nodes were the left frontal middle gyrus (orbital part) and the right inferior parietal gyrus. At the lower set threshold ( $t=2.3$ ) the hypoconnected network comprised 5 edges over 6 nodes ( $p=0.010$ , Appendix C).

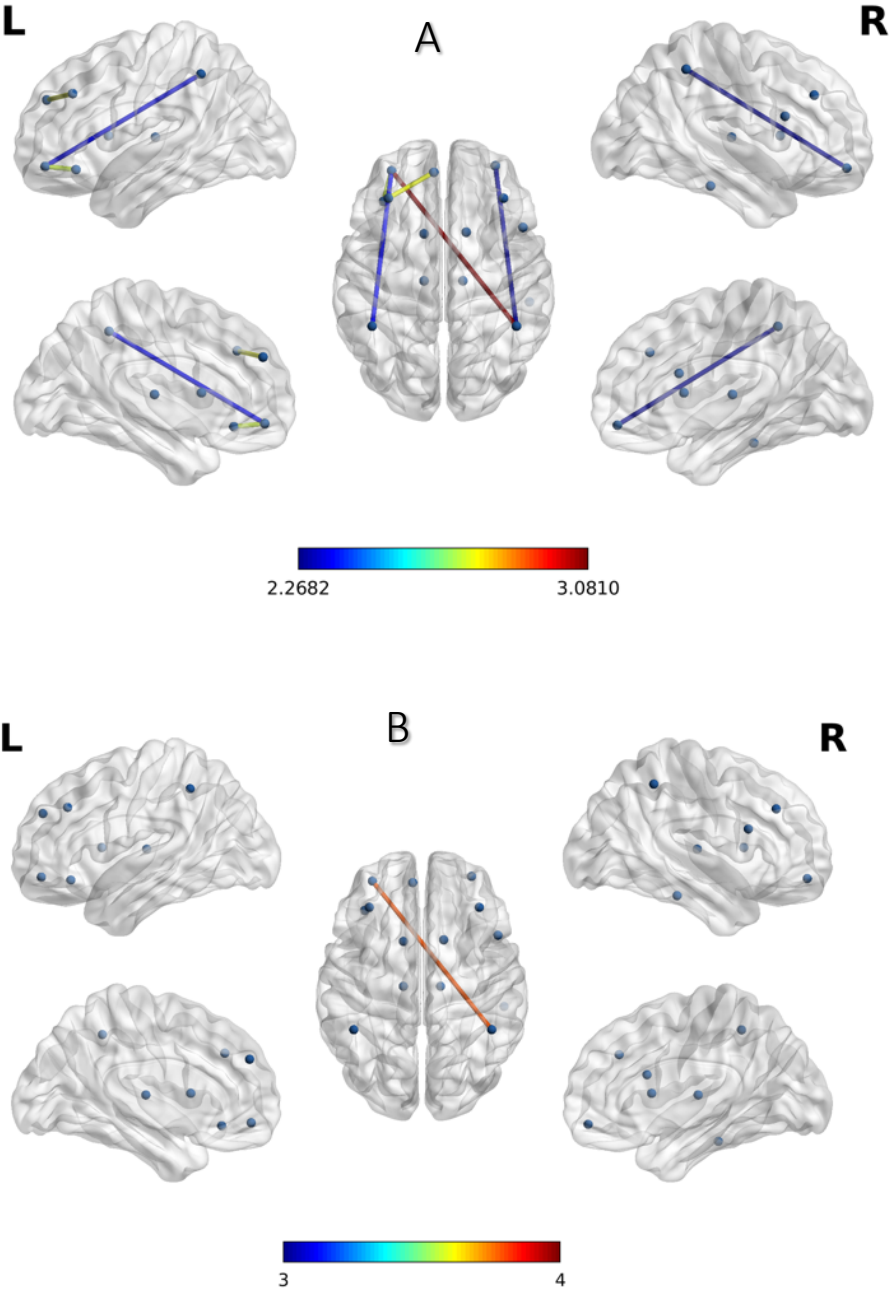


Figure 14 Subnetworks with reduced functional connectivity in patients with TS compared to healthy controls (A) and STEMI controls (B) in the central executive network.

Only subnetworks at the higher set thresholds are shown. The subnetworks at the lower set threshold are shown in the appendix with a table of the nodes. The colour bar signifies the t-value of the strength of the difference in connectivity between the subnetworks in each group.

#### 4.3.7.2 Whole brain

At the higher set threshold ( $t=3.1$ ), there was reduced connectivity in the TS-related network comprised of 5 edges over 6 nodes ( $p=0.024$ ; Appendix C). These nodes included the bilateral hippocampus, left superior temporal gyrus, right middle frontal gyrus, left superior parietal gyrus and the right inferior frontal gyrus (triangular part). At the lower set threshold ( $t=2.85$ ), the hypoconnected network demonstrated a trend towards significance and consisted of 8 nodes over 7 edges ( $p=0.062$ ; Appendix C). There were no networks demonstrating increased connectivity.

When compared to STEMI participants, there was reduced connectivity in the TS-related network at the higher threshold ( $t=4.7$ ) comprised 1 edge over 2 nodes ( $p=0.010$ , Appendix C). These nodes were the left superior temporal gyrus and the right inferior frontal gyrus (triangular part). At the lower threshold ( $t=3.0$ ) the network comprised 5 edges over 6 nodes ( $p=0.053$ , Appendix C).

### 4.3.8 CORRELATION BETWEEN VARIABLES AND FUNCTIONAL NETWORKS

#### 4.3.8.1 Sympathetic Network

There was a negative correlation between connectivity and anxiety scores in the sympathetic network in MINOCA patients. At the higher set threshold ( $t=1.6$ ) the network comprised 9 edges over 8 nodes ( $p=0.047$ , Figure 15A). At the lower set threshold ( $t=1.1$ ) the network comprised 18 edges over 9 nodes ( $p=0.049$ , Appendix C). There was no correlation seen in STEMI patients or healthy participants.

There was a negative correlation between connectivity and stress scores in the sympathetic network in MINOCA patients. At the higher set threshold ( $t=2.6$ ) the network comprised 3 edges over 4 nodes ( $p=0.010$ , Figure 15B). At the lower set threshold ( $t=1.4$ ) the network comprised 13 edges over 9 nodes ( $p=0.044$ , Appendix C). There was a negative correlation between connectivity and stress scores in the sympathetic network in STEMI patients. At the higher set threshold ( $t=2.5$ ) this comprised 3 edges over 4 nodes ( $p=0.035$ ; Appendix C). At the lower



set threshold ( $t=2.1$ ) this comprised 4 edges over 5 nodes ( $p=0.082$ , Appendix C). There was no significant correlation with stress score and connectivity in healthy participants.

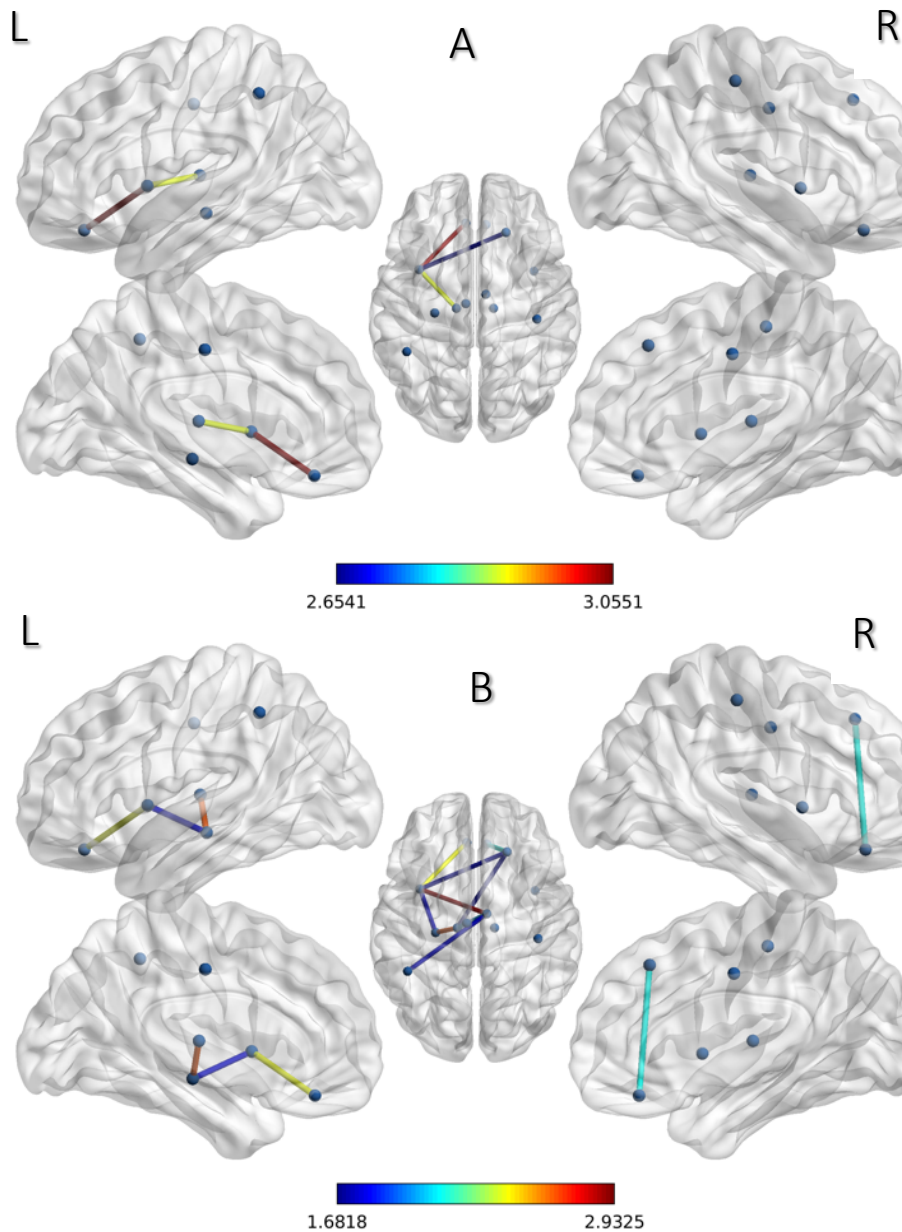


Figure 15 Subnetworks in MINOCA patients with a negative correlation with anxiety score (A) and with stress scores (B) in the sympathetic network.

Only subnetworks at the higher set thresholds are shown. The subnetworks at the lower set threshold are shown in the appendix with a table of the nodes. The colour bar signifies the strength of the association between the score and the connection between the two nodes.

There was no correlation between connectivity in the sympathetic network and GLS-CMR in MINOCA patients.

#### **4.3.8.2 Parasympathetic Network**

There was a negative correlation between connectivity and perceived stress score in the parasympathetic network in MINOCA patients. At the higher threshold ( $t=2.7$ ) this network comprised 2 edges over 3 nodes ( $p=0.016$ , Figure 16). These nodes included the right hippocampus, left insula and left amygdala. At the lower threshold ( $t=1.5$ ) the network comprised 10 edges over 6 nodes ( $p=0.011$ , Appendix C). There was no correlation in STEMI patients but there was a positive correlation in the parasympathetic network in healthy participants. At the higher threshold ( $t=1.2$ ), this network comprised 11 edges over 7 nodes ( $p=0.045$ , Appendix C). At the lower threshold ( $t=0.5$ ) this comprised 17 edges over 7 nodes ( $p=0.082$ , Appendix C).

There was no correlation with anxiety score or GLS-CMR in MINOCA patients.

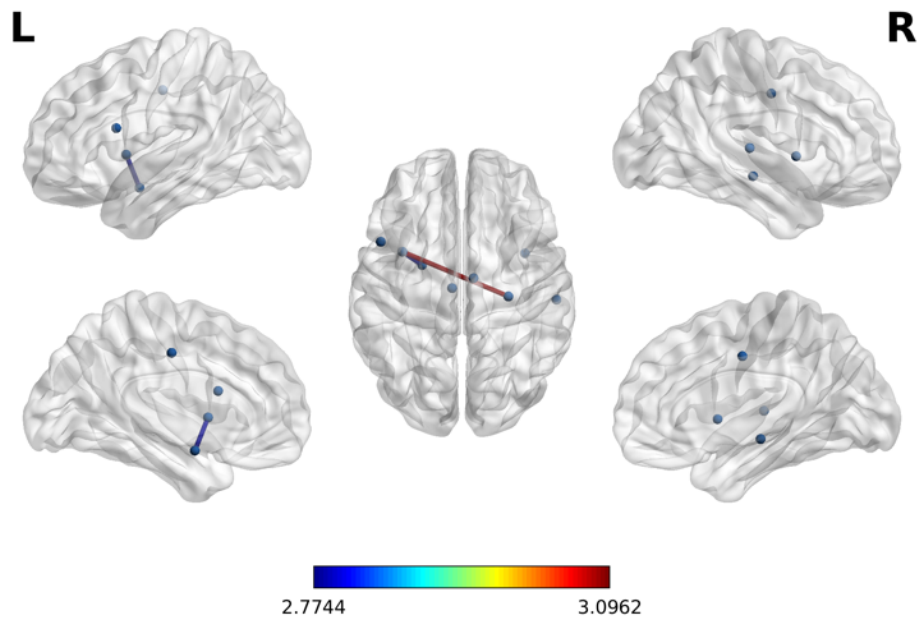


**Figure 16** Subnetworks in MINOCA patients with a negative correlation with stress score in the parasympathetic network.

Only subnetworks at the higher set thresholds are shown. The subnetworks at the lower set threshold are shown in the appendix with a table of the nodes. The colour bar signifies the strength of the association between the score and the connection between the two nodes.

#### 4.3.8.3 Default Mode Network

There was a negative correlation between anxiety scores and connectivity in MINOCA patients in the default mode network. At the higher set threshold ( $t=2.9$ ) this comprised 3 edges over 4 nodes ( $p=0.018$ , Figure 17) including the bilateral supramarginal gyri, left parahippocampus and left gyrus rectus. At the lower set threshold ( $t=1.9$ ) this comprised 21 edges over 13 nodes ( $p=0.014$ , Appendix C). In healthy participants there was a positive correlation between anxiety scores and connectivity. At the higher threshold ( $t=6.1$ ) this comprised 1 edge over 2 nodes ( $p<0.001$ ). At the lower threshold ( $t=4.1$ ) it comprised 1 edge over 2 nodes ( $p=0.034$ , Appendix C)

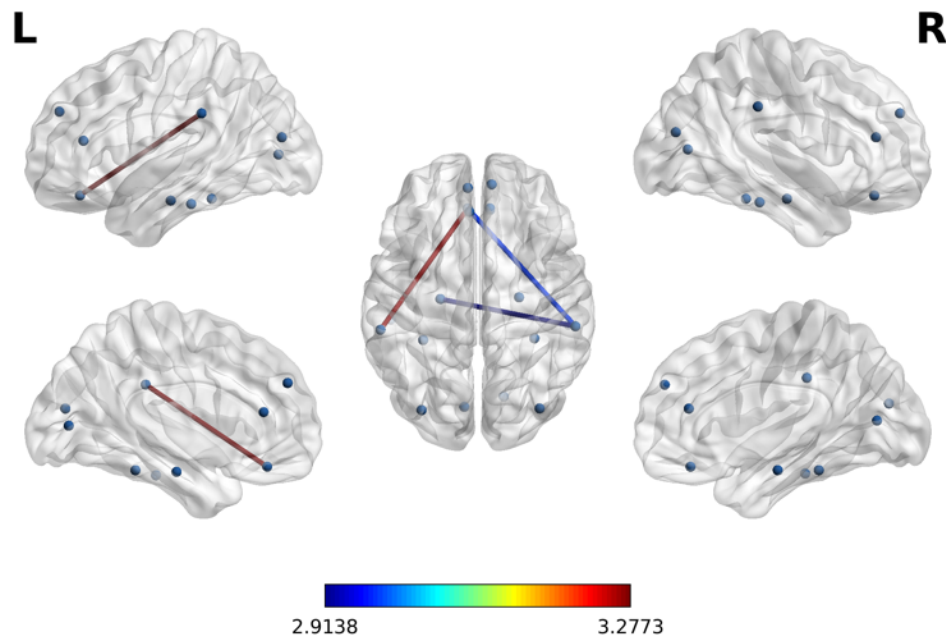


**Figure 17** Subnetworks in MINOCA patients with a negative correlation with anxiety score in the DMN.

Only subnetworks at the higher set thresholds are shown. The subnetworks at the lower set threshold are shown in the appendix with a table of the nodes. The colour bar signifies the strength of the association between the score and the connection between the two nodes.

There was a negative correlation between perceived stress scores and connectivity in MINOCA patients in the default mode network. At the higher set threshold ( $t=2.8$ ) this network comprised 3 edges over 4 nodes ( $p=0.033$ ; Figure 18) including the left supramarginal gyrus, left gyrus rectus, right mid occipital gyrus and right fusiform gyrus. At the lower set threshold ( $t=1.9$ ) the network comprised 23 edges over 17 nodes ( $p=0.007$ , Appendix C). In healthy participants there was a positive correlation between connectivity and perceived stress scores. At the higher set threshold ( $t=4.6$ ) the network comprised 1 edge over 2 nodes ( $p=0.020$ ). At the lower set threshold ( $t=3.8$ ) the network comprised 1 edge over 2 nodes ( $p=0.087$ , Appendix C) although this did not reach statistical significance. There were no correlations seen in STEMI patients.

There was no correlation with GLS-CMR and DMN connectivity in MINOCA patients.

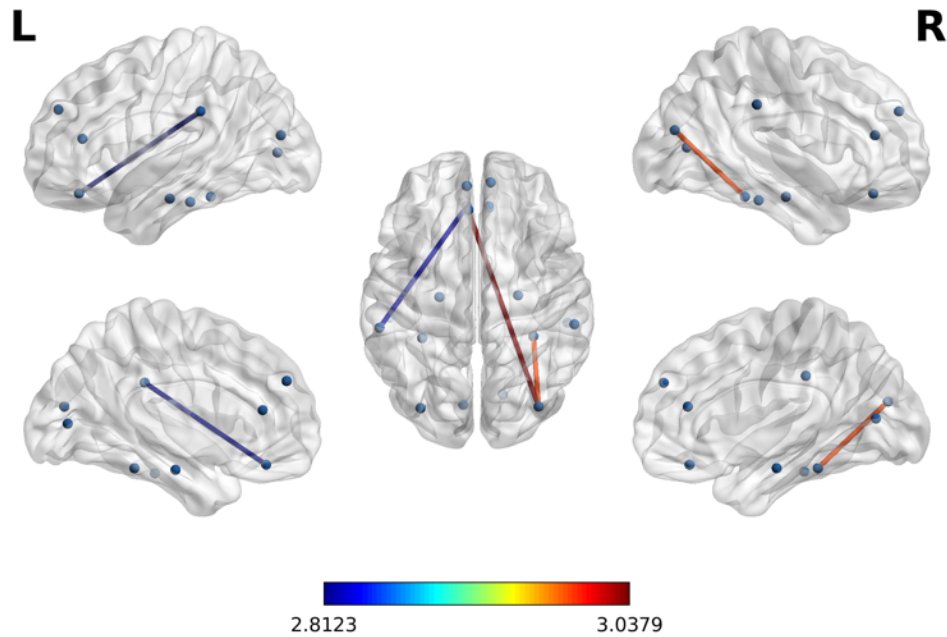


Figure 18 Subnetworks in MINOCA patients with a negative correlation with stress score in the DMN.

Only subnetworks at the higher set thresholds are shown. The subnetworks at the lower set threshold are shown in the appendix with a table of the nodes. The colour bar signifies the strength of the association between the score and the connection between the two nodes.

#### 4.3.8.4 Salience Network

There was a negative correlation between connectivity and perceived stress score in MINOCA patients. At the higher set threshold ( $t=2.5$ ) the network comprised 4 edges over 5 nodes ( $p=0.048$ ). These nodes included the left anterior cingulate and paracingulate gyrus, left amygdala, left supplementary motor area, right median cingulate and paracingulate gyri, and the left inferior parietal gyrus. At the lower set threshold ( $t=1.9$ ) the network comprised 25 edges over 16 nodes ( $p=0.009$ , Appendix C). There was no correlation in STEMI or healthy controls.

There was no correlation between GLS-CMR and connectivity in MINOCA patients.

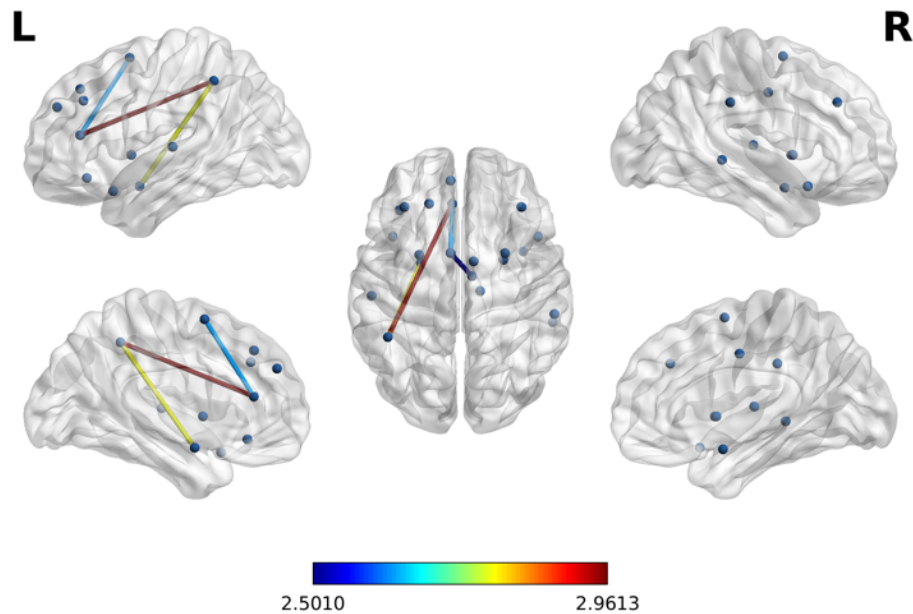


**Figure 19** Subnetworks in MINOCA patients with a negative correlation with perceived stress score in the salience network.

Only subnetworks at the higher set thresholds are shown. The subnetworks at the lower set threshold are shown in the appendix with a table of the nodes. The colour bar signifies the strength of the association between the score and the connection between the two nodes.

#### 4.3.8.5 Central Executive Network

There was a negative correlation between connectivity and anxiety scores in MINOCA patients. At the higher set threshold ( $t=3.35$ ) this comprised 1 edge over 2 nodes ( $p=0.047$ , Figure 20A) including the left thalamus and right middle frontal middle frontal gyrus (orbital part). At the lower set threshold ( $t=2.6$ ) this comprised 3 edges over 4 nodes ( $p=0.015$ , Appendix C). There was no correlation in healthy or STEMI patients.

There was a negative correlation between connectivity and GLS-CMR in MINOCA patients. At the higher set threshold ( $t=3.6$ ) the network comprised 1 edge over 2 nodes ( $p=0.010$ , Figure 20B) including the left caudate nucleus and left middle frontal gyrus (orbital part). At the lower set threshold, the network comprised 3 edges over 4 nodes ( $p=0.020$ , Appendix C).

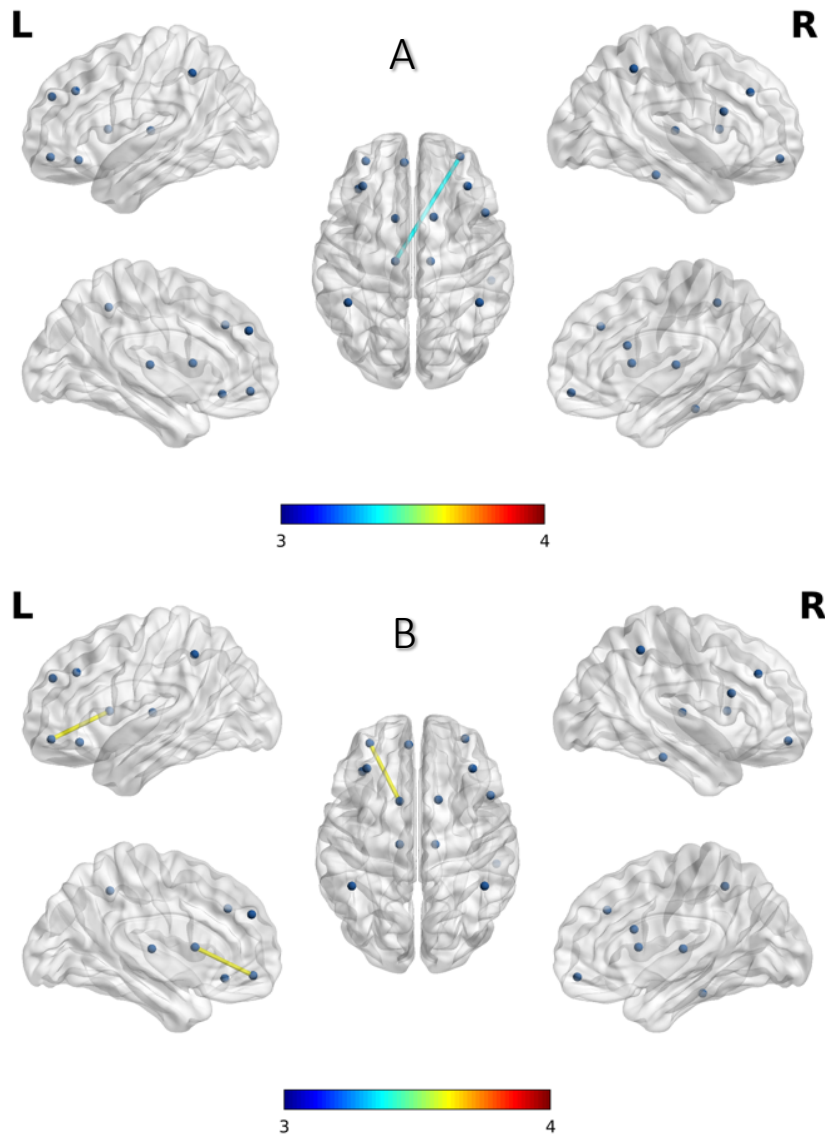


Figure 20 Subnetworks in MINOCA patients with a negative correlation with anxiety score (A) and GLS-CMR (B) in the CEN.

Only subnetworks at the higher set thresholds are shown. The subnetworks at the lower set threshold are shown in the appendix with a table of the nodes. The colour bar signifies the strength of the association between the score and the connection between the two nodes.

There was a positive correlation between connectivity and GLS-CMR in healthy participants. At the higher set threshold ( $t=4.1$ ) the network comprised 1 edge over 2 nodes ( $p=0.016$ ). At the lower set threshold ( $t=2.6$ ) the network comprised 8 edges over 8 nodes ( $p=0.002$ , Appendix C). There was no correlation in STEMI patients.

#### 4.3.8.6 Whole brain

There was a negative correlation between anxiety scores and connectivity in MINOCA patients on whole brain analysis. At the higher set threshold ( $t=3.0$ ) this network comprised 29 edges over 29 nodes ( $p=0.005$ , Appendix C). Amongst others, these nodes included the right hippocampus, left parahippocampus, bilateral precuneus, bilateral medial cingulate gyri, left insula and right amygdala. At the lower set threshold ( $t=2.6$ ) this network comprised 86 edges over 57 nodes ( $p=0.007$ ; Appendix C). In healthy participants there was a positive correlation between anxiety scores and connectivity. At the higher threshold ( $t=6.0$ ) the network comprised 1 edge over 2 nodes ( $p=0.008$ , Appendix C). At the lower set threshold ( $t=4.1$ ) the network comprised 2 edges over 3 nodes ( $p=0.105$ , Appendix C) although there was only a trend towards significance at this threshold. There was no correlation between anxiety scores and connectivity in STEMI patients.

There was a strong negative correlation between connectivity and perceived stress score in MINOCA patients on whole brain analysis. At the higher set threshold ( $t=3.6$ ) the network comprised 5 edges over 6 nodes ( $p=0.005$ ). These nodes included left posterior cingulate gyrus, left caudate nucleus and bilateral fusiform gyri. At the lower set threshold ( $t=2.8$ ) the network comprised 52 edges over 46 nodes ( $p=0.008$ , Appendix C). There was no association in STEMI or healthy participants.

There were no positive or negative correlations between GLS-CMR and functional connectivity in MINOCA patients on whole brain analysis.

#### 4.4 DISCUSSION

The main findings from our study were:

- i) patients presenting with MINOCA had higher anxiety scores than patients presenting with STEMI and greater anxiety, depression and perceived stress scores than healthy control patients.



- ii) there was no significant difference between global efficiency, modularity or SWP between MINOCA and control groups.
- iii) MINOCA patients with high anxiety scores had lower global efficiency and SWP than those with low anxiety; MINOCA patients with a high PSS had lower global efficiency than those with a low PSS.
- iv) patients presenting with MINOCA had increased connectivity in the DMN and reduced connectivity in the CEN compared to healthy controls, but only in the CEN when compared to STEMI controls.
- v) anxiety and perceived stress scores had multiple negative correlations with connectivity strength in MINOCA patients in sympathetic, parasympathetic, DMN, salience and CEN functional networks. These correlations were largely absent in the STEMI group and positive in the healthy controls (summarised in Table 21).

*TS Subgroup Analysis*

- vi) patients with TS had increased modularity compared to healthy controls.
- vii) patients with TS had decreased connectivity in the CEN compared to both healthy and STEMI controls and decreased connectivity in central autonomic regions on whole brain analysis compared to healthy controls.

**4.4.1 PSYCHOLOGICAL PROFILES**

We have compared for the first time prospectively enrolled patients with MINOCA with both age and sex matched healthy and acute STEMI control groups. Patients presenting with MINOCA had higher anxiety, depression and perceived stress scores than healthy controls. These scores reflect how participants had been feeling during the last week (anxiety and depression) and month (PSS) and therefore should not just represent their current mental state during the index hospital admission. They were designed to avoid physical symptoms (such as pain) which might confound the results(150). Compared to the STEMI group, who also were inpatients on the cardiology ward, MINOCA patients had higher anxiety

scores. This is in keeping with previous studies which showed patients with MINOCA recognised higher emotional stress compared to patients with obstructive coronary disease (173) and that anxiety and depression was higher compared to healthy controls (172). However, the latter study did not demonstrate a difference in anxiety score compared to patients with obstructive coronary disease, possibly because the questionnaire was applied 3 months after the acute event. Although only an association, rather than causality, can be shown, the fact that increased anxiety, depression and stress scores predate the onset of the acute cardiac event in our study suggests that there may be a role for these conditions in the aetiology of MINOCA.

#### 4.4.2 *NETWORK MEASURES*

There was no difference in global network measures between MINOCA patients and the control groups. However, MINOCA patients with high anxiety and perceived stress scores had lower global efficiency. There was no association between global efficiency and high anxiety or stress scores seen in the healthy or STEMI group suggesting this finding is unique to MINOCA patients.

Global efficiency was the most relevant global network measure in our analysis; no other network measure correlated with our variables in any group. Global efficiency is a measure of the inverse path length between nodes. That is, global efficiency is greater when the average number of connections between two nodes is lower. It is a measure of integration, with shorter average path length representing greater integration at a lower cost to the brain. There are no prior studies examining global network measures in MINOCA. Increased local efficiency and clustering coefficient (a measure of the density of connections between topographical neighbours) has been shown in hippocampal ROIs in TS patients in the chronic phase compared to healthy controls(63). The hippocampus has importance in the modulation of the central autonomic nervous system(217). Patients who suffer an emotional trauma prior to developing an emotional disorder demonstrate greater activity in the regions of the brain involved in experience, memory and emotional perception(218). The authors

speculated therefore that this could lead to patients with TS having a greater tendency to recall negative emotions, which might predispose them to more significant autonomic responses. There are mixed results looking at global efficiency in major depressive disorder. One study in older patients with untreated depression demonstrated lower global efficiency compared to controls(219), however in younger untreated subjects, global efficiency was found to be higher(208). There are few studies examining global efficiency and anxiety. Zhu et al showed no difference in global efficiency between patients with social anxiety disorder and controls (209) and Yang et al showed no difference in global efficiency in drug naïve patients with social anxiety disorder(220). In stress disorders, Wheelock et al showed decreased global efficiency during a stress task (221), Zi et al showed increased global efficiency in PTSD patients(222) and Sheynin et al showed no difference in global efficiency on whole brain analysis in adolescent patients with PTSD, although they did show decreased efficiency in the DMN of these patients(223). It is perhaps unsurprising there is little consistency between results since the populations, pathologies and methodology are extremely variable. Nevertheless, our results of reduced global efficiency in a MINOCA population with high anxiety or stress scores suggest these patients have greater average path lengths and less brain integration than those with lower anxiety or stress scores.

### 4.4.3 NETWORK CONNECTIVITY

Our results demonstrated reduced connectivity in the central executive network in MINOCA patients compared to both healthy and STEMI controls suggesting this finding is unique to MINOCA patients and therefore cannot purely be a function of an intercurrent cardiac illness or stressful hospital admission. The networks mainly involved nodes in the right middle frontal cortex, inferior parietal cortex and left caudate nucleus. Functional connectivity in the whole MINOCA population has not been studied previously, so no direct comparisons can be made with existing literature. However, the middle frontal gyrus has connections with important limbic emotional processing structures including the amygdala(64, 224, 225), which is a key region in the autonomic nervous system and increased

activity is known to be associated with major adverse cardiac events (MACE) (102). Reduced connectivity was shown by Templin et al(62) in the left dorsolateral prefrontal cortex and by Sabisz et al in the ventromedial prefrontal cortex(116) in TS patients in the chronic phase. The right middle frontal gyrus was one of the regions with reduced grey matter volume in MINOCA patients compared to healthy controls reported in chapter 3, which would be in keeping with reduced connectivity of this node. Reduced cortical thickness has been shown to correlate with functional connectivity in some brain regions and the theory that brain structure can predict (or is related to) function is a core assumption of neuroimaging (226, 227). The right middle frontal gyrus has also been shown to have reduced volume on VBM analysis in acute TS patients and to have decreased blood flow on SPECT (113, 115). The bilateral inferior parietal lobule has reduced resting state functional connectivity in TS(62). The caudate nuclei also have multiple projections to the amygdala and has roles in memory, learning and emotion and has inputs from the ipsilateral frontal lobes(228). It is plausible therefore that hypoconnectivity in the central executive network in MINOCA patients, perhaps due to their higher anxiety than the STEMI patients, has the potential to affect the autonomic nervous system.

Our results demonstrated increased connectivity in the DMN in MINOCA patients compared to healthy participants, but not compared to STEMI patients. The hyperconnected subnetwork consisted of the bilateral parahippocampal gyri and the right supramarginal gyrus. One other study in TS patients in the chronic phase showed increased connectivity in similar nodes(63). By contrast, lower DMN connectivity has also been reported in TS(62), although this result was not confirmed on the subgroup analysis of TS patients in our study. In addition, hypoconnectivity in the right precuneus, part of the DMN, has also been shown in TS(115). The DMN is intricately linked with anxiety(229), self-referential judgements(230) and the 'recollection of prior experiences'(201). The fact that these differences were only present compared to healthy controls and not to STEMI controls may signify an overlap in the pathophysiology between MINOCA and STEMI patients. Alternatively, it may be possible that the functional

connectivity differences that were seen in patients represented hyperconnectivity related to the anxiety and stress that can be associated with an acute illness and hospital admission, not experienced by the healthy controls. Previous studies did not include a STEMI control group so it is possible the previously described findings in TS are not unique and may be seen in other acute pathologies.

#### *4.4.4 NETWORK CONNECTIVITY IN TS*

Given the previous interest in the heart-brain interaction in TS patients specifically, we conducted a subgroup analysis to see if the findings could be explained by the TS patients alone. Patients with acute TS had decreased connectivity in the central executive network compared to both healthy and STEMI patients. In addition, on whole brain analysis, there was reduced connectivity in many regions involved in the autonomic control of the heart compared to healthy controls. These regions included multiple gyri in the prefrontal cortex, bilateral hippocampi, left superior temporal gyrus and bilateral inferior parietal gyri. Our results generally support the previously published literature. Decreased resting state connectivity has previously been shown in all these regions (the bilateral hippocampi, superior temporal gyrus and parietal gyri) (62, 64, 114, 115). The consistency of the results (excluding the Silva study which showed increased connectivity) is notable and the fact that some of these differences persist when compared to acute STEMI patients in our study adds substantial weight to the notion that TS patients have unique differences in the connectivity of the brain. This may have clinical implications for these patients. Further larger studies are required to see if these patients benefit from psychological or pharmacological treatments which can target autonomic pathways.

#### *4.4.5 RELATIONSHIP BETWEEN NETWORK MEASURES AND CLINICAL VARIABLES*

We have shown for the first time extensive negative correlations across all prespecified networks with both anxiety and stress scores in MINOCA patients. The only negative correlation in STEMI patients was between connectivity and

stress score and was found in the sympathetic network. Conversely positive correlations were found exclusively in healthy participants in the parasympathetic, DMN and CEN (Table 21).

**Table 21** Summary table showing direction of correlation seen on correlation analysis between variables and networks in each group.

Red = negative, grey = no correlation, green = positive correlation. GLS-CMR – global longitudinal strain on CMR; DMN – default mode network, CEN – central executive network.

Network	Variable	MINOCA	STEMI	Healthy
<b>Sympathetic</b>	Anxiety	Red	Grey	Grey
	Stress	Red	Red	Grey
	GLS-CMR	Grey	Grey	Grey
<b>Parasympathetic</b>	Anxiety	Grey	Grey	Grey
	Stress	Red	Grey	Green
	GLS-CMR	Grey	Grey	Grey
<b>DMN</b>	Anxiety	Red	Grey	Green
	Stress	Red	Grey	Green
	GLS-CMR	Grey	Grey	Grey
<b>Salience</b>	Anxiety	Grey	Grey	Grey
	Stress	Red	Grey	Grey
	GLS-CMR	Grey	Grey	Grey
<b>CEN</b>	Anxiety	Red	Grey	Grey
	Stress	Grey	Grey	Grey
	GLS-CMR	Red	Grey	Green
<b>Whole brain</b>	Anxiety	Red	Grey	Green
	Stress	Red	Grey	Grey
	GLS-CMR	Grey	Grey	Grey

This means that in patients presenting with MINOCA, the greater the anxiety or stress score, the lower the strength of the association between the specified nodes. Interestingly, the nodes involved again strongly reflect those involved in the autonomic and emotional processing regions with the amygdala, hippocampus, temporal gyri, cingulate cortex, caudate nuclei and thalamus appearing regularly on subnetwork analysis. On whole brain analysis across all 90 nodes, these nodes also feature prominently which demonstrates the specific regional nature of our findings. The positive correlation in healthy participants and the largely absent correlation in STEMI patients lends weight to the argument that there is disruption in the connectivity of patients with MINOCA and that this

is related to their underlying psychological status. The positive correlations seen in healthy participants suggest the greater the anxiety, stress or GLS\_CMV in the healthy state the stronger the strength of the association between the specified nodes. This may mean that healthy patients have an opposite response to MINOCA patients and perhaps have greater control over their autonomic nervous system.

The only network to be negatively correlated with GLS-CMV in MINOCA patients was the central executive network. The nodes involved were the left middle frontal gyrus (orbital part) and the left caudate nucleus. There was a positive correlation in healthy participants involving the left thalamus and left inferior parietal gyrus. This is a novel finding and suggests, for the first time, that there is a relationship between brain connectivity and cardiac function. As explored earlier the caudate nuclei and prefrontal cortex are closely integrated with the limbic system(228). Reduced connectivity in the limbic system inputs may alter the response to an emotional or physical stimulus via the autonomic nervous system. Therefore, a negative correlation with GLS-CMV might suggest that the lower connectivity in part of the limbic system may lead to a greater degree of LV dysfunction in MINOCA patients than those with higher connectivity. However, in healthy and STEMI patients this relationship does not exist and indeed reduced connectivity in the thalamus and inferior parietal cortex (part of the CEN) in healthy participants is associated with increased GLS.

Based on these results we speculate that patients with MINOCA have significant differences in connectivity, which is independent of their acute admission to hospital and which may predispose them to presenting with MINOCA. In addition, the degree of reduction in connectivity is related to their individual level of anxiety or stress. We believe that these results should encourage physicians to assess the psychological profile of these patients during their acute admission with MINOCA. There may be a role for established psychological, psychiatric, or pharmacological support for anxiety and stress to improve outcomes in these patients, Early studies have even shown that simple

heart rate variability biofeedback interventions can alter functional connectivity in the emotion-related resting state networks, which may be of benefit to these patients(231). Many more, larger outcome studies are now necessary. In addition, it may help physicians to understand which patients are particularly vulnerable, and which patients may need a higher level of psychological or psychiatric support.

### 4.4.6 LIMITATIONS

Our study has several limitations. Firstly, all images were acquired at 1.5T. This was decided at study design because of the need to acquire the images as early as possible after presentation and this necessitated using our clinical scanner. Although other comparable studies occurred at 3T, 1.5 T scanners have been used extensively in functional neuroimaging previously(63, 118) and although lower in sensitivity they do not suffer from the susceptibility artefacts from scanning at higher field strengths(155). During study design our scanner was found to generate high quality images suitable to answer our specific research questions. Secondly, we were not able to acquire cardiac physiological data during CMR acquisition as we were using the clinical scanner. This meant we were unable to control for possible nuisance variables due to cardiac and respiratory deformation. The STEMI and healthy control groups were significantly smaller than the MINOCA groups. This may mean that these groups lacked the power to detect small significant differences in connectivity or correlations. Nevertheless, these groups included 25 patients which is more than other comparable studies (64, 115). It should also be noted that only association can be inferred from our results, not causation.

### 4.5 CONCLUSIONS

Patients with MINOCA have a psychological profile which is different from the healthy and STEMI population. They have altered functional network connectivity which is distinct from another comparable acute illness (STEMI) and the connectivity correlates with their degree of stress, anxiety and GLS-CMR in



some networks. These novel findings need to be explored in larger studies including clinical outcomes. Studies examining possible psychological and pharmacological treatments which might alter the clinical outcomes of these patients are also warranted.

## Chapter 5      LONGITUDINAL CHANGES FROM THE ACUTE TO THE CHRONIC PHASE IN GREY MATTER VOLUME AND FUNCTIONAL CONNECTIVITY IN MINOCA

---

### 5.1 INTRODUCTION

Patients with MINOCA have a higher prevalence of anxiety and depression than the healthy population and are more likely to have preceding emotional stress or psychiatric illness compared to patients with obstructive coronary disease(172, 173). In addition, we have shown that anxiety scores are higher in acute MINOCA patients than age and sex matched acute STEMI patients, and that anxiety, depression and perceived stress scores are higher than matched healthy controls (Chapter 3). We have shown for the first time that patients with MINOCA have increased grey matter volume in the putamen and reduced grey matter in regions across the brain compared to healthy controls. MINOCA patients also have altered subnetwork connectivity in the DMN and CEN compared to controls (Chapter 4). This chapter will explore how these changes evolve over time.

There is surprisingly sparse data looking at longitudinal brain changes in other psychiatric conditions. In major depressive disorder, one study concluded that neuroanatomical differences were present in the temporal lobes, medulla and right hippocampus at baseline but were not found 11 years later, which the authors suggest are due to a beneficial effect of drug treatment on brain structure (232). In another study, 37 patients with major depressive disorder were followed for three years and showed increased or reduced grey matter volume at follow up in a large number of regions including the bilateral amygdala, bilateral cerebellar vermis, frontal gyri, left putamen, right hippocampus and right thalamus(233). Both these studies would suggest that grey matter volume is not stable in major depressive disorder. In contrast, another longitudinal study of

## Chapter 5 Longitudinal changes from the acute to the chronic phase in grey matter volume and functional connectivity in MINOCA

patients with anxiety or depression did not show any convincing changes in cortical volume with depression severity over time(234). A large meta-analysis of longitudinal studies in depressive disorder could not conclusively delineate if brain changes were pre-existing (chronic and largely fixed) or secondary to the depressive state (more acute and fluid)(235). With regard to stress, one study showed decreased right basolateral amygdala grey matter density in stressed individuals following an 8 week mindfulness course(236), and another suggested that taking part in meditation and yoga helped cope with stress and was associated with smaller right amygdala volume(237). Makovac et al showed that changes in amygdala functional connectivity over 12 months correlated with symptoms of generalised anxiety disorder(238). These studies would suggest overall that there is the potential for significant neuroplasticity associated with affective disorders, and that grey matter volume and functional connectivity can vary over time and correlate with symptoms.

However, in neuroimaging studies of patients with a previous episode of TS, anatomical and functional changes have been documented in similar regions in both the acute and chronic phase of TS compared to healthy controls(62, 102, 114-116). In the acute phase increased cerebral blood flow has been shown in subcortical structures (hippocampus, brainstem and basal ganglia) and reduced blood flow in the prefrontal cortex. The subcortical regions remained activated, but to a lesser degree into the chronic phase (113). Lower grey matter volume was seen in the acute phase in the right middle frontal gyrus, right subcallosal cortex, right insula, left central opercular cortex, right paracingulate gyrus, bilateral thalamus, left cerebral cortex and left amygdala. In addition, patient with acute TS showed lower functional connectivity in connections arising from the right anterior insula, temporal lobes and right precuneus (115). In the chronic phase Hiestand et al demonstrated decreased cortical thickness in both insulae and reduced grey matter volume in the bilateral amygdalae and at the amygdala/hippocampus border (114). In a functional study performed in the chronic phase, there was reduced connectivity in the sympathetic and parasympathetic networks and default mode networks comprising the bilateral

## Chapter 5 Longitudinal changes from the acute to the chronic phase in grey matter volume and functional connectivity in MINOCA

amygdala, bilateral hippocampus, bilateral superior and middle temporal gyri, left primary motor cortex, left supramarginal/angular gyrus, bilateral cerebellum, bilateral middle cingulate gyri, left dorsolateral prefrontal cortex, left superior parietal lobule/supramarginal gyrus, right hippocampus, left parahippocampal gyrus, bilateral posterior cingulate cortices, bilateral dorsal and ventral medial prefrontal cortex, left temporal pole, bilateral posterior inferior parietal lobule and the bilateral temporoparietal junction. Taken overall, this suggests that in TS these anatomical and functional differences persist. However, no study has examined the same TS patients over two time points or looked at MINOCA patients as a whole.

It is important to understand the causality between the onset of brain changes and the neurobiological changes over time. The brain changes that we have identified in the acute phase were either i) present prior to admission and may therefore represent an acute or chronic pathological state that might predispose to being admitted with MINOCA, or ii) reflect acute neurobiological changes occurring as a result of the MINOCA/stressful event (as has been postulated in major depressive disorder(239)) and therefore may or may not improve with time. If the brain changes predate MINOCA then there may be options for preventative psychological or pharmacological therapies to prevent disease onset. It was not possible in this study to address point i) as it is not feasible to image patients prior to disease onset as it is a relatively rare and unpredictable condition. However If brain changes evolve with time then these may be amenable or even reversible with antidepressant or anxiolytic medication(240).

Our study, for the first time, will compare the same patients with MINOCA at presentation and at 6 months to ascertain whether there are any differences in grey matter volume or connectivity from the acute phase to the chronic phase.

### 5.1.1 AIMS AND HYPOTHESES

The purpose of this study was to investigate if the changes in psychological state, grey matter volume or connectivity in MINOCA and TS patients at presentation are reversible at 6 months. Therefore, the hypotheses were limited only to investigate the longitudinal nature of any differences identified in chapters 3 or 4.

Our hypotheses for this study were that at 6 month follow up:

- i) patients with MINOCA would have higher anxiety and stress scores than both control groups
- ii) there would be no difference in grey matter volume in any region compared to MINOCA patients in the acute phase
- iii) there would be no change in the grey matter volume differences identified in the acute phase analysis compared to healthy controls.
- iv) there would be no change in the grey matter volume differences identified in the acute phase analysis between TS patients and healthy controls.
- v) there would be no difference in global efficiency, modularity and small world propensity compared to the acute phase.
- vi) there would be no difference in the connectivity changes seen on the DMN and CEN analysis in the acute phase between MINOCA and control patients.
- vii) there would be no difference in the connectivity changes seen on the CEN and whole brain analysis in the acute phase between TS and control patients.

## 5.2 *METHODS*

### 5.2.1 *OVERVIEW*

This was a prospective cohort study carried out at a large tertiary cardiac centre in the South-West. All patients who presented to the Bristol Heart Institute with MINOCA, as defined in chapter 2, were approached for inclusion in the study. Exclusion criteria were no diagnostic coronary angiogram (CT or invasive), age <18 or >80 years, current prisoners, pregnancy, contraindication to CMR, inability to perform CMR within 14 days of presentation, cardiac arrest at presentation or inability to meet the follow up requirements. Two control groups were recruited, an age and sex matched group who had been admitted with a STEMI and an age and sex matched healthy group. Participants underwent bloods, psychological questionnaires, CMR and brain MRI at presentation and at 6 months following their admission. The full study methods have been explained in chapters 2, 3 and 4.

Our CMR scanner (Magnetom Avanto 1.5-T, Siemens Healthineers, Erlangen, Germany) was replaced with a new scanner in April 2021 (Magnetom Sola 1.5-T, Siemens Healthineers, Erlangen, Germany) just prior to the delayed end of the study.

Only participants who returned for the follow up study and, so who had two data sets, were included in the longitudinal analysis.

### 5.2.2 *VOXEL-BASED MORPHOMETRY*

As previously described in detail in chapter 3, VBM was used to quantify grey matter volume. In brief, the images were checked to ensure they matched the standard MNI space and orientation, then they were segmented into tissue classes, normalised into the standard MNI space, and finally smoothed using a full

Chapter 5 Longitudinal changes from the acute to the chronic phase in grey matter volume and functional connectivity in MINOCA

width half maximum of 8 mm. The results were visualised using xjView toolbox

(<https://www.alivelearn.net/xjview>).

### 5.2.3 FUNCTIONAL CONNECTIVITY ANALYSIS

Chapter 4 describes in full the method used for analysis. In brief the images were corrected for slice timing, realigned, segmented, normalised to MNI space and smoothed. CSF, white matter and movement were then regressed out of the 4D image and the time series for each region were extracted and bandpass filtered. A weighted Pearson correlation matrix was created (excluding the cerebellum) and this was Fisher transformed. All negative correlations were removed leaving just the strength of the correlation. This final weighted correlation matrix was used for analysis.

The global efficiency, modularity and small world propensity were calculated using scripts as previously described in chapter 4.

NBS was used to analyse the connectivity matrices to test the pre-specified hypotheses. Thresholds were manually determined through experimentation and an FWE-corrected p value was calculated using permutation testing to determine the significance of supra-threshold topological connections. For the comparison between acute and chronic MINOCA or TS patients, exchange blocks were specified to constrain the analysis for repeated measurements within the same subjects (paired data).

### 5.2.4 STATISTICAL ANALYSIS

Data is presented as previously described depending on its normality and nature. Comparison of means between groups was assessed using the students unpaired two-way t-test (parametric data) or the Wilcoxon rank sums test (non-parametric data). The chi square test was used to compare categorical variables.

For the anatomical analysis, age, sex and TIV were again used as covariates. Comparison of grey matter volume across the whole brain between

## Chapter 5 Longitudinal changes from the acute to the chronic phase in grey matter volume and functional connectivity in MINOCA

acute or chronic MINOCA or TS patients was performed using a two-way paired student t-test. Comparison between chronic MINOCA or TS patients and healthy or STEMI controls was performed using a two-way unpaired student t-test. The results will be presented as FWE-corrected as this is the most stringent method.

A one-tailed paired t-test using NBS was used to assess for differences in connectivity between every connection in the specified networks in acute and chronic MINOCA patients. A one-tailed unpaired t-test was used to test for differences between MINOCA and control groups. Two  $t$  thresholds were chosen to demonstrate the nature of any effect shown. Effects seen at the more stringent thresholds are likely to be characterised by strong, topologically focal differences and at the lower threshold, subtle yet topologically extended differences.

A  $p$  value  $< 0.05$  was considered as strong evidence against the null hypothesis.

### 5.3 RESULTS

The study flow chart is shown in Figure 21. Of the 13 MINOCA patients lost to follow up, 2 had myocarditis, 5 had an MI, 2 had TS, 1 had another cardiomyopathy and 3 had normal/non-specific scans. Five STEMI patients were lost to follow up (1 due to COVID concerns, 3 withdrew without reason, 1 died). 59 patients were included in the anatomical analysis and 56 in the functional analysis as 3 of the patients who returned did not have the correct number of slices acquired on the initial scans at presentation (1 myocarditis, 1 MI and 1 normal scan). 14 of the follow up scans were performed on the Siemens Sola scanner (10 MINOCA, 4 STEMI controls).



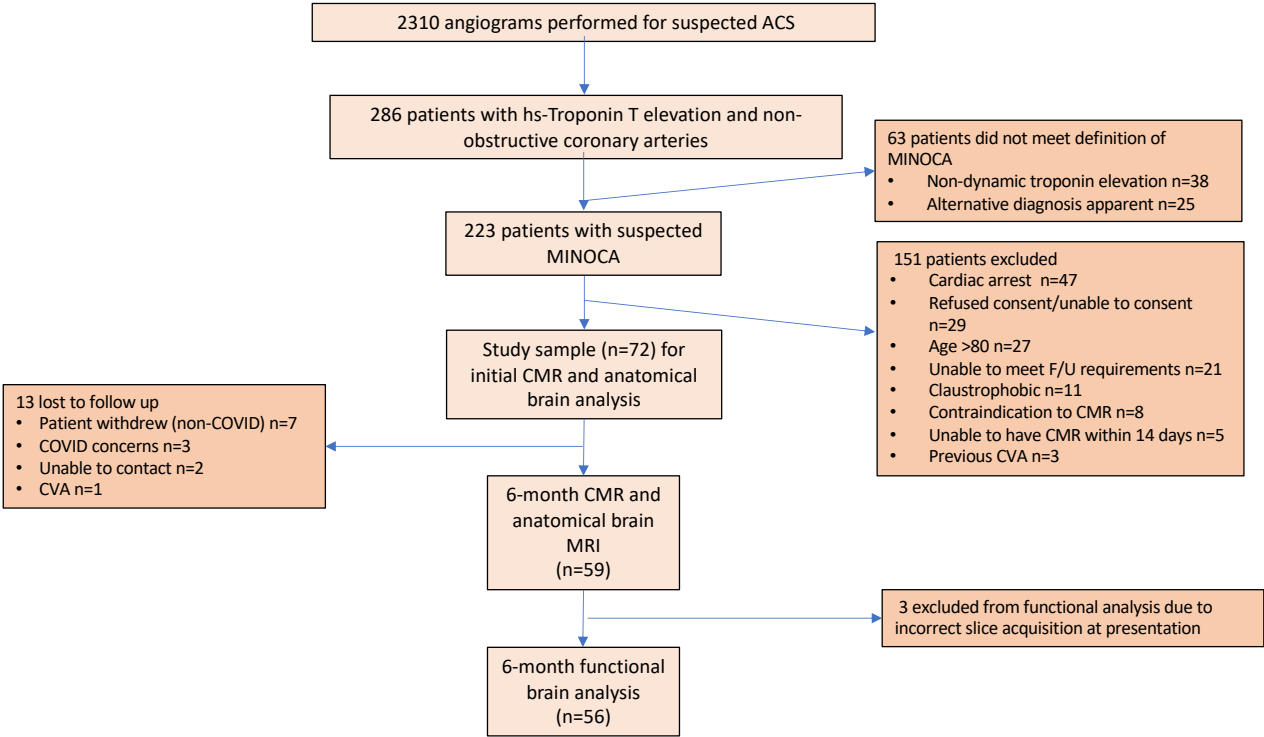


Figure 21 Study Flow Chart

Table 22 shows the demographics, investigations, questionnaire scores and CMR findings for the 59 acute and chronic phase MINOCA patients who completed both study visits, the chronic phase STEMI patients and healthy controls. Acute phase data for the STEMI patients is not shown again here as it is not central to our hypotheses. The follow up MRI imaging was acquired at a median of 231 [192-336] days after presentation in the MINOCA group and 217 [183-359] days in the STEMI group ( $p=0.552$ ). Due to the coronavirus pandemic, research was temporarily suspended meaning that follow up visits were delayed beyond the planned 6 months.

Table 22 Demographics, investigations, questionnaire and CMR findings for the different study groups.

Variable	MINOCA acute phase (n=59)	MINOCA chronic phase (n=59)	P value MINOCA acute v chronic	STEMI chronic phase (n=22)	P value chronic MINOCA v chronic STEMI	Healthy Controls (n=26)	P value chronic MINOCA v Healthy
Age at presentation, median [IQR], years	56 [47-64]	56 [47-64]	nn/a	61 [49-70]	0.195	53 [47-60]	0.244
Female sex, n (%)	26 (44)	26 (44)	nn/a	6 (27)	0.169	15 (58)	0.247
Right-handed, n (%)	51 (86)	51 (86)	nn/a	20 (91)	0.587	21 (81)	0.351
<b>Laboratory Investigations</b>							
Peak Troponin T, median [IQR], ng/L	183 [53-573]	6.5 [5-9]	<b>&lt;0.001</b>	7 [5-9]	0.69	5 [5-6]	<b>0.012</b>
CRP, median [IQR], mg/L	5 [1-23]	1 [1-2]	<b>&lt;0.001</b>	1 [1-3]	0.750	1 [1-2]	0.370
NT-pro-BNP, median [IQR], pg/ml	136 [75-517]	81 [39-161]	<b>&lt;0.001</b>	133 [106-241]	<b>0.037</b>	42 [21-59]	<b>0.002</b>
<b>Questionnaire scores</b>							
MMSE, median [IQR]	29 [28-29]	29 [28-30]	0.108	30 [29-30]	0.096	30 [29-30]	0.066
Anxiety, mean [SD]	8.1 [4.0]	8.2 [4.5]	0.858	5.0 [3.0]	<b>0.003</b>	4.4 [3.2]	<b>&lt;0.001</b>
Depression, median [IQR]	4 [2-6]	4 [1-8]	0.945	2 [1-4]	0.207	1 [0-3]	<b>&lt;0.001</b>
Perceived Stress Scale, mean [SD]	17.3 [8.0]	15.8 [8.8]	0.082	12.8 [6.9]	0.157	9.5 [6.2]	<b>0.001</b>
Impact of Events, median [IQR]	n/a	16 [7-35]	n/a	13 [5-28]	0.234	n/a	n/a
<b>Cardiac MRI findings</b>							
Days from admission to CMR, median [IQR]	5 [2-7]	231 [192-336]	nn/a	217 [183-359]	0.552	n/a	n/a
LVEF, median [IQR], %	59 [53-62]	60 [58-64]	<b>00.003</b>	57 [55-59]	<b>0.004</b>	62 [60-65]	0.228
iLVEDV, median [IQR], ml/m <sup>2</sup>	78 [74-95]	77 [73-92]	00.243	82 [76-86]	0.534	86 [68-97]	0.538
iLV mass, median [IQR], g/m <sup>2</sup>	54 [48-66]	53 [47-60]	<b>&lt;0.001</b>	54 [47-56]	0.655	51 [46-62]	0.611
RVEF, median [IQR], %	57 [53-61]	58 [52-62]	00.594	58 [53-63]	0.470	58 [51-63]	0.760
GLS, median [IQR]	15.9 [-17.4-13.5]	16.7 [-17.9 -15.1]	<b>00.012</b>	-15.8 [-18.1 -14.3]	0.764	-17.9 [-20 -15.9]	<b>0.028</b>
Presence of LGE, n (%)	36 (61)	28 (47)	<b>00.010</b>	20 (91)	<b>&lt;0.001</b>	0 (0)	<b>&lt;0.001</b>
<b>Pattern of LGE n. (%)</b>							
Ischaemic	21 (58)	19 (68)	00.490	20 (100)	<b>0.011</b>	n/a	n/a
Mid-wall	6 (17)	4 (14)		0 (0)		n/a	n/a
Subepicardial	7 (19)	3 (2)		0 (0)		n/a	n/a
Diffuse/patchy	1 (3)	2 (7)		0 (0)		n/a	n/a
Insertion point	1 (3)	0 (0)		0 (0)		n/a	n/a
LGE mass, median [IQR], g	0.6 [0-4.8]	0 [0-2.6]	00.089	9.3 [5.8 -17.1]	<b>&lt;0.001</b>	0 [0]	<b>&lt;0.001</b>
Presence of oedema, n (%)	37 (63)	0 (0)	<b>&lt;0.001</b>	3 (17)	<b>0.004</b>	0 (0)	n/a
Oedema mass, median [IQR], g	6.9 [0-29.6]	0 [0-0]	<b>&lt;0.001</b>	0 [0-0]	<b>0.004</b>	0 [0]	n/a

### 5.3.1 INVESTIGATIONS

There was no difference in age, sex or handedness between any of the groups. MINOCA patients continued to have an elevated BNP and Troponin-T at

follow up compared to healthy controls, but this was less than STEMI patients.

MINOCA patients had significantly higher anxiety scores at follow up compared to STEMI and healthy controls, and higher depression and perceived stress scores than healthy controls (Figure 22). GLS-CMR in MINOCA patients improved from presentation but still was significantly impaired compared to healthy controls.

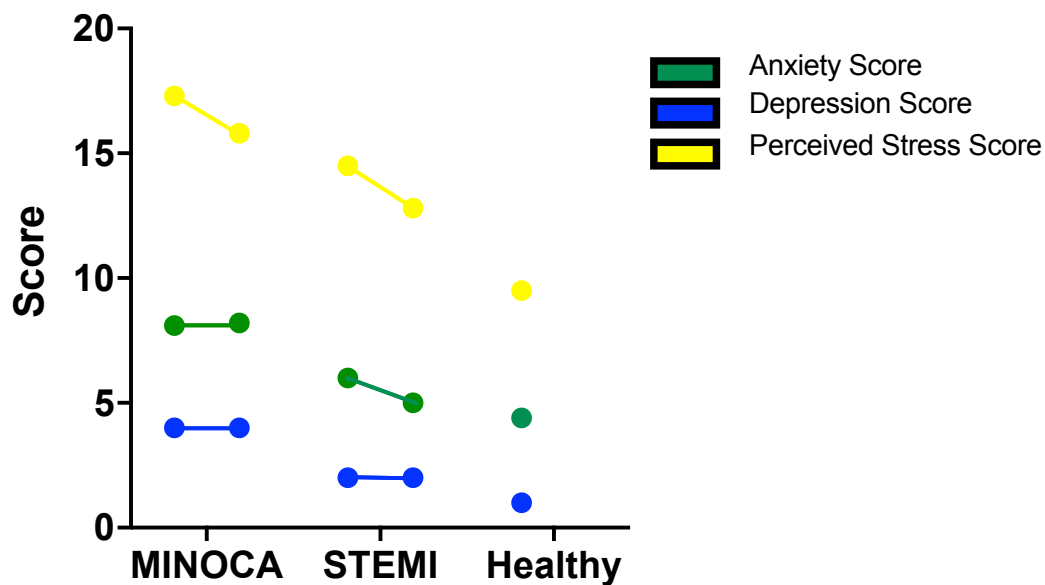


Figure 22 Before and after plot showing change in psychological scores at each study visit.

The first dot represents the mean score at presentation, the second dot represents the mean score at follow up (healthy participants only had one study visit)

### 5.3.2 ANATOMICAL ANALYSIS

59 MINOCA patients and 22 STEMI patients who undertook both study visits were included.

#### 5.3.2.1 Acute phase MINOCA v chronic phase MINOCA

Figure 32 shows the grey matter regions of the brain which demonstrated increased volume in the chronic phase compared to the acute phase. The threshold was set at  $>5$ . The full list of anatomical regions and coordinates is listed in Appendix D but mainly included regions in the bilateral inferior and medial frontal gyrus, bilateral superior and medial temporal gyrus, bilateral insula and cerebellum.

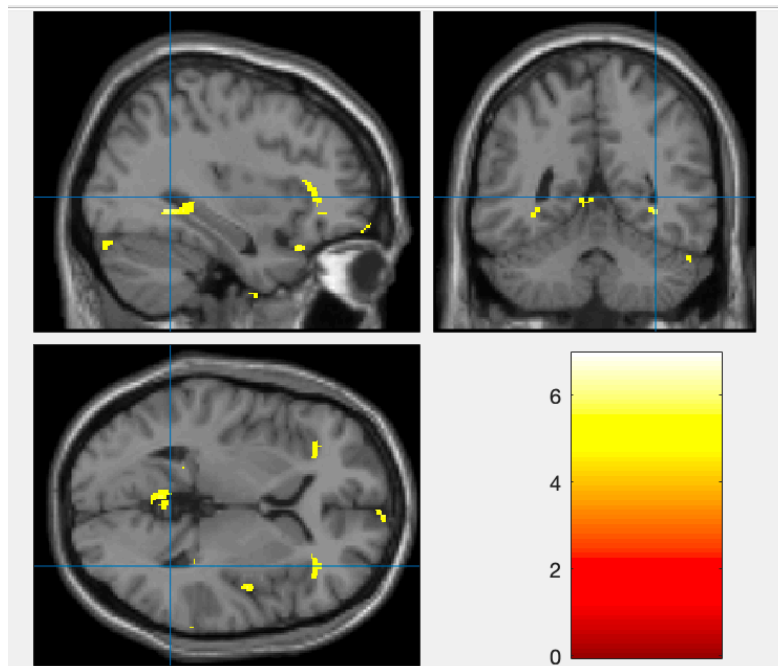


Figure 23 Brain activation map showing grey matter regions in MINOCA patients demonstrating significantly increased volume in the chronic phase compared to the acute phase.

The colour bar represents the T value and results are corrected for multiple comparisons (FWE corrected). Only results with a T threshold  $>5$  are displayed.

Figure 24 shows the grey matter regions in MINOCA patients which demonstrated reduced volume in the chronic phase compared to the acute phase. The t threshold was set at  $>5$ . The full list of anatomical regions is listed in Appendix D but most notably included the bilateral putamen, bilateral insula, bilateral cingulate gyrus, left hippocampus and parahippocampus, left thalamus, and middle and superior temporal gyri.

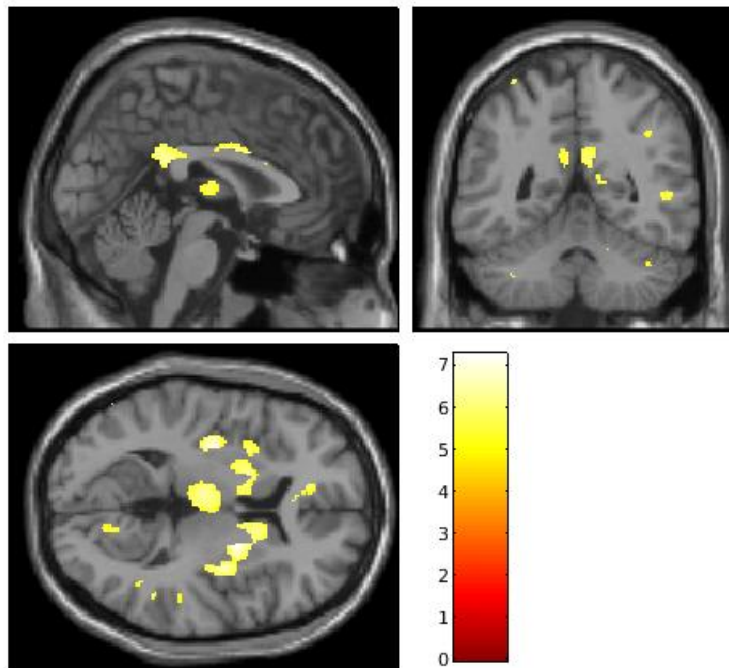


Figure 24 Brain activation map showing grey matter regions in MINOCA patients demonstrating significantly reduced volume in the chronic phase compared to the acute phase.

The colour bar represents the T value and results are corrected for multiple comparisons (FWE corrected). Only results with a T threshold >5 are displayed.

#### 5.3.2.2 Chronic phase MINOCA v healthy controls

MINOCA patients in the chronic phase had reduced grey matter volume in 4 regions compared to healthy controls (Figure 25). No regions had increased grey matter volume compared to healthy controls. The full list of anatomical regions is listed in Appendix D and included the left middle temporal gyrus, left precentral gyrus and bilateral postcentral gyri.

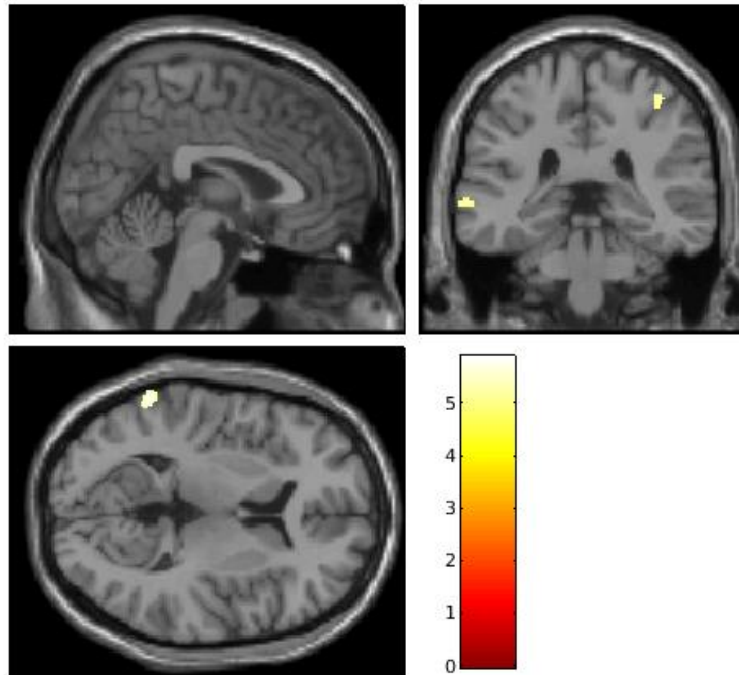


Figure 25 Regions of the brain with reduced grey matter volume in chronic MINOCA patients versus healthy control patients.

The colour bar represents the T value and results are corrected for multiple comparisons (FWE corrected). Only results with a T threshold  $>5$  are displayed.

#### 5.3.2.3 Chronic phase MINOCA v chronic phase STEMI controls

There was no difference in grey matter volume between MINOCA and STEMI patients at follow up.

#### 5.3.3 SUBGROUP ANATOMICAL ANALYSIS

9/11 patients with TS completed both study visits and were included in the TS subgroup analyses. 1 patient withdrew and 1 patient was excluded between the first and second visit due to an ischaemic stroke. Median scan interval for the TS group at follow up was 257 days (IQR 199-308). This group with TS was only compared with the 25 healthy control patients as no difference was seen between TS and STEMI patients at presentation.

##### 5.3.3.1 Acute phase TS v chronic phase TS

There was no difference in grey matter volume in any brain region between the acute and chronic phase.

### 5.3.3.2 Chronic phase TS v healthy participants

There was no difference in grey matter volume between chronic TS patients and healthy controls.

### 5.3.4 GLOBAL BRAIN MEASURES

There was no difference in any network measure between the acute and chronic phases. However, in the chronic phase of MINOCA modularity was significantly higher compared to healthy participants (Table 23). There were no other differences in any other network measures. There was no difference in TIV between the groups.

Table 23 Global network measures in acute and chronic phase MINOCA patients and control patients

Variable	MINOCA acute phase (n=56)	MINOCA chronic phase (n=56)	P value MINOCA acute v chronic	STEMI chronic phase (n=22)	P value chronic MINOCA v chronic phase STEMI	Healthy Controls (n=25)	P value chronic MINOCA v Healthy
Total intracranial volume, mean [SD]	1544 [195]	1539 [195]	0.618	1552 [146]	0.782	1534 [171]	0.922
Global efficiency, median [IQR]	0.325 [0.304-0.353]	0.331 [0.306-0.381]	0.342	0.332 [0.309-0.358]	0.750	0.319 [0.305 – 0.352]	0.411
Modularity, mean [SD]	0.131 [0.017]	0.135 [0.017]	0.189	0.138 [0.017]	0.532	0.127 [0.018]	<b>0.049</b>
Small world propensity, median [IQR]	0.675 [0.586-0.760]	0.708 [0.617-0.743]	0.458	0.699 [0.605-0.749]	0.882	0.690 [0.580 – 0.763]	0.856

### 5.3.5 FUNCTIONAL CONNECTIVITY ANALYSIS

#### 5.3.5.1 Acute phase MINOCA v chronic phase MINOCA network connectivity analysis

There were no differences in connectivity in any ROI analysis or on the whole brain analysis.

### 5.3.5.2 Chronic phase MINOCA v STEMI and healthy controls

56 MINOCA patients were included in this network connectivity analysis. Only functional networks where there was a significant difference at presentation were analysed (e.g. DMN and CEN).

#### 5.3.5.2.1 *Default Mode Network*

At the higher set threshold ( $t=2.2$ ), there was increased connectivity in the MINOCA-related subnetwork compared to healthy participants consisting of 9 edges over 7 nodes ( $p=0.020$ , Figure 26). The nodes involved were the bilateral parahippocampus, bilateral supramarginal gyri, bilateral medial superior frontal gyrus and the left inferior temporal gyrus. At the lower set threshold ( $t=1.9$ ), there was greater connectivity compared to healthy participants in the DMN comprising 13 edges over 10 nodes ( $p=0.042$ , Appendix D).



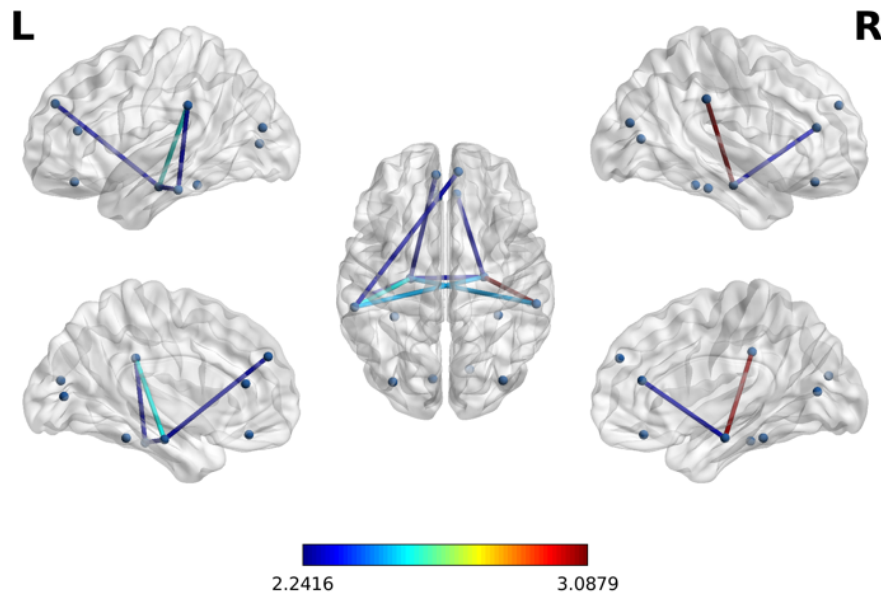


Figure 26 Subnetworks with greater functional connectivity in chronic phase MINOCA patients compared to healthy controls in the default mode network.

Only subnetworks at the higher set threshold ( $t=2.2$ ) are shown. The subnetworks at the lower set threshold are shown in Appendix D with a table of the nodes. The colour bar signifies the t-value of the strength of the difference in connectivity between the subnetworks in each group.

#### 5.3.5.2.2 Central Executive Network

At the higher set threshold ( $t=3.7$ ), there was reduced connectivity in the chronic phase MINOCA-related subnetwork compared to healthy participants. This comprised 1 edge over 2 nodes ( $p=0.03$ , Figure 27). The nodes involved were the left frontal middle gyrus (orbital part) and the left frontal inferior gyrus (orbital part). At the lower set threshold ( $t=3.0$ ), the network consisted of 3 edges over 4 nodes ( $p=0.006$ , Appendix D).

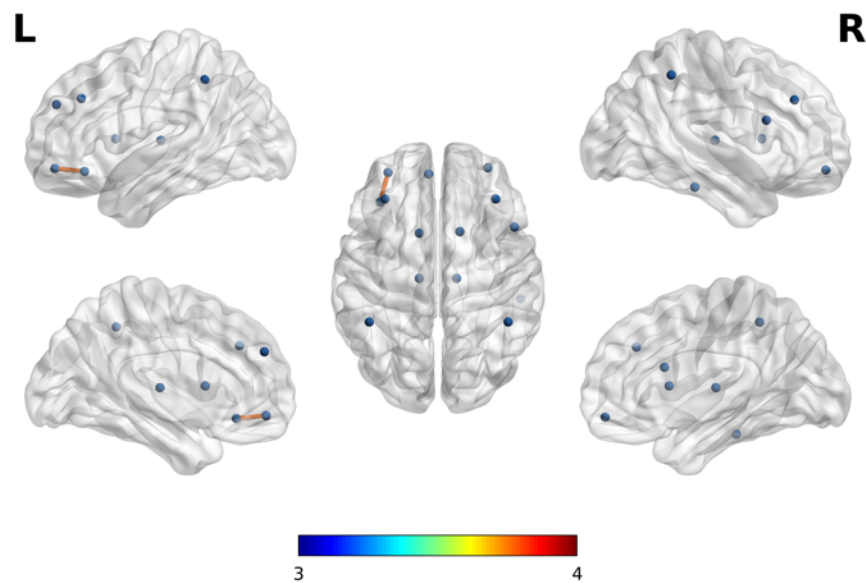


Figure 27 Subnetworks with lower functional connectivity in chronic phase MINOCA patients compared to healthy controls in the central executive network.

Only subnetworks at the higher set threshold ( $t=3.7$ ) are shown. The subnetworks at the lower set threshold are shown in Appendix D with a table of the nodes. The colour bar signifies the t-value of the strength of the difference in connectivity between the subnetworks in each group.

There was no difference in connectivity between chronic MINOCA and STEMI patients in the central executive network.

Table 24 summarises the changes from the same analyses performed in the acute phase in Chapter 4.

Table 24 Table illustrating the changes in connectivity over time in MINOCA versus control patients

Red cells indicate reduced connectivity and green cells highlight increased connectivity.

Network	Acute MINOCA v Acute STEMI	Chronic MINOCA v Chronic STEMI	Acute MINOCA v Healthy	Chronic MINOCA v Healthy
DMN	Nil	Not tested	Bilateral parahippocampus, right supramarginal gyrus	Bilateral parahippocampus, bilateral supramarginal gyri, bilateral medial superior frontal gyrus, left inferior temporal gyrus
CEN	Bilateral frontal middle gyri (orbital part), right thalamus, right inferior temporal gyrus, bilateral inferior parietal gyri	Nil	Left frontal middle and inferior gyri (orbital parts)	Left frontal middle and inferior gyri (orbital parts)

### 5.3.6 SUBGROUP FUNCTIONAL ANALYSIS

#### 5.3.6.1 Acute vs chronic phase TS

This subgroup analysis included the 9 acute patients with TS compared to the same 9 patients in the chronic phase.

##### 5.3.6.1.1 ROI Analysis

There was no difference in connectivity between acute and chronic phase TS patients in any of the pre-specified ROI analyses.

##### 5.3.6.1.2 Whole Brain

At the higher set threshold ( $t=5.7$ ) there was reduced connectivity in the acute TS patients compared to chronic phase TS patients in a subnetwork comprising 1 edge over 2 nodes ( $p=0.035$ ; Figure 28; Appendix D). The nodes involved were the left superior temporal gyrus and the left superior occipital

gyrus. There were no significant hypoconnected networks at any lower set threshold. There were no subnetworks with greater connectivity in the acute phase compared to the chronic phase.

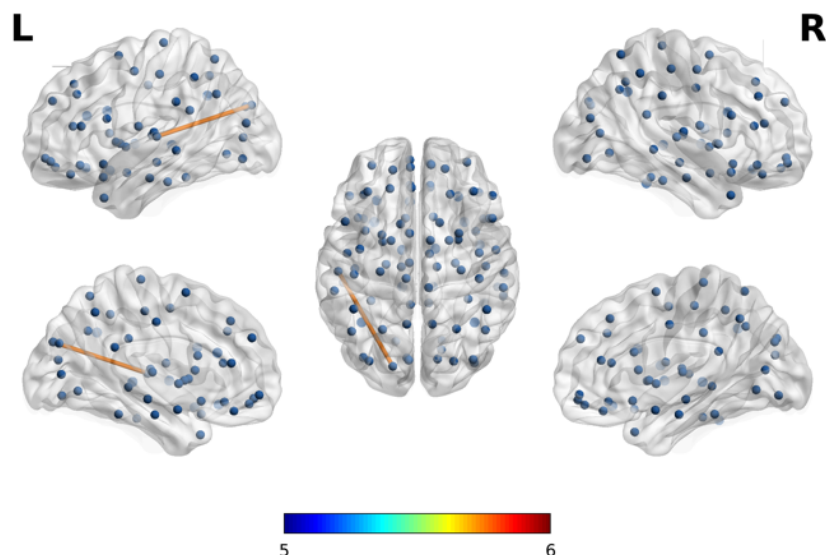


Figure 28 Subnetworks with reduced functional connectivity in acute phase TS patients compared to chronic phase TS patients on whole brain connectivity analysis.

Only subnetworks at the higher set threshold ( $t=5.7$ ) are shown. The subnetworks at the lower set threshold are shown in the appendix with a table of the nodes. The colour bar signifies the t-value of the strength of the difference in connectivity between the subnetworks in each group.

### 5.3.6.2 Chronic phase TS v controls

9 TS patients were included in this analysis compared to 25 healthy controls or 22 STEMI controls.

#### 5.3.6.2.1 Central Executive Network

At the higher set threshold ( $t=2.7$ ) there was greater connectivity in the chronic phase TS subnetwork compared to healthy controls comprising 4 edges over 5 nodes ( $p=0.029$ , Figure 29). The nodes involved were the right inferior frontal gyrus (opercular part), left thalamus, left middle frontal gyrus (orbital part), right caudate nucleus and the right middle frontal gyrus. At the lower set

threshold ( $t=2.3$ ) the network comprised 7 edges over 7 nodes ( $p=0.040$ ; Appendix D).

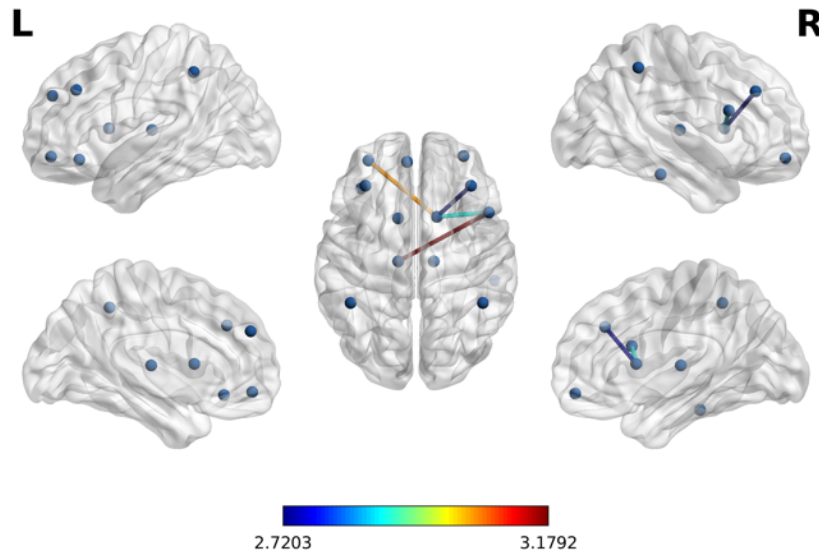


Figure 29 Subnetworks with greater functional connectivity in chronic phase TS patients compared to healthy controls in the central executive network.

Only subnetworks at the higher set threshold ( $t=2.7$ ) are shown. The subnetworks at the lower set threshold are shown in Appendix D with a table of the nodes. The colour bar signifies the t-value of the strength of the difference in connectivity between the subnetworks in each group.

There was also lower connectivity in the chronic phase TS group compared to healthy controls at a set threshold of  $t=2.4$  comprising 3 edges over 3 nodes ( $p=0.019$ ; Figure 30; Appendix D but there was no significantly lower connectivity at a lower set threshold. The nodes involved were the left middle frontal gyrus (orbital part), right inferior parietal gyrus and the left inferior frontal gyrus (orbital part).

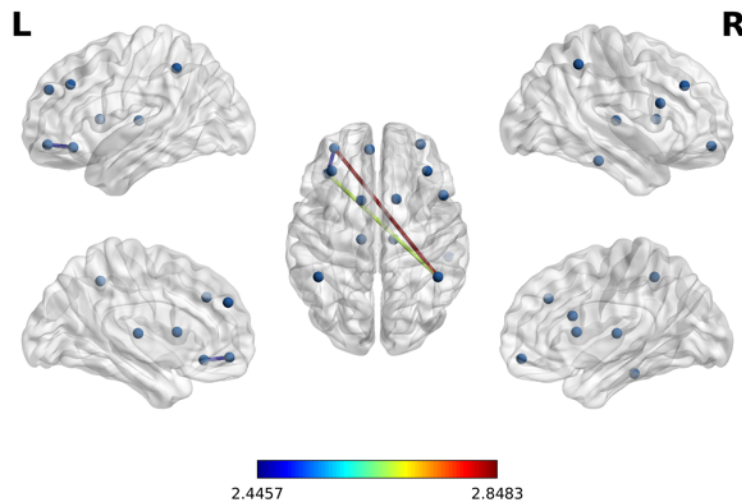


Figure 30 Subnetworks with lower functional connectivity in chronic phase TS patients compared to healthy controls in the central executive network.

Only subnetworks at the higher set threshold ( $t=2.4$ ) are shown. The subnetworks at the lower set threshold are shown in the Appendix D with a table of the nodes. The colour bar signifies the t-value of the strength of the difference in connectivity between the subnetworks in each group.

At the higher set threshold ( $t=2.8$ ) there was lower connectivity in the chronic phase TS patients compared to STEMI controls in a subnetwork comprised 2 edges over 3 nodes ( $p=0.016$ , Figure 31). These were the left inferior frontal gyrus (orbital part) and the bilateral inferior parietal gyri. At the lower set threshold ( $t=2.0$ ) this network comprised 6 edges over 5 nodes ( $p=0.031$ , Appendix D).

There were no subnetworks with higher connectivity in chronic phase TS patients compared to STEMI controls.

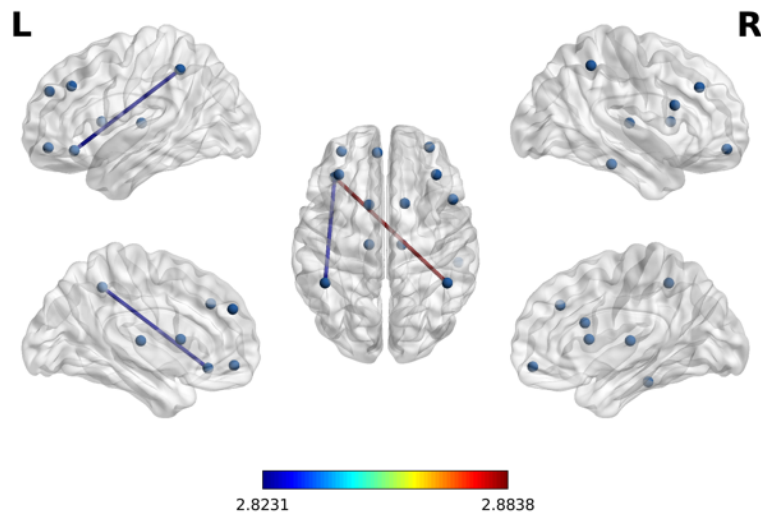


Figure 31 Subnetworks with lower functional connectivity in chronic phase TS patients compared to STEMI controls in the central executive network.

Only subnetworks at the higher set threshold ( $t=2.8$ ) are shown. The subnetworks at the lower set threshold are shown in the Appendix D with a table of the nodes. The colour bar signifies the t-value of the strength of the difference in connectivity between the subnetworks in each group.

#### 5.3.6.2.2 Whole Brain

There was no difference in connectivity between any brain regions in patients with a previous episode of TS and healthy or STEMI controls.

Table 25 Table illustrating changes in functional connectivity from the acute to chronic phase compared to controls in TS

Red cells indicate reduced connectivity and green cells highlight increased connectivity.

Network	Acute TS v chronic STEMI	Chronic TS v chronic STEMI	Acute TS v healthy	Chronic TS v healthy
<b>CEN</b>	Left frontal middle gyrus (orbital part), right inferior parietal gyrus	Left inferior frontal gyrus (orbital part) bilateral inferior parietal gyri.	Left frontal middle gyrus (orbital part), bilateral inferior parietal gyri, left frontal middle gyrus, left medial frontal superior gyrus, bilateral frontal inferior gyri (orbital parts)	Left middle frontal gyrus (orbital part), right inferior frontal gyrus (opercular part), left thalamus, right caudate nucleus and the right middle frontal gyrus
				Left middle frontal gyrus (orbital part), right inferior parietal gyrus and the left inferior frontal gyrus (orbital part).
<b>Whole brain</b>	Left superior temporal gyrus and the right inferior frontal gyrus (triangular part)	No difference	Bilateral hippocampus, left superior temporal gyrus, right middle frontal gyrus, left superior parietal gyrus, right inferior frontal gyrus (triangular part).	No difference



## 5.4 *DISCUSSION*

The principal results are:

- i) patients with MINOCA had higher anxiety scores than both control groups in the chronic phase.
- ii) there were multiple regions of grey matter volume differences between acute and chronic phase MINOCA patients.
- iii) there was reduced grey matter volume in 4 clusters in chronic phase MINOCA patients compared to healthy controls.
- iv) grey matter volume differences seen in the acute phase between TS patients and healthy controls did not persist into the chronic phase.
- v) there was no difference in global efficiency, global modularity and small world propensity in chronic phase MINOCA when compared to the acute phase, although global modularity was higher in chronic phase MINOCA patients compared to healthy controls.
- vi) there were no differences in connectivity between the acute and chronic phase MINOCA patients.
- vii) the connectivity differences seen in the DMN and CEN between acute phase MINOCA patients and healthy controls largely persisted into the chronic phase. However, the changes seen in the CEN when compared to STEMI patients did not persist.
- viii) the connectivity differences seen in the CEN and on whole brain analysis in the acute phase between TS and control patients partially persisted into the chronic phase.
- ix) Connectivity increased between the acute and chronic phase of patients with TS in a single subnetwork comprising 2 nodes on whole brain analysis.

#### *5.4.1 LONGITUDINAL PSYCHOLOGICAL PROFILES*

There was no change in the psychological profile between the groups over time. At follow up MINOCA patients still had significantly higher anxiety scores compared to STEMI controls and healthy participants. Anxiety scores stayed similar in the MINOCA group but trended lower in the STEMI group although were not significantly different. Stress scores trended lower in both groups. MINOCA patients experience greater anxiety into the chronic phase of their condition suggesting that this is not an acute phenomenon related to the acute admission and may represent their chronic underlying mental state. This would be in keeping with the fact there was no difference in functional connectivity between the acute and chronic phase demonstrated in our study. In addition, we demonstrated in Chapter 4 that MINOCA patients with high anxiety scores had multiple negative correlations with connectivity strength in the sympathetic, parasympathetic, DMN, CEN and salience networks which may suggest the functional connectivity is driven by high anxiety.

#### *5.4.2 LONGITUDINAL GREY MATTER VOLUME AND FUNCTIONAL CONNECTIVITY DIFFERENCES*

##### **5.4.2.1 Acute v chronic phase MINOCA**

There were extensive differences in GMV over the follow up period. GMV increased over time in mainly frontal regions, but also notably in the bilateral insula and right middle and superior temporal gyri. In addition, there were widespread reductions in grey matter volume over time. Many AAL regions were involved but most significantly the bilateral putamen, left insula, bilateral posterior cingulate gyri, left thalamus, left parahippocampal gyrus and left hippocampus. Firstly, a few of these AAL regions overlap (e.g. the insula); this is likely to be because each AAL region includes a range of MNI coordinates depending on its size. It is theoretically possible for GMV to increase in one part of the AAL region but decrease in another. This restriction in spatial resolution is a limitation of using anatomical parcellation to describe complex architecture.

Secondly, it is noticeable that the reductions in GMV occurred in many of the areas we have identified previously as being part of the limbic and autonomic nervous systems. Grey matter comprises cell bodies, unmyelinated axons and glial cells. Reduction in grey matter volume is thought to reflect cortical atrophy (loss of neurones). Grey matter however is known to show relatively rapid plasticity which is confirmed in this study. Grey matter in the occipito-parietal regions increases over time (even after as little as 7 days) in people learning to juggle(241) and increased grey matter has been shown in people undertaking cognitive tasks as well(242). Changes in grey matter volume may represent neuronal or extra-neuronal changes. Neuronal changes can include neurogenesis, synaptogenesis, myelination or even neuronal morphological changes. Extra neuronal changes can include increases in glial cell size or number and angiogenesis(243). Neurogenesis can occur in the hippocampus(244) but it is controversial in the cortex and thus is unlikely to be a major driver of increased GMV in our study. Glial cells outnumber neurones 6:1(243) and have been shown to increase in response to learning and experience(245) and are therefore a more likely driver of increased grey matter volume along with myelination of unmyelinated axons. However, it is not possible without histology to be certain of the under aetiology for the cause of the increase in GMV in this study.

There were no differences in network connectivity over time in any of our ROIs or on whole brain analysis. This would suggest that the anatomical differences described above did not have any measurable influence on connectivity in any of our ROIs. This may be because the change in connectivity was too small to be detected with our sample size, the mixed picture of increases and decreases in GMV or perhaps because GMV is not proportionately related to connectivity or function of the node as is typically assumed(226, 227). The only change in the psychological profile of MINOCA patients over time was a non-significant fall in the stress score, similar to the STEMI cohort. Although there was no significant change in connectivity, the reductions over time in GMV in the limbic regions (hippocampus, cingulate cortex, insula) may be due to, or indeed

be responsible for, reduced stress in MINOCA patients. Nevertheless, our results suggest that grey matter volume is dynamic in MINOCA patients over time.

#### 5.4.2.2 Chronic phase MINOCA v healthy or chronic STEMI controls

In the acute phase there was increased GMV in the right putamen and reduced GMV in multiple areas (Chapter 3) compared to healthy controls. In the chronic phase there were no areas of increased GMV and only 4 areas of reduced grey volume persisted (left middle temporal gyrus, bilateral postcentral and left precentral gyri). Once again this suggests a plasticity in GMV over time akin to the fluidity in GMV in major depressive disorder described in the introduction. This could reflect the brains response over time to the acute event and subsequent recovery/therapy or could suggest that the diffuse anatomical changes seen at presentation precipitated the MINOCA event in the first place. There was no difference in GMV at presentation or at follow up between MINOCA and STEMI controls. This suggests that the changes seen above are not unique to MINOCA patients. This raises the possibility that the changes in GMV identified reflect a more general stress response to acute physical illness. Interestingly, in the COVID-19 population there is early evidence suggesting that the acute systemic inflammation seen commonly in COVID-19 predicts changes in brain structure (GMV and white matter volume), function and PTSD and depression severity(246). In rheumatoid arthritis (another inflammatory condition), levels of peripheral inflammation correlate with reductions in GMV(247). Both COVID-19 and rheumatoid arthritis are associated with increased risk of MI(248, 249) due to their pro-inflammatory state. This suggests that GMV changes are not unique to the MINOCA or STEMI population. Together with the fact that GMV changes reduced over time, we postulate that the changes in GMV we have identified compared to healthy controls represent a more non-specific neuroanatomical response to an acute inflammatory illness which largely resolves over time.

In the acute phase in the DMN there was increased connectivity in the bilateral parahippocampal gyri and right supramarginal gyrus compared to healthy controls, whereas at follow up there was increased connectivity involving more

nodes including the bilateral parahippocampal gyri, bilateral supramarginal gyrus, bilateral superior medial frontal gyri and the left inferior temporal gyrus. This is in keeping with the results of the GMV analysis over time which showed a widespread increase in GMV (or more precisely a resolution of the reduction in GMV) in MINOCA patients compared to healthy controls which may partly explain the subsequent increase in the number of nodes demonstrating increased connectivity. The parahippocampal gyrus is part of the cortical-limbic-subcortical circuit(250) and in addition to regulating emotional behaviour has a particular role in episodic memory encoding and retrieval and visuospatial processes(251). Our results suggest that top-down control of limbic regions in the DMN by the prefrontal cortex is greater than healthy controls which may suggest these patients have exaggerated responses to emotion than healthy patients. Connectivity increases over time. The reason for this increase is not clear but could explain why these patients tend to have an ongoing mortality risk and risk of future events(8, 112). It could also represent a homeostatic overcorrection in response to the MINOCA event or a response to treatment. Increased connectivity in the DMN could feasibly affect cortical control of the limbic regions. This may influence the downstream subcortical structures, such as the amygdala, which can cause dysregulation in the autonomic nervous system(102). It can increase the risk of major adverse cardiac events (including MINOCA) possibly via increased inflammation and atherosclerotic plaque instability mediated by increased bone marrow activity and macrophage activation(102, 111).

In the CEN there was reduced connectivity in the left middle and inferior frontal gyri (orbital parts) and these changes persisted into the chronic phase when compared to healthy controls. When compared to STEMI patients there was reduced connectivity in the left middle frontal gyrus (orbital part), right middle frontal gyrus, right thalamus, right inferior temporal gyrus and the bilateral inferior parietal gyri acutely, but there was no difference in connectivity in the chronic phase. The fact that there was a difference in connectivity in the CEN between both healthy and STEMI controls suggests these changes are unique to MINOCA patients as discussed in chapter 4. However, the reduced connectivity

persists when compared to healthy controls but resolves when compared to STEMI patients. This suggests that connectivity decreases over time in STEMI patients in the CEN, which is responsible for integrating inputs from many other networks to initiate task selection and executive function and is disrupted in many neuropsychiatric disorders(252). The lower connectivity of the CEN in MINOCA, notably the left middle and inferior frontal gyri, which as previously discussed have close links with the amygdala, may reflect a persistent psychopathological state with subsequent downstream dysregulation of critical limbic/autonomic systems providing the milieu for an acute cardiac event. The reduction in connectivity over time in the STEMI group compared to MINOCA is interesting and unexplained. There was no significant difference in the psychological profile of STEMI patients over time suggesting that variation in anxiety, depressive or stress symptoms cannot explain the decrease. It could represent a treatment effect as STEMI patients are typically prescribed medications including beta-blockers which antagonise cardiac sympathetic beta-adrenoceptors. STEMI patients also undergo a period of cardiac rehabilitation including counselling and a managed exercise programme. It is plausible that these interventions unique to the STEMI group could influence CEN connectivity.

#### **5.4.2.3 Acute v chronic phase TS**

There was no difference in GMV between the acute and chronic phase of TS. There was reduced connectivity in only one network in the acute phase of TS when compared to the chronic phase. This implies that the functional and anatomical changes identified in TS largely persist into the chronic phase and are not 'acute'. The one difference between the acute and chronic phase involved the left superior temporal gyrus and the left superior occipital gyrus on whole brain analysis. Occipito-temporal connections are well established(253). The left superior temporal gyrus contains the auditory cortex and Wernicke's area. However, it also thought to be part of a pathway involving the amygdala and the prefrontal cortex which is involved in processing social stimuli and in the regulation of social cognition(254). Embarrassment and guilt have been associated with increased activation in the superior temporal cortex(255, 256). In

addition, the occipital cortex, although primarily involved in visual processing, is also linked to the amygdala and both increased and reduced connectivity between the amygdala and the visual cortex has been demonstrated in the fear response(253, 257, 258). The increased connectivity seen in this network over time may suggest adaptations in the response to fear or social stimuli, once again perhaps as a protective adaptation to reduce the risk of recurrence of the cardiac event. In addition, the persistence of anatomical and functional changes over time suggests that there is either permanent change induced by the TS event, or that patients with TS have long term structural and functional anomalies in their brain which may have predisposed them to TS. This may be partly responsible for the relatively high recurrence rate in TS (1-6%)(49, 62) as these changes persist into the chronic phase.

#### 5.4.2.4 Chronic phase TS v healthy or STEMI controls

The reduced grey matter volume in the left calcarine fissure and surrounding cortex and the cerebellar vermis seen in TS patients compared to healthy controls did not persist into the chronic phase. This conflicts with there being no difference between acute and chronic TS patients but this may simply reflect the smaller sample size of the TS group. Furthermore, comparing TS v TS patients is comparing 'within subjects' whereas comparing TS with controls is comparing 'between' subjects where there will be greater variance in the data.

The lower connectivity, compared to healthy controls in the CEN, comprised the left middle frontal gyrus (orbital part), bilateral inferior frontal gyri (orbital parts), bilateral inferior parietal gyri, left middle frontal gyrus and left medial superior frontal gyrus. However, in the chronic phase only lower connectivity in the left middle frontal gyrus (orbital part), left inferior frontal gyrus (orbital part) and right inferior parietal gyrus persisted. Therefore, during the study period there was an increase in connectivity in TS patients involving nodes mainly in the prefrontal cortex (right inferior frontal gyrus (orbital part), left middle frontal gyrus, left medial superior frontal gyrus and the left inferior parietal gyrus). In addition, in the chronic phase of TS compared to healthy

controls there was now greater connectivity in the right inferior frontal gyrus (opercular part), left middle frontal gyrus (opercular part), left thalamus, right caudate nucleus and right middle frontal gyrus. Putting this together, in patients with TS over time there is an increase in connectivity in several nodes in the CEN suggesting partial neurofunctional improvement although the network remains disrupted. There is no difference in stress or anxiety scores between the two groups which may reflect the ongoing disruption of the CEN. Overall this fits with the existing literature; and previous studies of patients with TS imaged in the acute and chronic phases have shown differences in frontal and parietal regions compared to healthy controls (62, 64, 114, 115).

Other than further decreased connectivity involving the left inferior parietal gyrus, the other reductions in connectivity in the CEN persisted into the chronic phase compared to STEMI patients. This suggests that the changes seen in the left middle frontal gyrus and bilateral inferior parietal gyri are unique to TS patients.

Finally on the whole brain analysis, where there will be some overlap with the more specific ROI analyses performed, all the reductions in connectivity seen acutely compared to STEMI and healthy control patients resolved in follow up. These connections are not part of our pre-specified networks but mainly involved reductions in connectivity in subnetworks between the bilateral hippocampi and the prefrontal cortex. These regions are consistent with the previous TS literature showing reduced connectivity (involving the bilateral hippocampi, superior temporal gyrus and parietal gyri) (62, 64, 114, 115). The fact that connectivity in these areas increases over time suggests that these particular reductions in connectivity are acute and either represent adaptation of connectivity in response to the acute event or a response to treatment.

#### 5.4.3 GLOBAL NETWORK MEASURES

There was no difference in any global network measure between acute and chronic phase MINOCA patients. In the acute phase there was no difference



in any network measure compared to controls, but in the chronic phase modularity increased and was significantly higher than healthy controls.

Modularity in the chronic phase of STEMI patients was also significantly higher than healthy controls. Networks with high modularity have dense intramodular connections but few connections between other modules. The presence of modules is consistent with functional segregation and implies robustness and adaptability(58). Modularity has been shown to increase when patients with OCD receive an SSRI(259). The fact that modularity is similar to healthy patients in the acute phase and then rises in the chronic phase of MINOCA and STEMI patients compared to healthy controls favours a rise following the event rather than low modularity at the time of the presentation. We postulate that the rise in modularity reflects neuroadaptation following a stressful event to improve the brain's robustness perhaps to try and reduce the risk of future events.

#### *5.4.4 STUDY LIMITATIONS*

In addition to the limitations described in chapters 3 and 4, there are some further points that may affect the results of the longitudinal study. Firstly 13 MINOCA participants were lost to follow up. This is likely to introduce bias into the population as it is possible those who did not wish or were not able to return for follow up were sicker or had more significant mental health disorder. Second, a different MRI scanner was used for 14 of the follow up scans. Although it was conducted at the same field strength and using an MRI scanner from the same manufacturer, using the same protocols, there are likely to be some differences in the homogeneity and stability of the static magnetic field which have not been accounted for. Finally, the 'ideal' time to follow up these patients is not known, and patients were likely to be in different stages of physical and psychological 'recovery'. It may be that changes in connectivity and GMV do not occur at the same speed and that perhaps over a longer follow up period the changes in connectivity may follow the changes in GMV.

#### *5.5 CONCLUSIONS*

## Chapter 5 Longitudinal changes from the acute to the chronic phase in grey matter volume and functional connectivity in MINOCA

Patients with MINOCA in the chronic phase have significant differences in GMV and functional connectivity compared to control patients. There is evidence that some of these changes, especially regarding GMV, change over time. We postulate this reflects significant plasticity in GMV in MINOCA patients, although changes in connectivity are more variable and nuanced and require further evaluation in future studies.

## Chapter 6      GENERAL DISCUSSION, FUTURE DIRECTIONS AND CONCLUSION

---

### 6.1 *GENERAL SUMMARY OF RESULTS*

#### 6.1.1 *MINOCA PATIENTS*

There were widespread reductions in GMV and increased GMV in only one region in the putamen in patients with MINOCA compared to healthy controls, but no differences in GMV compared to STEMI controls. Regions with reduced GMV included the bilateral middle temporal gyrus, bilateral postcentral and precentral gyrus, left anterior cingulate gyrus, right median cingulate gyrus, right inferior temporal gyrus, left middle frontal gyrus and right inferior frontal gyrus. At follow up, there were only 4 regions with reduced GMV compared to healthy controls suggesting a degree of ‘normalisation’ over time in GMV.

There was increased connectivity in the DMN (bilateral hippocampus, right supramarginal gyrus) compared to healthy controls and reduced connectivity in the CEN (left middle frontal gyrus and left inferior frontal gyrus) compared to both control groups. At follow up there was greater connectivity involving more nodes in the DMN but the reduced connectivity in the CEN remained.

There was a positive correlation between GMV and GLS-CMR (improving cardiac function) in many regions, most notably in the cingulate gyrus and hippocampus/parahippocampus. There were negative correlations between connectivity and stress scores in the sympathetic network, parasympathetic network, DMN and salience network. There were negative correlations between connectivity and anxiety scores in the sympathetic network, DMN and CEN. There was a negative correlation between connectivity and GLS-CMR in the CEN. There were only positive correlations between connectivity and anxiety, stress or GLS-CMR scores in healthy participants.

There was no difference in global network measures between MINOCA patients and controls. At follow up there was evidence of increased modularity compared to healthy participants.

Anxiety scores were greater in the MINOCA patients than both control groups and depression and perceived stress scores were greater than the healthy population at presentation. These differences persisted over time. The presence of anxiety (score  $\geq 8$ ) or stress (PSS $>20$ ) was associated with reduced global efficiency.

#### *6.1.2 TAKOTSUBO SYNDROME PATIENTS*

There is reduced GMV in the cerebellar vermis and left calcarine fissure and surrounding cortex (in the region of the posterior cingulate cortex) compared to healthy controls. At follow up there was no difference in GMV once again suggesting plasticity in GMV over time.

There was reduced connectivity in the CEN (left frontal middle gyrus (orbital part), bilateral inferior parietal gyri, left frontal middle gyrus, left medial frontal superior gyrus and the bilateral frontal inferior gyri (orbital parts)) compared to both control groups and in autonomic/emotional processing regions on global brain analysis compared to healthy controls. At follow up there was both increased (versus healthy control only), and reduced connectivity (versus both control groups) in regions of the CEN. There was no difference in connectivity on the whole brain analysis.

Patients with TS had greater modularity compared to healthy controls and reduced GLS-CMR (worse cardiac function) was associated with lower modularity.

### *6.2 SYNTHESIS OF THEMES*

#### *6.2.1 DISRUPTION OF THE AUTONOMIC AND LIMBIC SYSTEMS IN MINOCA PATIENTS*

Our results confirm that MINOCA patients have a unique neuropsychological profile when compared to STEMI patients and healthy

individuals. We have shown the anatomical and functional differences previously described in TS and discussed in Chapter 1 extend beyond this cohort and into the wider MINOCA and the STEMI group (and by extension, possibly into the wider cardiology/hospital population). The areas with reductions in GMV tend to correlate with areas with reduced connectivity (e.g. middle and inferior frontal gyrus) suggesting that there is some overlap between anatomy and function. The prefrontal cortex, and particularly the middle frontal gyrus, has connections with important limbic emotional processing structures including the amygdala(64, 224, 225). This is entirely in keeping with the narrative throughout this thesis that MINOCA patients have disruption in the autonomic/limbic areas of the brain. As discussed in the Introduction, disruption in these centres has been shown to contribute to endothelial dysfunction and plaque instability(102, 111) (increasing adverse cardiac events) and is thought to lead to overactivity of the SNS which may trigger a Takotsubo event(119, 260). These changes in GMV and connectivity partly resolve in the chronic phase. Without neuroimaging before the MINOCA event it is not possible to ascertain if these changes predispose to the MINOCA event or occur acutely because of the MINOCA event. Our regression analyses in the MINOCA group demonstrated that high stress or high anxiety scores correlated with reduced connectivity in most of our networks of interest. High stress or anxiety scores were also associated with reduced global efficiency. This adds weight to our narrative that it is stress and/or anxiety that either leads to these changes in structure and connectivity (or perhaps occurs because of them).

Some of the reductions in functional connectivity in the CEN are unique to the MINOCA population (i.e. there was a significant difference between MINOCA and *both* control groups). As discussed in Chapter 4, this may reflect the higher anxiety seen in the MINOCA group compared to both control groups as the CEN (particularly caudate nuclei and prefrontal cortex) have intricate connections to the amygdala. How this leads to a MINOCA event, rather than a STEMI event, is not clear and there is no research to explain this yet. We postulate that the difference in connectivity may reflect the heterogeneity of the MINOCA group or perhaps the lack of power in the smaller STEMI group.

### 6.2.2 *DISRUPTION IN THE CEN IN TAKOTSUBO SYNDROME*

The anatomical differences we have shown in TS in the cerebellar vermis and left calcarine fissure were not entirely in keeping with the existing literature (62, 114) and did not directly explain the reduction in connectivity in the CEN and on whole brain analysis that we found. However, the differences we did find were largely unique to TS patients. This may simply reflect our smaller sample size compared to the previous studies and perhaps some heterogeneity between our populations. Nevertheless, the calcarine fissure is in the region of the posterior cingulate cortex which is an established part of the default mode network and as such has strong links to emotional salience(261). Reductions in cortical thickness were also shown in this region by Hiestand (114) suggesting some overlap with our results. As discussed in Chapter 3, the cerebellar vermis is primarily involved in movement but has recently been implicated in cognitive and mood dysregulation(193, 194). Connections from the vermis to the hypothalamus and limbic system have been demonstrated(195). The reduction in connectivity in the CEN and in limbic areas (bilateral hippocampus) on whole brain analysis is entirely in keeping with the existing literature (62, 114) and is in keeping with the hypothesis that dysregulation in the emotional processing centres leads to exaggerated systemic responses as suggested in **Error! Reference source not found.**, Chapter 1 page **Error! Bookmark not defined.**. The consistency of these findings across the literature is notable.

At follow up (median 257 days; IQR 199-308), our results were mixed. There was no difference in GMV at follow up suggesting that these changes normalised over time. However, there was significant fluidity in connectivity in the CEN with some nodes demonstrating increased and reduced connectivity in the CEN compared to healthy controls. The decreased connectivity in the CEN compared to STEMI patients persisted. There may be a degree of 'neurofunctional recovery' in patients with TS with some improvement in connectivity but clearly there is ongoing disruption in the CEN.

### 6.3 *CLINICAL IMPLICATIONS*

Our results provide novel insights into the pathophysiology of this intriguing condition. Firstly, the MINOCA population is unique and as such requires a more personalised approach to investigation and management. We would suggest that our results demonstrate it would be useful as a minimum to assess the psychological state of these patients at admission. Taken in context with the rest of the literature there is growing evidence that anxiety and/or stress and the associated neuroanatomical and neurofunctional brain changes are an important risk factor for MINOCA and acute coronary syndromes in general. Although not assessed in this study, there may be a role for behavioural, pharmaco- or psychotherapies for these conditions (or in a yet unspecified subset of this population). It may also be reasonable to offer these patients closer follow up and as part of their assessment, reassess their psychological state since many of the differences we have identified persist once the acute event has recovered perhaps leaving them at risk of recurrent events. However, the main implication of our study is that it provides valuable data for further studies and/or grant applications which may be used to change management/guidelines as discussed in section 6.4.

### 6.4 *FUTURE DIRECTIONS*

One of the main criticisms that could be levelled at this study results from the heterogeneity of the original MINOCA working diagnosis. As we have demonstrated in this study a MINOCA working diagnosis mainly comprises patients with acute myocarditis, acute myocardial infarction and TS. It could be questioned now whether these different diagnoses, with potentially different aetiological mechanisms and outcomes, should be analysed together. As discussed in Chapter 1, the field has moved on during the period of this PhD, and MINOCA in its current form now only refers to patients with an ischaemic basis to their presentation. At the time of study concept and design in 2017/2018 MINOCA was a valid working diagnosis and a legitimate target for research. Even at study design, we recognised this issue and as such aimed to recruit enough

patients to allow a meaningful subgroup analysis as well as analysis of the whole group. In addition, work published since we designed this study has suggested the potential importance of the heart-brain interaction in patients with myocardial infarction and has demonstrated correlations between stress related amygdala activity and acute plaque instability (102, 110, 111). Cardiovascular disease is the leading cause of death globally and therefore any future therapeutic interventions have the potential to have a large public health impact. We propose that future studies should focus on the heart-brain interaction in patients with ST elevation myocardial infarction. It would be interesting to assess, compared to control patients admitted with another non-inflammatory cardiac condition (e.g. arrhythmia), whether these patients have any pathological structural or functional changes in autonomic/limbic control regions of the brain which may be driving arterial atherosclerotic inflammation and subsequent plaque instability. Taking this concept further, it would be interesting to study patients with recurrent cardiovascular events, perhaps with no obvious established cardiovascular risk factors such as diabetes, smoking etc. It is possible that this particular cohort of patients might have centrally driven autonomic/limbic dysfunction driving plaque instability. Any psychological intervention or novel therapeutic intervention that could interrupt this neurobiological pathway, should there be a link, has the potential to improve global health outcomes in myocardial infarction.

Establishing causality is a major issue in observational studies. It is difficult to show whether any brain changes identified are because of the acute cardiac pathology or cause (or contribute to) the cardiac pathology. The UK biobank is a large-scale biomedical database of 40–69-year-old volunteers and has performed brain, cardiac and abdominal magnetic resonance imaging, dual-energy X-ray absorptiometry and carotid ultrasound on 100,000 volunteers. The brain MRI protocol includes T1 anatomical imaging and rs-fMRI timeseries data, along with emotional processing task-based fMRI. It also collects general demographic data, ECGs and psychological questionnaire data (anxiety and stress measures). The database is open access and linked to NHS records. If possible, it would be interesting to identify patients who, subsequent to their participation, have had a



myocardial infarction or a TS event and invite them back for repeat imaging. To our knowledge this has not yet been performed. Using a similar analysis methodology as we have used in this study, it would be possible to identify if there are any pre-existing brain differences which, when compared to healthy age and sex matched controls, predisposed them to having the event.

Modern medicine is driven by evidence, and the most influential studies demonstrate cost-effective changes in outcome and/or management of patients. Ultimately these studies are what will be required to change guidelines and international clinical practice. Management of these patients varies hugely, even between consultants in our department. Accordingly, there is a need for large randomised, outcome-based studies in patients with MINOCA. This includes studies using existing therapies (for example heart failure medications in TS, or therapeutic anticoagulation/PFO closure in patients with 'embolic' MI) but also novel treatments such as antidepressant medication or cognitive behavioural therapy for anxiety or stress in patients following TS. Studies are also needed to demonstrate that CMR in these patients changes outcomes e.g., mortality/readmission to further strengthen and expand access to early CMR globally.

## 6.5 CONCLUSION

This was a large, novel, prospective, longitudinal observational study examining the pathophysiological association of the heart and brain in patients with MINOCA compared to both STEMI and healthy controls. We have shown that MINOCA patients have high levels of stress and anxiety at presentation and have disruption in the limbic and autonomic brain networks. There are correlations between stress and anxiety scores and reduced connectivity and global brain efficiency which may partly explain these findings, although causality cannot be inferred. Finally, we have demonstrated that there is neuroanatomical recovery in grey matter volume in the MINOCA population over time and there are subsequent complex changes in connectivity. Further larger studies are needed in this area and in the wider myocardial infarction population. There are potentially

important future clinical implications for the follow up and management of these patients that require investigation.

## Chapter 7 REFERENCES

---

1. Heart and Circulatory Disease Statistics 2020. British Heart Foundation; 2020.
2. Amsterdam EA, Wenger NK, Brindis RG, Casey DE, Jr., Ganiats TG, Holmes DR, Jr., et al. 2014 AHA/ACC Guideline for the Management of Patients with Non-ST-Elevation Acute Coronary Syndromes: a report of the American College of Cardiology/American Heart Association Task Force on Practice Guidelines. *J Am Coll Cardiol*. 2014;64(24):e139-e228.
3. Ibanez B, James S, Agewall S, Antunes MJ, Bucciarelli-Ducci C, Bueno H, et al. 2017 ESC Guidelines for the management of acute myocardial infarction in patients presenting with ST-segment elevation. *European Heart Journal*. 2017;119:77.
4. Collet JP, Thiele H, Barbato E, Barthélémy O, Bauersachs J, Bhatt DL, et al. 2020 ESC Guidelines for the management of acute coronary syndromes in patients presenting without persistent ST-segment elevation. *Eur Heart J*. 2021;42(14):1289-367.
5. Larsen AI, Galbraith PD, Ghali WA, Norris CM, Graham MM, Knudtson ML. Characteristics and outcomes of patients with acute myocardial infarction and angiographically normal coronary arteries. *American Journal of Cardiology*. 2005;95:261-3.
6. Kang WY, Jeong MH, Ahn YK, Kim JH, Chae SC, Kim YJ, et al. Are patients with angiographically near-normal coronary arteries who present as acute myocardial infarction actually safe? *International Journal of Cardiology*. 2011;146:207-12.
7. Gehrie ER, Reynolds HR, Chen AY, Neelon BH, Roe MT, Gibler WB, et al. Characterization and outcomes of women and men with non-ST-segment elevation myocardial infarction and nonobstructive coronary artery disease: Results from the Can Rapid Risk Stratification of Unstable Angina Patients Suppress Adverse Outcomes with Early. *American Heart Journal*. 2009;158:688-94.
8. Pasupathy S, Air T, Dreyer RP, Tavella R, Beltrame JF. Systematic review of patients presenting with suspected myocardial infarction and nonobstructive coronary arteries. *Circulation*. 2015;131:861-70.
9. Agewall S, Beltrame JF, Reynolds HR, Niessner A, Rosano G, Caforio ALP, et al. ESC working group position paper on myocardial infarction with non-obstructive coronary arteries. *European Heart Journal*. 2017;38:143-53.
10. DeWood M, Stifter W, Simpson C, Spores J, Eugster G, Judge T, et al. Coronary arteriographic findings soon after non-Q-wave myocardial infarction. *New England Journal of Medicine*. 1986;317:417-23.
11. DeWood MA, Spores J, Notske R, Mouser LT, Burroughs R, Golden MS, et al. Prevalence of Total Coronary Occlusion during the Early Hours of Transmural Myocardial Infarction. *New England Journal of Medicine*. 1980;303:897-902.
12. Alpert JS. Myocardial infarction with angiographically normal coronary arteries. *Arch Intern Med*. 1994;154(3):265-9.
13. Agewall S, Eurenus L, Hofman-Bang C, Malmqvist K, Frick M, Jernberg T, et al. Myocardial infarction with angiographically normal coronary arteries. *Atherosclerosis*. 2011;219:10-4.

14. Tamis-Holland JE, Jneid H, Reynolds HR, Agewall S, Brilakis ES, Brown TM, et al. Contemporary Diagnosis and Management of Patients With Myocardial Infarction in the Absence of Obstructive Coronary Artery Disease: A Scientific Statement From the American Heart Association. 2019;139(18):e891-e908.
15. Thygesen K. 'Ten Commandments' for the Fourth Universal Definition of Myocardial Infarction 2018. *Eur Heart J*. 2019;40(3):226.
16. Pathik B, Raman B, Amin NHM, Mahadavan D, Rajendran S, McGavigan AD, et al. Troponin-positive chest pain with unobstructed coronary arteries: Incremental diagnostic value of cardiovascular magnetic resonance imaging. *European Heart Journal Cardiovascular Imaging*. 2016;17:1146-52.
17. Dastidar AG, Rodrigues JCL, Johnson TW, De Garate E, Singhal P, Baritussio A, et al. Myocardial Infarction With Nonobstructed Coronary Arteries: Impact of CMR Early After Presentation. *JACC: Cardiovascular Imaging*. 2017;10:1204-6.
18. Luetkens JA, Homsí R, Sprinkart AM, Doerner J, Dabir D, Kuetting DL, et al. Incremental value of quantitative CMR including parametric mapping for the diagnosis of acute myocarditis. *European Heart Journal-Cardiovascular Imaging*. 2016;17:154-61.
19. Radunski UK, Lund GK, Muellerleile K. Reply: Diagnostic value of quantitative CMR in patients suspected of having myocarditis: a question of timing. *JACC Cardiovasc Imaging*. 2015;8(1):110.
20. Cabral M, Brito MJ, Conde M, Oliveira M, Ferreira GC. Fulminant myocarditis associated with pandemic H1N1 influenza A virus. *Rev Port Cardiol*. 2012;31(7-8):517-20.
21. Gerbaud E, Harcaut E, Coste P, Erickson M, Lederlin M, Labèque JN, et al. Cardiac magnetic resonance imaging for the diagnosis of patients presenting with chest pain, raised troponin, and unobstructed coronary arteries. *The international journal of cardiovascular imaging*. 2012;28:783-94.
22. Dastidar AG, Singhal P, Rodrigues JC, Ahmed N, Palazzuoli A, Townsend M, et al. Improved diagnostic role of CMR in acute coronary syndromes and unobstructed coronary arteries: The importance of time-to-CMR. *Journal of Cardiovascular Magnetic Resonance*. 2015:1-2.
23. Stensaeth KH, Fossum E, Hoffmann P, Mangschau A, Klow NE. Clinical characteristics and role of early cardiac magnetic resonance imaging in patients with suspected ST-elevation myocardial infarction and normal coronary arteries. *International Journal of Cardiovascular Imaging*. 2011;27:355-65.
24. Assomull RG, Lyne JC, Keenan N, Gulati A, Bunce NH, Davies SW, et al. The role of cardiovascular magnetic resonance in patients presenting with chest pain, raised troponin, and unobstructed coronary arteries. *European Heart Journal*. 2007;28:1242-9.
25. Monney PA, Sekhri N, Burchell T, Knight C, Davies C, Deaner A, et al. Acute myocarditis presenting as acute coronary syndrome: Role of early cardiac magnetic resonance in its diagnosis. *Heart*. 2011;97:1312-8.
26. Reynolds HR, Maehara A, Kwong RY, Sedlak T, Saw J, Smilowitz NR, et al. Coronary Optical Coherence Tomography and Cardiac Magnetic Resonance Imaging to Determine Underlying Causes of MINOCA in Women. *Circulation*. 2020.
27. Opolski MP, Spiewak M, Marczak M, Debski A, Knaapen P, Schumacher SP, et al. Mechanisms of Myocardial Infarction in Patients With Nonobstructive

- Coronary Artery Disease: Results From the Optical Coherence Tomography Study. *JACC Cardiovasc Imaging*. 2019;12(11 Pt 1):2210-21.
28. Montone RA, Niccoli G, Fracassi F, Russo M, Gurgoglione F, Camma G, et al. Patients with acute myocardial infarction and non-obstructive coronary arteries: safety and prognostic relevance of invasive coronary provocative tests. *Eur Heart J*. 2018;39(2):91-8.
29. Friedrich MG, Sechtem U, Schulz-Menger J, Holmvang G, Alakija P, Cooper LT, et al. Cardiovascular Magnetic Resonance in Myocarditis: A JACC White Paper. *Journal of the American College of Cardiology*. 2009;53:1475-87.
30. Ferreira VM, Schulz-Menger J, Holmvang G, Kramer CM, Carbone I, Sechtem U, et al. Cardiovascular Magnetic Resonance in Nonischemic Myocardial Inflammation: Expert Recommendations. *J Am Coll Cardiol*. 2018;72(24):3158-76.
31. Caforio AL, Pankuweit S, Arbustini E, Basso C, Gimeno-Blanes J, Felix SB, et al. Current state of knowledge on aetiology, diagnosis, management, and therapy of myocarditis: a position statement of the European Society of Cardiology Working Group on Myocardial and Pericardial Diseases. *Eur Heart J*. 2013;34(33):2636-48, 48a-48d.
32. Lurz P, Eitel I, Adam J, Steiner J, Grothoff M, Desch S, et al. Diagnostic performance of CMR imaging compared with EMB in patients with suspected myocarditis. *JACC: Cardiovascular Imaging*. 2012;5:513-24.
33. Gutberlet M, Spors B, Thoma T, Bertram H, Denecke T, Felix R, et al. Suspected Chronic Myocarditis at Cardiac MR: Diagnostic Accuracy and Association with Immunohistologically Detected Inflammation and Viral Persistence. *Radiology*. 2008;246:401-9.
34. Abdel-Aty H, Boyé P, Zagrosek A, Wassmuth R, Kumar A, Messroghli D, et al. Diagnostic performance of cardiovascular magnetic resonance in patients with suspected acute myocarditis: Comparison of different approaches. *Journal of the American College of Cardiology*. 2005;45:1815-22.
35. Radunski UK, Lund GK, Stehning C, Schnackenburg B, Bohnen S, Adam G, et al. CMR in patients with severe myocarditis: Diagnostic value of quantitative tissue markers including extracellular volume imaging. *JACC: Cardiovascular Imaging*. 2014;7:667-75.
36. Thavendiranathan P, Walls M, Giri S, Verhaert D, Rajagopalan S, Moore S, et al. Improved detection of myocardial involvement in acute inflammatory cardiomyopathies using T2 mapping. *Circulation: Cardiovascular Imaging*. 2012;5:102-10.
37. Ferreira VM, Piechnik SK, Dallarmellina E, Karamitsos TD, Francis JM, Choudhury RP, et al. Non-contrast T1-mapping detects acute myocardial edema with high diagnostic accuracy: A comparison to T2-weighted cardiovascular magnetic resonance. *Journal of Cardiovascular Magnetic Resonance*. 2012;14.
38. Lurz P, Luecke C, Eitel I, Föhrenbach F, Frank C, Grothoff M, et al. Comprehensive Cardiac Magnetic Resonance Imaging in Patients with Suspected Myocarditis the MyoRacer-Trial. *Journal of the American College of Cardiology*. 2016;67:1800-11.
39. André F, Stock FT, Riffel J, Giannitsis E, Steen H, Scharhag J, et al. Incremental value of cardiac deformation analysis in acute myocarditis: a cardiovascular magnetic resonance imaging study. *The International Journal of Cardiovascular Imaging*. 2016;32:1093-101.

40. Scatteia A, Baritussio A, Bucciarelli-Ducci C. Strain imaging using cardiac magnetic resonance. *Heart Fail Rev.* 2017;22(4):465-76.
41. Baeßler B, Treutlein M, Schaarschmidt F, Stehning C, Schnackenburg B, Michels G, et al. A novel multiparametric imaging approach to acute myocarditis using T2-mapping and CMR feature tracking. *Journal of Cardiovascular Magnetic Resonance.* 2017;19:1-10.
42. Friedrich MG, Strohm O, Schulz-Menger J, Marciniak H, Luft FC, Dietz R. Contrast media-enhanced magnetic resonance imaging visualizes myocardial changes in the course of viral myocarditis. *Circulation.* 1998;97(18):1802-9.
43. Bohnen S, Radunski UK, Lund GK, Ojeda F, Looft Y, Senel M, et al. Tissue characterization by T1 and T2 mapping cardiovascular magnetic resonance imaging to monitor myocardial inflammation in healing myocarditis. *European Heart Journal Cardiovascular Imaging.* 2017;18:744-51.
44. Ghadri JR, Wittstein IS, Prasad A, Sharkey S, Dote K, Akashi YJ, et al. International Expert Consensus Document on Takotsubo Syndrome (Part I): Clinical Characteristics, Diagnostic Criteria, and Pathophysiology. *European Heart Journal.* 2018.
45. Eitel I, von Knobelsdorff-Brenkenhoff F, Bernhardt P, Carbone I, Muellerleile K, Aldrovandi A, et al. Clinical characteristics and cardiovascular magnetic resonance findings in stress (takotsubo) cardiomyopathy. *Jama.* 2011;306(3):277-86.
46. Lyon AR, Citro R, Schneider B, Morel O, Ghadri JR, Templin C, et al. Pathophysiology of Takotsubo Syndrome: JACC State-of-the-Art Review. *J Am Coll Cardiol.* 2021;77(7):902-21.
47. Scally C, Ahearn T, Rudd A, Neil CJ, Srivanasan J, Jagpal B, et al. Right ventricular involvement and recovery after acute stress-induced (Tako-tsubo) cardiomyopathy. *American Journal of Cardiology.* 2016;117:775-80.
48. Dawson DK. Acute stress-induced (takotsubo) cardiomyopathy. *Heart.* 2017;heartjnl-2017-311579.
49. Lyon AR, Bossone E, B S. 2016 ESC - Position statement on current knowledge of TCM.pdf. *European Journal of Heart Failure.* 2016;18:8-27.
50. Ahtarovski KA, Iversen KK, Christensen TE, Andersson H, Grande P, Holmvang L, et al. Takotsubo cardiomyopathy, a two-stage recovery of left ventricular systolic and diastolic function as determined by cardiac magnetic resonance imaging. *European Heart Journal Cardiovascular Imaging.* 2014;15:855-62.
51. Scally C, Rudd A, Mezincescu A, Wilson H, Srivanasan J, Horgan G, et al. Persistent Long-Term Structural, Functional, and Metabolic Changes After Stress-Induced (Takotsubo) Cardiomyopathy. *Circulation.* 2018;137(10):1039-48.
52. Whitwell JL, Jack CR, Jr. Comparisons between Alzheimer disease, frontotemporal lobar degeneration, and normal aging with brain mapping. *Top Magn Reson Imaging.* 2005;16(6):409-25.
53. Williams LM. Voxel-based morphometry in schizophrenia: implications for neurodevelopmental connectivity models, cognition and affect. *Expert Rev Neurother.* 2008;8(7):1049-65.
54. Whitwell JL, Josephs KA. Voxel-based morphometry and its application to movement disorders. *Parkinsonism Relat Disord.* 2007;13 Suppl 3:S406-16.
55. Good CD, Scahill RI, Fox NC, Ashburner J, Friston KJ, Chan D, et al. Automatic differentiation of anatomical patterns in the human brain: validation with studies of degenerative dementias. *Neuroimage.* 2002;17(1):29-46.

56. Davies RR, Scahill VL, Graham A, Williams GB, Graham KS, Hodges JR. Development of an MRI rating scale for multiple brain regions: comparison with volumetrics and with voxel-based morphometry. *Neuroradiology*. 2009;51(8):491-503.
57. Glover GH. Overview of functional magnetic resonance imaging. *Neurosurg Clin N Am*. 2011;22(2):133-9, vii.
58. Bullmore E, Sporns O. Complex brain networks: graph theoretical analysis of structural and functional systems. *Nat Rev Neurosci*. 2009;10(3):186-98.
59. Onias H, Viol A, Palhano-Fontes F, Andrade KC, Sturzbecher M, Viswanathan G, et al. Brain complex network analysis by means of resting state fMRI and graph analysis: will it be helpful in clinical epilepsy? *Epilepsy Behav*. 2014;38:71-80.
60. Rubinov M, Sporns O. Complex network measures of brain connectivity: uses and interpretations. *Neuroimage*. 2010;52(3):1059-69.
61. Tzourio-Mazoyer N, Landeau B, Papathanassiou D, Crivello F, Etard O, Delcroix N, et al. Automated anatomical labeling of activations in SPM using a macroscopic anatomical parcellation of the MNI MRI single-subject brain. *Neuroimage*. 2002;15(1):273-89.
62. Templin C, Hanggi J, Klein C, Topka MS, Hiestand T, Levinson RA, et al. Altered limbic and autonomic processing supports brain-heart axis in Takotsubo syndrome. *Eur Heart J*. 2019.
63. Silva AR, Magalhaes R, Arantes C, Moreira PS, Rodrigues M, Marques P, et al. Brain functional connectivity is altered in patients with Takotsubo Syndrome. *Sci Rep*. 2019;9(1):4187.
64. Klein C, Hiestand T, Ghadri J-R, Templin C, Jäncke L, Hänggi J. Takotsubo Syndrome – Predictable from brain imaging data. *Scientific Reports*. 2017;7:5434.
65. Buckner RL, Andrews-Hanna JR, Schacter DL. The brain's default network: anatomy, function, and relevance to disease. *Ann N Y Acad Sci*. 2008;1124:1-38.
66. Menon V. *Brain Mapping: An Encyclopaedic Reference*: Elsevier; 2015.
67. Menon V. Large-scale brain networks and psychopathology: a unifying triple network model. *Trends Cogn Sci*. 2011;15(10):483-506.
68. Gordan R, Gwathmey JK, Xie LH. Autonomic and endocrine control of cardiovascular function. *World J Cardiol*. 2015;7(4):204-14.
69. Hildebrand R. Robert Willis (1799-1878): the works of William Harvey, M. D., London 1847. A bibliographical note. *Sudhoffs Arch*. 2007;91(1):118-21.
70. Barber M, Morton JJ, Macfarlane PW, Barlow N, Roditi G, Stott DJ. Elevated troponin levels are associated with sympathoadrenal activation in acute ischaemic stroke. *Cerebrovascular Diseases*. 2007;23:260-6.
71. Breteler MM, Claus JJ, Grobbee DE, Hofman A. Cardiovascular disease and distribution of cognitive function in elderly people: the Rotterdam Study. *BMJ*. 1994;308(6944):1604-8.
72. Yaghi S, Chang AD, Ricci BA, Jayaraman MV, McTaggart RA, Hemendinger M, et al. Early Elevated Troponin Levels After Ischemic Stroke Suggests a Cardioembolic Source. *Stroke*. 2018;49(1):121-6.
73. Doehner W, Ural D, Haeusler KG, Čelutkienė J, Bestetti R, Cavusoglu Y, et al. Heart and brain interaction in patients with heart failure: Overview and proposal for a taxonomy. A position paper from the Study Group on Heart and

- Brain Interaction of the Heart Failure Association. *European Journal of Heart Failure*. 2017.
74. Santangeli P, Di Biase L, Bai R, Mohanty S, Pump A, Cereceda Brantes M, et al. Atrial fibrillation and the risk of incident dementia: a meta-analysis. *Heart Rhythm*. 2012;9(11):1761-8.
75. Luchsinger JA, Reitz C, Honig LS, Tang MX, Shea S, Mayeux R. Aggregation of vascular risk factors and risk of incident Alzheimer disease. *Neurology*. 2005;65(4):545-51.
76. Sposato LA, Asperg S, Scheitz JF, Fisher M. The World Stroke Organization Brain & Heart Task Force: collaborations between stroke physicians and cardiologists. *European Heart Journal*. 2021.
77. Samuels MA. The brain-heart connection. *Circulation*. 2007;116(1):77-84.
78. Palma JA, Benarroch EE. Neural control of the heart: recent concepts and clinical correlations. *Neurology*. 2014;83(3):261-71.
79. Kawashima T. The autonomic nervous system of the human heart with special reference to its origin, course, and peripheral distribution. *Anat Embryol (Berl)*. 2005;209(6):425-38.
80. McAllen RM, Spyer KM. The location of cardiac vagal preganglionic motoneurons in the medulla of the cat. *J Physiol*. 1976;258(1):187-204.
81. Ciriello J, Calaresu FR. Medullary origin of vagal preganglionic axons to the heart of the cat. *J Auton Nerv Syst*. 1982;5(1):9-22.
82. Nieuwenhuys R. The insular cortex: a review. *Prog Brain Res*. 2012;195:123-63.
83. Seeley WW, Menon V, Schatzberg AF, Keller J, Glover GH, Kenna H, et al. Dissociable intrinsic connectivity networks for salience processing and executive control. *J Neurosci*. 2007;27(9):2349-56.
84. Critchley HD. Psychophysiology of neural, cognitive and affective integration: fMRI and autonomic indicants. *Int J Psychophysiol*. 2009;73(2):88-94.
85. LeDoux J. The amygdala. *Curr Biol*. 2007;17(20):R868-74.
86. Lane RD, McRae K, Reiman EM, Chen K, Ahern GL, Thayer JF. Neural correlates of heart rate variability during emotion. *Neuroimage*. 2009;44(1):213-22.
87. Kim MJ, Loucks RA, Palmer AL, Brown AC, Solomon KM, Marchante AN, et al. The structural and functional connectivity of the amygdala: from normal emotion to pathological anxiety. *Behav Brain Res*. 2011;223(2):403-10.
88. Saper CB, Loewy AD, Swanson LW, Cowan WM. Direct hypothalamo-autonomic connections. *Brain Res*. 1976;117(2):305-12.
89. Saper CB. The central autonomic nervous system: conscious visceral perception and autonomic pattern generation. *Annu Rev Neurosci*. 2002;25:433-69.
90. Smyth A, O'Donnell M, Lamelas P, Teo K, Rangarajan S, Yusuf S, et al. Physical Activity and Anger or Emotional Upset as Triggers of Acute Myocardial Infarction: The INTERHEART Study. *Circulation*. 2016;134(15):1059-67.
91. Verrier RL, Mittleman MA. Life-threatening cardiovascular consequences of anger in patients with coronary heart disease. *Cardiology Clinics*. 14(2):289-307.
92. Strike PC, Steptoe A. Systematic review of mental stress-induced myocardial ischaemia. *Eur Heart J*. 2003;24(8):690-703.



93. Chandola T, Britton A, Brunner E, Hemingway H, Malik M, Kumari M, et al. Work stress and coronary heart disease: what are the mechanisms? *European Heart Journal*. 2008;29(5):640-8.
94. Smeijers L, Mostofsky E, Tofler GH, Muller JE, Kop WJ, Mittleman MA. Anxiety and anger immediately prior to myocardial infarction and long-term mortality: Characteristics of high-risk patients. *J Psychosom Res*. 2017;93:19-27.
95. Willich SN, Lowel H, Lewis M, Hormann A, Arntz HR, Keil U. Weekly variation of acute myocardial infarction. Increased Monday risk in the working population. *Circulation*. 1994;90(1):87-93.
96. Nabi H, Kivimaki M, Batty GD, Shipley MJ, Britton A, Brunner EJ, et al. Increased risk of coronary heart disease among individuals reporting adverse impact of stress on their health: the Whitehall II prospective cohort study. *Eur Heart J*. 2013;34(34):2697-705.
97. Ghiadoni L, Donald AE, Cropley M, Mullen MJ, Oakley G, Taylor M, et al. Mental stress induces transient endothelial dysfunction in humans. *Circulation*. 2000;102(20):2473-8.
98. Hammadah M, Sullivan S, Pearce B, Al Mheid I, Wilmot K, Ramadan R, et al. Inflammatory response to mental stress and mental stress induced myocardial ischemia. *Brain Behav Immun*. 2018;68:90-7.
99. Lima BB, Hammadah M, Wilmot K, Pearce BD, Shah A, Levantsevych O, et al. Posttraumatic stress disorder is associated with enhanced interleukin-6 response to mental stress in subjects with a recent myocardial infarction. *Brain Behav Immun*. 2019;75:26-33.
100. Chrapko WE, Jurasz P, Radomski MW, Lara N, Archer SL, Le Melleo JM. Decreased platelet nitric oxide synthase activity and plasma nitric oxide metabolites in major depressive disorder. *Biol Psychiatry*. 2004;56(2):129-34.
101. Strike PC, Magid K, Whitehead DL, Brydon L, Bhattacharyya MR, Steptoe A. Pathophysiological processes underlying emotional triggering of acute cardiac events. *Proc Natl Acad Sci U S A*. 2006;103(11):4322-7.
102. Tawakol A, Ishai A, Takx RA, Figueroa AL, Ali A, Kaiser Y, et al. Relation between resting amygdalar activity and cardiovascular events: a longitudinal and cohort study. *Lancet (London, England)*. 2017;389(10071):834-45.
103. Wang SS, Yan XB, Hofman MA, Swaab DF, Zhou JN. Increased expression level of corticotropin-releasing hormone in the amygdala and in the hypothalamus in rats exposed to chronic unpredictable mild stress. *Neurosci Bull*. 2010;26(4):297-303.
104. Lagraauw HM, Kuiper J, Bot I. Acute and chronic psychological stress as risk factors for cardiovascular disease: Insights gained from epidemiological, clinical and experimental studies. *Brain Behav Immun*. 2015;50:18-30.
105. Schultz WM, Kelli HM, Lisko JC, Varghese T, Shen J, Sandesara P, et al. Socioeconomic Status and Cardiovascular Outcomes: Challenges and Interventions. *Circulation*. 2018;137(20):2166-78.
106. Hatch SL, Dohrenwend BP. Distribution of traumatic and other stressful life events by race/ethnicity, gender, SES and age: a review of the research. *Am J Community Psychol*. 2007;40(3-4):313-32.
107. Grzywacz JG, Almeida DM, Neupert SD, Ettner SL. Socioeconomic status and health: a micro-level analysis of exposure and vulnerability to daily stressors. *J Health Soc Behav*. 2004;45(1):1-16.

108. Heidt T, Sager HB, Courties G, Dutta P, Iwamoto Y, Zaltsman A, et al. Chronic variable stress activates hematopoietic stem cells. *Nat Med*. 2014;20(7):754-8.
109. Libby P. Inflammation in atherosclerosis. *Nature*. 2002;420(6917):868-74.
110. Tawakol A, Osborne MT, Wang Y, Hammed B, Tung B, Patrich T, et al. Stress-Associated Neurobiological Pathway Linking Socioeconomic Disparities to Cardiovascular Disease. *J Am Coll Cardiol*. 2019;73(25):3243-55.
111. Kang DO, Eo JS, Park EJ, Nam HS, Song JW, Park YH, et al. Stress-associated neurobiological activity is linked with acute plaque instability via enhanced macrophage activity: a prospective serial 18F-FDG-PET/CT imaging assessment. *Eur Heart J*. 2021.
112. Templin C, Ghadri JR, Diekmann J, Napp LC, Bataiosu DR, Jaguszewski M, et al. Clinical Features and Outcomes of Takotsubo (Stress) Cardiomyopathy. *New England Journal of Medicine*. 2015;373:929-38.
113. Suzuki H, Matsumoto Y, Kaneta T, Sugimura K, Takahashi J, Fukumoto Y, et al. Evidence for brain activation in patients with takotsubo cardiomyopathy. *Circ J*. 2014;78(1):256-8.
114. Hiestand T, Hänggi J, Klein C, Topka MS, Jaguszewski M, Ghadri JR, et al. Takotsubo Syndrome Associated With Structural Brain Alterations of the Limbic System. *Journal of the American College of Cardiology*. 2018;71:809-11.
115. Dichtl W, Tuovinen N, Barbieri F, Adukauskaitė A, Senoner T, Rubatscher A, et al. Functional neuroimaging in the acute phase of Takotsubo syndrome: volumetric and functional changes of the right insular cortex. *Clin Res Cardiol*. 2020;109(9):1107-13.
116. Sabisz A, Treder N, Fijalkowska M, Sieminski M, Fijalkowska J, Naumczyk P, et al. Brain resting state functional magnetic resonance imaging in patients with takotsubo cardiomyopathy an inseparable pair of brain and heart. *Int J Cardiol*. 2016;224:376-81.
117. Hiestand T, Hanggi J, Klein C, Topka MS, Jaguszewski M, Ghadri JR, et al. Takotsubo Syndrome Associated With Structural Brain Alterations of the Limbic System. *J Am Coll Cardiol*. 2018;71(7):809-11.
118. Pereira VH, Marques P, Magalhaes R, Portugues J, Calvo L, Cerqueira JJ, et al. Central autonomic nervous system response to autonomic challenges is altered in patients with a previous episode of Takotsubo cardiomyopathy. *Eur Heart J Acute Cardiovasc Care*. 2016;5(2):152-63.
119. Radfar A, Abohashem S, Osborne MT, Wang Y, Dar T, Hassan MZO, et al. Stress-associated neurobiological activity associates with the risk for and timing of subsequent Takotsubo syndrome. *Eur Heart J*. 2021.
120. Ma L, Del Buono MG, Moeller FG. Cannabis Use as a Risk Factor for Takotsubo (Stress) Cardiomyopathy: Exploring the Evidence from Brain-Heart Link. *Curr Cardiol Rep*. 2019;21(10):121.
121. Suzuki H, Yasuda S, Shimokawa H. Brain-heart connection in Takotsubo syndrome before onset. *Eur Heart J*. 2021;42(19):1909-11.
122. Naidech AM, Kreiter KT, Janjua N, Ostapkovich ND, Parra A, Commichau C, et al. Cardiac troponin elevation, cardiovascular morbidity, and outcome after subarachnoid hemorrhage. *Circulation*. 2005;112(18):2851-6.
123. Wybraniec MT, Mizia-Stec K, Krzych L. Neurocardiogenic injury in subarachnoid hemorrhage: A wide spectrum of catecholamin-mediated brain-heart interactions. *Cardiology Journal*. 21(3):220-8.

124. Lee M, Oh JH, Lee KB, Kang GH, Park YH, Jang WJ, et al. Clinical and Echocardiographic Characteristics of Acute Cardiac Dysfunction Associated With Acute Brain Hemorrhage- Difference From Takotsubo Cardiomyopathy. *Circ J*. 2016;80(9):2026-32.
125. Ancona F, Bertoldi LF, Ruggieri F, Cerri M, Magnoni M, Beretta L, et al. Takotsubo cardiomyopathy and neurogenic stunned myocardium: similar albeit different. *European Heart Journal*.37(37):2830-2.
126. Stress Cardiomyopathy Diagnosis and Treatment: JACC State-of-the-Art Review, (2018).
127. Chen Z, Venkat P, Seyfried D, Chopp M, Yan T, Chen J. Brain-Heart Interaction: Cardiac Complications After Stroke. *Circulation Research*.121(4):451-68.
128. Nagai M, Dote K, Kato M, Sasaki S, Oda N, Kagawa E, et al. The Insular Cortex and Takotsubo Cardiomyopathy. *Curr Pharm Des*. 2017;23(6):879-88.
129. Ay H, Koroshetz WJ, Benner T, Vangel MG, Melinosky C, Arsava EM, et al. Neuroanatomic correlates of stroke-related myocardial injury. *Neurology*. 2006;66(9):1325-9.
130. Nagai M, Dote K, Kato M. Central autonomic network and Takotsubo cardiomyopathy: how left insular cortex interact? *Eur Heart J*. 2019.
131. Jung JM, Kim JG, Kim JB, Cho KH, Yu S, Oh K, et al. Takotsubo-Like Myocardial Dysfunction in Ischemic Stroke: A Hospital-Based Registry and Systematic Literature Review. *Stroke*. 2016;47(11):2729-36.
132. Oppenheimer SM, Gelb A, Girvin JP, Hachinski VC. Cardiovascular effects of human insular cortex stimulation. *Neurology*. 1992;42(9):1727-32.
133. Alalade E, Denny K, Potter G, Steffens D, Wang L. Altered cerebellar-cerebral functional connectivity in geriatric depression. *PloS one*. 2011;6(5):e20035.
134. Pannekoek JN, van der Werff SJ, Meens PH, van den Bulk BG, Jolles DD, Veer IM, et al. Aberrant resting-state functional connectivity in limbic and salience networks in treatment-naïve clinically depressed adolescents. *J Child Psychol Psychiatry*. 2014;55(12):1317-27.
135. Alexopoulos GS, Hoptman MJ, Kanellopoulos D, Murphy CF, Lim KO, Gunning FM. Functional connectivity in the cognitive control network and the default mode network in late-life depression. *J Affect Disord*. 2012;139(1):56-65.
136. Wu B, Li X, Zhou J, Zhang M, Long Q. Altered Whole-Brain Functional Networks in Drug-Naïve, First-Episode Adolescents With Major Depression Disorder. *Journal of Magnetic Resonance Imaging*. 2020;52(6):1790-8.
137. Zhuo C, Li G, Lin X, Jiang D, Xu Y, Tian H, et al. The rise and fall of MRI studies in major depressive disorder. *Transl Psychiatry*. 2019;9(1):335.
138. Makovac E, Meeten F, Watson DR, Herman A, Garfinkel SN, D. Critchley H, et al. Alterations in Amygdala-Prefrontal Functional Connectivity Account for Excessive Worry and Autonomic Dysregulation in Generalized Anxiety Disorder. *Biological Psychiatry*. 2016;80(10):786-95.
139. Makovac E, Mancini M, Fagioli S, Watson DR, Meeten F, Rae CL, et al. Network abnormalities in generalized anxiety pervade beyond the amygdala-prefrontal cortex circuit: Insights from graph theory. *Psychiatry Research: Neuroimaging*. 2018;281:107-16.
140. Thygesen K, Alpert JS, Jaffe AS, Simoons ML, Chaitman BR, White HD, et al. Third universal definition of myocardial infarction. *European Heart Journal*. 2012;33:2551-67.

141. Szucs D, Ioannidis JP. Sample size evolution in neuroimaging research: An evaluation of highly-cited studies (1990-2012) and of latest practices (2017-2018) in high-impact journals. *Neuroimage*. 2020;221:117164.
142. Burkhouse KL, Jacobs RH, Peters AT, Ajilore O, Watkins ER, Langenecker SA. Neural correlates of rumination in adolescents with remitted major depressive disorder and healthy controls. *Cogn Affect Behav Neurosci*. 2017;17(2):394-405.
143. Feher EP, Mahurin RK, Doody RS, Cooke N, Sims J, Pirozzolo FJ. Establishing the limits of the Mini-Mental State. Examination of 'subtests'. *Archives of neurology*. 1992;49(1):87-92.
144. Tombaugh TN, McIntyre NJ. The mini-mental state examination: a comprehensive review. *J Am Geriatr Soc*. 1992;40(9):922-35.
145. Bjelland I, Dahl AA, Haug TT, Neckelmann D. The validity of the Hospital Anxiety and Depression Scale. An updated literature review. *J Psychosom Res*. 2002;52(2):69-77.
146. Lee EH. Review of the psychometric evidence of the perceived stress scale. *Asian Nurs Res (Korean Soc Nurs Sci)*. 2012;6(4):121-7.
147. Broadbent E, Wilkes C, Koschwanetz H, Weinman J, Norton S, Petrie KJ. A systematic review and meta-analysis of the Brief Illness Perception Questionnaire. *Psychol Health*. 2015;30(11):1361-85.
148. Weiss DS. The Impact of Event Scale: Revised. In: Wilson J.P. TCS, editor. *Cross-Cultural Assessment of Psychological Trauma and PTSD International and Cultural Psychology Series* Boston, MA. : Springer; 2007.
149. Naugle RI, Kawczak K. Limitations of the Mini-Mental State Examination. *Cleve Clin J Med*. 1989;56(3):277-81.
150. Zigmond AS, Snaith RP. The hospital anxiety and depression scale. *Acta Psychiatr Scand*. 1983;67(6):361-70.
151. Malarkey WB, Pearl DK, Demers LM, Kiecolt-Glaser JK, Glaser R. Influence of academic stress and season on 24-hour mean concentrations of ACTH, cortisol, and beta-endorphin. *Psychoneuroendocrinology*. 1995;20(5):499-508.
152. [http%3A%2F%2Fpodcast.uctv.tv%2Fwebdocuments%2FCOHEN-PERCEIVED-STRESS-Scale.pdf](http://3A%2F%2Fpodcast.uctv.tv%2Fwebdocuments%2FCOHEN-PERCEIVED-STRESS-Scale.pdf). [
153. Petrie KJ, Broadbent, E., & Meechan, G. Self-regulatory interventions for improving the management of chronic illness. In: Leventhal DCH, editor. *The self-regulation of health and illness behaviour*: Routledge; 2003. p. 257–77.
154. Creamer M, Bell R, Failla S. Psychometric properties of the Impact of Event Scale - Revised. *Behav Res Ther*. 2003;41(12):1489-96.
155. Garcia-Eulate R, Garcia-Garcia D, Dominguez PD, Noguera JJ, De Luis E, Rodriguez-Oroz MC, et al. Functional bold MRI: advantages of the 3 T vs. the 1.5 T. *Clin Imaging*. 2011;35(3):236-41.
156. Potter E, Marwick TH. Assessment of Left Ventricular Function by Echocardiography: The Case for Routinely Adding Global Longitudinal Strain to Ejection Fraction. *JACC Cardiovasc Imaging*. 2018;11(2 Pt 1):260-74.
157. McAlindon EJ, Pufulete M, Harris JM, Lawton CB, Moon JC, Manghat N, et al. Measurement of myocardium at risk with cardiovascular MR: comparison of techniques for edema imaging. *Radiology*. 2015;275(1):61-70.
158. Otsu N. Threshold selection method from gray-level histograms. *IEEE Trans Syst Man Cyb*. 1979;9:62-6.

159. McAlindon E, Pufulete M, Lawton C, Angelini GD, Bucciarelli-Ducci C. Quantification of infarct size and myocardium at risk: evaluation of different techniques and its implications. *Eur Heart J Cardiovasc Imaging*. 2015;16(7):738-46.
160. Hsu LY, Natanzon A, Kellman P, Hirsch GA, Aletras AH, Arai AE. Quantitative myocardial infarction on delayed enhancement MRI. Part I: Animal validation of an automated feature analysis and combined thresholding infarct sizing algorithm. *J Magn Reson Imaging*. 2006;23(3):298-308.
161. Ghadri JR, Wittstein IS, Prasad A, Sharkey S, Dote K, Akashi YJ, et al. International Expert Consensus Document on Takotsubo Syndrome (Part II): Diagnostic Workup, Outcome, and Management. *European Heart Journal*. 2018.
162. R.S.J. Frackowiak KJF, C.D. Frith, R.J. Dolan, and J.C. Mazziotta,. *Human Brain Function*: Academic Press USA; 1997.
163. Ashburner J, Friston KJ. Voxel-based morphometry--the methods. *Neuroimage*. 2000;11(6 Pt 1):805-21.
164. Whitwell JL. Voxel-based morphometry: an automated technique for assessing structural changes in the brain. *J Neurosci*. 2009;29(31):9661-4.
165. Ashburner J. *Computational Neuroanatomy* 2000.
166. Worsley KJ, Marrett S, Neelin P, Vandal AC, Friston KJ, Evans AC. A unified statistical approach for determining significant signals in images of cerebral activation. *Hum Brain Mapp*. 1996;4(1):58-73.
167. Muldoon SF, Bridgeford EW, Bassett DS. Small-World Propensity and Weighted Brain Networks. *Sci Rep*. 2016;6:22057.
168. Beissner F, Meissner K, Bar KJ, Napadow V. The autonomic brain: an activation likelihood estimation meta-analysis for central processing of autonomic function. *J Neurosci*. 2013;33(25):10503-11.
169. Andrews-Hanna JR, Reidler JS, Sepulcre J, Poulin R, Buckner RL. Functional-anatomic fractionation of the brain's default network. *Neuron*. 2010;65(4):550-62.
170. Klein C, Leipold S, Ghadri JR, Jurisic S, Hiestand T, Hanggi J, et al. Takotsubo syndrome: How the broken heart deals with negative emotions. *Neuroimage Clin*. 2020;25:102124.
171. Christensen TE, Bang LE, Holmvang L, Hasbak P, Kjær A, Bech P, et al. Neuroticism, depression and anxiety in takotsubo cardiomyopathy. *BMC Cardiovasc Disord*. 2016;16:118.
172. Daniel M, Agewall S, Berglund F, Caidahl K, Collste O, Ekenbäck C, et al. Prevalence of Anxiety and Depression Symptoms in Patients with Myocardial Infarction with Non-Obstructive Coronary Arteries. *Am J Med*. 2018;131(9):1118-24.
173. Pais JL, Izquierdo Coronel B, Galan Gil D, Espinosa Pascual MJ, Martinez Peredo CG, Awamleh Garcia P, et al. Psycho-emotional disorders as incoming risk factors for myocardial infarction with non-obstructive coronary arteries. *Cardiol J*. 2018;25(1):24-31.
174. Brett MP, W; Kiebel, S. *An Introduction to Random Field Theory*. MRC Cognition and Brain Sciences Unit, Cambridge 2003.
175. Ridgway GR, Henley SM, Rohrer JD, Scallill RI, Warren JD, Fox NC. Ten simple rules for reporting voxel-based morphometry studies. *Neuroimage*. 2008;40(4):1429-35.

176. Grieve SM, Korgaonkar MS, Koslow SH, Gordon E, Williams LM. Widespread reductions in gray matter volume in depression. *NeuroImage: Clinical*. 2013;3:332-9.
177. Wise T, Radua J, Via E, Cardoner N, Abe O, Adams TM, et al. Common and distinct patterns of grey-matter volume alteration in major depression and bipolar disorder: evidence from voxel-based meta-analysis. *Mol Psychiatry*. 2017;22(10):1455-63.
178. Moon CM, Kim GW, Jeong GW. Whole-brain gray matter volume abnormalities in patients with generalized anxiety disorder: voxel-based morphometry. *Neuroreport*. 2014;25(3):184-9.
179. Schienle A, Ebner F, Schafer A. Localized gray matter volume abnormalities in generalized anxiety disorder. *Eur Arch Psychiatry Clin Neurosci*. 2011;261(4):303-7.
180. Abdallah CG, Coplan JD, Jackowski A, Sato JR, Mao X, Shungu DC, et al. A pilot study of hippocampal volume and N-acetylaspartate (NAA) as response biomarkers in riluzole-treated patients with GAD. *Eur Neuropsychopharmacol*. 2013;23(4):276-84.
181. Kolesar TA, Bilevicius E, Wilson AD, Kornelsen J. Systematic review and meta-analyses of neural structural and functional differences in generalized anxiety disorder and healthy controls using magnetic resonance imaging. *Neuroimage Clin*. 2019;24:102016.
182. Pourtois G, de Gelder B, Bol A, Crommelinck M. Perception of facial expressions and voices and of their combination in the human brain. *Cortex*. 2005;41(1):49-59.
183. Hayden BY, Platt ML. Neurons in anterior cingulate cortex multiplex information about reward and action. *J Neurosci*. 2010;30(9):3339-46.
184. van Tol MJ, van der Wee NJ, van den Heuvel OA, Nielen MM, Demenescu LR, Aleman A, et al. Regional brain volume in depression and anxiety disorders. *Arch Gen Psychiatry*. 2010;67(10):1002-11.
185. Frodl T, Koutsouleris N, Bottlender R, Born C, Jager M, Morgenthaler M, et al. Reduced gray matter brain volumes are associated with variants of the serotonin transporter gene in major depression. *Mol Psychiatry*. 2008;13(12):1093-101.
186. Liakakis G, Nickel J, Seitz RJ. Diversity of the inferior frontal gyrus--a meta-analysis of neuroimaging studies. *Behav Brain Res*. 2011;225(1):341-7.
187. Delgado MR. Reward-related responses in the human striatum. *Ann N Y Acad Sci*. 2007;1104:70-88.
188. Potts NL, Book S, Davidson JR. The neurobiology of social phobia. *Int Clin Psychopharmacol*. 1996;11 Suppl 3:43-8.
189. Wang X, Cheng B, Luo Q, Qiu L, Wang S. Gray Matter Structural Alterations in Social Anxiety Disorder: A Voxel-Based Meta-Analysis. *Front Psychiatry*. 2018;9:449.
190. Suga M, Yamasue H, Abe O, Yamasaki S, Yamada H, Inoue H, et al. Reduced gray matter volume of Brodmann's Area 45 is associated with severe psychotic symptoms in patients with schizophrenia. *Eur Arch Psychiatry Clin Neurosci*. 2010;260(6):465-73.
191. Barbas H, De Olmos J. Projections from the amygdala to basoventral and mediodorsal prefrontal regions in the rhesus monkey. *J Comp Neurol*. 1990;300(4):549-71.

192. Cho C, Smith DV, Delgado MR. Reward Sensitivity Enhances Ventrolateral Prefrontal Cortex Activation during Free Choice. *Frontiers in neuroscience*. 2016;10:529-.
193. Lupo M, Olivito G, Gragnani A, Sættoni M, Siciliano L, Pancheri C, et al. Comparison of Cerebellar Grey Matter Alterations in Bipolar and Cerebellar Patients: Evidence from Voxel-Based Analysis. *Int J Mol Sci*. 2021;22(7).
194. Sacchetti B, Scelfo B, Strata P. Cerebellum and emotional behavior. *Neuroscience*. 2009;162(3):756-62.
195. Anand BK, Malhotra CL, Singh B, Dua S. Cerebellar projections to limbic system. *J Neurophysiol*. 1959;22(4):451-7.
196. Strata P. The emotional cerebellum. *Cerebellum*. 2015;14(5):570-7.
197. Gusnard DA, Raichle ME, Raichle ME. Searching for a baseline: functional imaging and the resting human brain. *Nat Rev Neurosci*. 2001;2(10):685-94.
198. Fox MD, Snyder AZ, Vincent JL, Corbetta M, Van Essen DC, Raichle ME. The human brain is intrinsically organized into dynamic, anticorrelated functional networks. *Proc Natl Acad Sci U S A*. 2005;102(27):9673-8.
199. Lee MH, Smyser CD, Shimony JS. Resting-state fMRI: a review of methods and clinical applications. *AJNR American journal of neuroradiology*. 2013;34(10):1866-72.
200. Raichle ME, MacLeod AM, Snyder AZ, Powers WJ, Gusnard DA, Shulman GL. A default mode of brain function. *Proc Natl Acad Sci U S A*. 2001;98(2):676-82.
201. Raichle ME. The brain's default mode network. *Annu Rev Neurosci*. 2015;38:433-47.
202. Stein MB, Simmons AN, Feinstein JS, Paulus MP. Increased amygdala and insula activation during emotion processing in anxiety-prone subjects. *Am J Psychiatry*. 2007;164(2):318-27.
203. Latora V, Marchiori M. Efficient behavior of small-world networks. *Phys Rev Lett*. 2001;87(19):198701.
204. Newman MEJ. Analysis of weighted networks. *Physical Review E*. 2004;70.
205. Oliveira CL, Morais PA, Moreira AA, Andrade JS, Jr. Enhanced flow in small-world networks. *Phys Rev Lett*. 2014;112(14):148701.
206. Nishikawa T, Motter AE, Lai YC, Hoppensteadt FC. Heterogeneity in oscillator networks: are smaller worlds easier to synchronize? *Phys Rev Lett*. 2003;91(1):014101.
207. Ajilore O, Lamar M, Kumar A. Association of brain network efficiency with aging, depression, and cognition. *The American journal of geriatric psychiatry : official journal of the American Association for Geriatric Psychiatry*. 2014;22(2):102-10.
208. Zhang J, Wang J, Wu Q, Kuang W, Huang X, He Y, et al. Disrupted brain connectivity networks in drug-naïve, first-episode major depressive disorder. *Biol Psychiatry*. 2011;70(4):334-42.
209. Zhu H, Qiu C, Meng Y, Yuan M, Zhang Y, Ren Z, et al. Altered Topological Properties of Brain Networks in Social Anxiety Disorder: A Resting-state Functional MRI Study. *Scientific Reports*. 2017;7(1):43089.
210. Templin C, Hanggi J, Klein C, Topka MS, Hiestand T, Levinson RA, et al. Altered limbic and autonomic processing supports brain-heart axis in Takotsubo syndrome. *European Heart Journal*. 40(15):1183-7.

211. Onishi T, Saha SK, Delgado-Montero A, Ludwig DR, Onishi T, Schelbert EB, et al. Global longitudinal strain and global circumferential strain by speckle-tracking echocardiography and feature-tracking cardiac magnetic resonance imaging: comparison with left ventricular ejection fraction. *J Am Soc Echocardiogr*. 2015;28(5):587-96.
212. Schuster A, Hor KN, Kowallick JT, Beerbaum P, Kutty S. Cardiovascular Magnetic Resonance Myocardial Feature Tracking: Concepts and Clinical Applications. *Circulation: Cardiovascular Imaging*. 2016.
213. Reindl M, Tiller C, Holzknecht M, Lechner I, Beck A, Plappert D, et al. Prognostic Implications of Global Longitudinal Strain by Feature-Tracking Cardiac Magnetic Resonance in ST-Elevation Myocardial Infarction. *Circ Cardiovasc Imaging*. 2019;12(11):e009404.
214. Ezzati A, Jiang J, Katz MJ, Sliwinski MJ, Zimmerman ME, Lipton RB. Validation of the Perceived Stress Scale in a community sample of older adults. *Int J Geriatr Psychiatry*. 2014;29(6):645-52.
215. Zalesky A, Fornito A, Bullmore ET. Network-based statistic: identifying differences in brain networks. *Neuroimage*. 2010;53(4):1197-207.
216. Cohen S, Kamarck T, Mermelstein R. A global measure of perceived stress. *J Health Soc Behav*. 1983;24(4):385-96.
217. Shoemaker JK, Norton KN, Baker J, Luchyshyn T. Forebrain organization for autonomic cardiovascular control. *Auton Neurosci*. 2015;188:5-9.
218. Li G, Ma X, Bian H, Sun X, Zhai N, Yao M, et al. A pilot fMRI study of the effect of stressful factors on the onset of depression in female patients. *Brain Imaging Behav*. 2016;10(1):195-202.
219. Ajilore O, Lamar M, Leow A, Zhang A, Yang S, Kumar A. Graph theory analysis of cortical-subcortical networks in late-life depression. *Am J Geriatr Psychiatry*. 2014;22(2):195-206.
220. Yang X, Liu J, Meng Y, Xia M, Cui Z, Wu X, et al. Network analysis reveals disrupted functional brain circuitry in drug-naïve social anxiety disorder. *Neuroimage*. 2019;190:213-23.
221. Wheelock MD, Rangaprakash D, Harnett NG, Wood KH, Orem TR, Mrug S, et al. Psychosocial stress reactivity is associated with decreased whole-brain network efficiency and increased amygdala centrality. *Behav Neurosci*. 2018;132(6):561-72.
222. Lei D, Li K, Li L, Chen F, Huang X, Lui S, et al. Disrupted Functional Brain Connectome in Patients with Posttraumatic Stress Disorder. *Radiology*. 2015;276(3):818-27.
223. Sheynin J, Duval ER, King AP, Angstadt M, Phan KL, Simon NM, et al. Associations between resting-state functional connectivity and treatment response in a randomized clinical trial for posttraumatic stress disorder. *Depress Anxiety*. 2020;37(10):1037-46.
224. Thayer JF, Lane RD. Claude Bernard and the heart-brain connection: further elaboration of a model of neurovisceral integration. *Neurosci Biobehav Rev*. 2009;33(2):81-8.
225. Wager TD, Waugh CE, Lindquist M, Noll DC, Fredrickson BL, Taylor SF. Brain mediators of cardiovascular responses to social threat: part I: Reciprocal dorsal and ventral sub-regions of the medial prefrontal cortex and heart-rate reactivity. *Neuroimage*. 2009;47(3):821-35.



226. Park H, Park YH, Cha J, Seo SW, Na DL, Lee JM. Agreement between functional connectivity and cortical thickness-driven correlation maps of the medial frontal cortex. *PloS one*. 2017;12(3):e0171803.
227. Segall J, Allen E, Jung R, Erhardt E, Arja S, Kiehl K, et al. Correspondence between structure and function in the human brain at rest. *Frontiers in Neuroinformatics*. 2012;6.
228. Driscoll ME BP, Tadi P. *Neuroanatomy, Nucleus Caudate*: StatPearls Publishing; 2021.
229. Simpson JR, Jr., Drevets WC, Snyder AZ, Gusnard DA, Raichle ME. Emotion-induced changes in human medial prefrontal cortex: II. During anticipatory anxiety. *Proc Natl Acad Sci U S A*. 2001;98(2):688-93.
230. Gusnard DA, Akbudak E, Shulman GL, Raichle ME. Medial prefrontal cortex and self-referential mental activity: relation to a default mode of brain function. *Proc Natl Acad Sci U S A*. 2001;98(7):4259-64.
231. Nashiro K, Min J, Yoo HJ, Cho C, Bachman SL, Dutt S, et al. Enhancing the brain's emotion regulation capacity with a randomised trial of a 5-week heart rate variability biofeedback intervention. *medRxiv*. 2021:2021.09.28.21264206.
232. Ahdidan J, Hviid LB, Chakravarty MM, Ravnkilde B, Rosenberg R, Rodell A, et al. Longitudinal MR study of brain structure and hippocampus volume in major depressive disorder. *Acta Psychiatr Scand*. 2011;123(3):211-9.
233. Yuksel D, Engelen J, Schuster V, Dietsche B, Konrad C, Jansen A, et al. Longitudinal brain volume changes in major depressive disorder. *J Neural Transm (Vienna)*. 2018;125(10):1433-47.
234. Binnewies J, Nawijn L, van Tol MJ, van der Wee NJA, Veltman DJ, Penninx B. Associations between depression, lifestyle and brain structure: A longitudinal MRI study. *Neuroimage*. 2021;231:117834.
235. Dohm K, Redlich R, Zwieterlood P, Dannlowski U. Trajectories of major depression disorders: A systematic review of longitudinal neuroimaging findings. *Aust N Z J Psychiatry*. 2017;51(5):441-54.
236. Hölzel BK, Carmody J, Evans KC, Hoge EA, Dusek JA, Morgan L, et al. Stress reduction correlates with structural changes in the amygdala. *Soc Cogn Affect Neurosci*. 2010;5(1):11-7.
237. Gotink RA, Vernooij MW, Ikram MA, Niessen WJ, Krestin GP, Hofman A, et al. Meditation and yoga practice are associated with smaller right amygdala volume: the Rotterdam study. *Brain Imaging Behav*. 2018;12(6):1631-9.
238. Makovac E, Watson DR, Meeten F, Garfinkel SN, Cercignani M, Critchley HD, et al. Amygdala functional connectivity as a longitudinal biomarker of symptom changes in generalized anxiety. *Soc Cogn Affect Neurosci*. 2016;11(11):1719-28.
239. Sapolsky RM. Why stress is bad for your brain. *Science*. 1996;273(5276):749-50.
240. Arnone D, McKie S, Elliott R, Juhasz G, Thomas EJ, Downey D, et al. State-dependent changes in hippocampal grey matter in depression. *Mol Psychiatry*. 2013;18(12):1265-72.
241. Driemeyer J, Boyke J, Gaser C, Buchel C, May A. Changes in gray matter induced by learning--revisited. *PloS one*. 2008;3(7):e2669.
242. Takeuchi H, Sekiguchi A, Taki Y, Yokoyama S, Yomogida Y, Komuro N, et al. Training of working memory impacts structural connectivity. *J Neurosci*. 2010;30(9):3297-303.

243. Zatorre RJ, Fields RD, Johansen-Berg H. Plasticity in gray and white: neuroimaging changes in brain structure during learning. *Nat Neurosci.* 2012;15(4):528-36.
244. Aimone JB, Wiles J, Gage FH. Computational influence of adult neurogenesis on memory encoding. *Neuron.* 2009;61(2):187-202.
245. Dong WK, Greenough WT. Plasticity of nonneuronal brain tissue: roles in developmental disorders. *Ment Retard Dev Disabil Res Rev.* 2004;10(2):85-90.
246. Benedetti F, Palladini M, Paolini M, Melloni E, Vai B, De Lorenzo R, et al. Brain correlates of depression, post-traumatic distress, and inflammatory biomarkers in COVID-19 survivors: A multimodal magnetic resonance imaging study. *Brain Behav Immun Health.* 2021;18:100387.
247. Schrepf A, Kaplan CM, Ichescio E, Larkin T, Harte SE, Harris RE, et al. A multi-modal MRI study of the central response to inflammation in rheumatoid arthritis. *Nature Communications.* 2018;9(1):2243.
248. Crowson CS, Liao KP, Davis JM, 3rd, Solomon DH, Matteson EL, Knutson KL, et al. Rheumatoid arthritis and cardiovascular disease. *American heart journal.* 2013;166(4):622-8.e1.
249. Katsoularis I, Fonseca-Rodriguez O, Farrington P, Lindmark K, Fors Connolly AM. Risk of acute myocardial infarction and ischaemic stroke following COVID-19 in Sweden: a self-controlled case series and matched cohort study. *Lancet (London, England).* 2021;398(10300):599-607.
250. Drevets WC, Price JL, Furey ML. Brain structural and functional abnormalities in mood disorders: implications for neurocircuitry models of depression. *Brain Struct Funct.* 2008;213(1-2):93-118.
251. Baumann O, Mattingley JB. Functional Organization of the Parahippocampal Cortex: Dissociable Roles for Context Representations and the Perception of Visual Scenes. *J Neurosci.* 2016;36(8):2536-42.
252. Sha Z, Xia M, Lin Q, Cao M, Tang Y, Xu K, et al. Meta-Connectomic Analysis Reveals Commonly Disrupted Functional Architectures in Network Modules and Connectors across Brain Disorders. *Cereb Cortex.* 2018;28(12):4179-94.
253. Catani M, Jones DK, Donato R, Ffytche DH. Occipito-temporal connections in the human brain. *Brain.* 2003;126(Pt 9):2093-107.
254. Bigler ED, Mortensen S, Neeley ES, Ozonoff S, Krasny L, Johnson M, et al. Superior temporal gyrus, language function, and autism. *Dev Neuropsychol.* 2007;31(2):217-38.
255. Takahashi H, Yahata N, Koeda M, Matsuda T, Asai K, Okubo Y. Brain activation associated with evaluative processes of guilt and embarrassment: an fMRI study. *Neuroimage.* 2004;23(3):967-74.
256. Adolphs R. Cognitive neuroscience of human social behaviour. *Nat Rev Neurosci.* 2003;4(3):165-78.
257. Das P, Kemp AH, Liddell BJ, Brown KJ, Olivieri G, Peduto A, et al. Pathways for fear perception: modulation of amygdala activity by thalamo-cortical systems. *Neuroimage.* 2005;26(1):141-8.
258. Lithari C, Moratti S, Weisz N. Limbic areas are functionally decoupled and visual cortex takes a more central role during fear conditioning in humans. *Sci Rep.* 2016;6:29220.
259. Shin DJ, Jung WH, He Y, Wang J, Shim G, Byun MS, et al. The effects of pharmacological treatment on functional brain connectome in obsessive-compulsive disorder. *Biol Psychiatry.* 2014;75(8):606-14.

260. Lyon AR, Rees PSC, Prasad S, Poole-Wilson PA, Harding SE. Stress (Takotsubo) cardiomyopathy—a novel pathophysiological hypothesis to explain catecholamine-induced acute myocardial stunning. *Nature Clinical Practice Cardiovascular Medicine*. 2008;5(1):22-9.
261. Maddock RJ, Garrett AS, Buonocore MH. Posterior cingulate cortex activation by emotional words: fMRI evidence from a valence decision task. *Hum Brain Mapp*. 2003;18(1):30-41.

## Chapter 8 APPENDICES

### 8.1 APPENDIX A

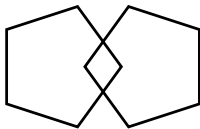
Appendix A is a copy of the psychological questionnaires including the MMSE, HADS, PSS and B-IPQ and the IES-R.

### MINI MENTAL STATE EXAMINATION (MMSE)

Name:

DOB:

Hospital Number:

One point for each answer		DATE:			
<b>ORIENTATION</b>					
Year	Season	Month	Date	Time	
Country	Town	District	Hospital	Ward/Floor	
		...../ 5	...../ 5	...../ 5	...../ 5
<b>REGISTRATION</b>					
Examiner names three objects (e.g. apple, table, penny) and asks the patient to repeat (1 point for each correct. THEN the patient learns the 3 names repeating until correct).		...../ 3	...../ 3	...../ 3	...../ 3
<b>ATTENTION AND CALCULATION</b>					
Subtract 7 from 100, then repeat from result. Continue five times: 100, 93, 86, 79, 65. (Alternative: spell "WORLD" backwards: DLROW).		...../ 5	...../ 5	...../ 5	...../ 5
<b>RECALL</b>					
Ask for the names of the three objects learned earlier.		...../ 3	...../ 3	...../ 3	...../ 3
<b>LANGUAGE</b>					
Name two objects (e.g. pen, watch).		...../ 2	...../ 2	...../ 2	...../ 2
Repeat "No ifs, ands, or buts".		...../ 1	...../ 1	...../ 1	...../ 1
Give a three-stage command. Score 1 for each stage. (e.g. "Place index finger of right hand on your nose and then on your left ear").		...../ 3	...../ 3	...../ 3	...../ 3
Ask the patient to read and obey a written command on a piece of paper. The written instruction is: "Close your eyes".		...../ 1	...../ 1	...../ 1	...../ 1
Ask the patient to write a sentence. Score 1 if it is sensible and has a subject and a verb.		...../ 1	...../ 1	...../ 1	...../ 1
<b>COPYING:</b> Ask the patient to copy a pair of intersecting pentagons					
		...../ 1	...../ 1	...../ 1	...../ 1
<b>TOTAL:</b>		...../ 30	...../ 30	...../ 30	...../ 30

#### MMSE scoring

24-30: no cognitive impairment

18-23: mild cognitive impairment

0-17: severe cognitive impairment

**Hospital Anxiety and Depression Score (HADS)**

This questionnaire helps your physician to know how you are feeling. Read every sentence. Place an "X" on the answer that best describes how you have been feeling during the LAST WEEK. You do not have to think too much to answer. In this questionnaire, spontaneous answers are more important

<b>A</b>	<b>I feel tense or 'wound up':</b> Most of the time A lot of the time From time to time (occ.) Not at all	3 2 1 0
<b>D</b>	<b>I still enjoy the things I used to enjoy:</b> Definitely as much Not quite as much Only a little Hardly at all	0 1 2 3
<b>A</b>	<b>I get a sort of frightened feeling as if something awful is about to happen:</b> Very definitely and quite badly Yes, but not too badly A little, but it doesn't worry me Not at all	3 2 1 0
<b>D</b>	<b>I can laugh and see the funny side of things:</b> As much as I always could Not quite so much now Definitely not so much now Not at all	0 1 2 3
<b>A</b>	<b>Worrying thoughts go through my mind:</b> A great deal of the time A lot of the time From time to time, but not often Only occasionally	3 2 1 0
<b>D</b>	<b>I feel cheerful:</b> Not at all Not often Sometimes Most of the time	3 2 1 0
<b>A</b>	<b>I can sit at ease and feel relaxed:</b> Definitely Usually Not often Not at all	0 1 2 3

<b>D</b>	<b>I feel as if I am slowed down:</b> Nearly all the time Very often Sometimes Not at all	3 2 1 0
<b>A</b>	<b>I get a sort of frightened feeling like "butterflies" in the stomach:</b> Not at all Occasionally Quite often Very often	0 1 2 3
<b>D</b>	<b>I have lost interest in my appearance:</b> Definitely I don't take as much care as I should I may not take quite as much care I take just as much care	3 2 1 0
<b>A</b>	<b>I feel restless as I have to be on the move:</b> Very much indeed Quite a lot Not very much Not at all	3 2 1 0
<b>D</b>	<b>I look forward with enjoyment to things:</b> As much as I ever did Rather less than I used to Definitely less than I used to Hardly at all	0 1 2 3
<b>A</b>	<b>I get sudden feelings of panic:</b> Very often indeed Quite often Not very often Not at all	3 2 1 0
<b>D</b>	<b>I can enjoy a good book or radio/TV program:</b> Often Sometimes Not often Very seldom	0 1 2 3

## Perceived Stress Scale

A more precise measure of personal stress can be determined by using a variety of instruments that have been designed to help measure individual stress levels. The first of these is called the **Perceived Stress Scale**.

The Perceived Stress Scale (PSS) is a classic stress assessment instrument. The tool, while originally developed in 1983, remains a popular choice for helping us understand how different situations affect our feelings and our perceived stress. The questions in this scale ask about your feelings and thoughts during the last month. In each case, you will be asked to indicate how often you felt or thought a certain way. Although some of the questions are similar, there are differences between them and you should treat each one as a separate question. The best approach is to answer fairly quickly. That is, don't try to count up the number of times you felt a particular way; rather indicate the alternative that seems like a reasonable estimate.

**For each question choose from the following alternatives:**

**0 - never    1 - almost never    2 - sometimes    3 - fairly often    4 - very often**

- \_\_\_\_\_ 1. In the last month, how often have you been upset because of something that happened unexpectedly?
- \_\_\_\_\_ 2. In the last month, how often have you felt that you were unable to control the important things in your life?
- \_\_\_\_\_ 3. In the last month, how often have you felt nervous and stressed?
- \_\_\_\_\_ 4. In the last month, how often have you felt confident about your ability to handle your personal problems?
- \_\_\_\_\_ 5. In the last month, how often have you felt that things were going your way?
- \_\_\_\_\_ 6. In the last month, how often have you found that you could not cope with all the things that you had to do?
- \_\_\_\_\_ 7. In the last month, how often have you been able to control irritations in your life?
- \_\_\_\_\_ 8. In the last month, how often have you felt that you were on top of things?
- \_\_\_\_\_ 9. In the last month, how often have you been angered because of things that happened that were outside of your control?
- \_\_\_\_\_ 10. In the last month, how often have you felt difficulties were piling up so high that you could not overcome them?

### The Brief Illness Perception Questionnaire

For the following questions, please circle the number that best corresponds to your views:

<b>How much does your illness affect your life?</b> <div style="display: flex; justify-content: space-between; padding: 5px;"> <span>0 no affect at all</span> <span>1</span> <span>2</span> <span>3</span> <span>4</span> <span>5</span> <span>6</span> <span>7</span> <span>8</span> <span>9</span> <span>10 severely affects my life</span> </div>											
<b>How long do you think your illness will continue?</b> <div style="display: flex; justify-content: space-between; padding: 5px;"> <span>0 a very short time</span> <span>1</span> <span>2</span> <span>3</span> <span>4</span> <span>5</span> <span>6</span> <span>7</span> <span>8</span> <span>9</span> <span>10 forever</span> </div>											
<b>How much control do you feel you have over your illness?</b> <div style="display: flex; justify-content: space-between; padding: 5px;"> <span>0 absolutely no control</span> <span>1</span> <span>2</span> <span>3</span> <span>4</span> <span>5</span> <span>6</span> <span>7</span> <span>8</span> <span>9</span> <span>10 extreme amount of control</span> </div>											
<b>How much do you think your treatment can help your illness?</b> <div style="display: flex; justify-content: space-between; padding: 5px;"> <span>0 not at all</span> <span>1</span> <span>2</span> <span>3</span> <span>4</span> <span>5</span> <span>6</span> <span>7</span> <span>8</span> <span>9</span> <span>10 extremely helpful</span> </div>											
<b>How much do you experience symptoms from your illness?</b> <div style="display: flex; justify-content: space-between; padding: 5px;"> <span>0 no symptoms at all</span> <span>1</span> <span>2</span> <span>3</span> <span>4</span> <span>5</span> <span>6</span> <span>7</span> <span>8</span> <span>9</span> <span>10 many severe symptoms</span> </div>											
<b>How concerned are you about your illness?</b> <div style="display: flex; justify-content: space-between; padding: 5px;"> <span>0 not at all concerned</span> <span>1</span> <span>2</span> <span>3</span> <span>4</span> <span>5</span> <span>6</span> <span>7</span> <span>8</span> <span>9</span> <span>10 extremely concerned</span> </div>											
<b>How well do you feel you understand your illness?</b> <div style="display: flex; justify-content: space-between; padding: 5px;"> <span>0 don't understand at all</span> <span>1</span> <span>2</span> <span>3</span> <span>4</span> <span>5</span> <span>6</span> <span>7</span> <span>8</span> <span>9</span> <span>10 understand very clearly</span> </div>											
<b>How much does your illness affect you emotionally? (e.g. does it make you angry, scared, upset or depressed?)</b> <div style="display: flex; justify-content: space-between; padding: 5px;"> <span>0 not at all affected emotionally</span> <span>1</span> <span>2</span> <span>3</span> <span>4</span> <span>5</span> <span>6</span> <span>7</span> <span>8</span> <span>9</span> <span>10 extremely affected emotionally</span> </div>											
<b>Please list in rank-order the three most important factors that you believe caused <u>your</u> illness. The most important causes for me:-</b>  <div style="margin-top: 10px;"> 1. _____  2. _____  3. _____ </div>											

© All rights reserved. For permission to use the scale please contact: lizbroadbent@clear.net.nz

**IMPACT OF EVENT SCALE - REVISED**

**INSTRUCTIONS:** Below is a list of difficulties people sometimes have after stressful life events.

Please read each item, and then indicate how distressing each difficulty has been for you **DURING THE PAST SEVEN DAYS** with respect to \_\_\_\_\_, how much were you distressed or bothered by these difficulties?

		Not at All	A little Bit	Moderately	Quite a Bit	Extremely
1.	Any reminder brought back feelings about it.	0	1	2	3	4
2.	I had trouble staying asleep.	0	1	2	3	4
3.	Other things kept making me think about it.	0	1	2	3	4
4.	I felt irritable and angry.	0	1	2	3	4
5.	I avoided letting myself get upset when I thought about it or was reminded of it.	0	1	2	3	4
6.	I thought about it when I didn't mean to.	0	1	2	3	4
7.	I felt as if it hadn't happened or wasn't real.	0	1	2	3	4
8.	I stayed away from reminders about it.	0	1	2	3	4
9.	Pictures about it popped into my mind.	0	1	2	3	4
10.	I was jumpy and easily startled.	0	1	2	3	4
11.	I tried not to think about it.	0	1	2	3	4
12.	I was aware that I still had a lot of feelings about it, but I didn't deal with them.	0	1	2	3	4
13.	My feelings about it were kind of numb.	0	1	2	3	4
14.	I found myself acting or feeling like I was back at that time.	0	1	2	3	4
15.	I had trouble falling asleep.	0	1	2	3	4
16.	I had waves of strong feelings about it.	0	1	2	3	4
17.	I tried to remove it from my memory.	0	1	2	3	4
18.	I had trouble concentrating.	0	1	2	3	4
19.	Reminders of it caused me to have physical reactions, such as sweating, trouble breathing, nausea, or a pounding heart.	0	1	2	3	4
20.	I had dreams about it.	0	1	2	3	4
21.	I felt watchful and on guard.	0	1	2	3	4
22.	I tried not to talk about it.	0	1	2	3	4



## 8.2 APPENDIX B

Appendix B includes the supplementary results from Chapter 3.

Table 26 Regions where grey matter volume negatively correlates with MMSE score

Hemisphere	AAL region	p(FWE-corr)	T	x	y	z
Right	Putamen	0.019	5.33	32	-20	-3

Table 27 Regions of the brain in which grey matter volume positively correlates with GLS in STEMI patients

Hemisphere	AAL brain region	p(FWE-corr)	T	x	y	z
Right	Frontal_Sup*	0.004	8.42	15	36	54
Left	Frontal_Inf_Orb*	0.007	8	-42	36	-3
Right	Frontal_Sup_Orb*	0.01	7.76	18	33	-24
Right	Olfactory	0.01	7.72	8	24	-9
Right	Frontal_Mid*	0.013	7.56	27	36	48
Right	Frontal_Med_Orb	0.023	7.18	12	46	-3
Left	Temporal_Inf	0.032	6.98	-45	-38	-26
Right	Frontal_Mid_Orb	0.034	6.95	20	58	-12
Left	Temporal_Mid*	0.042	6.81	-56	-20	-2
Left	Fusiform	0.044	6.77	-34	-20	-30
Left	Temporal_Inf*	0.046	6.75	-44	-36	-27

AAL – automated anatomic labelling, GLS – global longitudinal strain.

\* Represents AAL regions also seen in MINOCA patients.

All p values are corrected for multiple comparisons (FWE corrected). Only results with a T threshold >5 are included.

Table 28 Regions of the brain in which grey matter volume positively correlate with LVEF in healthy controls patients

Hemisphere	AAL brain region	p(FWE-corr)	T	x	y	z
Left	Hippocampus	0.005	8.03	-24	-8	-26
Right	Parahippocampal	0.007	7.81	24	-8	-27
Right	Frontal_Sup	0.007	7.8	20	18	66
Right	Hippocampus	0.012	7.44	32	-6	-21
Right	Cingulum_Mid	0.016	7.27	6	-18	42
Left	Frontal_Mid_Orb	0.019	7.16	-20	56	-12
Right	Insula	0.021	7.09	42	24	-3
Right	Cingulum_Mid_R	0.033	6.8	8	20	40

## Chapter 8 Appendices

Left	Frontal_Inf_Orb	0.034	6.8	-28	27	-9
Right	Temporal_Inf	0.048	6.57	56	-14	-38
Left	Temporal_Pole_Mid	0.049	6.56	-44	9	-28

AAL – automated anatomic labelling

All p values are corrected for multiple comparisons (FWE corrected). Only results with a T threshold >5 are included.

## 8.3 APPENDIX C

Appendix C included the supplementary results from Chapter 4.

Table 29 Table demonstrating network measures by anxiety, depression, stress and GLS-CMR groups in STEMI control patients and healthy volunteers.

STEMI Controls (n=25)			
Variable	Global Efficiency	Modularity	SWP
Anxiety <8 (n=16)	0.330 [0.299-0.366]	0.128 [0.023]	0.686 [0.608-0.755]
Anxiety ≥8 (n=9)	0.332 [0.297-0.342]	0.138 [0.028]	0.635 [0.622-0.670]
P value	0.428	0.385	0.571
Depression <8 (n=21)	0.331 [0.297-0.360]	0.132 [0.026]	0.670 [0.600-0.756]
Depression ≥8 (n=4)	0.312 [0.294-0.331]	0.127 [0.021]	0.628 [0.619-0.637]
P value	0.266	0.701	0.299
PSS <21 (n=19)	0.342 [0.297-0.361]	0.133 [0.026]	0.730 [0.628-0.757]
PSS ≥21 (n=6)	0.312 [0.284-0.330]	0.127 [0.020]	0.619 [0.548-0.635]
P value	0.086	0.593	<b>0.036</b>
GLS-CMR ≤-17.9% (n=0)	n/a	n/a	n/a
GLS-CMR >-17.9% (n=25)	0.331 [0.297-0.354]	0.132 [0.025]	0.640 [0.615-0.755]
P value	n/a	n/a	n/a
Healthy Volunteers (n=25)			
Anxiety <8 (n=20)	0.318 [0.306-0.350]	0.127 [0.018]	0.684 [0.581-0.758]
Anxiety ≥8 (n=5)	0.335 [0.305-0.367]	0.125 [0.022]	0.690 [0.574-0.779]
P value	0.786	0.795	0.892
Depression <8 (n=25)	0.319 [0.305-0.352]	0.127 [0.018]	0.690 [0.580-0.763]
Depression ≥8 (n=0)	n/a	n/a	n/a
P value	n/a	n/a	n/a
PSS <21 (n=23)	0.319 [0.304-0.352]	0.126 [0.017]	0.702 [0.580-0.777]
PSS ≥21 (n=2)	0.357 [0.305-0.408]	0.135 [0.034]	0.630 [0.571-0.690]
P value	0.617	0.501	0.367
GLS-CMR ≤-17.9% (n=13)	0.315 [0.304-0.333]	0.129 [0.018]	0.644 [0.574-0.763]
GLS-CMR >-17.9% (n=12)	0.339 [0.310-0.371]	0.124 [0.019]	0.696 [0.621-0.755]
P value	0.115	0.473	0.703

Table 30 Increased connectivity in patients with MINOCA compared to healthy controls in the default mode network at two set thresholds.

At the higher threshold ( $t=3.1$ )  $p=0.012$ , FWE-corrected; 5000 permutations, at the lower threshold ( $t=2.35$ )  $p=0.016$ , FWE-corrected, 5000 permutations. Edges described in bold were demonstrated at both the higher and lower thresholds

Node	Node	t-value
<b>ParaHippocampal_R</b>	<b>Supramarginal_R</b>	<b>3.30</b>
<b>ParaHippocampal_L</b>	<b>Supramarginal_R</b>	<b>3.19</b>
ParaHippocampal_R	Supramarginal_L	2.63
ParaHippocampal_L	ParaHippocampal_R	2.60
Supramarginal_L	Temporal_Inf_L	2.43
Frontal_Sup_Medial_L	ParaHippocampal_L	2.42
ParaHippocampal_L	Supramarginal_L	2.38

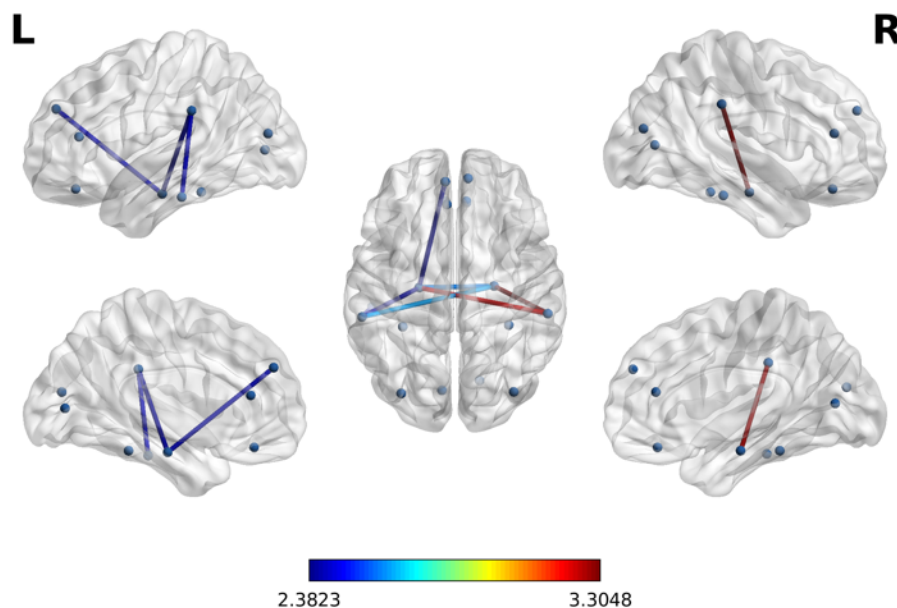


Table 31 Reduced connectivity in patients with MINOCA compared to healthy controls in the central executive network at two different set thresholds.

At the higher threshold ( $t=3.8$ )  $p=0.02$ , FWE-corrected; 5000 permutations, at the lower threshold ( $t=1.9$ )  $p=0.048$ , FWE-corrected, 5000 permutations. Edges described in bold were demonstrated at both the higher and lower thresholds

Node	Node	t-value
<b>Frontal_Mid_Orb_L</b>	<b>Frontal_Inf_Orb_L</b>	<b>3.83</b>
Frontal_Mid_Orb_R	Temporal_Inf_R	2.46

Frontal_Mid_Orb_L	Parietal_Inf_R	2.33
Frontal_Mid_Orb_L	Caudate_L	2.27
Parietal_Inf_R	Caudate_L	2.25
Frontal_Mid_Orb_L	Frontal_Inf_Oper_R	2.02
Frontal_Mid_Orb_R	Caudate_L	1.95
Frontal_Mid_Orb_L	Parietal_Inf_L	1.94
Frontal_Mid_Orb_L	Frontal_Mid_Orb_R	1.90

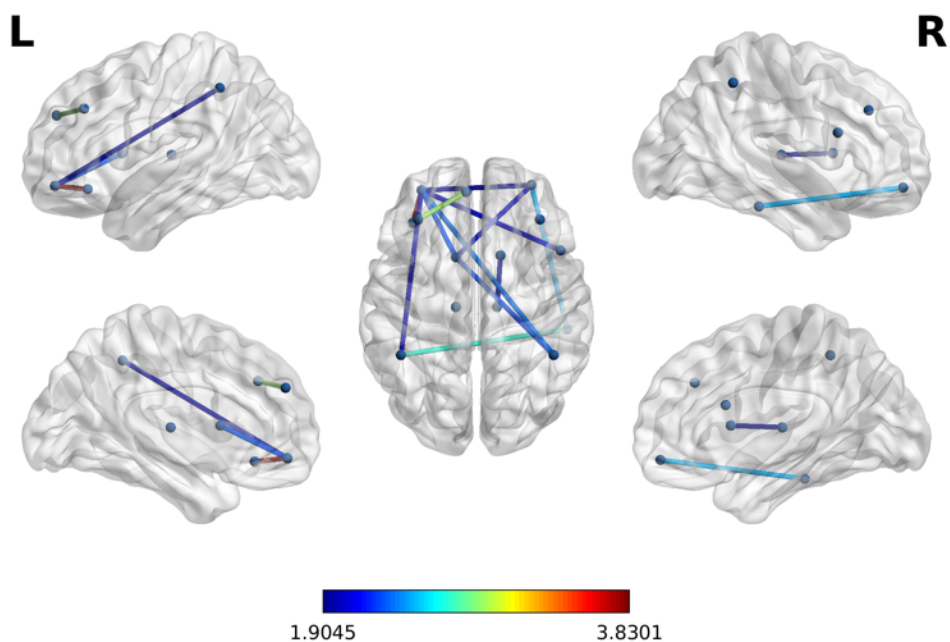


Table 32 Reduced connectivity in patients with MINOCA compared to STEMI controls in the central executive network

At the higher threshold ( $t=2.2$ )  $p=0.050$ , FWE-corrected; 5000 permutations, at the lower threshold ( $t=1.8$ )  $p=0.045$ , FWE-corrected, 5000 permutations. Edges described in bold were demonstrated at both the higher and lower thresholds

Node	Node	t-value
<b>Frontal_Mid_Orb_L</b>	<b>Parietal_Inf_R</b>	<b>2.72</b>
<b>Frontal_Mid_R</b>	<b>Parietal_Inf_L</b>	<b>2.60</b>
<b>Frontal_Mid_R</b>	<b>Thalamus_R</b>	<b>2.29</b>
<b>Frontal_Mid_R</b>	<b>Parietal_Inf_R</b>	<b>2.24</b>
<b>Frontal_Mid_R</b>	<b>Temporal_Inf_R</b>	<b>2.21</b>
Frontal_Mid_Orb_R	Temporal_Inf_R	2.10

Frontal_Inf_Orb_L	Thalamus_R	2.07
Frontal_Mid_Orb_L	Parietal_Inf_L	2.02
Parietal_Inf_R	Thalamus_R	1.98
Thalamus_L	Thalamus_R	1.88
Frontal_Mid_Orb_L	Thalamus_R	1.81

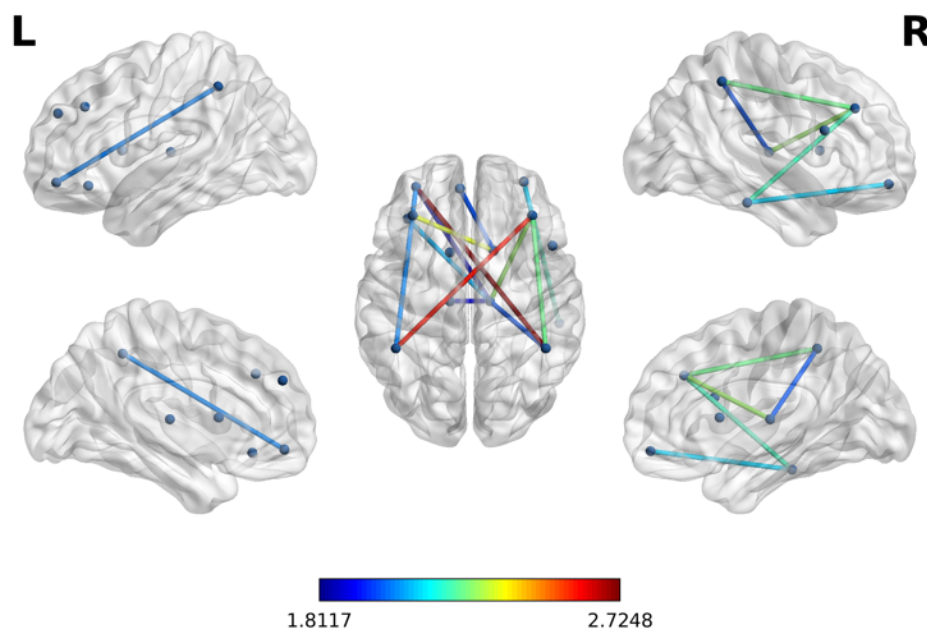


Table 33 Reduced connectivity in patients with TS compared to healthy controls in the central executive network.

At the higher threshold ( $t=2.2$ )  $p=0.030$ , FWE-corrected; 5000 permutations, at the lower threshold ( $t=1.7$ ),  $p=0.053$ , FWE-corrected; 5000 permutations.. Edges described in bold were demonstrated at both the higher and lower thresholds.

Node	Node	t-value
<b>Frontal_Mid_Orb_L</b>	<b>Parietal_Inf_R</b>	<b>3.08</b>
<b>Frontal_Sup_Medial_L</b>	<b>Frontal_Mid_L</b>	<b>2.76</b>
<b>Frontal_Mid_Orb_L</b>	<b>Frontal_Inf_Orb_L</b>	<b>2.73</b>
<b>Frontal_Mid_Orb_L</b>	<b>Parietal_Inf_L</b>	<b>2.35</b>
Frontal_Mid_R	Frontal_Inf_Oper_R	2.30
<b>Frontal_Mid_Orb_R</b>	<b>Parietal_Inf_R</b>	<b>2.27</b>
Frontal_Inf_Orb_L	Parietal_Inf_R	1.90
Frontal_Mid_R	Parietal_Inf_L	1.86
Frontal_Inf_Oper_R	Parietal_Inf_R	1.79

Frontal_Mid_R	Frontal_Mid_Orb_R	1.74
Parietal_Inf_R	Caudate_L	1.71

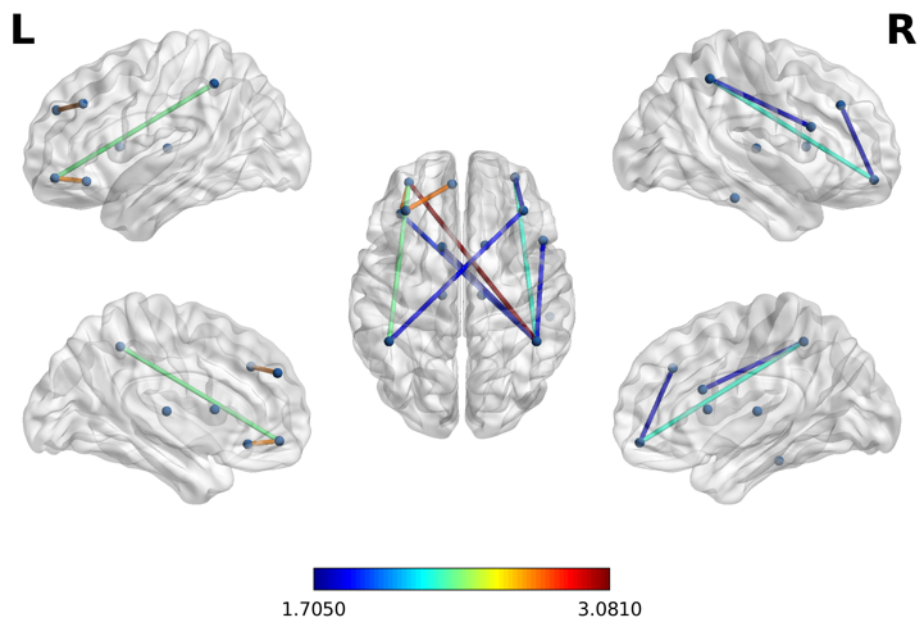


Table 34 Reduced connectivity in patients with TS compared to STEMI controls in the central executive network.

At the higher threshold ( $t=3.7$ )  $p=0.008$ , FWE-corrected; 5000 permutations, at the lower threshold ( $t=2.3$ ),  $p=0.010$ , FWE-corrected; 5000 permutations. Edges described in bold were demonstrated at both the higher and lower thresholds.

Node	Node	t-value
<b>Frontal_Mid_Orb_L</b>	<b>Parietal_Inf_R</b>	<b>3.80</b>
Parietal_Inf_L	Thalamus_R	2.60
Frontal_Inf_Orb_L	Parietal_Inf_R	2.41
Frontal_Mid_Orb_R	Parietal_Inf_R	2.40
Frontal_Mid_Orb_L	Parietal_Inf_L	2.39

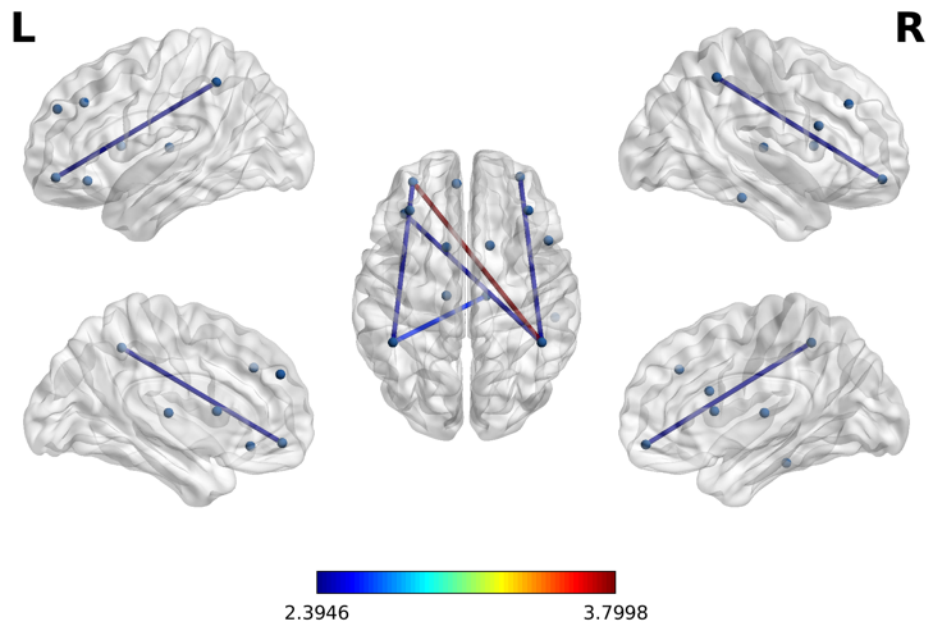


Table 35 Reduced connectivity in patients with TS compared to healthy controls on whole brain analysis.

At the higher threshold ( $t=3.1$ )  $p=0.024$ , FWE-corrected; 5000 permutations, at the lower threshold ( $t=2.85$ )  $p=0.062$ , FWE-corrected, 5000 permutations. Edges described in bold were demonstrated at both the higher and lower thresholds.

Node	Node	t-value
<b>Frontal_Mid_R</b>	<b>Hippocampus_R</b>	<b>3.65</b>
<b>Frontal_Mid_R</b>	<b>Hippocampus_L</b>	<b>3.45</b>
<b>Frontal_Inf_Tri_R</b>	<b>Temporal_Sup_L</b>	<b>3.32</b>
<b>Frontal_Inf_Tri_R</b>	<b>Hippocampus_R</b>	<b>3.23</b>
<b>Parietal_Sup_L</b>	<b>Temporal_Sup_L</b>	<b>3.14</b>
Frontal_Mid_R	Parietal_Inf_R	3.08
Frontal_Mid_R	Parietal_Sup_R	2.90



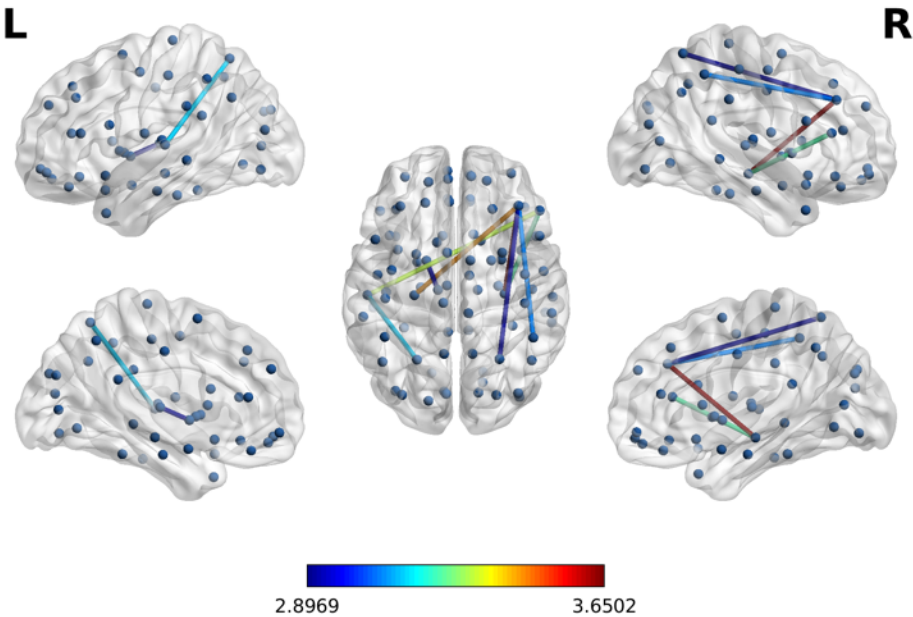


Table 36 Reduced connectivity in patients with TS compared to STEMI controls on whole brain analysis.

At the higher threshold ( $t=4.7$ )  $p=0.010$ , FWE-corrected; 5000 permutations, at the lower threshold ( $t=3.0$ ),  $p=0.053$ , FWE-corrected; 5000 permutations. Edges described in bold were demonstrated at both the higher and lower thresholds.

Node	Node	t-value
<b>Frontal_Inf_Tri_R</b>	<b>Temporal_Sup_L</b>	<b>4.75</b>
Frontal_Mid_R	Parietal_Inf_R	3.80
Frontal_Mid_R	Hippocampus_R	3.19
Frontal_Inf_Tri_R	Parietal_Inf_R	3.15
Frontal_Inf_Tri_R	Supramarginal_L	3.01

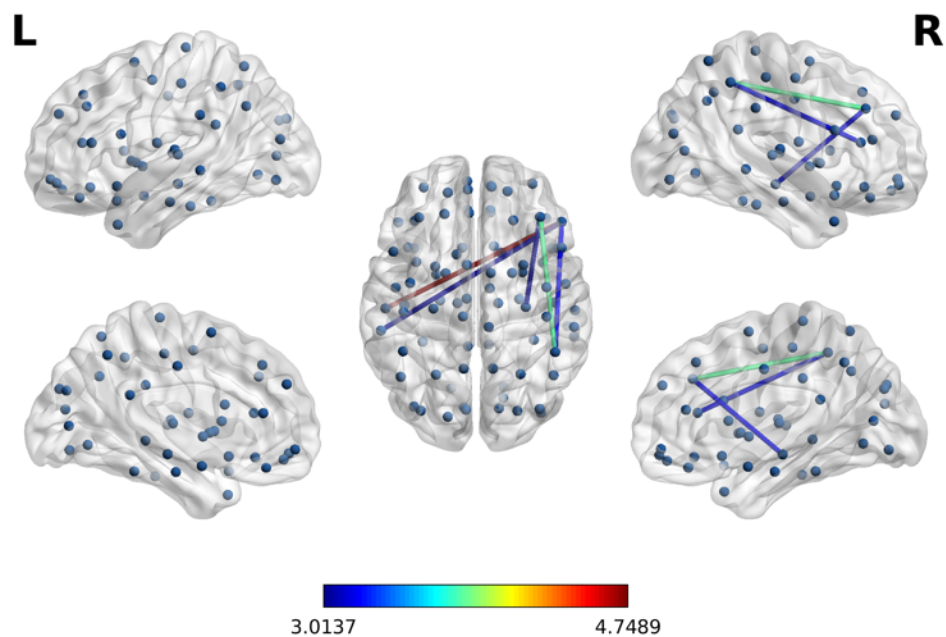


Table 37 Networks with a negative correlation between connectivity and anxiety scores in the sympathetic network in MINOCA patients.

At the higher threshold ( $t=1.6$ )  $p=0.047$ , FWE-corrected; 5000 permutations, at the lower threshold ( $t=1.1$ ),  $p=0.049$ , FWE-corrected; 5000 permutations. Edges described in bold were demonstrated at both the higher and lower thresholds.

Node	Node	t-value
<b>Hippocampus_L</b>	<b>Insula_L.</b>	<b>2.93</b>
<b>Insula_R</b>	<b>Parietal_Inf_L.</b>	<b>2.68</b>
<b>Cingulum_Mid_R</b>	<b>Hippocampus_L.</b>	<b>2.44</b>
<b>Cingulum_Mid_L</b>	<b>Postcentral_R.</b>	<b>2.17</b>
<b>Insula_L</b>	<b>Parietal_Inf_L.</b>	<b>2.05</b>
<b>Hippocampus_L</b>	<b>Insula_R.</b>	<b>1.73</b>
<b>Cingulum_Mid_L</b>	<b>Hippocampus_L.</b>	<b>1.72</b>
<b>Insula_L</b>	<b>Thalamus_R.</b>	<b>1.72</b>
<b>Cingulum_Mid_L</b>	<b>Parietal_Inf_L.</b>	<b>1.68</b>
Hippocampus_L	Parietal_Inf_L.	1.55
Postcentral_R	Parietal_Inf_L.	1.47
Insula_L	Thalamus_L.	1.38
Cingulum_Mid_R	Parietal_Inf_L.	1.38
Hippocampus_L	Thalamus_R.	1.37

Cingulum_Mid_L	Insula_R.	1.29
Cingulum_Mid_L	Cingulum_Mid_R.	1.19
Hippocampus_L	Thalamus_L.	1.19
Insula_L	Insula_R.	1.12

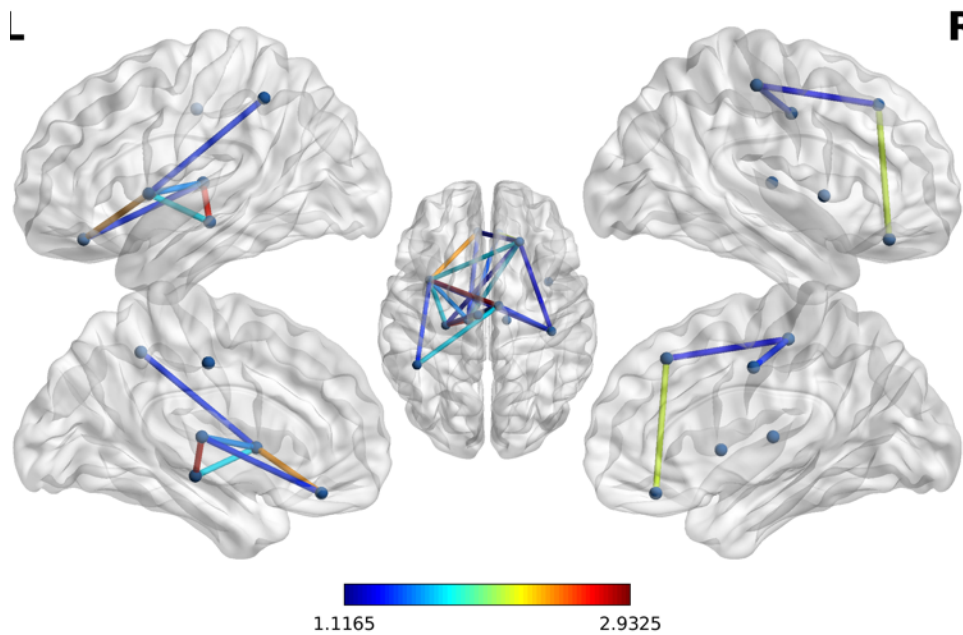


Table 38 Networks with a negative correlation between connectivity and stress scores in the sympathetic network in MINOCA patients.

At the higher threshold ( $t=2.6$ ),  $p=0.010$ , FWE-corrected; 5000 permutations, at the lower threshold ( $t=1.4$ ),  $p=0.044$ , FWE-corrected; 5000 permutations. Edges described in bold were demonstrated at both the higher and lower thresholds.

Node	Node	t-value
<b>Cingulum_Mid_R</b>	<b>Hippocampus_L.</b>	<b>3.06</b>
<b>Hippocampus_L</b>	<b>Parietal_Inf_L.</b>	<b>2.89</b>
<b>Cingulum_Mid_L</b>	<b>Hippocampus_L.</b>	<b>2.65</b>
Cingulum_Mid_L	Parietal_Inf_L.	1.93
Cingulum_Mid_R	Frontal_Sup_R.	1.79
Hippocampus_L	Insula_R.	1.77
Postcentral_R	Parietal_Inf_L.	1.7
Hippocampus_L	Insula_L.	1.66
Cingulum_Mid_R	Parietal_Inf_L.	1.64
Postcentral_R	Thalamus_L.	1.57

Postcentral_R	Hippocampus_L.	1.47
Cingulum_Mid_L	Cingulum_Mid_R.	1.45
Insula_R	Parietal_Inf_L.	1.43

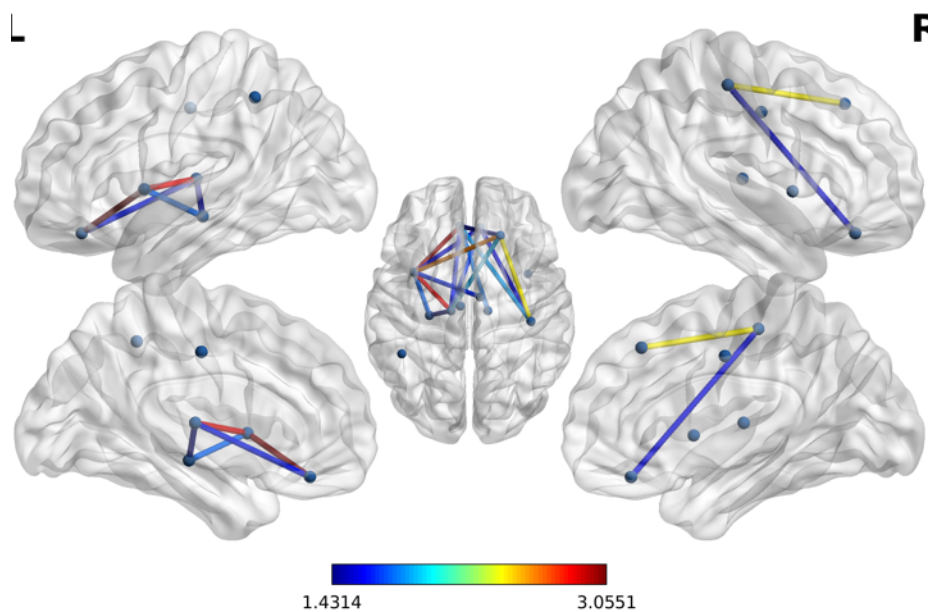


Table 39 Networks with a negative correlation between connectivity and stress scores in the sympathetic network in STEMI patients.

At the higher threshold ( $t=2.5$ ),  $p=0.035$ , FWE-corrected; 5000 permutations, at the lower threshold ( $t=2.1$ ),  $p=0.082$ , FWE-corrected; 5000 permutations. Edges described in bold were demonstrated at both the higher and lower thresholds.

Node	Node	t-value
Thalamus_L	<b>Frontal_Sup_R.</b>	<b>3.03</b>
Postcentral_R	<b>Rectus_R.</b>	<b>2.97</b>
Rectus_R	<b>Frontal_Sup_R.</b>	<b>2.52</b>
Cingulum_Mid_L	Thalamus_L.	2.19

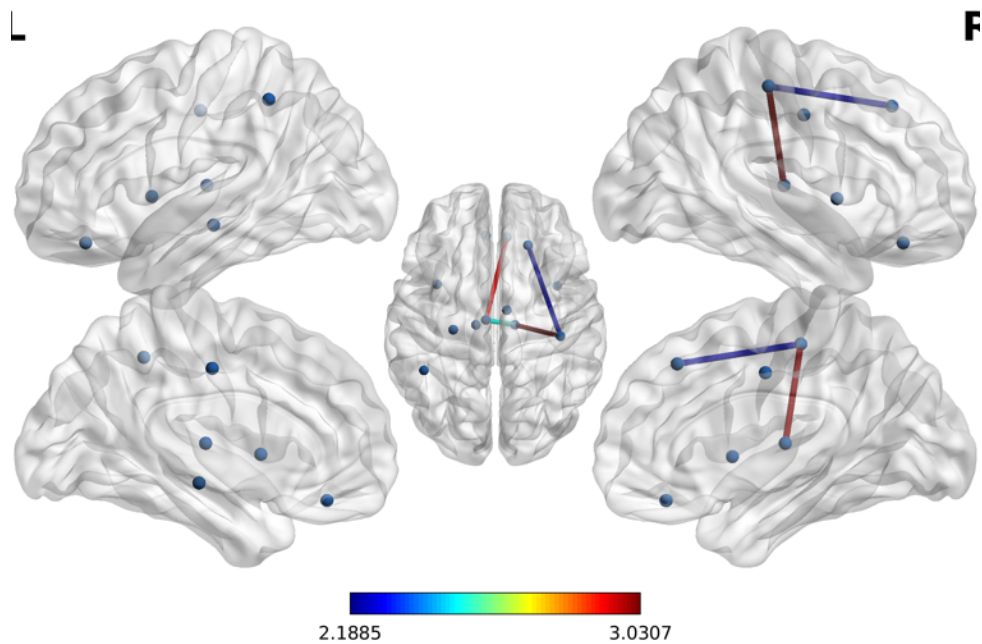


Table 40 Networks with a negative correlation between connectivity and stress scores in the parasympathetic network in MINOCA patients.

At the higher threshold ( $t=2.7$ ),  $p=0.016$ , FWE-corrected; 5000 permutations, at the lower threshold ( $t=1.5$ ),  $p=0.011$ , FWE-corrected; 5000 permutations. Edges described in bold were demonstrated at both the higher and lower thresholds.

Node	Node	t-value
<b>Insula_L</b>	<b>Hippocampus_R.</b>	<b>3.1</b>
<b>Insula_L</b>	<b>Amygdala_L.</b>	<b>2.77</b>
Frontal_Inf_Oper_L	Cingulum_Mid_R.	2.69
Insula_L	Cingulum_Mid_R.	2.15
Frontal_Inf_Oper_L	Hippocampus_R.	1.94
Frontal_Inf_Oper_L	Insula_R.	1.92
Cingulum_Mid_R	Amygdala_L.	1.64
Frontal_Inf_Oper_L	Insula_L.	1.61
Hippocampus_R	Amygdala_L.	1.59
Insula_L	Insula_R.	1.51

Table 41 Networks with a positive correlation between connectivity and stress scores in the parasympathetic network in healthy patients.

At the higher threshold ( $t=1.2$ ),  $p=0.045$ , FWE-corrected; 5000 permutations, at the lower threshold ( $t=0.5$ ),  $p=0.082$ , FWE-corrected; 5000 permutations. Edges described in bold were demonstrated at both the higher and lower thresholds.

Node	Node	t-value
Amygdala_L	Temporal_Sup_R.	<b>2.36</b>
Frontal_Inf_Oper_L	Temporal_Sup_R.	<b>2.19</b>
Frontal_Inf_Oper_L	Insula_R.	<b>1.53</b>
Cingulum_Mid_L	Cingulum_Mid_R.	<b>1.5</b>
Frontal_Inf_Oper_L	Cingulum_Mid_L.	<b>1.45</b>
Insula_R	Amygdala_L.	<b>1.37</b>
Cingulum_Mid_L	Temporal_Sup_R.	<b>1.36</b>
Hippocampus_R	Temporal_Sup_R.	<b>1.36</b>
Frontal_Inf_Oper_L	Hippocampus_R.	<b>1.34</b>
Frontal_Inf_Oper_L	Amygdala_L.	<b>1.27</b>
Frontal_Inf_Oper_L	Cingulum_Mid_R.	<b>1.25</b>
Cingulum_Mid_L	Amygdala_L.	1.1
Insula_R	Hippocampus_R.	0.86
Cingulum_Mid_R	Amygdala_L.	0.83
Hippocampus_R	Amygdala_L.	0.63
Cingulum_Mid_R	Temporal_Sup_R.	0.62
Insula_R	Cingulum_Mid_R.	0.55

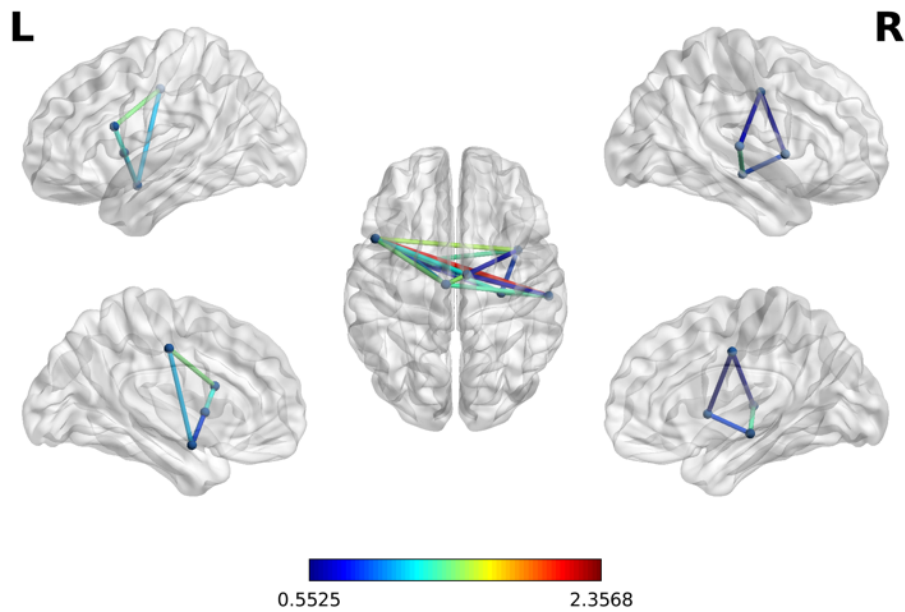


Table 42 Networks with a negative correlation between connectivity and anxiety scores in the default mode network in MINOCA patients.

At the higher threshold ( $t=2.9$ ),  $p=0.018$ , FWE-corrected; 5000 permutations, at the lower threshold ( $t=1.9$ ),  $p=0.014$ , FWE-corrected; 5000 permutations. Edges described in bold were demonstrated at both the higher and lower thresholds.

Node	Node	t-value
<b>Rectus_L</b>	<b>SupraMarginal_L.</b>	<b>3.28</b>
Occipital_Mid_R	Fusiform_R.	3.23
Occipital_Mid_L	Fusiform_R.	3.01
<b>Rectus_L</b>	<b>SupraMarginal_R.</b>	<b>2.97</b>
<b>ParaHippocampal_L</b>	<b>SupraMarginal_R.</b>	<b>2.91</b>
Frontal_Sup_Medial_R	Fusiform_R.	2.74
Cingulum_Ant_L	SupraMarginal_L.	2.7
Rectus_R	ParaHippocampal_L.	2.62
Rectus_L	Occipital_Mid_R.	2.53
Rectus_R	SupraMarginal_L.	2.36
Rectus_L	Occipital_Mid_L.	2.33
Rectus_L	ParaHippocampal_L.	2.1
Occipital_Mid_L	Fusiform_L.	2.09
Frontal_Sup_Medial_R	SupraMarginal_L.	2.07
Rectus_R	SupraMarginal_R.	2.04

Occipital_Mid_R	Fusiform_L.	2
Fusiform_L	Temporal_Inf_L.	1.99
Rectus_R	Occipital_Mid_R.	1.94
Frontal_Sup_Medial_R	ParaHippocampal_L.	1.92
Frontal_Sup_Medial_L	Fusiform_R.	1.92
Frontal_Sup_Medial_L	SupraMarginal_L.	1.91

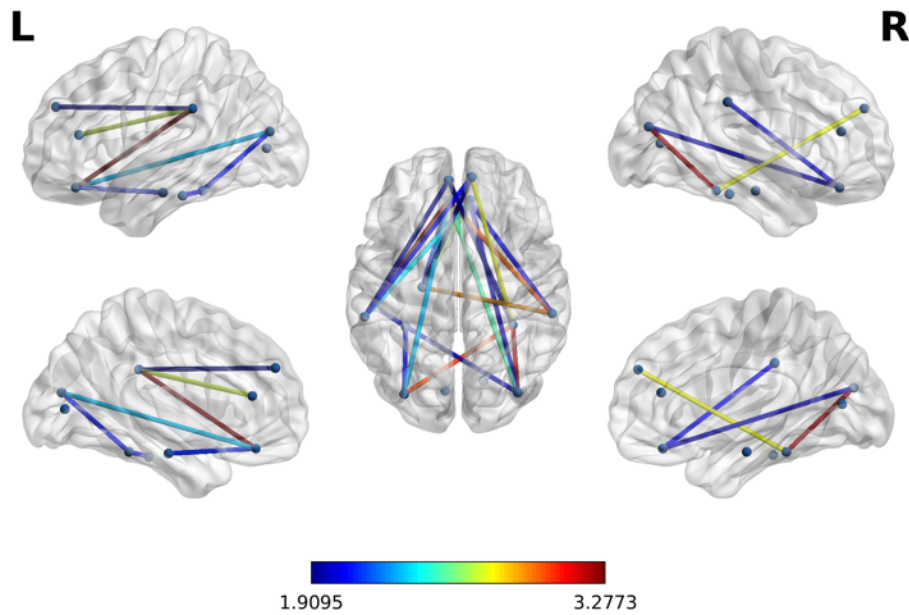


Table 43 Networks with a negative correlation between connectivity and perceived stress scores in the default mode network in MINOCA patients.

At the higher threshold ( $t=2.8$ ),  $p=0.033$ , FWE-corrected; 5000 permutations, at the lower threshold ( $t=1.9$ ),  $p=0.007$ , FWE-corrected; 5000 permutations. Edges described in bold were demonstrated at both the higher and lower thresholds.

Node	Node	t-value
<b>Rectus_L</b>	<b>Occipital_Mid_R.</b>	<b>3.04</b>
<b>Occipital_Mid_R</b>	<b>Fusiform_R.</b>	<b>3</b>
<b>Rectus_L</b>	<b>SupraMarginal_L.</b>	<b>2.81</b>
ParaHippocampal_R	Temporal_Inf_R.	2.79
Occipital_Mid_L	Fusiform_L.	2.44
Rectus_L	SupraMarginal_R.	2.4
Rectus_L	Occipital_Mid_L.	2.37
Rectus_R	SupraMarginal_L.	2.37
Calcarine_L	SupraMarginal_R.	2.33



Occipital_Mid_R	Fusiform_L.	2.25
Occipital_Mid_L	Fusiform_R.	2.25
Frontal_Sup_Medial_R	Fusiform_R.	2.18
Temporal_Inf_L	Temporal_Inf_R.	2.16
Rectus_R	Occipital_Mid_R.	2.1
ParaHippocampal_L	ParaHippocampal_R.	2.09
Frontal_Sup_Medial_L	Frontal_Sup_Medial_R.	2.08
ParaHippocampal_R	Temporal_Inf_L.	2.07
SupraMarginal_L	SupraMarginal_R.	2.03
Cingulum_Ant_R	Temporal_Inf_R.	1.98
Cingulum_Ant_L	SupraMarginal_L.	1.96
ParaHippocampal_R	Fusiform_R.	1.94
Frontal_Sup_Medial_L	SupraMarginal_L.	1.94
Occipital_Mid_L	Occipital_Mid_R.	1.91

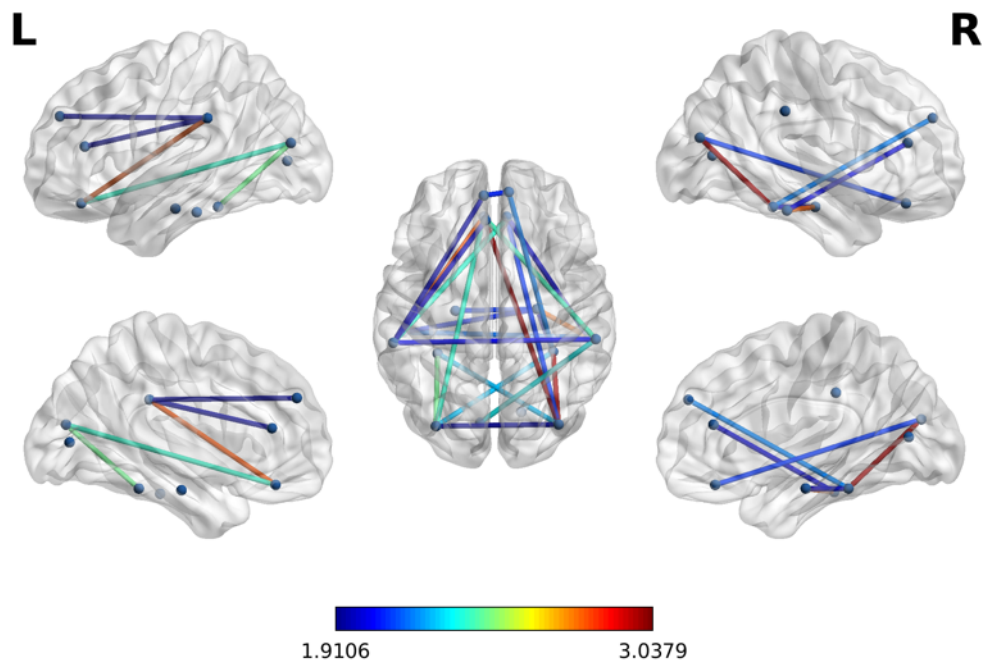


Table 44 Networks with a positive correlation between connectivity and anxiety in the default mode network in healthy patients.

At the higher threshold ( $t=6.1$ ),  $p<0.001$ , FWE-corrected; 5000 permutations, at the lower threshold ( $t=4.1$ ),  $p=0.034$ , FWE-corrected; 5000 permutations

Node	Node	t-value
Calcarine L	Occipital Mid L	6.15
ParaHippocampal_L	SupraMarginal_R	4.22

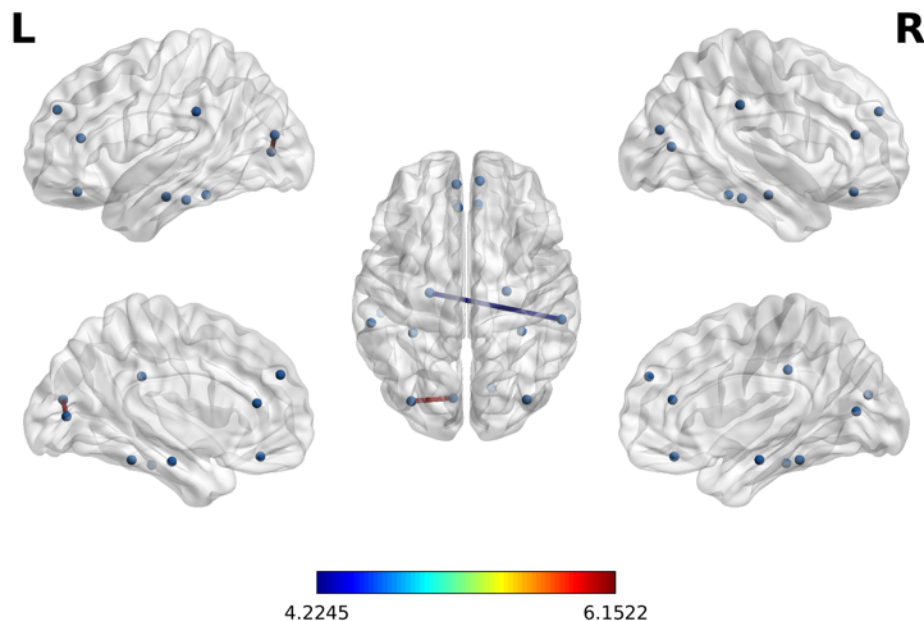


Table 45 Networks with a positive correlation between connectivity and perceived stress scores in the default mode network in healthy patients.

At the higher threshold ( $t=4.6$ )  $p=0.020$ , FWE-corrected; 5000 permutations, at the lower threshold ( $t=3.8$ ),  $p=0.087$ , FWE-corrected; 5000 permutations. Edges described in bold were demonstrated at both the higher and lower thresholds.

Node	Node	t-value
<b>Calcarine_L</b>	<b>Occipital_Mid_L</b>	<b>4.64</b>

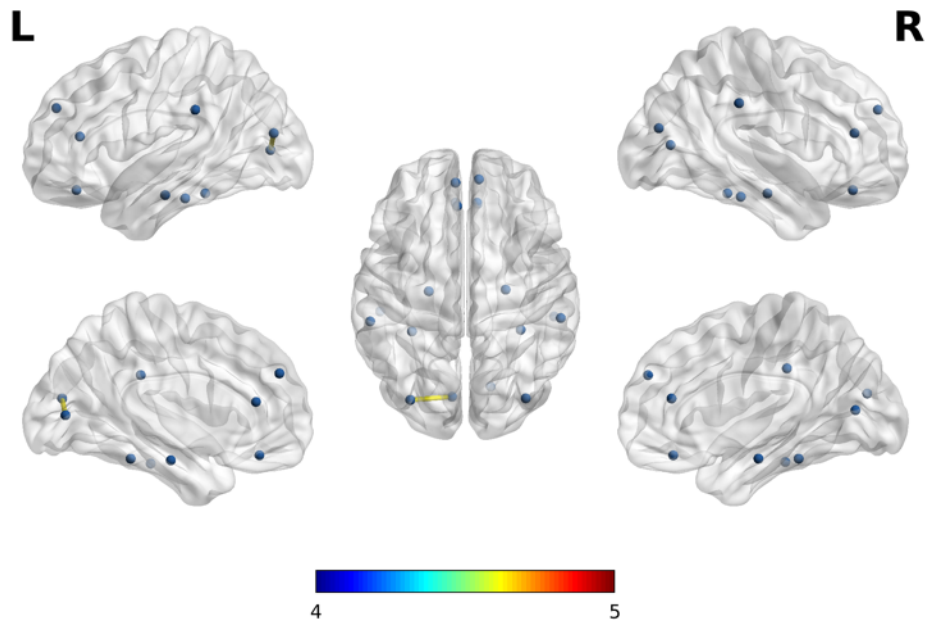


Table 46 Networks with a negative correlation between connectivity and perceived stress scores in MINOCA patients.

At the higher threshold ( $t=2.5$ )  $p=0.048$ , FWE-corrected; 5000 permutations, at the lower threshold ( $t=1.9$ ),  $p=0.009$ , FWE-corrected; 5000 permutations. Edges described in bold were demonstrated at both the higher and lower thresholds.

Node	Node	t-value
Supp_Motor_Area_R	Temporal_Pole_Sup_R.	3.1
<b>Cingulum_Ant_L</b>	<b>Parietal_Inf_L.</b>	<b>2.96</b>
<b>Amygdala_L</b>	<b>Parietal_Inf_L.</b>	<b>2.78</b>
<b>Supp_Motor_Area_L</b>	<b>Cingulum_Ant_L.</b>	<b>2.62</b>
SupraMarginal_R	Putamen_L.	2.54
<b>Supp_Motor_Area_L</b>	<b>Cingulum_Mid_R.</b>	<b>2.5</b>
Amygdala_R	Temporal_Mid_R.	2.48
Supp_Motor_Area_L	SupraMarginal_R.	2.31
Supp_Motor_Area_R	Cingulum_Ant_L.	2.27
Amygdala_R	Thalamus_R.	2.27
Supp_Motor_Area_L	Supp_Motor_Area_R.	2.24
Frontal_Mid_R	Parietal_Inf_L.	2.21
Supp_Motor_Area_R	Cingulum_Mid_R.	2.19
Supp_Motor_Area_R	Insula_R.	2.18

Amygdala_L	Putamen_L.	2.18
Frontal_Mid_R	Supp_Motor_Area_R.	2.15
Supp_Motor_Area_R	Amygdala_R.	2.14
Amygdala_R	Temporal_Pole_Sup_R.	2.06
Frontal_Inf_Orb_L	Parietal_Inf_L.	2.05
Supp_Motor_Area_L	Putamen_L.	1.98
Frontal_Mid_L	Supp_Motor_Area_R.	1.94
Amygdala_L	SupraMarginal_R.	1.94
Insula_R	Putamen_L.	1.93
Frontal_Inf_Orb_L	Putamen_L.	1.92
Parietal_Inf_L	Temporal_Pole_Sup_R.	1.91

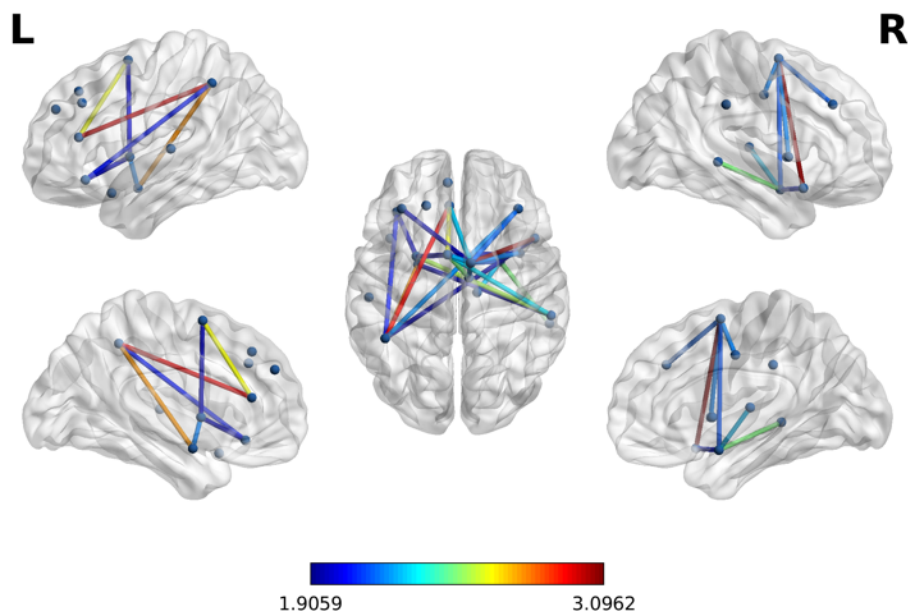


Table 47 Networks with a negative correlation between connectivity and anxiety scores in the central executive network in MINOCA patients.

At the higher threshold ( $t=3.35$ )  $p=0.047$ , FWE-corrected; 5000 permutations, at the lower threshold ( $t=2.6$ ),  $p=0.015$ , FWE-corrected; 5000 permutation. Edges described in bold were demonstrated at both the higher and lower thresholds.

Node	Node	t-value
<b>Frontal_Mid_Orb_R</b>	<b>Thalamus_L.</b>	<b>3.36</b>
Thalamus_L	Thalamus_R.	2.75
Caudate_R	Thalamus_R.	2.68

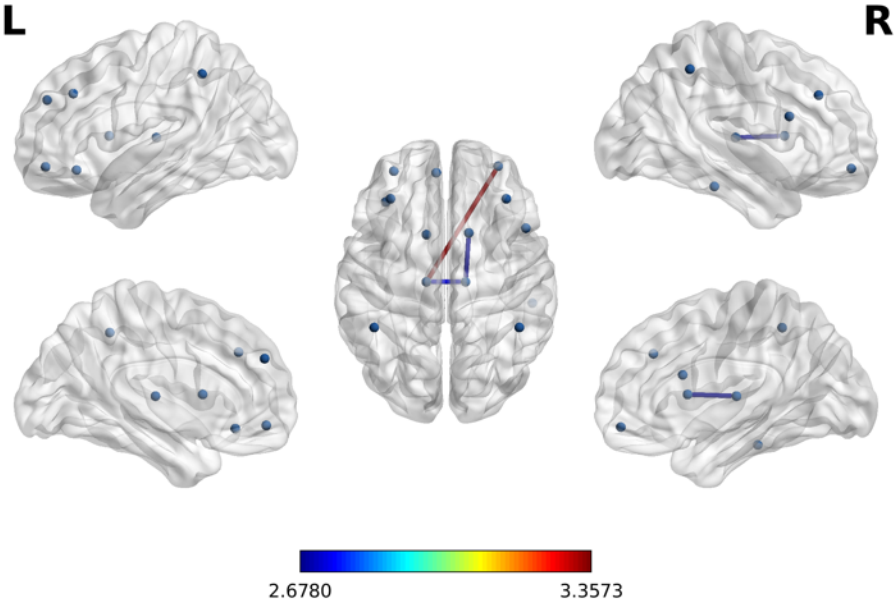


Table 48 Networks with a negative correlation between connectivity and GLS-CMR in the central executive network in MINOCA patients.

At the higher threshold ( $t=3.6$ )  $p=0.010$ , FWE-corrected; 5000 permutations, at the lower threshold ( $t=2.5$ ),  $p=0.020$ , FWE-corrected; 5000 permutations. Edges described in bold were demonstrated at both the higher and lower thresholds.

Node	Node	t-value
<b>Frontal_Mid_Orb_L</b>	<b>Caudate_L.</b>	<b>3.62</b>
Frontal_Mid_Orb_L	Caudate_R.	2.64
Frontal_Mid_R	Caudate_L.	2.56

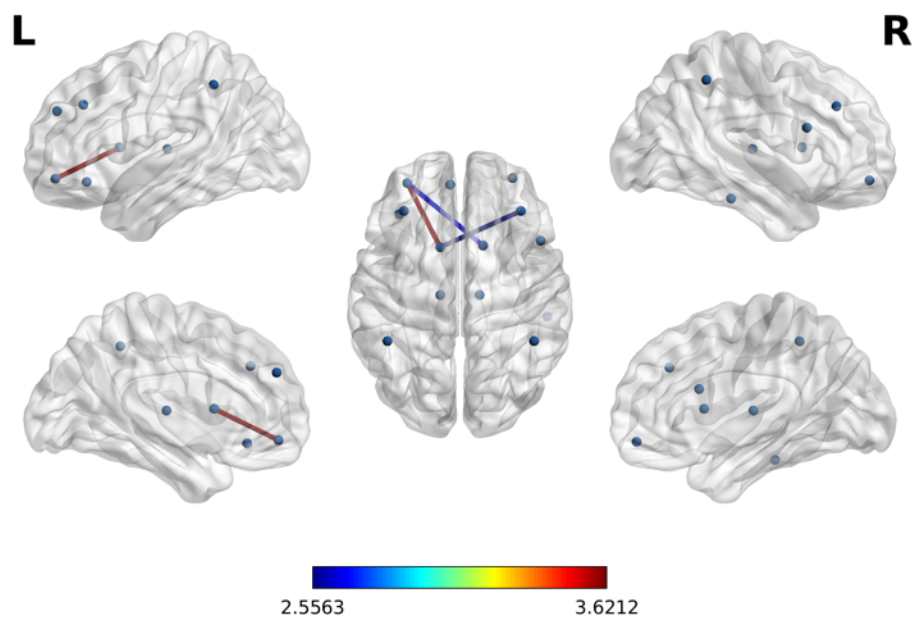


Table 49 Networks with a positive correlation between connectivity and GLS-CMR in the central executive network in healthy patients.

At the higher threshold ( $t=4.1$ )  $p=0.016$ , FWE-corrected; 5000 permutations, at the lower threshold ( $t=2.6$ ),  $p=0.002$ , FWE-corrected; 5000 permutations. Edges described in bold were demonstrated at both the higher and lower thresholds.

Node	Node	t-value
<b>Parietal_Inf_L</b>	<b>Thalamus_L.</b>	<b>4.16</b>
Caudate_R	Thalamus_L.	3.3
Frontal_Mid_R	Frontal_Inf_Orb_L.	3.03
Frontal_Inf_Orb_L	Caudate_L.	2.96
Thalamus_R	Temporal_Inf_R.	2.74
Frontal_Inf_Orb_L	Temporal_Inf_R.	2.72
Frontal_Inf_Orb_L	Thalamus_R.	2.66
Frontal_Mid_R	Thalamus_L.	2.65

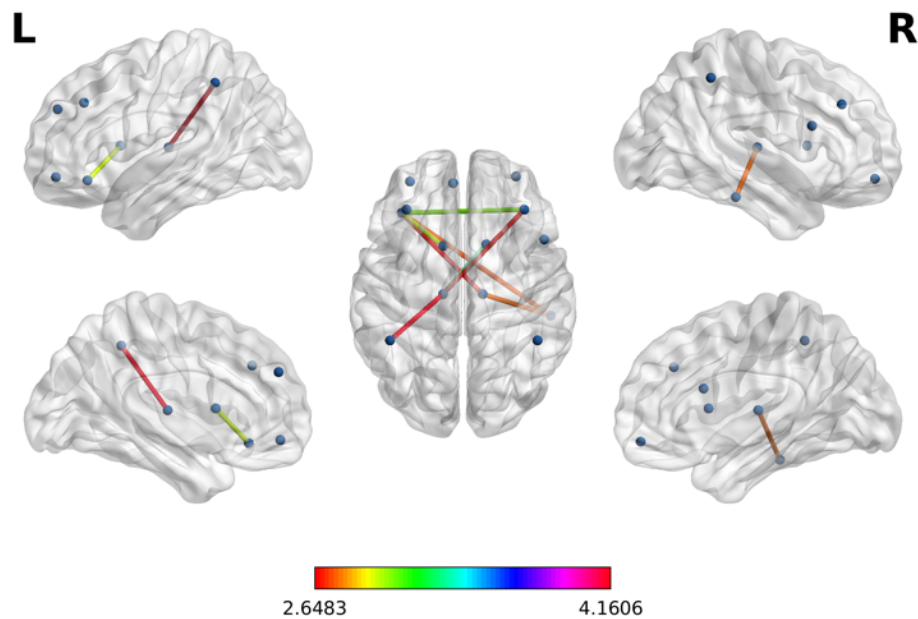


Table 50 Networks with a negative correlation with anxiety score in MINOCA patients on whole brain analysis

At the higher threshold ( $t=3.0$ )  $p=0.005$ , FWE-corrected; 5000 permutations, at the lower threshold ( $t=2.6$ ),  $p=0.007$ , FWE-corrected; 5000 permutations. Edges described in bold were demonstrated at both the higher and lower thresholds.

Node	Node	t-value
Occipital_Inf_R	Parietal_Sup_R.	4.03
Cingulum_Mid_R	Precuneus_R.	3.75
Insula_L	Paracentral_Lobule_R.	3.67
Precentral_R	Fusiform_L.	3.64
Calcarine_L	Putamen_L.	3.46
Parietal_Sup_L	Paracentral_Lobule_L.	3.44
Precuneus_L	Paracentral_Lobule_R.	3.36
Frontal_Mid_Orb_L	Caudate_R.	3.36
Putamen_L	Temporal_Pole_Mid_R.	3.34
Cingulum_Mid_L	Fusiform_L.	3.32
Frontal_Sup_Orb_R	Occipital_Inf_L.	3.3
Occipital_Mid_R	Parietal_Inf_L.	3.3
Frontal_Sup_Medial_L	Fusiform_L.	3.28
SupraMarginal_L	Precuneus_L.	3.27
Parietal_Inf_L	Precuneus_R.	3.26

Olfactory_R	Hippocampus_R.	3.25
Precuneus_R	Paracentral_Lobule_L.	3.25
Frontal_Sup_Orb_R	Hippocampus_R.	3.24
Calcarine_R	Occipital_Mid_R.	3.23
Olfactory_L	Caudate_L.	3.2
Insula_L	ParaHippocampal_L.	3.19
Occipital_Inf_L	Precuneus_R.	3.15
Calcarine_R	Caudate_L.	3.08
Frontal_Sup_Orb_L	Hippocampus_R.	3.07
Cingulum_Mid_L	Postcentral_L.	3.07
Cingulum_Mid_R	Precuneus_L.	3.07
SupraMarginal_R	Precuneus_R.	3.05
Precentral_R	Occipital_Inf_R.	3.04
Cingulum_Mid_L	Amygdala_R.	3.02
Precentral_R	Parietal_Sup_L.	3.02
Cingulum_Mid_L	Precuneus_R.	3.02
Calcarine_R	Occipital_Mid_L.	3.01
Parietal_Sup_L	Precuneus_R.	3
Insula_L	Paracentral_Lobule_L.	3
Parietal_Sup_R	Precuneus_L.	2.99
Calcarine_R	Putamen_L.	2.98
Insula_L	Occipital_Mid_R.	2.97
Frontal_Sup_Medial_L	Fusiform_R.	2.97
Parietal_Inf_L	Precuneus_L.	2.97
Precuneus_L	Paracentral_Lobule_L.	2.97
Frontal_Inf_Tri_L	Calcarine_R.	2.95
Insula_L	Hippocampus_L.	2.93
Frontal_Inf_Tri_L	Occipital_Mid_R.	2.92
Hippocampus_R	Putamen_L.	2.92
Fusiform_R	Temporal_Inf_L.	2.91
Fusiform_L	Parietal_Inf_L.	2.9
Precentral_L	Hippocampus_L.	2.85
Frontal_Sup_L	Fusiform_L.	2.82
Occipital_Mid_R	Precuneus_L.	2.82



Frontal_Inf_Tri_L	Cuneus_L.	2.8
Insula_L	Parietal_Sup_R.	2.79
Olfacry_R	Angular_R.	2.79
Lingual_L	Pallidum_R.	2.79
Occipital_Inf_R	Temporal_Inf_L.	2.79
Parietal_Sup_R	Paracentral_Lobule_L.	2.78
Precentral_R	Occipital_Inf_L.	2.76
Cingulum_Mid_L	Precuneus_L.	2.76
Caudate_R	Thalamus_L.	2.75
Frontal_Inf_Oper_L	Calcarine_R.	2.74
Cingulum_Ant_R	Calcarine_R.	2.74
Lingual_L	Angular_R.	2.74
Occipital_Inf_L	Precuneus_L.	2.74
Frontal_Inf_Orb_R	Postcentral_R.	2.73
Insula_L	Cuneus_R.	2.72
Frontal_Inf_Oper_L	Lingual_L.	2.72
Insula_R	Paracentral_Lobule_R.	2.71
Fusiform_L	SupraMarginal_L.	2.7
SupraMarginal_L	Caudate_L.	2.7
Frontal_Mid_Orb_L	Occipital_Mid_L.	2.69
Frontal_Inf_Oper_L	Fusiform_L.	2.69
Occipital_Inf_L	Parietal_Sup_R.	2.69
Calcarine_L	Pallidum_L.	2.69
Frontal_Inf_Orb_R	Postcentral_L.	2.68
Insula_R	Parietal_Inf_L.	2.68
Cingulum_Mid_R	SupraMarginal_R.	2.68
Frontal_Inf_Tri_L	Paracentral_Lobule_L.	2.68
Caudate_L	Thalamus_L.	2.68
Calcarine_R	Occipital_Sup_R.	2.66
Insula_L	Hippocampus_R.	2.65
Hippocampus_R	Putamen_R.	2.65
Frontal_Sup_L	Fusiform_R.	2.64
Frontal_Inf_Tri_L	Parietal_Sup_L.	2.62
Frontal_Sup_Medial_R	Temporal_Inf_L.	2.62

Cingulum_Mid_R	Parietal_Inf_R.	2.61
Frontal_Mid_Orb_R	SupraMarginal_R.	2.61
Amygdala_R	Putamen_L.	2.61

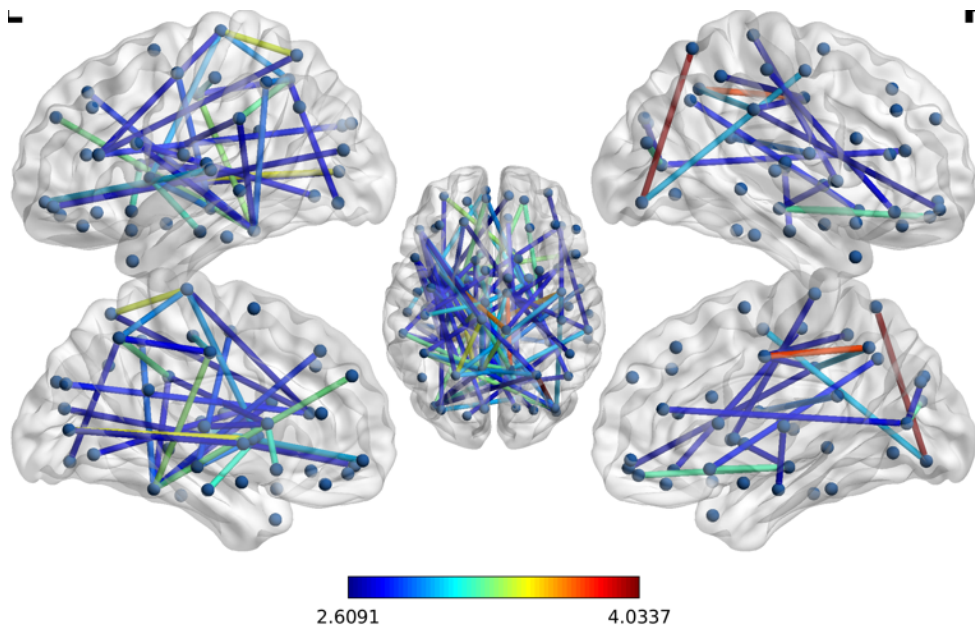


Table 51 Networks with a negative correlation with perceived stress score in MINOCA patients on whole brain analysis

At the higher threshold ( $t=3.6$ )  $p=0.005$ , FWE-corrected; 5000 permutations, at the lower threshold ( $t=2.8$ ),  $p=0.008$ , FWE-corrected; 5000 permutations. Edges described in bold were demonstrated at both the higher and lower thresholds.

Node	Node	t-value
Cingulum_Post_L	Fusiform_L.	<b>4.48</b>
Frontal_Mid_L	Occipital_Mid_L.	4.42
Cingulum_Post_L	Fusiform_R.	<b>3.86</b>
Calcarine_L	Heschl_L.	3.81
Fusiform_L	Caudate_L.	<b>3.8</b>
Cingulum_Mid_R	ParaHippocampal_L.	3.66
Caudate_L	Temporal_Mid_L.	<b>3.64</b>
Occipital_Inf_L	Caudate_L.	<b>3.63</b>

Frontal_Inf_Orb_R	Occipital_Inf_L.	3.54
Occipital_Mid_R	Parietal_Inf_L.	3.5
ParaHippocampal_R	Temporal_Pole_Sup_R.	3.42
Cingulum_Mid_L	ParaHippocampal_L.	3.4
Lingual_R	Caudate_L.	3.31
Frontal_Sup_Medial_L	Occipital_Sup_R.	3.3
Cuneus_R	Caudate_L.	3.28
Occipital_Inf_L	Precuneus_R.	3.23
Precuneus_L	Paracentral_Lobule_L.	3.19
Frontal_Inf_Oper_L	Fusiform_L.	3.18
Fusiform_L	Parietal_Inf_L.	3.16
Parietal_Inf_L	Paracentral_Lobule_L.	3.16
Occipital_Mid_L	Caudate_L.	3.14
Cingulum_Mid_R	Amygdala_L.	3.1
Supp_Motor_Area_L	Angular_R.	3.1
Parietal_Inf_R	Heschl_L.	3.07
Cingulum_Mid_R	Hippocampus_L.	3.06
Frontal_Inf_Orb_R	Fusiform_R.	3.06
Frontal_Sup_Medial_L	Occipital_Mid_R.	3.04
Fusiform_L	Temporal_Pole_Sup_R.	3.03
Occipital_Inf_L	Caudate_R.	3.02
Calcarine_R	Occipital_Mid_R.	3
Fusiform_L	Angular_L.	2.98
Frontal_Mid_L	Occipital_Sup_L.	2.97
Precuneus_L	Paracentral_Lobule_R.	2.97
Supp_Motor_Area_R	Parietal_Inf_L.	2.96
Frontal_Inf_Oper_L	Amygdala_R.	2.94
Insula_R	ParaHippocampal_L.	2.91
Lingual_L	Occipital_Mid_L.	2.91
Hippocampus_R	Heschl_L.	2.9
Hippocampus_L	Parietal_Inf_L.	2.89
Precuneus_R	Paracentral_Lobule_L.	2.89
Cingulum_Mid_L	Temporal_Mid_R.	2.89
Amygdala_R	Angular_R.	2.88

Cingulum_Mid_R	Precuneus_R.	2.88
Fusiform_L	Parietal_Inf_R.	2.86
Occipital_Inf_R	Caudate_L.	2.86
Frontal_Inf_Oper_R	Amygdala_L.	2.85
Frontal_Mid_L	Occipital_Mid_R.	2.83
ParaHippocampal_L	Precuneus_L.	2.83
Parietal_Inf_R	Temporal_Sup_L.	2.83
Supp_Motor_Area_L	Frontal_Sup_Medial_R.	2.81
Frontal_Sup_Medial_L	Fusiform_L.	2.81
ParaHippocampal_R	Caudate_L.	2.8

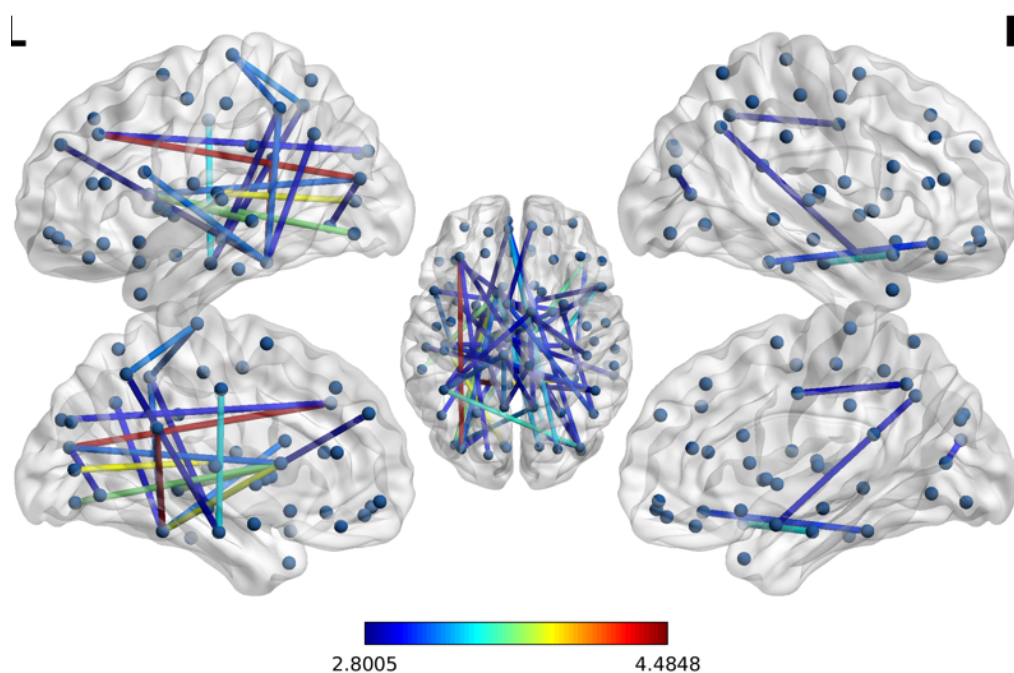
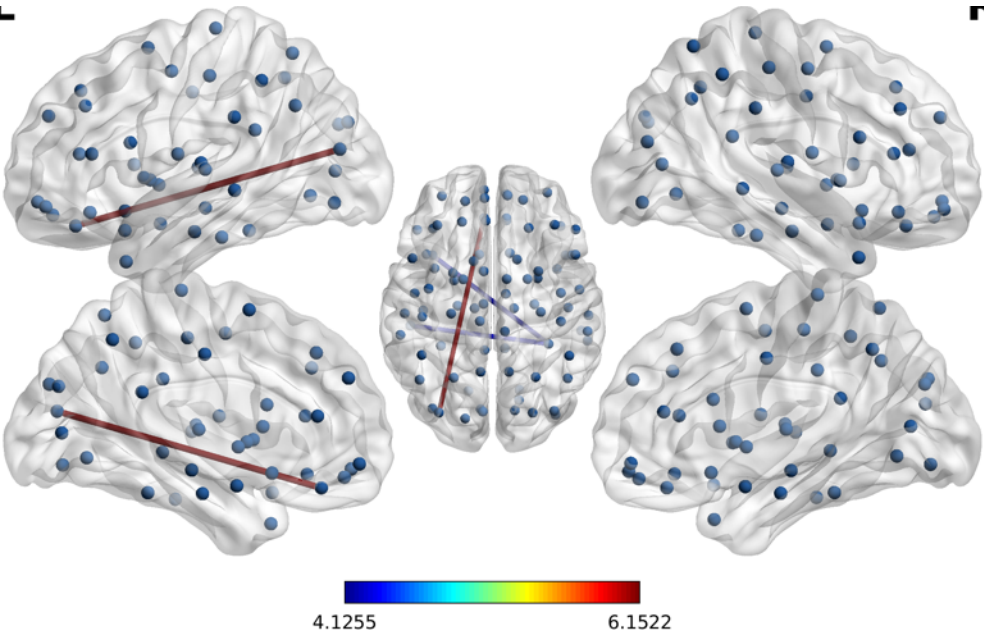


Table 52 Networks with a positive correlation with anxiety score in healthy participants on whole brain analysis

At the higher threshold ( $t=6.0$ )  $p=0.008$ , FWE-corrected; 5000 permutations, at the lower threshold ( $t=4.1$ ),  $p=0.105$ , FWE-corrected; 5000 permutations. Edges described in bold were demonstrated at both the higher and lower thresholds.

Node	Node	t-value
Rectus_L	Occipital_Mid_L	6.15
Fusiform_R	Temporal_Inf_L	4.22
Fusiform_R	Temporal_Pole_Mid_L	4.10



## 8.4 APPENDIX D

Appendix D included supplementary results from Chapter 5.

Table 53 Regions of the brain in MINOCA patients with *reduced* grey matter volume from the acute to chronic phase

Hemisphere	AAL region	p(FWE-corr)	T	x	y	z
Right	Temporal_Pole_Sup	0.001	6.6	45	26	-24
Left	Cerebellum_Crus2	0.004	5.99	0	-86	-26
Left	Cerebellum_4_5	0.007	5.81	-4	-58	0
Left	Frontal_Mid_Orb	0.002	6.19	-42	56	-10
Right	Cerebellum_Crus1	0.003	6.11	51	-70	-28
Right	Frontal_Mid_Orb	0.003	6.06	44	51	-16
Right	Frontal_Inf_Orb	0.026	5.42	52	34	-15
Left	Frontal_Inf_Orb	0.007	5.83	-46	26	-16
Left	Temporal_Pole_Sup	0.013	5.64	-39	26	-26
Left	Postcentral	0.009	5.75	-66	-8	14
Right	Cerebellum_Crus2	0.011	5.68	54	-57	-44
Right	Frontal_Sup_Medial	0.022	5.47	6	57	40
Right	Frontal_Inf_Oper	0.016	5.57	50	12	32
Right	Frontal_Inf_Orb	0.017	5.56	36	36	-6
Right	Insula	0.019	5.51	46	-6	3
Right	Temporal_Sup	0.021	5.49	70	-33	9
Left	Frontal_Inf_Tri	0.026	5.41	-33	34	2
Left	Insula	0.039	5.29	-27	30	8
Right	Temporal_Mid	0.038	5.29	70	-30	-4

Table 54 Regions of the brain in acute MINOCA patients with increased grey matter volume compared to chronic MINOCA patients

Hemisphere	AAL region	p(FWE-corr)	T	x	y	z
Right	Putamen	0	7.26	21	0	9
Left	Insula	0	6.82	-33	-14	8
Right	Cingulum_Post	0	6.73	4	-42	28
Left	Cingulum_Post	0.002	6.18	-4	-44	22
Left	Cingulum_Mid	0.004	5.97	-4	-20	39
Left	Paracentral_Lobule	0	6.65	-8	-30	52
Left	Thalamus	0.001	6.43	-6	-18	4

Left	ParaHippocampal	0.001	6.36	-22	-20	-22
Left	Hippocampus	0.002	6.16	-21	-14	-16
Right	Supp_Motor_Area	0.001	6.33	9	-21	56
Left	Putamen	0.002	6.21	-18	6	8
Right	Cerebellum_8	0.003	6.13	21	-70	-52
Left	Cingulum_Ant	0.005	5.92	-9	15	30
Left	Cerebellum_Crus1	0.003	6.07	-12	-68	-27
Left	Temporal_Inf	0.003	6.05	-58	-8	-34
Right	Frontal_Inf_Orb	0.003	6.05	33	34	-20
Left	Frontal_Mid	0.004	5.99	-44	9	54
Left	Precentral	0.016	5.57	-50	9	45
Left	Frontal_Sup	0.004	5.98	-15	26	63
Right	Cerebellum_Crus1	0.004	5.97	21	-78	-28
Right	Cerebellum_Crus2	0.007	5.83	30	-70	-39
Left	Caudate_L	0.006	5.88	-8	10	-12
Left	Cerebellum_8	0.011	5.7	-30	-62	-50
Right	Frontal_Inf_Tri	0.007	5.83	42	14	21
Right	Temporal_Sup	0.007	5.81	51	-27	4
Left	Rectus	0.008	5.8	-20	12	-15
Right	Temporal_Mid	0.008	5.79	52	-48	4
Left	Postcentral	0.008	5.79	-39	-12	40
Left	Temporal_Mid	0.01	5.73	-63	-4	-9
Right	Insula	0.01	5.71	38	14	-6
Left	Frontal_Inf_Oper	0.011	5.7	-42	12	21
Right	Cingulum_Ant	0.012	5.67	12	22	27
Right	Cingulum_Mid	0.034	5.33	10	15	33
Left	Parietal_Sup	0.013	5.63	-34	-50	68
Right	Frontal_Mid	0.014	5.61	24	38	26
Right	Rolandic_Oper	0.043	5.26	44	-16	21
Left	Cerebellum_Crus2	0.017	5.54	-16	-82	-34
Right	Temporal_Pole_Mid	0.02	5.5	46	20	-36
Left	Supp_Motor_Area	0.021	5.49	-8	-8	56
Left	Frontal_Inf_Orb	0.023	5.46	-33	36	-18
Right	Cingulum_Ant_R	0.023	5.45	12	44	24
Left	Cerebellum_4_5	0.025	5.43	-8	-56	-21
Left	Parietal_Inf	0.027	5.4	-42	-34	36
Right	Calcarine	0.027	5.4	12	-69	8
Left	SupraMarginal	0.033	5.34	-51	-26	21
Right	Precuneus	0.034	5.33	12	-50	15
Right	Parietal_Inf	0.036	5.31	40	-50	38

Table 55 Regions of the brain with reduced grey matter volume in chronic MINOCA patients versus healthy control patients.

Hemisphere	AAL region	p(FWE-corr)	T	x	y	z
Left	Temporal_Mid	0.001	5.88	-62	-50	8
Left	Precentral	0.01	5.35	-46	-8	51
Left	Postcentral	0.033	5	-51	-14	56
Right	Postcentral	0.015	5.23	40	-34	56

Table 56 Greater connectivity in patients with a previous episode of MINOCA compared to healthy controls in the default mode network.

At the higher threshold ( $t=2.2$ )  $p=0.020$ , FWE-corrected; 5000 permutations, at the lower threshold ( $t=1.9$ )  $p=0.042$ , FWE-corrected, 5000 permutations. Edges described in bold were demonstrated at both the higher and lower thresholds

Node	Node	T-value
<b>ParaHippocampal_R</b>	<b>SupraMarginal_R.</b>	<b>3.09</b>
<b>ParaHippocampal_L</b>	<b>SupraMarginal_L.</b>	<b>2.57</b>
<b>ParaHippocampal_R</b>	<b>SupraMarginal_L.</b>	<b>2.48</b>
<b>ParaHippocampal_L</b>	<b>SupraMarginal_R.</b>	<b>2.48</b>
<b>ParaHippocampal_L</b>	<b>Temporal_Inf_L.</b>	<b>2.28</b>
<b>Frontal_Sup_Medial_L</b>	<b>ParaHippocampal_L.</b>	<b>2.27</b>
<b>ParaHippocampal_L</b>	<b>ParaHippocampal_R.</b>	<b>2.27</b>
<b>Frontal_Sup_Medial_R</b>	<b>SupraMarginal_L.</b>	<b>2.26</b>
<b>SupraMarginal_L</b>	<b>Temporal_Inf_L.</b>	<b>2.24</b>
ParaHippocampal_R	Temporal_Inf_L.	2.14
SupraMarginal_L	Temporal_Inf_R.	2.12
Occipital_Mid_R	Temporal_Inf_L.	2.02
Occipital_Mid_R	Fusiform_R.	1.92

Table 57 Lower connectivity in patients with a previous episode of MINOCA compared to healthy controls in the central executive network.

At the higher threshold ( $t=3.7$ )  $p=0.03$ , FWE-corrected; 5000 permutations, at the lower threshold ( $t=3.0$ )  $p=0.006$ , FWE-corrected, 5000 permutations. Edges described in bold were demonstrated at both the higher and lower thresholds

Node	Node	T-value
<b>Frontal_Mid_Orb_L</b>	<b>Frontal_Inf_Orb_L.</b>	<b>3.79</b>
Parietal_Inf_R	Caudate_L.	3.47
Frontal_Mid_Orb_L	Parietal_Inf_R.	3.04



Table 58 Greater connectivity in patients with a previous episode of TS compared to healthy controls in the central executive network.

At the higher threshold ( $t=2.7$ )  $p=0.029$ , FWE-corrected; 5000 permutations, at the lower threshold ( $t=2.3$ )  $p=0.040$ , FWE-corrected, 5000 permutations. Edges described in bold were demonstrated at both the higher and lower thresholds

Node	Node	T-value
<b>Frontal_Inf_Oper_R</b>	<b>Thalamus_L.</b>	<b>3.18</b>
<b>Frontal_Mid_Orb_L</b>	<b>Caudate_R.</b>	<b>3.06</b>
<b>Frontal_Inf_Oper_R</b>	<b>Caudate_R.</b>	<b>2.89</b>
<b>Frontal_Mid_R</b>	<b>Caudate_R.</b>	<b>2.72</b>
Frontal_Mid_Orb_R	Caudate_R.	2.57
Frontal_Mid_Orb_L	Thalamus_L.	2.55
Caudate_L	Caudate_R.	2.33

Table 59 Lower connectivity in patients with a previous episode of TS compared to healthy controls in the central executive network.

At the higher threshold ( $t=2.4$ )  $p=0.019$ , FWE-corrected; 5000 permutations, there was no increased connectivity at lower thresholds.

Node	Node	T-value
Frontal_Mid_Orb_L	Parietal_Inf_R.	2.85
Frontal_Inf_Orb_L	Parietal_Inf_R.	2.67
Frontal_Mid_Orb_L	Frontal_Inf_Orb_L.	2.45

Table 60 Lower connectivity in patients with a previous episode of TS compared to patients with a previous STEMI in the central executive network.

At the higher threshold ( $t=2.8$ )  $p=0.016$ , FWE-corrected; 5000 permutations, at the lower threshold ( $t=2.0$ )  $p=0.031$ , FWE-corrected, 5000 permutations. Edges described in bold were demonstrated at both the higher and lower thresholds

Node	Node	T-value
<b>Frontal_Inf_Orb_L</b>	<b>Parietal_Inf_R.</b>	<b>2.88</b>
<b>Frontal_Inf_Orb_L</b>	<b>Parietal_Inf_L.</b>	<b>2.82</b>
Frontal_Mid_Orb_L	Parietal_Inf_R.	2.68
Frontal_Mid_L	Parietal_Inf_L.	2.55
Frontal_Mid_L	Frontal_Inf_Orb_L.	2.25
Parietal_Inf_L	Parietal_Inf_R.	2.09

Table 61 Reduced connectivity in patients with an acute episode TS compared to chronic TS on whole brain analysis.

At the higher threshold ( $t=5.7$ )  $p=0.035$ , FWE-corrected; 5000 permutations, there was no increased connectivity at lower thresholds.

Node	Node	T-value
Temporal_Sup_L	Occipital_Sup_L	5.76